

Small Molecule Inhibitors of Protein-Protein Interactions

by

Kareem Khoury

Bachelor of Science, University of Pittsburgh, 2008

Submitted to the Graduate Faculty of
School of Pharmacy in partial fulfillment
of the requirements for the degree of
Doctor of Philosophy

University of Pittsburgh

2013

UNIVERSITY OF PITTSBURGH
SCHOOL OF PHARMACY

This dissertation was presented

by

Kareem Khoury

It was defended on

December 5th, 2013

and approved by

Barry I. Gold, Professor, Department of Pharmaceutical Sciences

Xiang-Qun Xie, Professor, Department of Pharmaceutical Sciences

Song Li, Professor, Department of Pharmaceutical Sciences

Carlos Camacho, Department of Structural Biology

Dissertation Advisor: Alexander Doemling, Professor, Department of Pharmaceutical
Sciences

Copyright © by Kareem Khoury

2013

Discovery of Small Molecule Inhibitors for Protein-Protein Interactions

Kareem Khoury, PhD

University of Pittsburgh, 2013

Protein-protein interactions (PPIs) constitute a rising class of targets for the next generation of therapeutic intervention. Though they play a fundamental role in many biological processes and almost all pathological conditions including cancer, diabetes, and autoimmune diseases, PPIs remain underrepresented in drug discovery. Small molecules are the ideal candidates for PPI inhibitors due to low production cost and better absorption, distribution, metabolism, and excretion (ADME) properties compared to biological agents. Discovering small molecule inhibitors of PPIs has proven to be difficult because of the relatively large contact areas between proteins. Herein are described novel approaches to the chemical synthesis as well as a screening tool which will facilitate the discovery of small molecule inhibitors of PPIs.

Currently, molecules derived from multicomponent reactions (MCRs) are rarely distributed in general screening libraries. The exceptions are special scaffolds, e.g. dihydropyrimidines, whose class includes the blockbuster Ca antagonist, Nifedipine. Interestingly, however, MCR molecules have been frequently described as inhibitors of PPIs. Examples include p53/mdm2^{1,2}, Bcl2³, HIV-1/gp41⁴, CCR5⁵ and oxytocin antagonists⁶. These findings support the notion that MCR molecules are especially suitable for mimicking peptides. We have developed a virtual library of scaffolds derived from a diverse set of MCRs which are easily chemically accessible.

In addition, our lab has set forth to discover novel MCRs to add to our virtual library. One such scaffold described in this dissertation is derived from the Ugi-4-component-5-centered reaction. A novel amidation of this classic scaffold adds a true four-component reaction to our MCR database. The scope and limitations of this reaction are described in detail allowing for an accurate representation of compounds with a high probability of being synthesized. Various cyclizations of this scaffold are also explored and described in detail.

A receptor-based drug discovery approach can be applied when an accurate three-dimensional (3D) structure of a specific PPI complex is available. A novel, complementary and transformative docking approach for the rational design of small molecule inhibitors was developed for our virtual library based on the “anchor” concept. Applying our method, we efficiently discovered several new scaffolds of inhibitors of the p53/MDM2 interaction with lower micromolar affinity binding to MDM2, which can serve as starting point for medicinal chemistry optimization.

In summary, the methods and tools described in this dissertation are important contributions to the fields of medicinal chemistry and structure-based drug discovery because they combine structural insights and ligand design to expedite the discovery of novel small molecule inhibitors of PPIs.

TABLE OF CONTENTS

LIST OF SCHEMES	XIII
PREFACE.....	XIV
1.0 INTRODUCTION.....	1
1.1 PROTEIN-PROTEIN INTERACTIONS AS DRUG TARGETS.....	1
1.2 THE P53/MDM2 AXIS	3
1.2.1 p53/MDM2 Biology.....	4
1.2.2 p53/MDM2 interactions	8
1.2.3 Small molecule-MDM2 co-crystals	10
1.2.4 MDMX-co crystal	21
1.2.5 Clinical Trials.....	24
2.0 ANCHORQUERY: AN EASILY ACCESSIBLE VIRTUAL SCREENING LIBRARY/TOOL	26
2.1 COMPOUND SCREENING LIBRARY GENERATION.....	33
2.1.1 Isocyanide Based MCRs.....	34
2.1.1.1 Ugi Reaction.....	34
2.1.1.2 Tetrazole Reaction	35
2.1.1.3 Hydantoine Reaction.....	37
2.1.1.4 Imidazole.....	38

2.1.1.5	Diketopiperazine	39
2.1.1.6	Praziquantel (Ugi/Pictet-Spengler).....	40
2.1.1.7	Ugi 4-component-5-centered reaction	42
2.1.1.8	Ugi-deprotective Cyclization - Benzimidazole.....	43
2.1.1.9	Ugi-deprotective Cyclization - Dihydrobenzodiazepine-acetamide	45
2.1.1.10	Ugi-deprotective Cyclization - Tetrahydrobenzodiazepine - carboxamide	46
2.1.1.11	Ugi- deprotective Cyclization - Dihydrobenzodiazepine- carboxamide	47
2.1.1.12	Ugi- deprotective Cyclization - Tetrazolyl- dihydrobenzodiazepine.....	49
2.1.1.13	Groebke/Blackburn/Bienayme	50
2.1.1.14	Thienodiazepine	51
2.1.1.15	Orru.....	53
2.1.1.16	Schöllkopf reaction	54
2.1.1.17	Thiazole Amidation.....	56
2.1.2	Non-Isocyanide Based Multicomponent Reactions	58
2.1.2.1	Döbner.....	58
2.1.2.2	Gewald.....	59
2.1.2.3	Isoquinoline Amidation	61
2.1.2.4	Reaction mapping and smarts codes	62
2.1.3	Principal Moment of Inertia	68
2.2	ANCHORQUERY IMPLEMENTATION.....	70

3.0	DISCOVERY OF NEW MULTICOMPONENT REACTIONS FOR VIRTUAL SCREENING.....	74
3.1	IMINODICARBOXAMIDES BY VARIATION OF THE UGI-4-COMPONENT-5-CENTERED REACTION	75
3.1.1	Materials and Methods	85
3.2	CYCLIZATION SCAFFOLDS BY VARIATION OF THE UGI-4-COMPONENT-5-CENTERED REACTION	105
3.2.1	Isoindolinone	107
3.2.2	Dioxopyrrolidines	110
3.2.3	Pictet-Spengler	113
3.2.4	Materials and Methods	121
4.0	UGI-4-COMPONENT-5-CENTERED REACTION FOR USE IN P53/MDM2155	
4.1	ANCHORQUERY SEARCH AGAINST P53/MDM2	155
4.2	SYNTHESIS AND IN VITRO ACTIVITY OF SELECTED COMPOUNDS	
	158	
4.2.1	Materials and Methods	164
4.3	CO-CRYSTAL AND CELL BASED SCREENING	181
4.3.1	Materials and Methods	185
5.0	CONCLUSIONS AND FUTURE WORK	188
	APPENDIX A	189
	APPENDIX B	196
	APPENDIX C	205
	BIBLIOGRAPHY	206

LIST OF TABLES

Table 3-1 Ugi-4C-5Cr reaction products and yields.....	81
Table 3-2 Ugi4C5CR isoindolinone cyclization reaction products	110
Table 3-3 Ugi4C5CR dioxopyrrolidines cyclization reaction products	112
Table 3-4 Ugi4C5CR Pictet-Spengler cyclization reaction products	116
Table 3-5 Ugi4C5CR Pictet-Spengler cyclization reaction products	118
Table 4-1 SAR study of compounds 4.2-2.....	160
Table 4-2 SAR study of compounds 4.2-3 I	162
Table 4-3 SAR study of compounds 4.2-4.....	164
Table 4-4 Use of an extended isocyanide	185

LIST OF FIGURES

Figure 1.1 p53/MDM2 pathway	5
Figure 1.2 MDM2/MDMX alignment.	7
Figure 1.3 PPI contact surface.	9
Figure 1.4 p53/MDM2 "hot spot"	10
Figure 1.5 MDM2/nutlin Co-crystal	12
Figure 1.6 MDM2/benzodiazepine Co-crystal.	15
Figure 1.7 MDM2/Spirooxindole Co-crystal.....	18
Figure 1.8 MDM2/chromenotriazolopyrimidine Co-crystal.....	20
Figure 1.9 MDM2/imidazole Co-crystal.....	21
Figure 1.10 p53/MDMX Co crystal.....	22
Figure 1.11MDMX/imidazole Co-crystal.....	23
Figure 1.12 Clinical candidates.....	25
Figure 2.1 The p53/MDM2 protein-protein interaction and open-access <i>AnchorQuery</i> web interface.....	29
Figure 2.2 A representation of the chemical diversity of our multicomponent reaction-accessible, anchor-biased <i>AnchorQuery</i> libraries	32
Figure 2.3 Beta-lactam reaction.....	35

Figure 2.4 Tetrazole reaction	36
Figure 2.5 Hydantoine reaction.....	37
Figure 2.6 Imidazole reaction	38
Figure 2.7 Diketopiperazine reaction.....	40
Figure 2.8 Praziquantel reaction	41
Figure 2.9 Ugi-4C-5CR reaction.....	42
Figure 2.10 Ugi-4C-5CR amidation reaction.....	43
Figure 2.11 Benzimidazole reaction	44
Figure 2.12 Benzodiazepine reaction.....	45
Figure 2.13 Benzodiazepine reaction.....	47
Figure 2.14 Benzodiazepine reaction.....	48
Figure 2.15 Benzodiazepine reaction.....	50
Figure 2.16 Groebke reaction.	51
Figure 2.17 Thienodiazepine reaction.....	52
Figure 2.18 Orru reaction.....	53
Figure 2.19 Orru amidation reaction.....	54
Figure 2.20 Schöllkopf reaction.....	55
Figure 2.21 Schöllkopf amidation reaction.....	56
Figure 2.22 Thiazole amidation reaction	57
Figure 2.23 Döbner reaction.	59
Figure 2.24 Gewald reaction.....	60
Figure 2.25 Isoquinoline reaction	62
Figure 2.26 Principal moment of inertia.	69

Figure 2.27 An evaluation of an AnchorQuery-based virtual screen	72
Figure 3.1 Ugi4C5Cr Xray.	84
Figure 3.2 Structure of pyrrolidinedione product 3.2-2A in solid state.....	111
Figure 3.3 Structure of Pictet-Spengler cyclization product 3.2-3R in solid state.	114
Figure 3.4 Distribution of rotatable bonds of 1000 randomly generated compounds of all four scaffold classes.....	120
Figure 3.5 Principal Moment of Inertia (PMI).....	121
Figure 4.1 Pharmacophore-based virtual screening platform ANCHOR.QUERY	156
Figure 4.2 Crystallographic structure of 4.3-1 in complex with MDM2.....	182
Figure 4.3 Compound 4.3-1 showing two molecules binding to MDM2.....	183
Figure 4.4 Crystallographic structure of 4.3-2 in complex with MDM2.....	184

LIST OF SCHEMES

Scheme 1-1 Hoffmann la Roche's synthesis of Nutlin-3.....	12
Scheme 1-2 Enantioselective synthesis of Hoffmann-La Roche's Nutlin.....	13
Scheme 1-3 2 step synthesis of Johnson and Johnson's Benzodiazepines.	15
Scheme 1-4 Enantioselective synthesis of J&J' s BDZ scaffold.	16
Scheme 1-5 Synthesis of Spirooxindole by Wang et al.	19
Scheme 3-1 Classic Ugi-4-Component-5-Centered Reaction	75
Scheme 3-2 Ugi Proposed Intermediate	76
Scheme 3-3 Proposed reaction mechanism of Ugi cyclization to Dioxopyrrolidines	111
Scheme 3-4 Proposed reaction mechanism of Pictet-Spengler reaction for indole derivatives.	113
Scheme 3-5 Proposed reaction mechanism of the Pictet-Spengler isoquinoline derivative formation.....	117
Scheme 4-1 Classic Ugi4C5CR for use in p53/MDM2 inhibitor discovery	159
Scheme 4-2 Modified Ugi4C5CR for use in p53/MDM2 inhibitor discovery	161
Scheme 4-3 Synthesis of saponified Ugi4C5CR derivatives.....	163

PREFACE

I would like to take a moment to acknowledge those people who have contributed to my success in completing this dissertation.

First and foremost, I would like to express my gratitude to my research advisor and mentor, Professor Alexander Doemling, who has given me the opportunity to grow into an independent scientist. He has taught me more than I could have hoped for and I am truly grateful for the opportunity to work with him over these past few years. None of this work would have been possible without his support and guidance. I would also like to thank all my colleagues in the lab at the University of Pittsburgh (Dr. Mantosh Sinha, Dr. Yijun Huang, Dr. Wei Wang, Dr. Kan Wang, Dr. Barbara Beck, Dr. Haixia Liu, Dr. Haiping Cao, Dr. Tadamichi Nagashima), as well as my undergraduate students (Samantha Jones, Maura Williams, Nan Wang, James Gaugler, Yeong Han, Dabin Kim) and my colleagues from the University of Groningen for allowing me the opportunity to work with them while abroad.

This work would not have been possible without the contributions from some excellent collaborators. First and foremost I would like to thank Dr Carlos Camacho and Dr David Koes Meireles in Department of Computational and Systems Biology without whom ANCHOR.QUERY would not be possible. I would like to thank Dr. Holak and his research group in Max Planck Institute of Biochemistry, Germany. and Jagiellonian University for

running our p53 screens and co-crystallization studies. I wish to thank Dr Barbara Beck at the Helmholtz Zentrum Muenchen for running our p53 cell based assays.

I owe special thanks to Dr. Gold, Dr. Xie, Dr Li, and Dr. Camacho for the commitment on my doctoral committee. I really appreciate their input and invaluable advice for my training and education. In addition, I would like to thank the administration team at the PhD program in Department of Pharmaceutical Sciences, especially Dr. Folan and Dr. Smith. I am also very grateful to the faculty, staff, postdocs, and graduate students in School of Pharmacy and Drug Discovery Institute, and the entire 10th floor of the BST3.

Last, but certainly not least, I could not have made it through graduate school without the love and support of my family and friends. I would not be where I am today without them.

1.0 INTRODUCTION

1.1 PROTEIN-PROTEIN INTERACTIONS AS DRUG TARGETS

Protein-protein interactions (PPIs) are a rather new, large, but challenging subgroup of drug targets. Classical drug targets offer intragroup commonalities, such as enzymes and their specific reaction mechanisms, and thus have been highly successful starting points for the design of inhibitors and subsequently drugs. Kinase inhibitors in most of the cases were derived from mimicking the essential ATP substrate needed to phosphorylate their targets. Thus, the core chemotype is predefined by flat (hetero)aromatic rings with suitable adjacent hydrogen bond donor and acceptor functions to mimic the corresponding ATP adenine ring system and its interaction with the kinase. PPIs, however, are very diverse in form, shape and function, and currently there is no generally used classification system. Although PPIs can be classified according to protein architectures, lifetime of interaction, affinity, and function, none of these classification schemes has been extensively leveraged for drug design and discovery.^{7,8}

PPI interfaces are often large and hydrophobic, and their non-polar surface areas are buried.⁹ The interfaces typically have areas of 1,200-2,000 Å², with some larger ones up to 4,600 Å², and some as small as 600 Å².¹⁰⁻¹² Hydrophobicity and van der Waals energies are the leading forces of PPIs. Large energies result from the combination of two hydrophobic surfaces in an aqueous environment. The energy components that need to be taken into account are desolvation,

van der Waals interactions, entropy reduction and electrostatic forces.¹³ Electrostatic complementarity increases the energy of a typical PPI and the polar amino acids are often found at the rim of PPIs. They surround the center of the PPI and shelter it from the solvent, thereby representing an O-ring.¹⁴ The dynamics of the formation of PPIs has also been investigated and several models have been proposed.¹⁵ One such model is the “anchor model”, in which specific anchor side chains are found in conformations similar to those observed in the bound complex. Once the anchors are docked, an induced fit process further contributes to forming the final high-affinity complex. The on and off kinetics of PPIs are of high importance for small molecules to compete with the interaction.

PPIs are an emerging class of drug targets in terms of importance and certainly in terms of numbers while the number of classical targets, e.g., proteases or channels, is rather limited.. For instance, the number of proteases in the human genome is only ~600, thus even assuming that each protease contains a druggable allosteric site this would not significantly increase the total number of drug targets. Similarly, this applies to other classical targets including kinases, phosphatases, nuclear receptors, channels, etc. The number of PPIs, however, is estimated to be several hundred thousand and thus exceeds classical targets by several orders of magnitude.¹⁶ For example, the number of PPIs with structural characterization and Ångstrom resolution exceed 35,000 entries in the protein data bank (PDB) and this number is growing exponentially.^{17,8} PPIs are involved in all basic and disease-related biochemical events and thus are meaningful drug targets, which has been recently recognized now that more PPI targets are being pursued. The first success stories have moved into clinical trials and to the market. Well known examples are the Bcl-2 inhibitor ABT-737, or the oxytocin agonist GSK221149A, which are all currently

undergoing clinical trials. PPI (ant)agonists that have recently received market approval include eltrombopag, maraviroc and tirofiban.

While the surface area of a PPI is typically very large, it has been suggested that it might not be necessary for a small molecule to cover the entire protein. A subset of the interface usually contributes to the majority of the binding affinity (the "hot spot") and it is these interactions which should be mimicked.^{9,14} Mapping methodologies and computational analysis has helped to shed some light into which targets offer the most appealing hot spots for a small molecule to potentially bind. More and new efforts are needed early on in the drug discovery pipeline to continue to advance the drugability of PPIs as they continue to emerge as potential therapeutic targets.

1.2 THE P53/MDM2 AXIS¹⁸

p53 was discovered thirty years ago as the oncoprotein of a simian virus 40 large T-antigen.¹⁹ The first decade of p53 research focused on the cloning of p53 DNA; shortly after, however, it was realized that p53 is a tumor suppressor protein that is frequently mutated in human cancers^{20,21}. p53 was then uncovered as a transcription factor induced by stress, which can promote cell cycle arrest, apoptosis and senescence.^{22,23} In 1992 MDM2 was shown to bind tightly to p53 and inhibit its biological activity.²⁴ MDM2 has emerged as the key regulator of p53, and has been termed the "gatekeeper" of p53.²⁵ Currently many pharmaceutical companies and academic institutions are focusing on ways to enhance p53 activity in tumor cells in hopes of developing a novel, more effective and better tolerated form of cancer treatment.²⁶

Currently there are approximately 22 million people living with tumors that contain either an inactivating mutation of *TP53* (the human gene that encodes p53) or have tumors in which the activity of p53 is partially negated through the inactivation of other signaling or effector components.²⁷ Attention was recently drawn to a very aggressive brain tumor (*Glioblastoma multiforme*) when Sen. Ted Kennedy died from it only 15 months after diagnosis.²⁸ It is well established that many forms of glioblastoma carry cells highly overexpressing the negative regulators of p53, MDM2 and/or MDMX, causing a severe decrease in p53 expression.²⁹ Additionally, recent evidence suggests that the combined use of MDM2 and MDMX antagonists could activate p53 more effectively than MDM2 antagonists alone.³⁰

1.2.1 p53/MDM2 Biology

p53 is termed a tumor suppressor gene because its activity can stop the formation of tumors (**Figure 1.1**). It belongs to a small family of related proteins that includes only two other members (p67 and p73), however of the three, p53 is the main one utilized by the cell to prevent tumor growth. p53 plays an essential role in guarding cells in response to various stressors, such as hypoxia or DNA damage, by inducing cell cycle arrest, repair, or apoptosis. It is specifically involved in the effects of survival of proteins in the mitochondria, regulating microRNA processing, DNA repair, and protein translation (to name a few). p53 prevents damaged cells from multiplying and passing mutated genes to the next generation; impairment allows for these processes to go unregulated.³¹ In fact, p53 deficient mice develop normally but are prone to spontaneous tumor generation.³² Therefore, cells that lack p53 have the potential to pass mutations on to the next generation that can facilitate tumor growth. p53 is a potent growth

suppressive and proapoptotic protein that would harm normal proliferating cells if left uncontrolled.

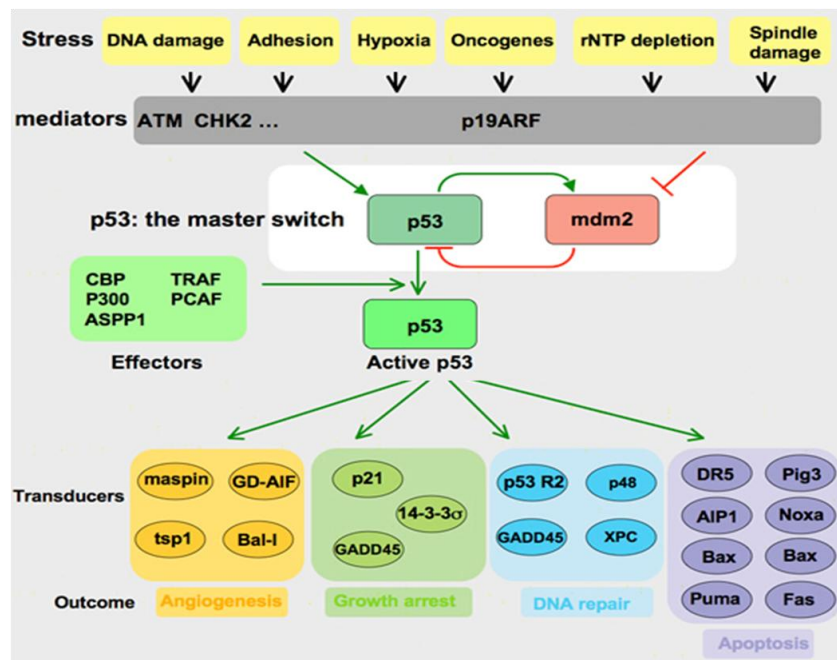


Figure 1.1 p53/MDM2 pathway Regulation of p53 by MDM2 showing the stress signals that activate the pathway, mediators that detect the signals, and downstream transcriptional activators affected by the pathway and their outcomes (Figure courtesy of Thierry Soussi, PhD http://p53.free.fr/p53_info/p53_Pathways.html)

The level of p53 protein in a cell is low and its concentration and activity are subject to tight control both under normal physiological conditions and during stress. The activity of p53 in a cell is regulated at the level of protein degradation, not at the level of expression of the p53 gene. In an unstressed cell, this is accomplished by MDM2-mediated degradation via the ubiquitin-proteasome pathway (regulation of p53 stability), and by inactivation of the p53 transcriptional activity primarily due to the MDMX-mediated occlusion of the p53 transactivation domain (inhibition of p53 activity). In addition, MDM2 and MDMX modify the activity of p53 by transporting p53 into cytoplasm, away from nuclear DNA. Thus the activity of p53 as a transcription factor is out of reach. After stress, MDM2 degrades itself and MDMX, leading to the accumulation and activation of p53; thus a transcriptional response of p53 is

mounting. MDM2 and MDMX are one of the p53 target genes, and increased nuclear levels of p53 activate MDM2/X gene transcription, leading to elevated levels of MDM2 and MDMX. As activated p53 transactivates MDM2, the increasingly abundant MDM2 degrades MDMX more efficiently, enabling full p53 activation: the transcriptional stress response is at its peak. Following stress relief, the accumulated MDM2 preferentially targets p53 again; p53 levels decrease, and MDMX levels increase, p53 activity also decreases. Small amounts of p53 will reduce the amount of MDM2 protein and this will result in an increase of p53 activity, thus completing the loop. The switch that makes MDM2 preferentially target p53 for degradation in unstressed cells, then target itself and MDMX after stress relief, is not precisely understood.^{33,34}

In cases where the cancer is not due to a mutation of p53 but due to an overexpression of a suppressor protein, such as MDM2/X, it is in principle possible to inhibit this interaction by a small molecule and release active p53 to the cell. In fact more than 50% of tumors show an overexpression and/or amplification of MDM2 and its gene. MDM2 is a special example of a protein that regulates p53 through an auto-regulatory feedback loop, in which p53 also regulates MDM2. p53 transcriptionally activates MDM2, and MDM2 in turn inhibits p53 in several ways.³⁵ MDM2 is an E3 ubiquitin ligase that either targets p53 for ubiquitin dependent degradation or inhibits p53 by modulating its activity and preventing interactions with other proteins.²⁴ Other than MDM2, MDMX also plays an important role in regulation of p53; however, it is much less well-characterized (MDMX is also known as MDM4, and human versions as HDMX, and HDMX). MDMX is structurally homologous to MDM2 with a high degree of sequence homology and structural similarity (**Figure 1.2**). MDMX can either act alone or form a heterocomplex with MDM2 and enhance ubiquitination of p53.^{25,36,37} There has been

extensive validation of MDM2 as a target showing that small reductions in MDM2 are significant enough to increase p53 activity.²⁵

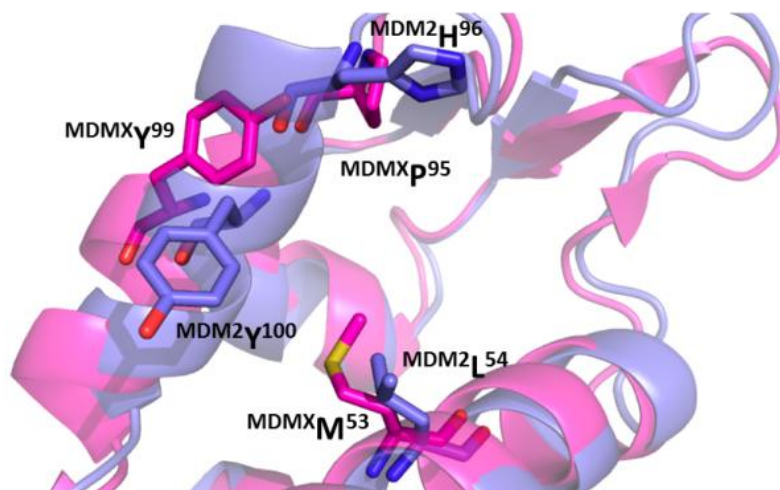


Figure 1.2 MDM2/MDMX alignment Alignment of the p53 receptors MDM2 (blue, PDB-ID 1YCR) and MDMX (pink, PDB-ID 3DAB). The changes in amino acids L54M and H96P, as well as a rotation of Y101 create a distinct sub binding pocket of MDMX and can help to explain the differences in binding of small molecule to MDM2 and not MDMX.

Activated p53 does not necessarily induce apoptosis in normal cells. It has been shown that tumor cells show a greater propensity to die in response to p53 than normal cells. The abnormal proliferation, loss of normal cell environment and stress on a tumor cell can lead to enhanced sensitivity to induce apoptosis in cancer cells.³¹ Therefore, there is great hope that specific p53/MDM2 inhibitors will act selectively on cancer cells. In certain animal experiments, however, a side effect of previous p53/MDM2 inhibitors was death of thymocytes and gut epithelium cells.³¹ Hence, there is a need for safer agents in the p53/MDM2 axis.

1.2.2 p53/MDM2 interactions

The p53/MDM2 interaction is defined as a protein-protein interaction (PPI). PPIs prove to be a difficult case for drug discovery in that the interface between two proteins is generally large (between 1,200 and 4,600 Å²) and involve contacts from as many as 30 side chains from each protein.³⁸ In typical drug discovery cases, smaller molecules are preferred (to enhance absorption, distribution, metabolism, and excretion (ADME) characteristics) but do not easily inhibit such a large area (**Figure 1.3**). It has been shown, however, that though two proteins make many contacts with each other there is often a small pocket of a few amino acids that make up for the majority of the binding energy. This pocket has been termed a “hot spot” and can be used to target small molecule inhibition of PPIs.³⁹

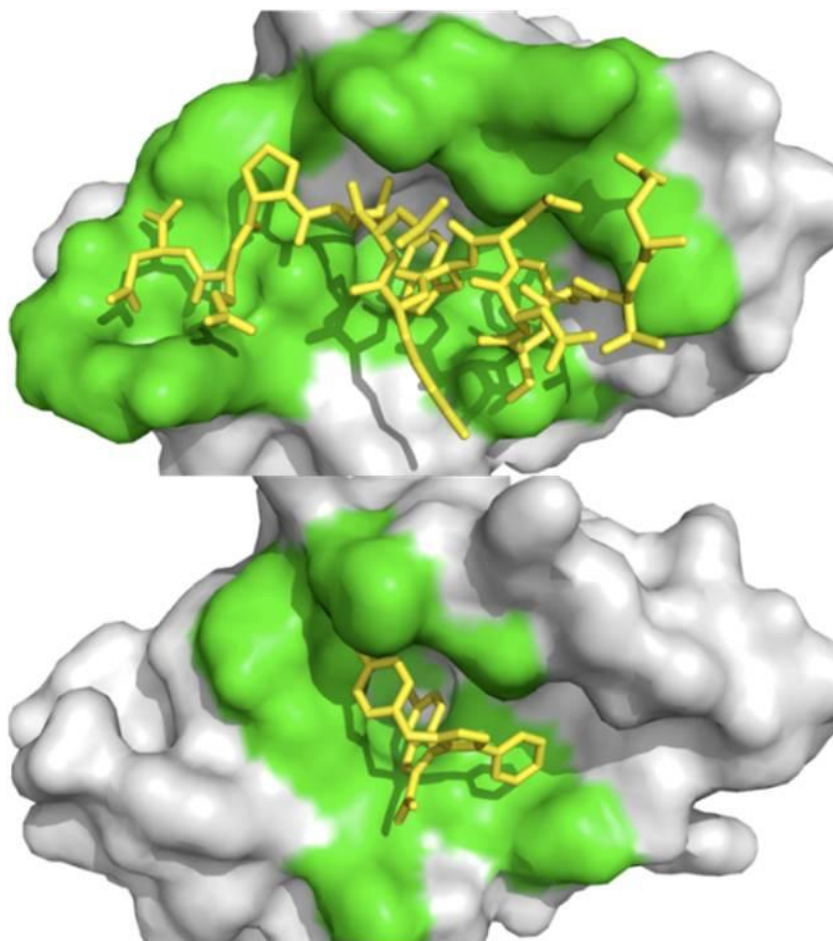


Figure 1.3 PPI contact surface Receptor contact surface covered by the native p53 peptide and a corresponding small molecule antagonist. The target protein (MDM2) is represented as a grey solid surface, and peptide binder p53 is shown as yellow sticks (PDB-ID 1YCR). The contact surface on the target protein with the peptide and small molecule binder is shown in green. The small molecule (PDB-ID 3LBK) shows much less interaction to MDM2. Contact surface was defined as an amino acid within 4Å of the peptide or small molecule.

The 3D structures of MDM2 and MDMX with and without p53 derived peptides and small molecules are extensively elaborated in more than 20 high resolution X-ray and NMR studies. In a seminal work in 1996, Pavletich's group described the first crystal structure of the interaction of p53/MDM2.⁴⁰ MDM2 has a deep and rigid binding pocket for p53 (**Figure 1.4**). The binding pocket measures only 18 Å² along the long edge, the size of a typical small molecule.⁴⁰ The p53/MDM2 complex has a "hot spot triad" made up of p53's Trp23, Leu26, and

Phe19, present analogously in the p53/MDMX complex. The three hydrophobic amino acids fit into three shape and electrostatic complementary hydrophobic pockets, and the indole nitrogen of p53's Trp23 forms a hydrogen bond with Leu54 of MDM2 (Met53 in MDMX). In fact much of the binding energy resides in these three amino acids.

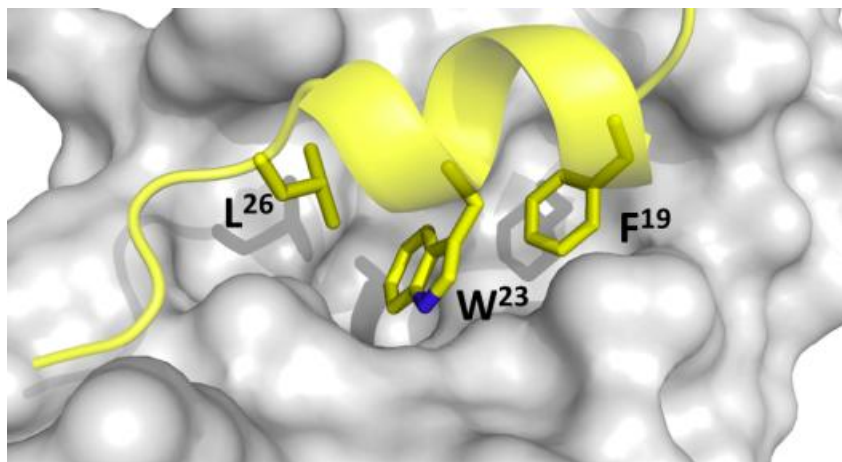


Figure 1.4 p53/MDM2 "hot spot" MDM2 (grey surface) and the key three amino acids (Leu26, Phe19, and Trp23, yellow sticks) mounted on a small amphipathic p53 derived α -helix (PDB-ID: 1YCR).

Alanine scan studies show that mutation of any of the three hot-spot amino acids destroys the affinity between p53 and MDM2.⁴¹ A prerequisite for high affinity MDM2 antagonists is therefore that certain moieties of the molecule must mimic the three amino acids of p53's hot spot triad: Trp23, Leu26, and Phe19. An illustrative model termed "three finger pharmacophore" has been created to describe this configuration.⁴²

1.2.3 Small molecule-MDM2 co-crystals

The first reported small molecule p53/MDM2 antagonist with *in vivo* activity is a class of cis-imidazoline compounds termed nutlins. The nutlins showed IC_{50} s in the low nanomolar range (18 nM) as determined by surface plasmon resonance. The crystal structure shows the nutlin-2

binding to MDM2 in the p53 pocket in a way that mimics the three essential amino acids Trp23, Leu26, and Phe19 (**Figure 1.5**). The bromophenyl moieties in positions 4 and 5 bind deeply into the Leu26 and Trp23 pockets, respectively. The isopropoxyloxy phenyl moiety of nutlin-2 mimics p53's Phe19. Additionally, the 4-methoxy function of nutlin-2 to a certain degree mimics p53's Leu22. HPLC.⁴³⁻⁴⁵

Roche's original synthesis of the Nutlin class of compound required an 8 step synthesis followed by chiral column separation (**Scheme 1-1**). Bromination of 3-Methoxyphenol (**1.2-1**) is followed by alkylation to give 1-bromo-2-isopropoxy-4-methoxybenzene (**1.2-3**). **1.2-3** then underwent palladium catalyzed cyanation and treatment of the cyanide with hydrogen chloride in ethanol gave the imidate (**1.2-4**). The imidate was coupled with *meso*-(4-chlorophenyl)ethane-1,2-diamine (**1.2-5**) to give the imidazoline intermediate (**1.2-6**). Treatment of the imidazoline with phosgene and reaction of the resulting carbamoyl chloride with piperazine afforded Nutlin-3 (**1.2-7**). The compound must then be separated on a chiral column to separate the enantiomers.⁴⁶

Recently Johnston and Davis from Vanderbilt University reported a novel enantioselective synthesis of (-)-Nutlin-3 in only six steps (Scheme 2). Johnston and Davis describe the first highly diastereo- and enantioselective addition of aryl nitromethane pronucleophiles (**1.2-8**) to aryl aldimines (**1.2-9**) using an electron rich chiral Bis(Amidine) catalyst (**1.2-10**) leading to the protected cis-stilbene (**1.2-11**). Boc-protected amide (**1.2-13**) was afforded via reduction of the nitro to amine using cobalt boride formed in situ and subsequent acylation with acid (**1.2-12**). Deprotection of the Boc group using trifluoroacetic acid was followed by acylation of the amine with carbonyl diimidazole forming an isocyanate intermediate. This intermediate was treated with piperazinone. Cyclizative dehydration to the desired enantiomerically pure imidazoline, Nutlin-3 (**1.2-14**), was done via phosphonium

anhydride formed by the combination of triphenylphosphine oxide and triflic anhydride. This synthesis removes Roche's reliance on preparatory chromatography using a chiral stationary phase and substitutes it with a readily chiral catalyst.⁴⁷

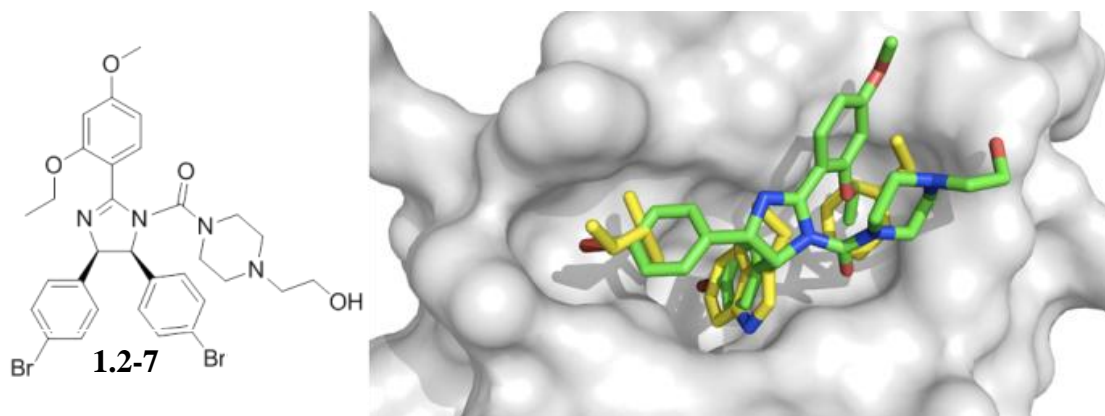
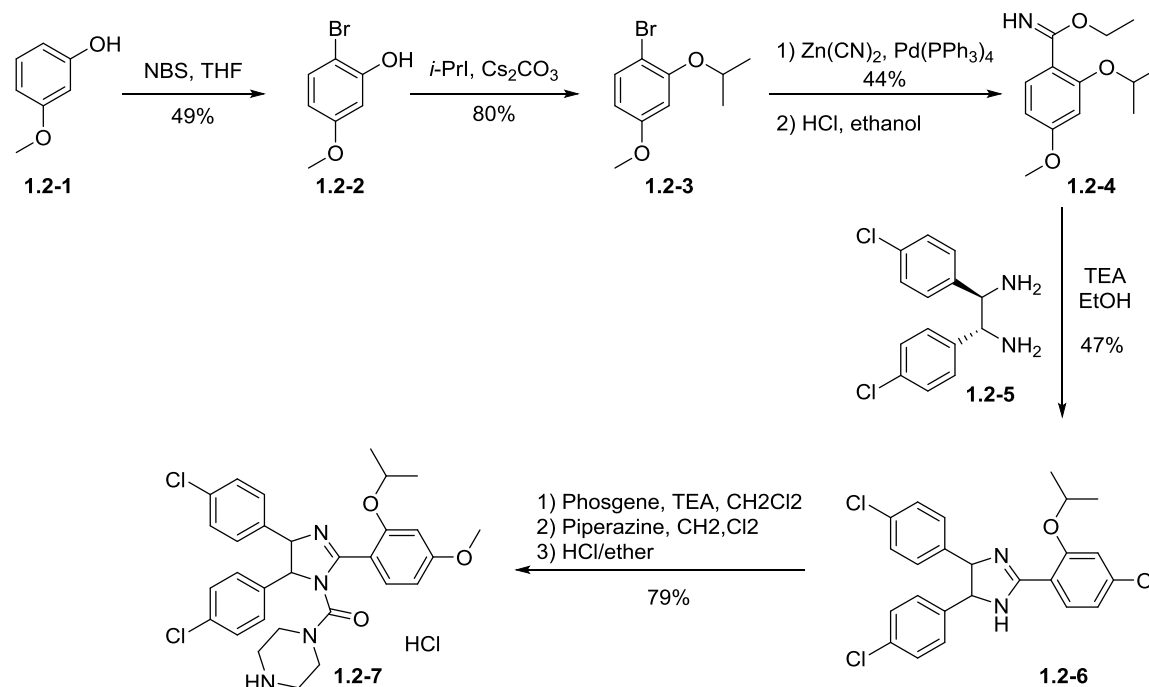


Figure 1.5 MDM2/nutlin Co-crystal structure of Hoffmann La-Roche's nutlin-2 (1.2-1) (green sticks), (PDB-ID: 1RV1) and MDM2 (grey surface) superimposed on the key amino acid side chain residues of the p53/MDM2 structure (yellow sticks, PDB-ID: 1YCR).



Scheme 1-1 Hoffmann la Roche's synthesis of Nutlin-3

properties. This benzodiazepine scaffold has been shown to be efficacious in animal models and acts in synergy with doxorubicin.^{49,50}

The BDPs were synthesized in two steps (**Scheme 1-3**), the first of which was the highly efficient Ugi 4 component reaction. Equal parts of aldehyde (**1.2-16**), amine (**1.2-17**), anthranilic acid (**1.2-18**), and 1-isocyanidecyclohexene (**1.2-19**) were combined in methanol to produce the Ugi product (**1.2-20**). This step was followed by acid-catalyzed cyclization to afford the desired BDP (**1.2-21**) (Yields not disclosed). Given that this class of promising compounds contained two stereocenters and that the different diastereomers were seen to have drastically different inhibitory activities, J&J set it upon themselves to obtain enantiomerically pure BDPs (**Scheme 1-4**). The synthetic strategy consisted of the preparation and selective crystallization of the diastereomeric camphanic esters. Compound **1.2-22** was treated with methyl lithium to give the corresponding racemic alcohol **1.2-23**, which was treated with camphanic chloride, followed by selective recrystallization to give **1.2-25**. **1.2-25** was then transformed to the corresponding amine **1.2-28** via hydrolysis (**1.2-26**), followed by the Mitsunobu reaction with phthalimide (to give **1.2-27**), and finally deprotection with hydrazine. This amine (**1.2-28**) is then ready for use in the Ugi reaction followed by cyclization as described above. The reaction gives a mix of the two different diastereomers (**1.2-32** and **1.2-33**) which are separated via column chromatography. The separated diastereomers (**1.2-32**) then undergoes alkylation followed by reduction of the nitro group to give the corresponding MDM2 antagonist (**1.2-34**); X-ray structure confirmed stereochemistry.⁵¹

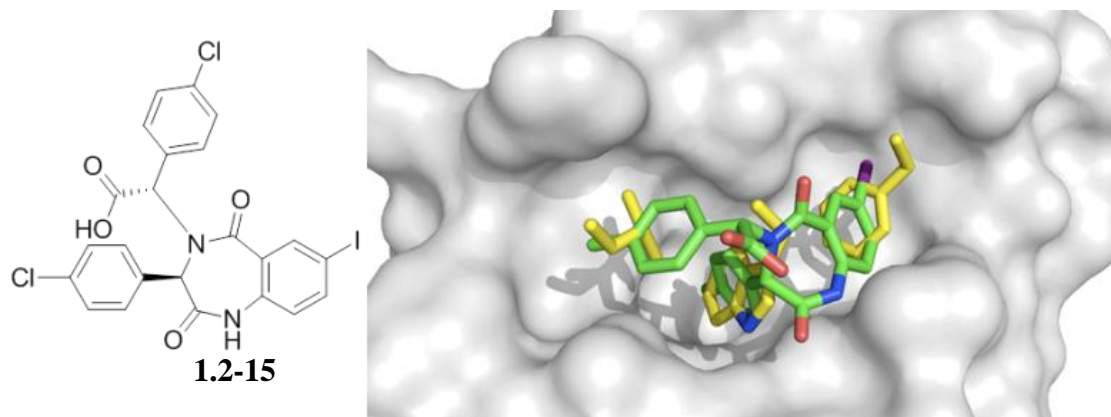
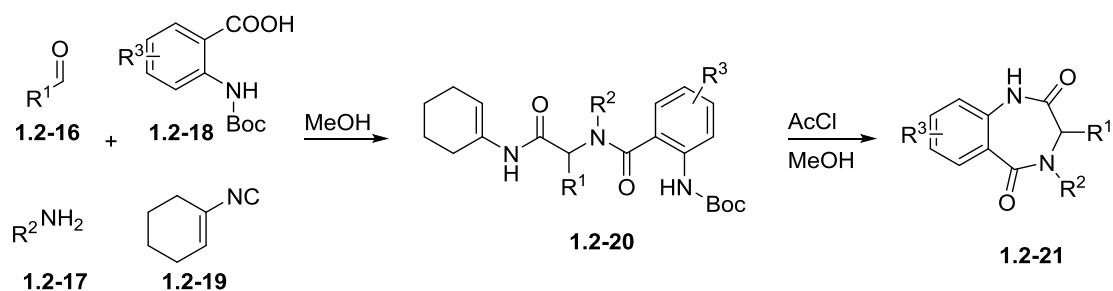
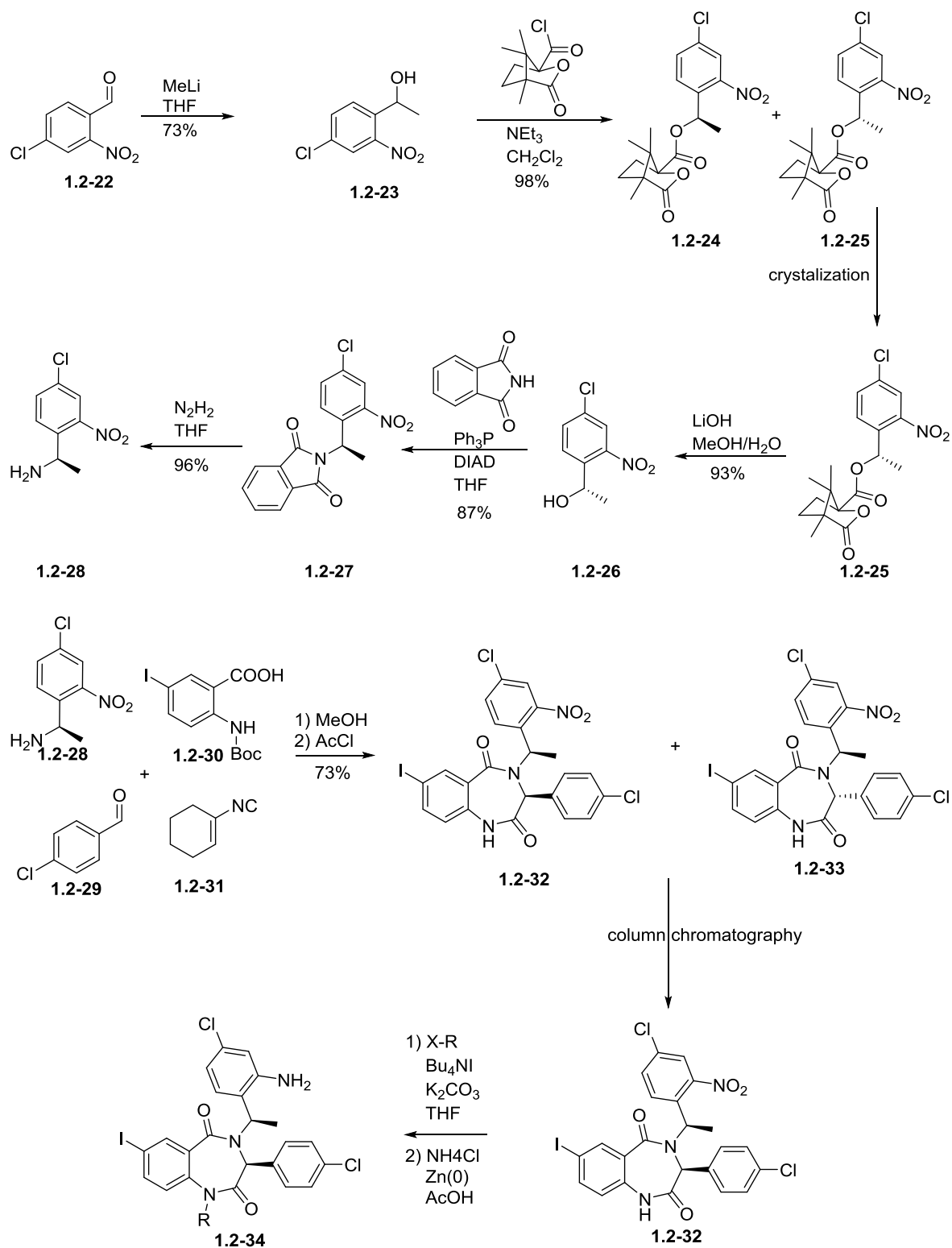


Figure 1.6 MDM2/benzodiazepine Co-crystal structure of Johnson & Johnson's benzodiazepine small molecule 1.2-2 (green sticks, PDB ID: 1T4E) and MDM2 (grey surface) superimposed on the key amino acid side chain residues of the p53/MDM2 structure (yellow sticks, PDB ID: 1YCR).



Scheme 1-3 2 step synthesis of Johnson and Johnson's Benzodiazepines.



Scheme 1-4 Enantioselective synthesis of J&J's BDZ scaffold.

A spiroindolone compound **1.2-35** was discovered by Wang et al. (2006) and is currently the most potent p53/MDM2 inhibitor scaffold published with a K_i of 3nM derived from fluorescence polarization.⁵² In addition, it has good cell based activity showing inhibition of cell growth in cancer cells with wild-type p53, excellent specificity in cancer cells with p53 knock-out and shows minimal toxicity in normal cells.⁵³ Structural analysis of the crystal structure demonstrates the oxindole group occupying the Trp26 pocket and also forming a hydrogen bond to MDM2's Leu54, much like p53's Trp26 (**Figure 1.7**).⁵⁴ This scaffold can be easily modified via an amidation step to allow for additional compounds with very potent inhibitor activity and good water solubility. The morpholino ethyl side chain does not show electron density but can be placed over the Leu22 of p53 based on the carbonyl His96 hydrogen bond interaction. Though this compound showed great affinity for MDM2, it had reduced cell permeability. A compound of the same class with a non-basic solubilizing side chain has recently been reported.⁵³ This compound inhibits p53/MDM2, activates the p53 pathway in cells with wild type p53 and leads to cell cycle arrest in all cells and selective apoptosis in tumour cells. It has been shown to be active in cancerous animal tissue, resulting in inhibition of cell reproduction, induction of apoptosis and complete tumour growth inhibition.⁵⁴

These compounds were synthesized via a multistep synthesis (Scheme 1-5), which yielded in high stereoselectivity. Briefly, oxindoles were condensed with different aromatic halides under basic conditions either in a microwave or under reflux to obtain E-3-aryl-1,3-dihydro-indol-2-ones (**1.2-36**). In order to obtain appropriate stereochemistry (5R,6S)-5,6-diphenylmorpholin-2-one (**1.2-38**) is used as a chiral auxiliary promoting the stereocontrol seen in the final product. This compound was then recrystallized from ethanol where X-ray analysis confirmed the E conformer. Asymmetric 1,3-dipolar cycloaddition was then done by heating the

recrystallized product **1.2-36** with alkyl aldehydes **1.2-37** and (5R,6S)-5,6-diphenylmorpholine **1.2-38** in toluene in the presence of a dehydrating agent. Compound (**1.2-39**) was partially purified by silica gel column and treated with 2M dimethylamine in THF to afford amides X (**1.2-40**) in overall good yield. Analysis of both the intermediate and the final compound by X-ray crystallography revealed absolute configuration of the stereocenters.⁵⁵

Modifications of the spirooxindole scaffold to modulate potency and fine-tune pharmacological properties led to the identification of SAR299155 (**Figure 1-12**). The compound binds to MDM2 with a K_i of 10 nM, and significantly inhibits the proliferation of a broad panel of wild-type p53 tumor cell lines. In acute pharmacokinetic/pharmacodynamics preclinical in vivo studies, the compound triggers a rapid and sustained target engagement when administered orally to tumor bearing mice as demonstrated by monitoring relevant biological read-outs such as p53, p21^{waf1}, HDM2 and PUMA. The pharmacological, biological and preclinical safety profiles of SAR299155 supported its clinical development and a modification of this drug is currently undergoing Phase I clinical trials in cancer patients⁵⁶

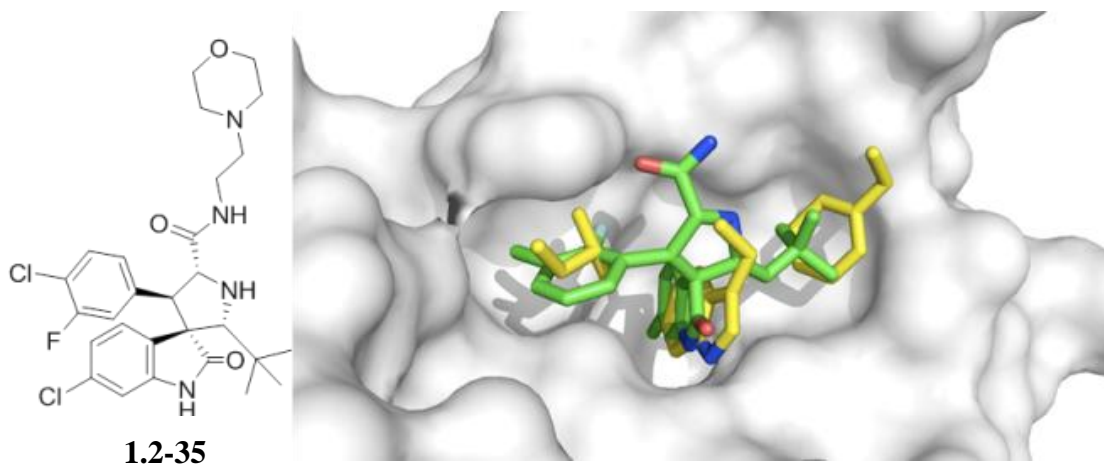
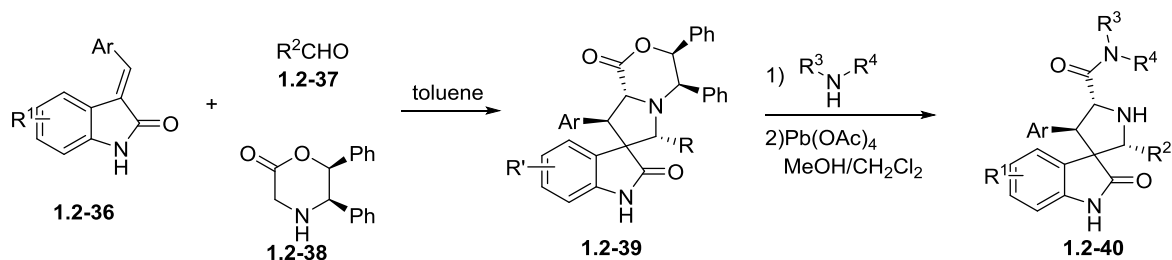


Figure 1.7 MDM2/Spirooxindole Co-crystal structure of a spiroindolone small molecule **1.2-3** (green sticks, PDB-ID: 3LBL) and MDM2 (grey surface) superimposed on the key amino acid side chain residues of the p53/MDM2 structure (yellow sticks, PDB-ID: 1YCR).



Scheme 1-5 Synthesis of Spirooxindole by Wang et al.

A chromenotriazolopyrimidine **1.2-41** was discovered to be a potent inhibitor ($IC_{50} = 1.23 \mu M$) of p53/MDM2 via homogeneous time-resolved fluorescence (HTRF) high-throughput screening by Amgen workers.⁵⁷ Crystal structure analysis shows that the small molecule is able to mimic the key amino acids of p53 (**Figure 1.8**). The two bromophenyl moieties bind to the Leu 26, and Trp23 pockets. The bromophenyl binding to the Leu26 pocket shows a weak π -stacking interaction with the nearby rim His96 imidazole of MDM2. The benzene ring on the backbone of the chromenotriazolopyrimidine binds into the Phe19 pocket. Efforts to optimize this compound included substitution of the two halogens, and additions to the benzene ring bound the Phe19 pocket. Such efforts showed an improvement in binding affinity with substitution of bromine to chlorine in the Trp23 binding site and addition of a methoxy group added to the 4 position of the benzene ring.⁵⁷

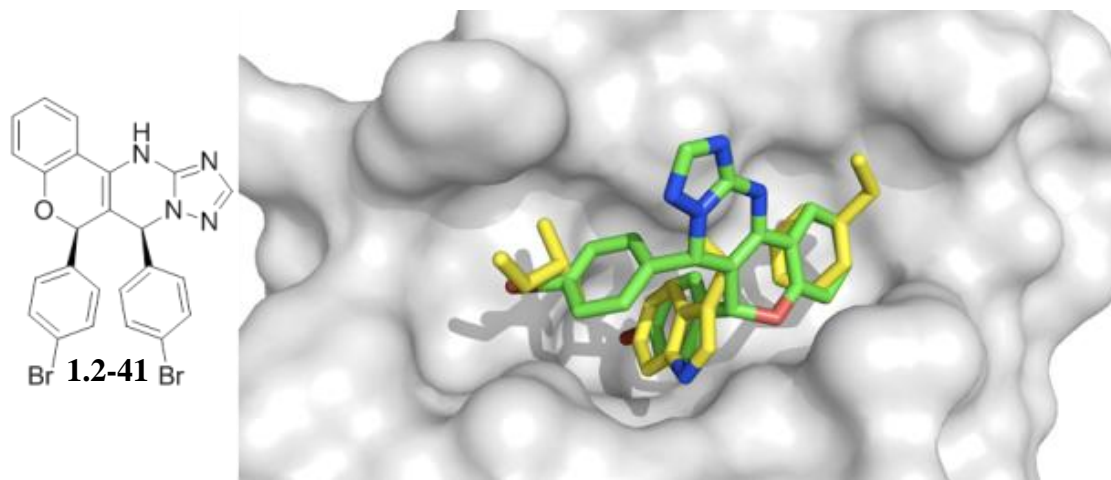


Figure 1.8 MDM2/chromenotriazolopyrimidine Co-crystal structure of Amgen's chromenotriazolopyrimidine small molecule 1.2-4 (green sticks, PDB ID: 3JZK) and MDM2 superimposed on the key amino acid side chain residues of the p53/MDM2 structure (yellow sticks, PDB ID: 1YCR).

A recent crystal structure of **1.2-42** based on a threefold substituted imidazole scaffold (**Figure 1.9**) discovered independently and at the same time by NOVARTIS and Dömling et al. from University of Pittsburgh adds to the p53/MDM2 structures.⁵⁴ This one step, multicomponent reaction product shows good activity in fluorescence polarization (900 nM). The structure shows the indole of the small molecule mimicking the Trp26 pocket of p53, and a para-chlorobenzyl group mimicking the Leu22 of p53, and a para-fluorophenyl group mimicking the Phe19 of p53. The alignment of the indole group of the small molecule and the indole moiety of the Trp23 is perfect. The ligand indole-NH forms a hydrogen bond (2.73 Å) to the backbone carbonyl of Leu54. The 6-chloro group in the indole resides in a hydrophobic pocket, which is not filled in the p53-MDM2 complex, brings additional hydrophobic interactions. The carboxyl group in 2 position of the indol forms two bridged hydrogen bond to two crystallographic water of distances 2.57 Å and 3.35 Å.⁵⁴

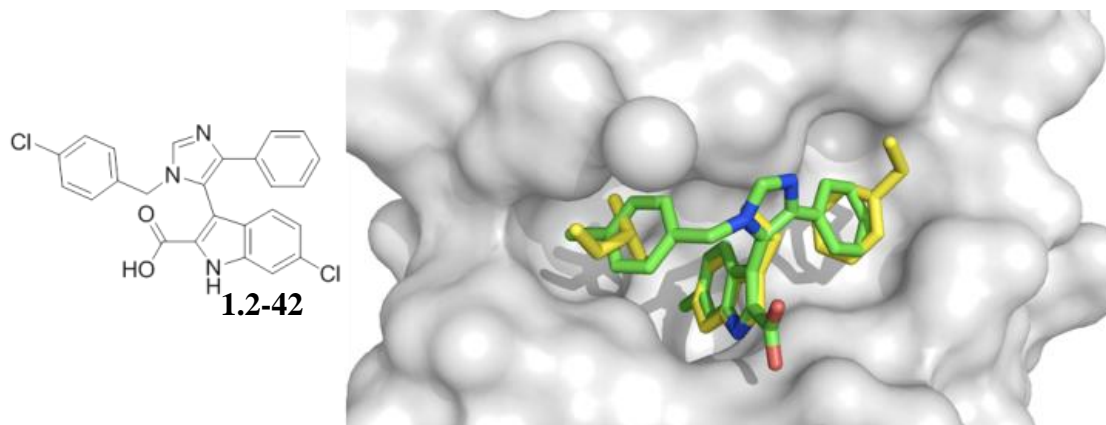


Figure 1.9 MDM2/imidazole Co-crystal structure of Dömling et al's imidazole small molecule 1.2-5 (green sticks, PDB ID: 3LBK) and MDM2 superimposed on the key amino acid side chain residues of the p53/MDM2 structure (yellow sticks, PDB ID: 1YCR).

1.2.4 MDMX-co crystal

Much less structural biology information is available for MDMX. Only one small molecule has been co-crystallized to date. Alignment of crystal structures of both MDM2 and MDMX can potentially draw pathways to selectively inhibit one or the other, or create a dual acting small molecule inhibitor for both proteins. Crystal structures reveal (**Figure 1.10**) that although principal features of the p53/MDM2 interaction are still present in p53/MDMX, the MDMX has a significantly altered hydrophobic cleft on which p53 binds compared to MDM2. MDMX's Met53 and Tyr99 protrude into the pocket causing a smaller and differently shaped, shallower binding pocket. Though the Met54 side chain of MDMX is in the same position as MDM2's Leu54, the bulkiness of methionine compared to leucine creates a smaller binding cleft. A shift of MDMX's helix $\alpha 2$ causes a conformational change, which contributes significantly to the alterations in the p53 binding pocket of MDMX. The conformation of MDMX's Tyr99 is altered

compared to MDM2's Tyr100. MDM2's Tyr100 is flipped away from the p53 binding pocket compared to MDMX's Tyr99, also contributing to a smaller binding pocket. (**Figure 1.10**)⁵⁸

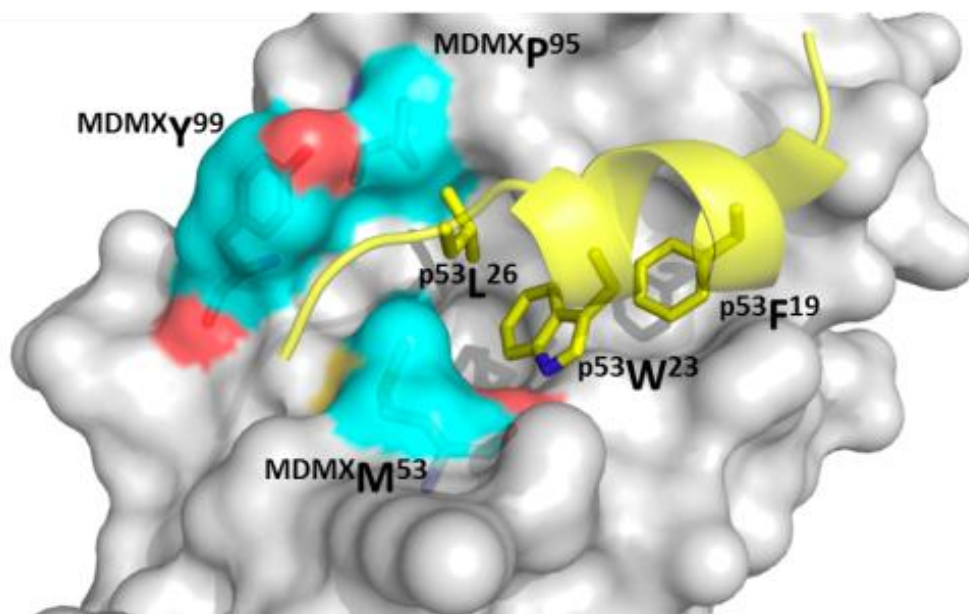


Figure 1.10 p53/MDMX Co crystal structure MDMX with p53 (yellow sticks). Highlighted in blue (surface and sticks) are the three key amino acids that contribute to the major differences in binding site between MDM2 and MDMX (PDB ID: 3DAB).

Popowicz et al. (2010) recently published the first co crystal structure of a small molecule inhibitor **1.2-43** and MDMX (**Figure 1.11**).⁵⁴ This imidazole compound **1.2-43** is similar to compound **1.2-42** binding to MDM2, and binds to MDMX in a way that mimics parts of the binding of p53. The central imidazole scaffold directs the three ligands into the three key sub binding pockets corresponding to ^{p53}Trp23, ^{p53}Phe19 and ^{p53}Leu26. The ^{p53}Trp23 pocket is filled with the 6-chloroindole substituent whose NH forms a hydrogen bond with the carbonyl atom of ^{MDMX}Met53 of 2.64 Å and thus mimics the same molecular interaction as seen with ^{p53}Trp23 and MDMX (2.77 Å). Additionally, the oxygen of the 2-carboxamide forms a solvent exposed hydrogen bond to the MDMX His54 of 3.28 Å. The 6-chloroindole substituent resides very similarly to the corresponding MDM2 structure (**Figure 1.11**) in the deep and hydrophobic

Trp23 pocket of MDMX making extensive hydrophobic contacts to the receptor amino acids Leu98, Phe90, Leu56, Ile60, Gly57, and Val92. The 4-chlorobenzyl ring of the imidazole penetrates the Leu26 pocket and the imidazole's phenyl ring fills the Phe19 pocket; however, the plane of this ring is nearly perpendicular to the plane of p53's Phe19. The carboxamide moiety of the molecule bends over the phenyl group and comprises an additional filling of the large and hydrophobic Phe19 pocket, thus shielding the hydrophobic region of Met61 from solvent. Similar compounds without the dimethylpropylamine side chain show much weaker inhibition of p53/MDMX. The amino acid exchanges from MDM2 to MDMX (L45M and H95P) form a distinct sub binding pocket and can explain the difference in binding of small molecules.⁵⁴

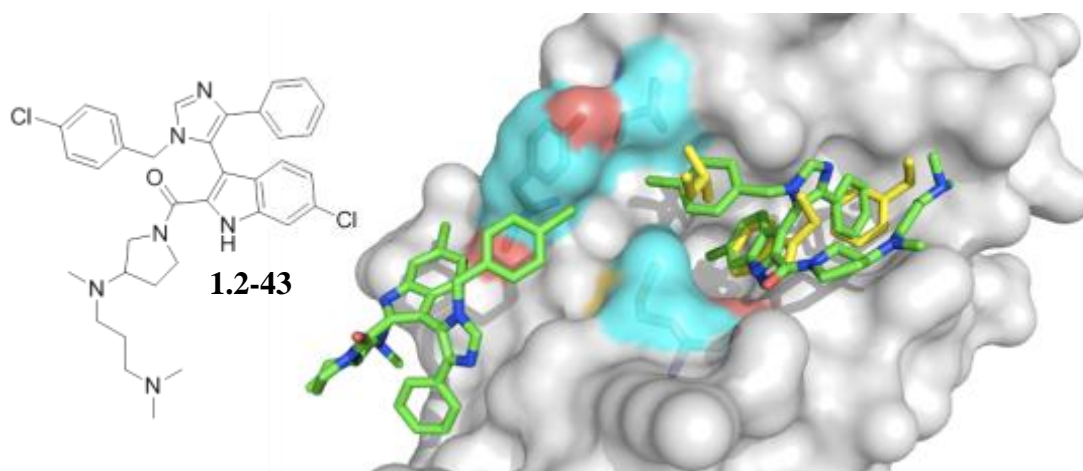


Figure 1.11MDMX/imidazole First co-crystal structure of MDMX (grey surface) with a small molecule inhibitor 1.2-6 (green sticks, PDB ID: 3LBJ) superimposed on the key amino acid side chain residues of the co-crystal of p53/MDMX (PDB ID: 3DAB). It is interesting to note that due to the slight difference in the amino acids of MDM2 and MDMX, MDMX forms an additional second pocket for a second small molecule inhibitor to bind to. This could allow for selectivity of MDMX over MDM2 when designing inhibitors.

1.2.5 Clinical Trials

Currently there are six p53/MDM2 inhibitor small compounds that have undergone or are undergoing phase 1 clinical trials, from Johnson & Johnson and one from Hoffman-La Roche, Sanofi Aventis, Novartis, Merck, and Daiichi Sankyo.

The Johnson & Johnson compound JNJ-26854165 (**Figure 1-12**) started in November of 2006 and was completed in February of 2010 (NCT00676910). Patients with advanced or refractory solid tumors were examined. Although JNJ-26854165 was well tolerated in these patients, no objective responses were observed.^{59,60}

Hoffman-La Roche's compound RG7112 (**Figure 1-12**) is undergoing or has undergone five different trials (NCT01143740, NCT01164033, NCT00559533, NCT00623870, and NCT01605526), for patients with liposarcomas (before debulking surgery), solid tumors, hematologic neoplasms, and soft tissue sarcomas.^{61,62}

Acceptable safety profiles and favorable clinical outcomes including complete remission, induction of apoptosis, and decrease in proliferation were seen in patients treated with RG7112 for leukemias, lymphomas, sarcomas, and other solid tumors. RG7112 has been tested in patients (oral doses ranged between 20 and 1920 mg/m²/day for 10 days followed by 18 days of rest between cycles) with advanced solid tumors (e.g., well-differentiated and dedifferentiated liposarcomas) or hematological malignancies (e.g., acute myelogenous leukemia). Evidence of target engagement at doses >320 mg/m²/day and clinical benefits have been recently reported.⁶³ The p53 transcriptional target and secreted protein, MIC-1 served as a pharmacodynamic marker and increased with increasing drug concentration. This protein is secreted in serum when p53 is activated and the use of its blood level avoids the awkwardness of needing tumor biopsies to demonstrate target modulation in clinical settings.

The most common and significant adverse events reported upon administration of RG7112 to cancer patients have been so far neutropenia and thrombocytopenia, which can be considered on target and intrinsic to the mechanism-of-action for this p53/hdm2 agent. Another p53/hdm2 inhibitor (RG7338, RO5503781) started Phase I clinical trials at the end of 2011, but its structure has not been disclosed yet.^{61,62}

A spirooxindole compound SR405838 derived from compound SAR299155 (**Figure 1-12**) from the university of Michigan has recently been licensed by Sanofi Aventis and is currently undergoing Phase I clinical trials (NCT01985191, NCT01636479). As discussed above derivatives of these compounds showed good pharmacological, biological, and preclinical safety profiles.⁵⁶ No results of the clinical trials have been published as of yet.

Merck introduced p53/MDM2 inhibitor SCH 900242 (MK-8242) into Phase I clinical trials (NCT01463696). CGM097, developed by Novartis, has also progressed into Phase I clinical trials in 2013 (NCT01760525). Very recently, Daiichi Sankyo Inc. has initiated Phase I clinical trial of DS-3032b (NCT01877382). None of these structures has been disclosed.⁶⁴

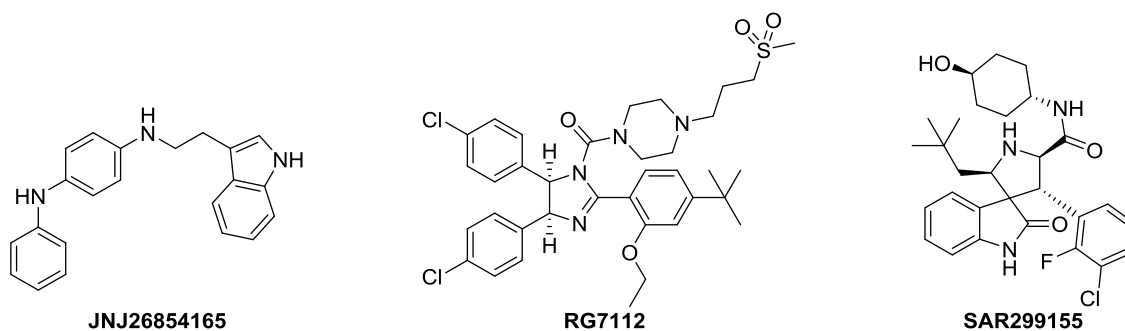


Figure 1.12 Clinical candidates JNJ26854165 from Johnson & Johnson and RG7112 from Hoffman La Roche, and pre-clinical candidate SAR299155 from the University of Michigan which led to clinical trials of SAR405838 currently licensed by Sanofi Aventis

2.0 ANCHORQUERY: AN EASILY ACCESSIBLE VIRTUAL SCREENING LIBRARY/TOOL⁶⁵

Computational screening methods, such as docking and pharmacophore searches, continue to be developed and improved as credible and complementary alternatives to high-throughput biochemical compound screening (HTS). Commercially available compound collections such as ZINC,⁶⁶ E-MOLECULES, or PubChem, are libraries used for traditional computational and high throughput screening. The advantage of using a database of commercially available compounds for virtual screening is the possibility of immediate validation of the virtual hit by acquiring the compound. Disadvantages of screening existing compound libraries are the limited and historically biased chemical space, the usually proprietary chemistry behind these commercial compounds, and the complex multi-step synthesis required for subsequent structure-activity relationship studies. In addition, such compounds will have potential issues with intellectual property as they proceed down the development pipeline. Our *AnchorQuery* technology avoids these disadvantages by screening libraries of completely novel compounds that are *chemically-accessible* (most compounds can be synthesized in less than a week).

Pharmacophore search based virtual screening is an established and effective mechanism for *in silico* drug discovery that has successfully identified novel inhibitors. A pharmacophore describes the structural arrangement of the essential features of an interaction. Common

pharmacophore features include hydrophobic, charged, or hydrogen bond features. With the exception of inverted-key fingerprint screening, which requires a very reduced search space, and Recore,⁶⁷ which is only applicable to a narrow scaffold hopping domain, traditional pharmacophore search technologies must screen every compound and therefore have difficulty scaling to very large databases. In contrast, our *AnchorQuery* specialized pharmacophore search technology is capable of screening a billion compound conformations in just seconds.⁶⁸ The core concept underlying *AnchorQuery* is the exploitation of biophysical, chemical, and computational insights regarding an anchor (deeply buried) side chains readily identified from crystal structures.⁶⁸

The *biophysical insight* of *AnchorQuery* is that chemical analogs of anchor side chains provide an ideal starting point for inhibitor design. Deeply buried anchors may initiate the recognition sequence leading to complex formation. Small molecules that include an anchor can mimic the binding of the target to the pocket, triggering a recognition event that opens up the neighboring pockets. Even when an anchor is not involved in recognition anchors are ideal starting points for the design of inhibitors. Mimicking a bulky, deeply-buried anchor increases the likelihood of sterically inhibiting an interaction. Furthermore, anchors are often hot-spots, so anchor mimics will also energetically inhibit an interaction.⁶⁸ Since in the normal case the anchor is the most buried site, mimicking and incorporating this site into a small molecule assures an energetically good starting point based on hydrophobicity.

Moreover the inclusion of amino acid analogs allows us to bias our libraries to specific “druggable” sites. To leverage this feature, we benefit from the growing structural information on protein-protein interactions exemplified by the Protein Data Bank (PDB), and target validated binding sites revealed by co-crystals of PPIs. The physicochemical characteristics of these

interfaces have so far proven to be very challenging for drug discovery: contact surfaces involved in protein–protein interactions are typically large (1,500–3,000 Å²), flat and full of electrostatic interactions,⁶⁹⁻⁷² and only a few success stories have been reported (e.g., Bcl2,⁷³ (X)IAP,⁷⁴ and p53/MDM2⁷⁵). However, a common element of several of these compounds is specific moieties that mimic the side chains that are found deeply buried in the acceptor protein. These deeply buried anchor side chains have been shown to play a critical role in molecular recognition by targeting relatively stable cavities in their corresponding receptors,^{76,77} providing a strong rationale for targeting these sites.

Our technology targets crystallographically validated anchor cavities by designing analogs of the burying side chain into our libraries. This rationale is highlighted in Figure 2.1, where the binding interface of MDM2 is shown before and after binding p53. Trp23 of p53 occupies a cavity that is an expansion of an existing cavity in the unbound structure. In contrast, two other hydrophobic cavities apparent in the bound structure are blocked in the unbound state, strongly suggesting that not all pockets in a PPI are the same for small molecule intervention. The presence of the anchor cavity in the unbound structure and the emergence of the fully structured p53 binding site upon peptide-ligand binding is further supported by recent molecular dynamics calculations.⁷⁸

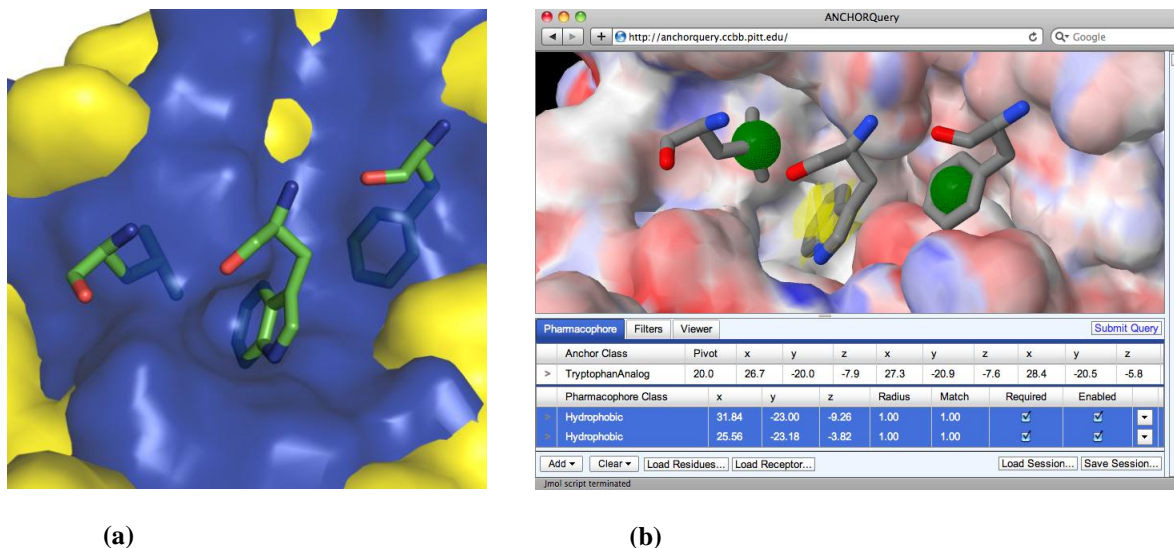


Figure 2.1 The p53/MDM2 protein-protein interaction and open-access *AnchorQuery* web interface. (a) In the p53/MDM2 complex (PDB 1YCR) three residues (F19, W23, L25) of p53 (green sticks) are buried in MDM2 (yellow surface). This binding cavity is not present in the unbound form of MDM2 (PDB 1Z1M), shown as blue surface. Only the W23 pocket retains any definition in the unbound structure, suggesting that W23 may play a major role in molecular recognition and initiating binding. (b) A screenshot of the online *AnchorQuery* software show a query pharmacophore for targeting the p53/MDM2 interface. Two hydrophobic features with a 1 Å radius (green) are extracted from the F19 and L25 amino acids of p53 while a Tryptophan analog pharmacophore feature (yellow), unique to *AnchorQuery*, with a pivot of 20° matches the indole fragment of tryptophan.

The chemical insight of *AnchorQuery* is that by using MCR chemistry we can incorporate a chemical analog of an anchor residue into a large and diverse virtual library of novel, chemically-accessible, compounds while complying with additional pharmacophore points useful for tight binding. These libraries, already biased towards PPIs due to the MCR chemistry, are further focused to target PPIs involving a specific anchor. Properly focused libraries can improve hit rates by more than an order of magnitude relative to randomly created or maximally diverse libraries.^{79,80} The inclusion of an anchor analog focuses our libraries, but it does not prevent the creation of a diverse set of chemotypes. We initially created a prototype tryptophan-biased library of ~600,000 chemical compounds that we successfully used to target

the p53/MDM2 interface. Using lessons learned from this prototype library, we have recently created a larger (700 million conformations of 5.8 million compounds), more diverse (23 reaction scaffolds with intelligent stereoisomeric sampling), and created not only tryptophan-biased virtual library but also leucine, valine, tyrosine, and phenylalanine biased libraries. In addition to well established multicomponent reaction products screened by *AnchorQuery* we are also in search of never before described backbones for use against PPI inhibition.

The computational insight of *AnchorQuery* is that the anchor analog present in every one of our virtual compounds can be used to define a coordinate system. The 3D pharmacophore features of each compound conformation can then be stored in a specially designed spatial index, a data structure that supports the efficient storage and retrieval of data indexed by spatial coordinates. This insight allows us to perform pharmacophore searches more than 100 times faster than current commercial solutions such as MOE⁸¹ or LigandScout.⁸² We only require that every pharmacophore query contain an anchor analog pharmacophore feature that corresponds to the position of the anchor analog in the original PPI crystal structure. The search performance of *AnchorQuery* enables us to search a much larger chemical space than would be practical with off-the-shelf solutions. Additionally, and perhaps more importantly, since most searches typically take less than a minute, *AnchorQuery* enables the integration of expert human insight into the search process through the iterative and interactive refinement of the pharmacophore search.⁶⁸

Due to the high costs of traditional HTS approaches⁸³ and often complex hit optimization chemistry, most academic researchers lack the infrastructure to embark in drug discovery efforts. This is especially true for PPIs whose chemotypes are poorly represented in existing small molecular weight libraries.^{70-72,84-87} To address this problem, we use multi-component reaction

chemistry (MCR)⁸⁸ an efficient “one-step, one pot” class of reactions that yields highly complex, drug-like and screening-ready products. Although not common in existing compound libraries, MCR compounds are well represented among known small-molecule PPI inhibitors.⁸⁹ More importantly, peptido-mimetic MCR chemotypes allow us to design compound libraries that include chemical mimics of key amino acids important for molecular recognition.⁹⁰ For instance, using 23 MCR chemistries and a curated set of starting materials, we have designed libraries of >5 million compounds targeting the amino acids phenylalanine, tyrosine, tryptophan, leucine/valine, and aspartic/glutamic acid, the nucleotides uracil, and adenine, and the cofactor thiamine where every compound contains a chemical analog of the targeted anchor. The diversity analysis of our 16.8 million anchor-biased compounds and the 17.5 million compounds of the ZINC database⁹¹ shown in Figure 2.2 confirms that these MCR compounds encompass an untapped region of chemical space that is a departure from historical targets, such as kinase inhibitors, while highly amenable to PPI targets, such as the p53/MDM2 interaction.

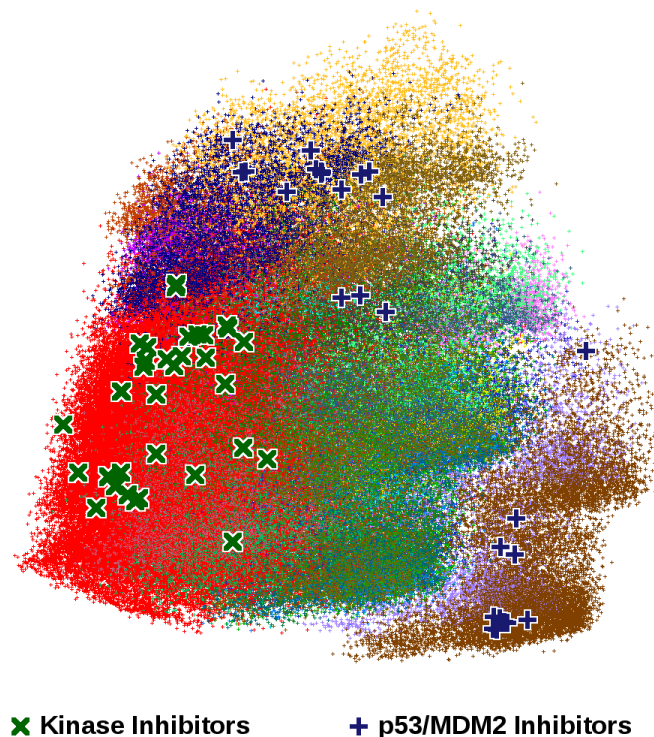


Figure 2.2 A representation of the chemical diversity of our multicomponent reaction-accessible, anchor-biased *AnchorQuery* libraries (different reaction chemistries shown in different colors) relative to the ZINC database (shown in red).⁹¹ The diversity space is visualized by plotting the top two principal components of the OpenBabel FP2 (<http://openbabel.org>) fingerprints of 200,000 compounds randomly selected from the 17.5 million compounds of the entire ZINC database and the 16.8 million compounds comprising the publicly available phenylalanine, tyrosine, and tryptophan biased *AnchorQuery* libraries. The PPI-biased *AnchorQuery* compounds are focused on a different region of chemical space than the historically-biased ZINC database. Indeed, a selection of kinase inhibitors, including inhibitors containing a tryptophan analog, falls squarely in the space covered by ZINC, while a selection of inhibitors of the p53/MDM2 interaction, including inhibitors without a tryptophan analog, are located in the space covered by the *AnchorQuery* libraries.

2.1 COMPOUND SCREENING LIBRARY GENERATION

We created our prototype tryptophan-biased virtual library by selecting indole-containing compounds from a diverse set of 20 multi-component reactions. A total of 54,000 reactions were performed using randomly chosen reactants and ChemAxons REACTOR software (<http://www.chemaxon.com>). OpenEye OMEGA (<http://eyesopen.com/>) was used with the default settings to enumerate 591,227 stereoisomers and generate 97.9 million conformations.

Our ultimate goal was to develop libraries for all meaningful anchor amino acids. Based on our experience with the prototype library, we have currently created larger anchor-oriented libraries for phenylalanine, tyrosine, tryptophan, leucine/valine, aspartic/glutamic acid, uracil, adenine, and thiamine anchors. These libraries are created from an expanded set of 23 MCR chemistries and starting materials that are curated for affordability, diversity, and synthesizability. All scaffolds are either described in detail in publications or have been studied extensively in house. We do not exhaustively enumerate all stereoisomers of compounds, instead only sampling stereoisomers around stereocenters that significantly change the geometry of the resulting conformations. About 100 conformations are generated per molecule with OMEGA with a RMS cutoff of 0.7, resulting in roughly 6×10^8 conformations per AA-based MCR library. The scope and limitation of each scaffold was examined in detail to provide only compounds with a high chance of successful synthesis.

2.1.1 Isocyanide Based MCRs

2.1.1.1 Ugi Reaction

In 1959, Ugi et al. described the most important variants of the four-component condensation, the U-4CRs.⁹² In the first step the oxo-component and a primary amine condense to the imine, the Schiff base, via a hydroxy aminal. The acid component protonates the nitrogen of the Schiff base increasing the electrophilicity of the C=N bond. The electrophilic imine ion and the nucleophilic acid anion add to the isocyanide carbon atom forming the α -adduct. After intramolecular acylation, and subsequent hydroxyimine to amide rearrangement the stable Ugi product is obtained. This reaction has been studied greatly over the years and has been seen to work well with most combinations of aromatic or aliphatic aldehydes/ketones, primary amines, isocyanides, and acids.⁹³

In 1962 Ugi presented an easy access to beta-lactam synthesis using a B-amino acid to act as both an amine and carboxylic acid in the Ugi reaction.⁹⁴ While there may not be a plethora of beta-amino acids commercially available, Weaver et al.⁹⁵ described a convenient MCR method to synthesize substituted beta-amino acids from aromatic aldehydes, malonic acid, and ammonium acetate in ethanol thereby increasing the potential for substitution of Ugi's beta-lactam synthesis.

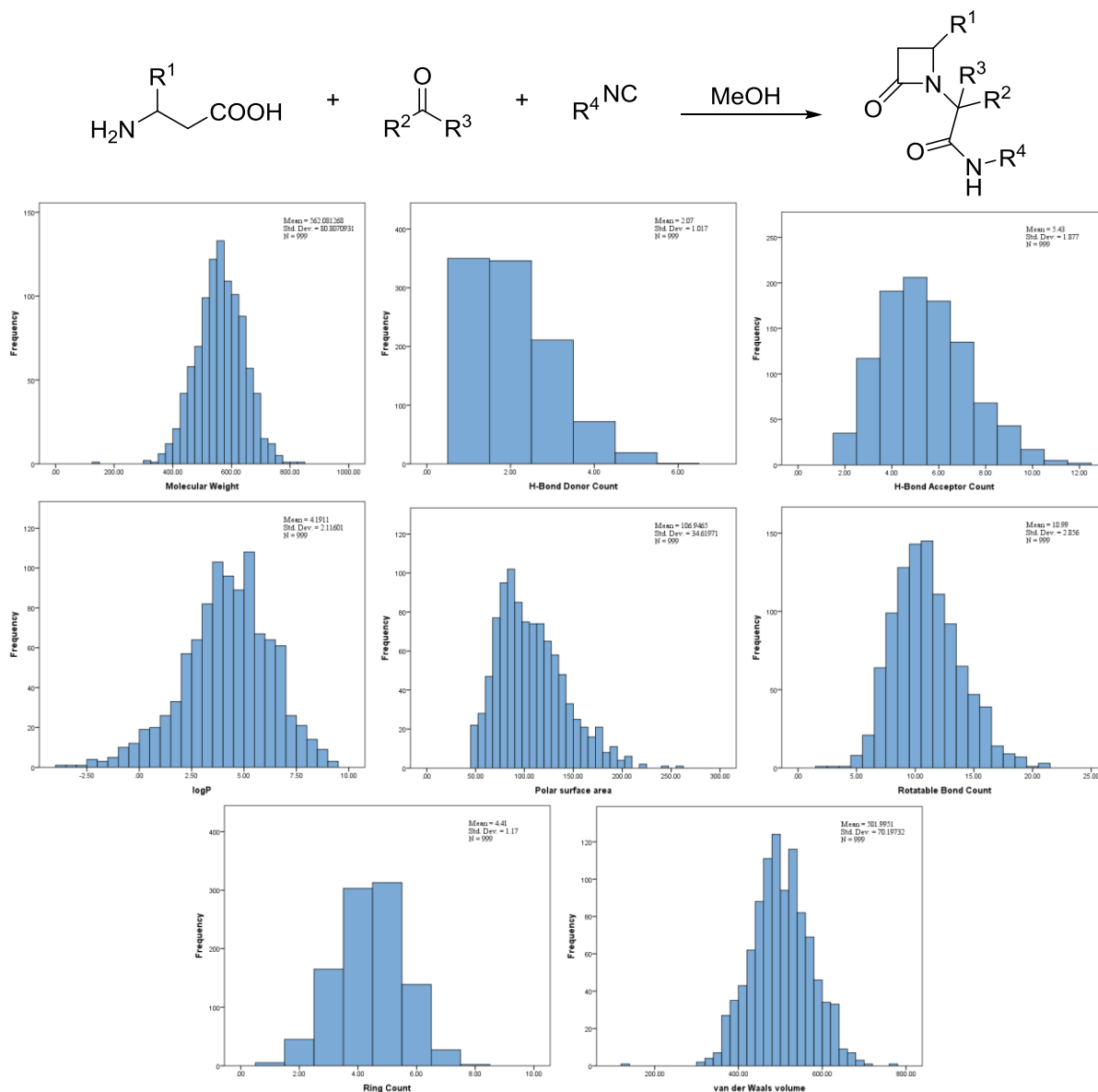


Figure 2.3 Beta-lactam reaction implemented in the AnchorQuery library as well as graphs displaying the distribution of select properties of 1000 randomly selected compounds from this scaffold.

2.1.1.2 Tetrazole Reaction

This Ugi reaction utilizes an azide in lieu of the carboxylic acid component to achieve a one-step synthesis of a tetrazole-containing compound.⁹⁶ This is a very versatile reaction as many different aliphatic and aromatic aldehydes/ketones and primary/secondary amines have

been seen to work well. In addition, use of cleavable isocyanides allows for the formation of α -amino methyl tetrazoles. This can be seen as very useful from a drug discovery point of view as the free tetrazole has been seen to mimic carboxylic acid functionality.⁹⁷ In addition, Dömling et al. recently introduced a way to synthesize N-unsubstituted α -aminotetrazoles by using tritylamine as the amine component which can be cleaved in a second step.⁹⁸ Using both cleavages, α -amino acid mimics could be synthesized.

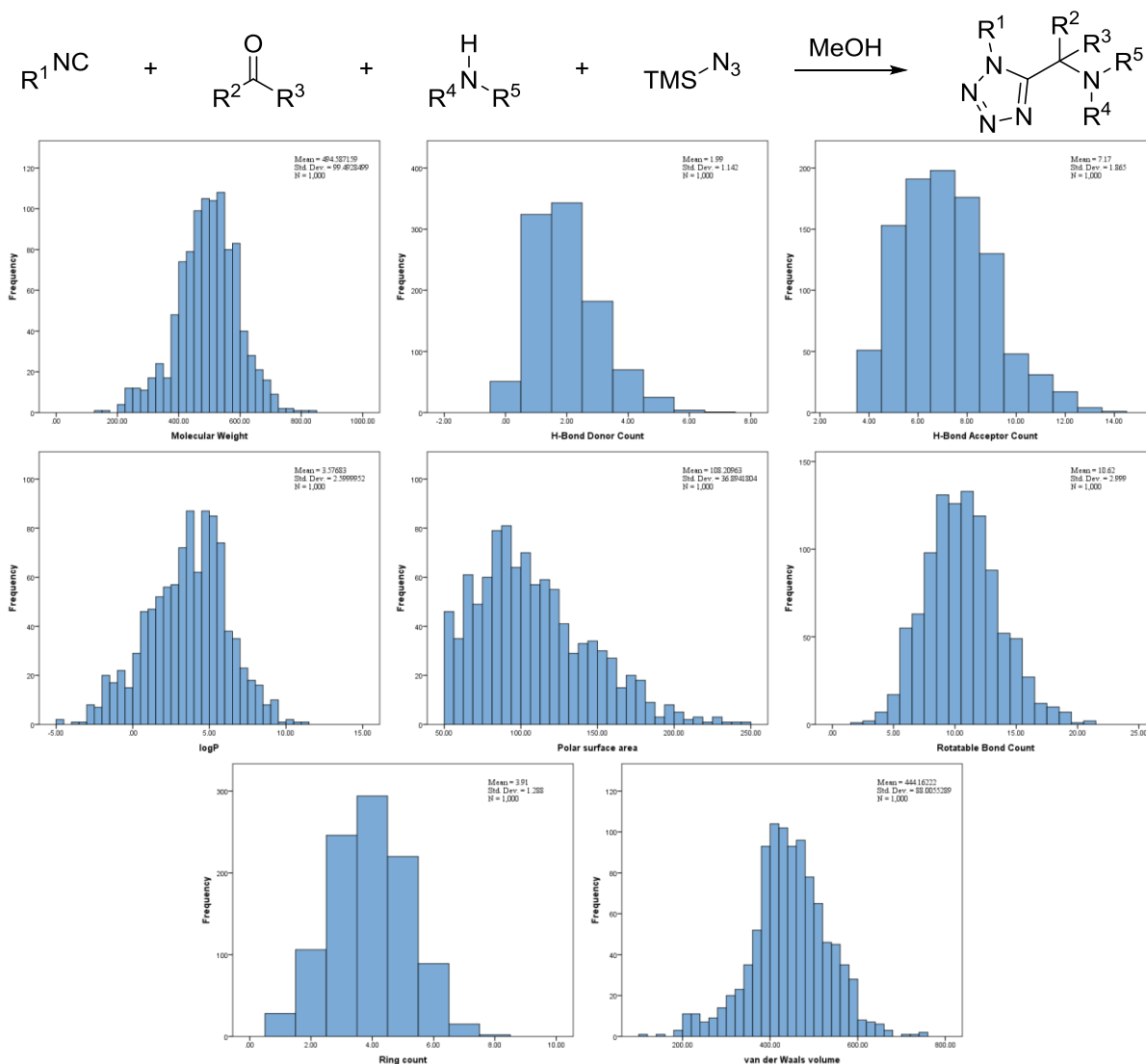


Figure 2.4 Tetrazole reaction implemented in the AnchorQuery library as well as graphs displaying the distribution of select properties of 1000 randomly selected compounds from this scaffold.

2.1.1.3 Hydantoine Reaction

The Hydantoine variation of the Ugi reaction, described by Ugi in 1964⁹⁹, utilizes an amine, an oxo-component, an isocyanide, and potassium cyanate to form this hydantoin-imide. Both aromatic and aliphatic amines have been described and shown to work well, and for the oxo-component, both aromatic and aliphatic aldehydes and symmetric aliphatic ketones have been described. This class of compounds have been seen to show inhibition against beta-secretase.¹⁰⁰

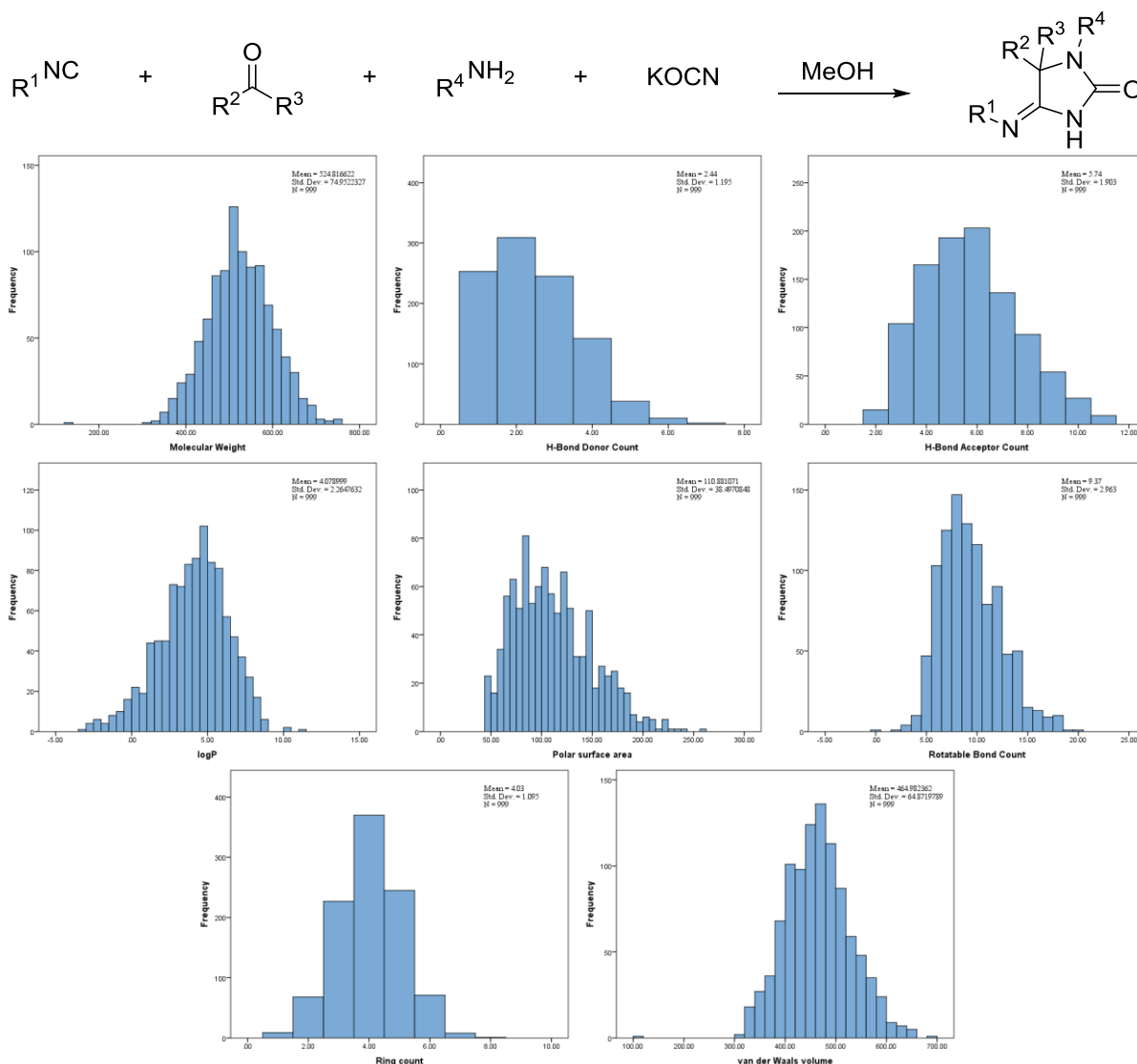


Figure 2.5 Hydantoine reaction implemented in the AnchorQuery library as well as graphs displaying the distribution of select properties of 1000 randomly selected compounds from this scaffold.

2.1.1.4 Imidazole

Tetra substituted imidazoles were introduced by means of an Ugi 4-component reaction using an arylglyoxal as the oxo-component, an amine, a carboxylic acid on isocyanide-functionalized Wang resin. Subsequent cyclization with ammonium acetate afforded the final tetra substituted imidazole.¹⁰¹ This reaction has also been described in solvent.¹⁰² Imidazoles are important to medicinal chemistry as they serve as the derivatives for a number of fungal creams (ketoconazole), antibiotics (nitromiddazole) and sedatives (midazolam).

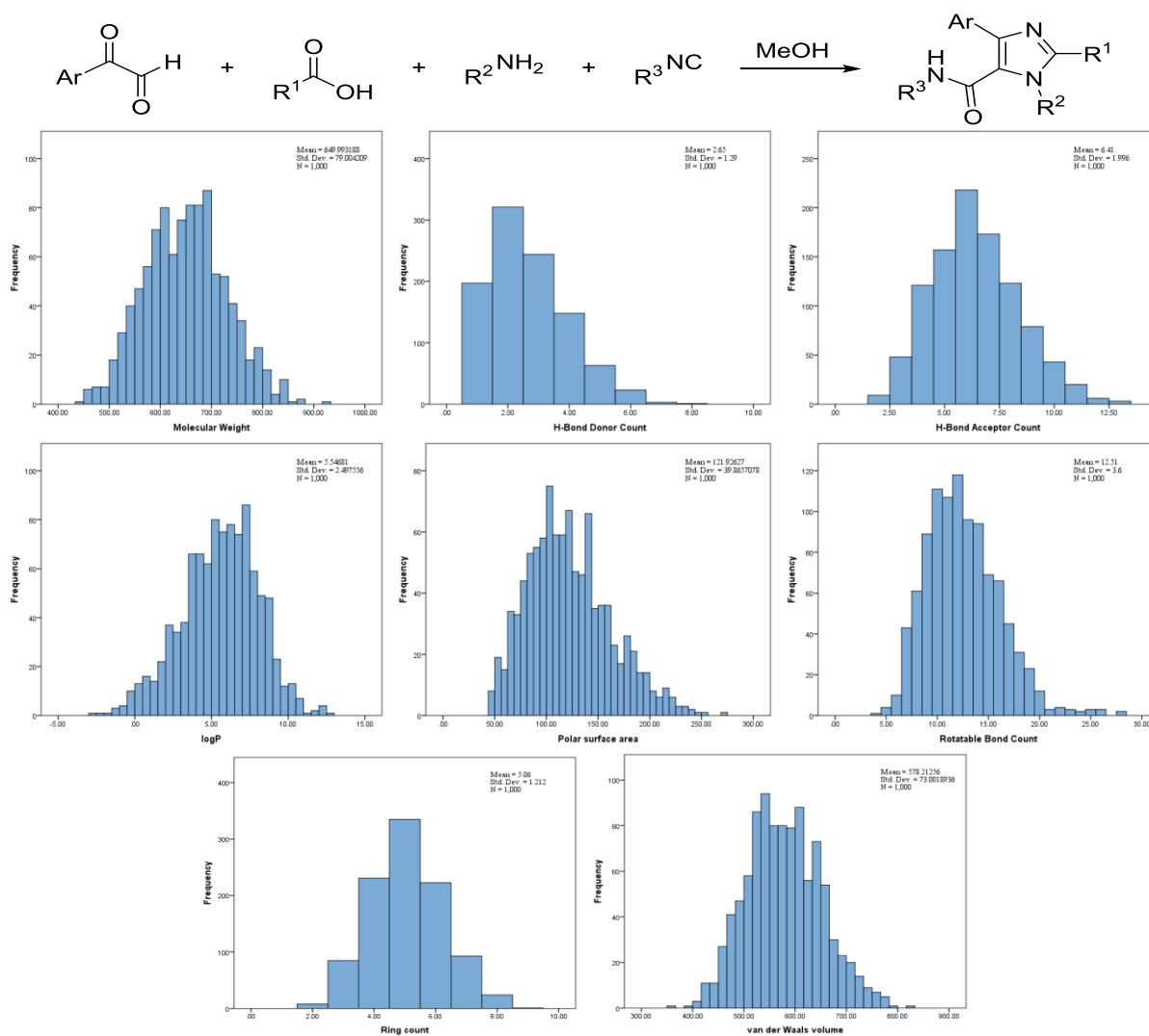


Figure 2.6 Imidazole reaction implemented in the AnchorQuery library as well as graphs displaying the distribution of select properties of 1000 randomly selected compounds from this scaffold.

2.1.1.5 Diketopiperazine

Piperazine derivatives have been intensively investigated in structural biology studies due to their unique scaffolds. According to a substructure search in Relibase ¹⁰³, 1,011 ligands containing piperazine motif were found in the Protein Data Bank. Many of the ligands serve as molecular probes of proteins, as well as leads of small molecular weight inhibitors.¹⁰⁴ In fact, Glaxo Smith Kline recently introduced retosiban (an diketopiperazine, oxytocin inhibitor) into phase II clinical trials.¹⁰⁵ Szardenings et al. introduced this two step synthesis of DKPs with an Ugi reaction utilizing two amino acids: one N-Boc protected, and the other methyl protected on the carboxylic acid. These, together with an aldehyde or ketone, and an isocyanide, form the Ugi product, which is followed by deprotection of the amine, and cyclization to the methyl ester to form the DKP with four points of diversity.^{106,107}

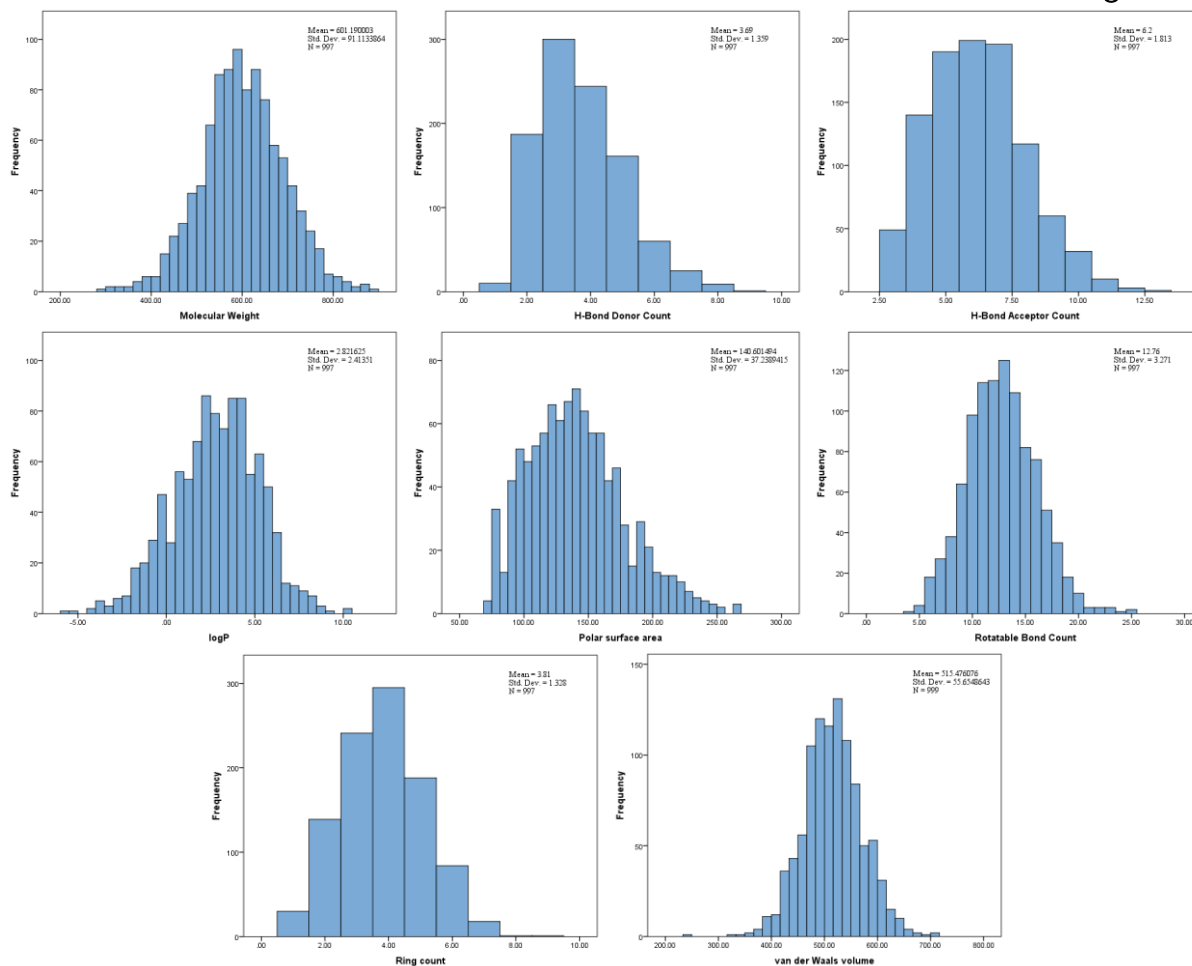
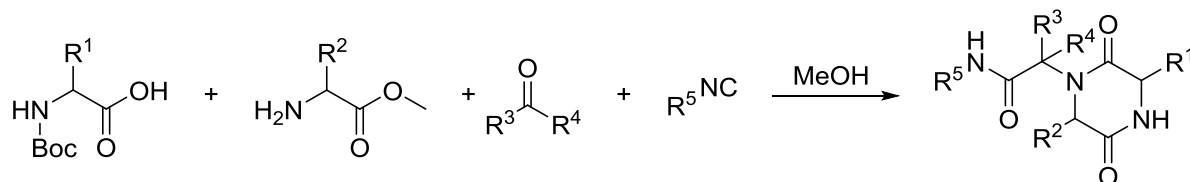


Figure 2.7 Diketopiperazine reaction implemented in the AnchorQuery library as well as graphs displaying the distribution of select properties of 1000 randomly selected compounds from this scaffold.

2.1.1.6 Praziquantel (Ugi/Pictet-Spengler)

Dömling et al. recently introduced an efficient two step method to produce the anti-parasitic drug Praziquantel via an Ugi/Pictet-Spengler reaction. Including the use of phenylethyl isocyanide derivatives, tryptophan and tryptamine derived isocyanides also were shown to work nicely in the secondary Pictet Spengler reaction. Both aliphatic and aromatic aldehydes and

isocyanides were used, and all seem to produce reasonable yields. In addition a 7 membered rings were introduced by use of a bi-functional amine aldehyde 1,3-Dioxolane-2-ethylamine; this acts as an amine in the Ugi reaction and subsequently cyclizes in the second Pictet Spengler step to form the 7-membered ring.^{108,109}

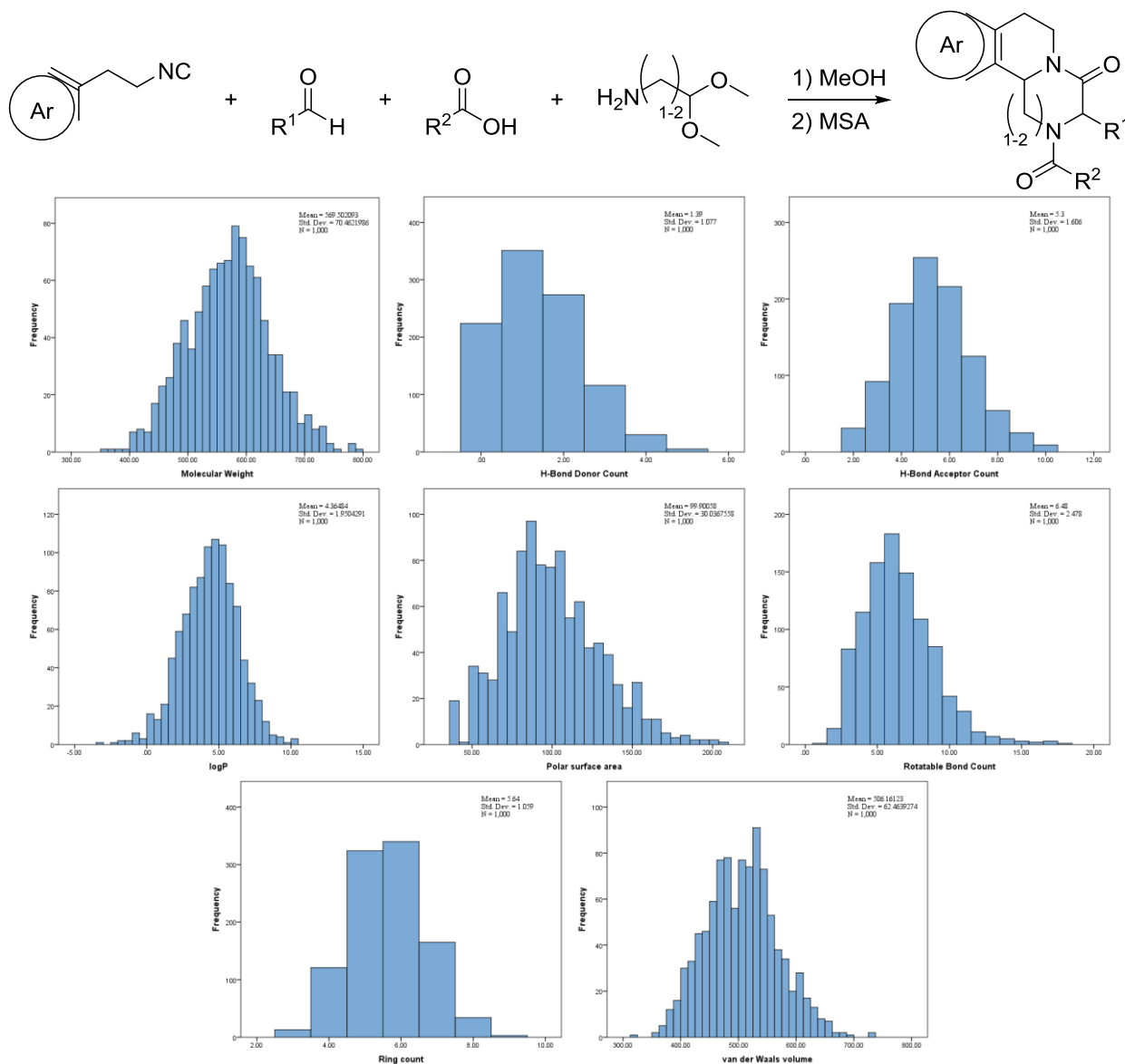


Figure 2.8 Praziquantel reaction implemented in the AnchorQuery library as well as graphs displaying the distribution of select properties of 1000 randomly selected compounds from this scaffold.

2.1.1.7 Ugi 4-component-5-centered reaction

As the amidation of this particular Ugi reaction was developed by the author of this thesis please see chapter 3 for a detailed description of its scope and limitation.

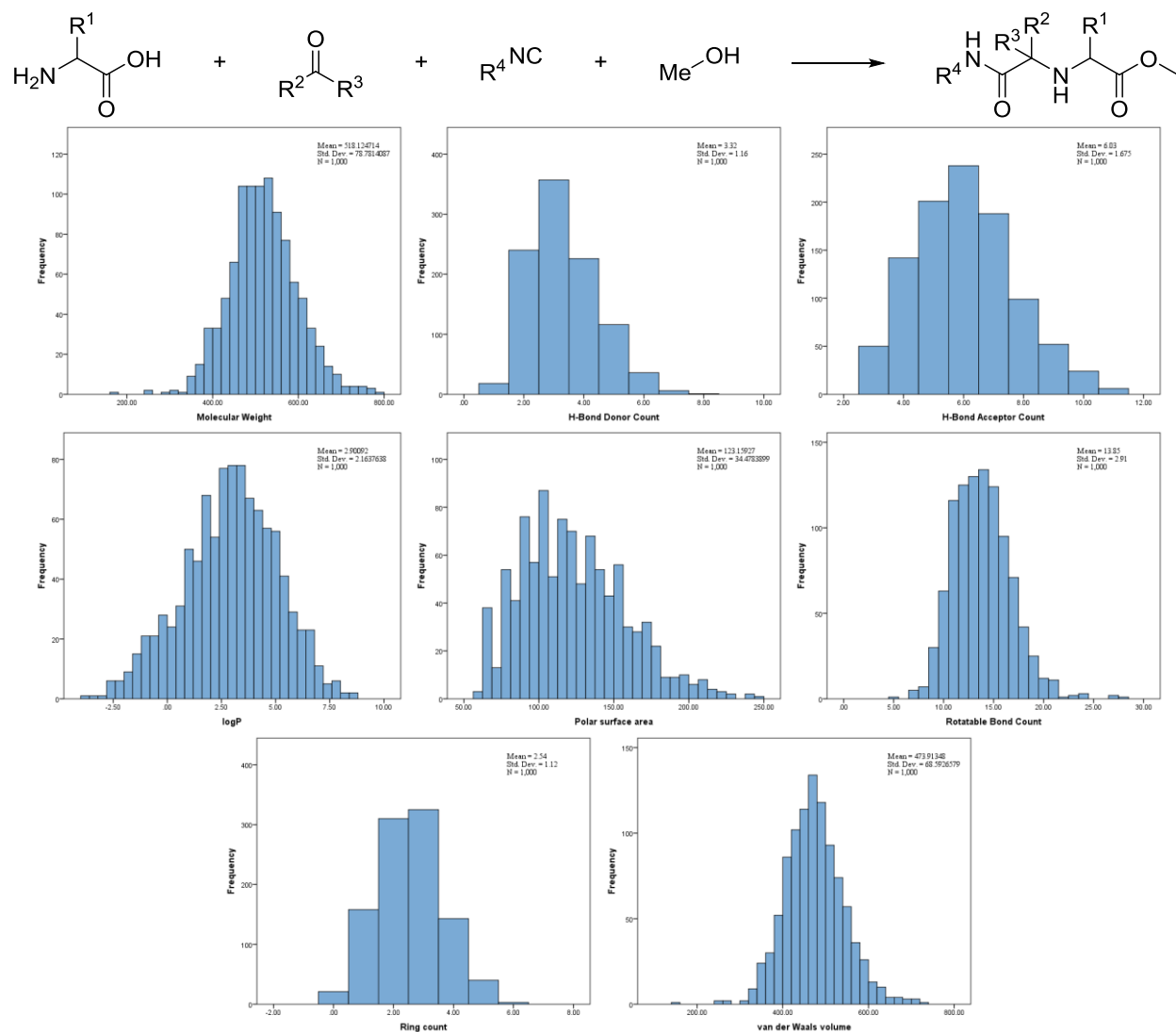


Figure 2.9 Ugi-4C-5CR reaction implemented in the AnchorQuery library as well as graphs displaying the distribution of select properties of 1000 randomly selected compounds from this scaffold.

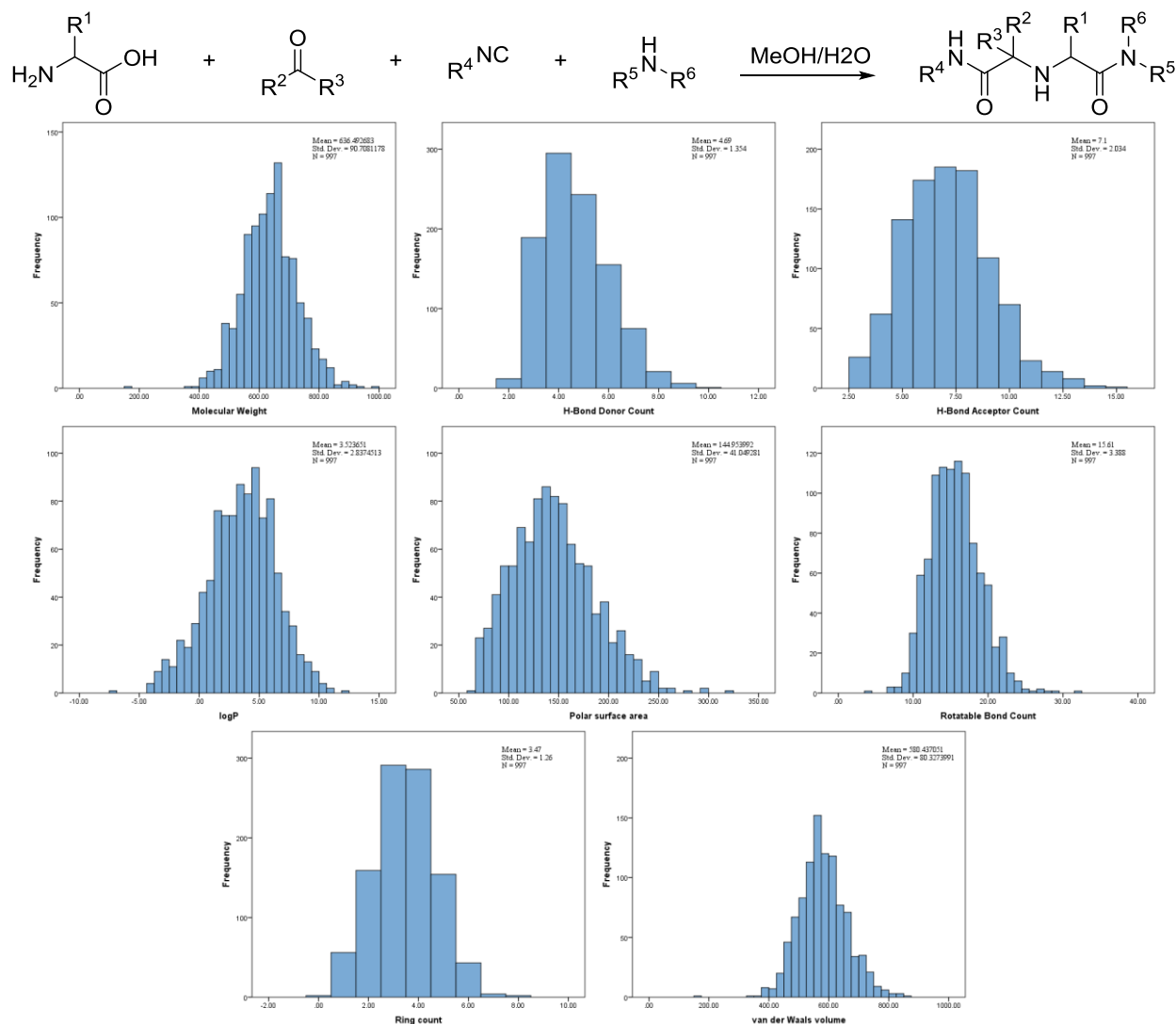


Figure 2.10 Ugi-4C-5CR amidation reaction implemented in the AnchorQuery library as well as graphs displaying the distribution of select properties of 1000 randomly selected compounds from this scaffold.

2.1.1.8 Ugi-protective Cyclization - Benzimidazole

Use of a post Ugi condensation reaction was described by Hulme et al. to produce biologically relevant benzimidazoles.¹¹⁰ Using N-Boc-ortho-phenylene diamine as the amine component in the Ugi reaction followed by acid-mediated removal of Boc and polystyrene-supported base-catalyzed cyclization, the final product can be observed. The generalities of this

reaction have been described in detail and can accommodate aliphatic and aromatic aldehydes/ketones, acids and isocyanides.¹¹⁰

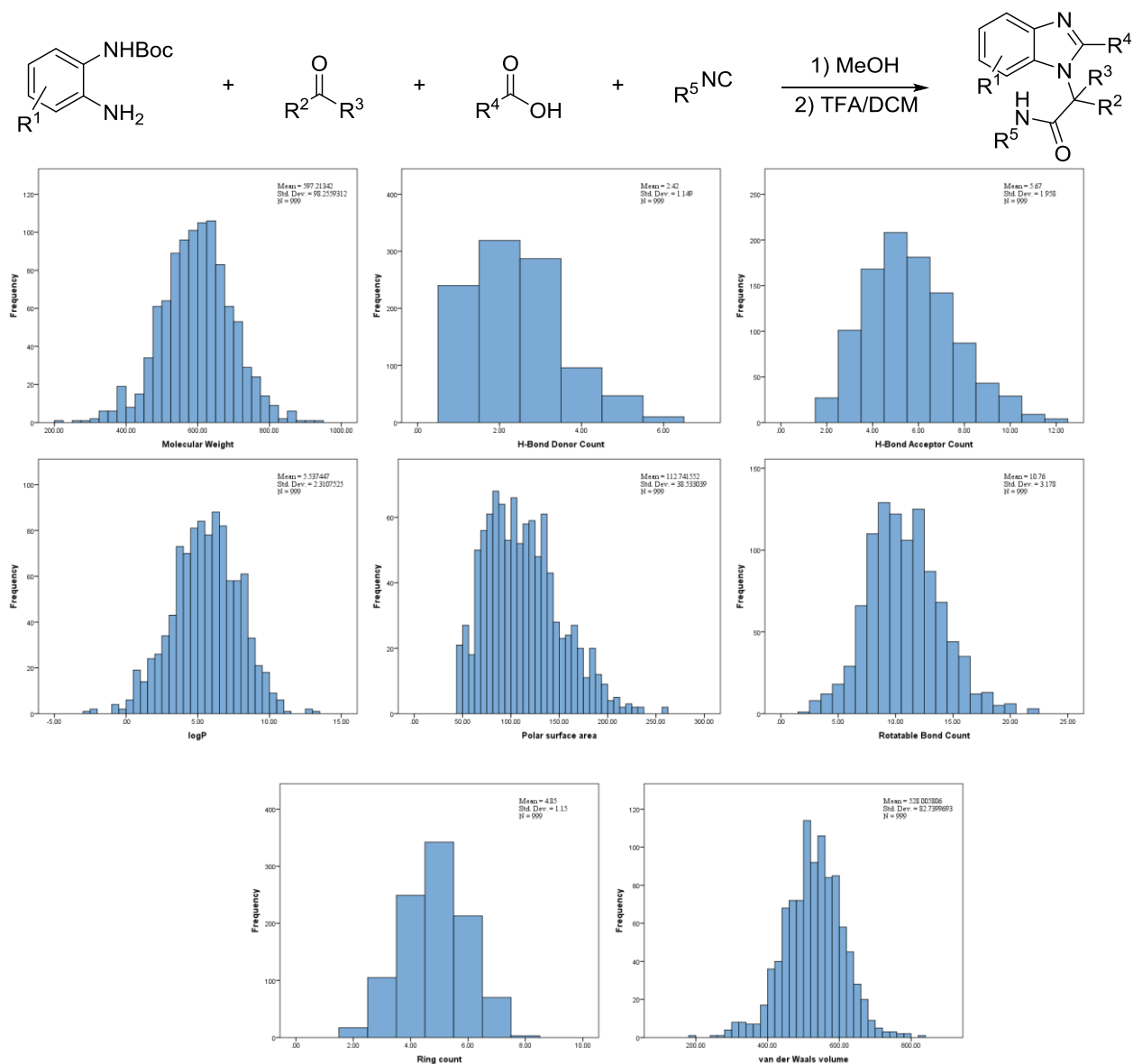


Figure 2.11 Benzimidazole reaction implemented in the AnchorQuery library as well as graphs displaying the distribution of select properties of 1000 randomly selected compounds from this scaffold.

2.1.1.9 Ugi-deprotective Cyclization - Dihydrobenzodiazepine-acetamide

Dömling et al. set forth to use an N-Boc-protected amino acid as an acid component to employ a two step UDC strategy. Using an aminophenylketone as an amine component, along with an aldehyde, and an isocyanide, the Ugi product is formed. Ugi product does not need to be isolated but the crude mixture can be treated with TFA in dichloroethane to deprotect and cyclize the amine to the ketone to afford the 1,4-BDA with four points of diversity.

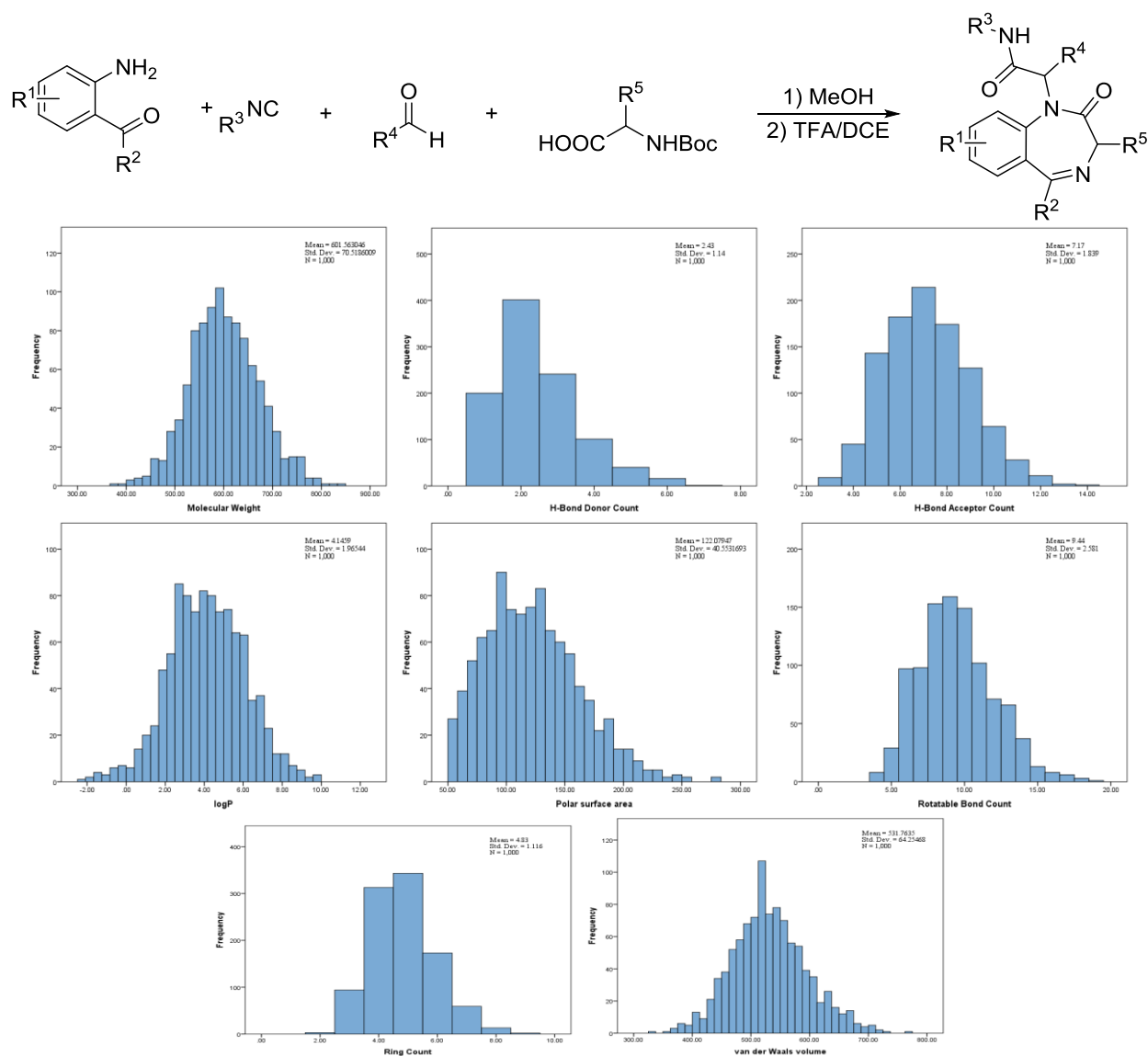


Figure 2.12 Benzodiazepine reaction implemented in the AnchorQuery library as well as graphs displaying the distribution of select properties of 1000 randomly selected compounds from this scaffold.

2.1.1.10 Ugi-deprotective Cyclization - Tetrahydrobenzodiazepine -carboxamide

The two-step reaction described by Dömling et al.¹¹¹ based on the classic Ugi 4 component reaction. An N-Boc- α -amino-aldehyde as an aldehyde component, and methyl anthranilate as an amine component are used as building blocks for this 1,4-benzodiazepine scaffold. Once the Ugi reaction is complete using any isocyanide or carboxylic acid known to work in the Ugi reaction, the Boc protecting group is cleaved and the free amine is condensed to the orthogonal ester group to form a 1,4-diazepine ring. This UDC strategy allows for access of the 1,4-benzodiazepine-6-ones with different substitution patterns derived from the isocyanide, carboxylic acid, or α -amino-aldehyde input.

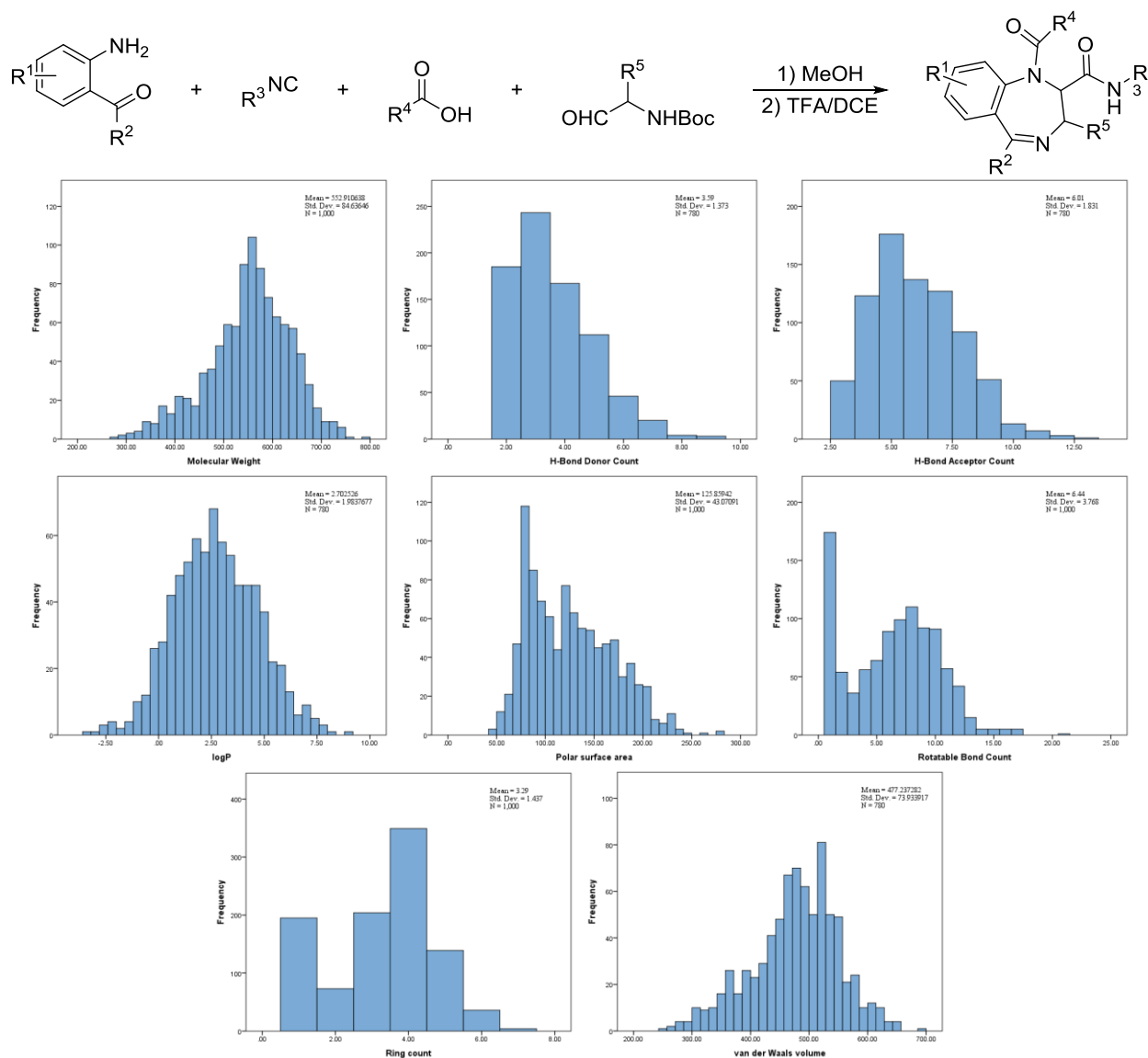


Figure 2.13 Benzodiazepine reaction implemented in the AnchorQuery library as well as graphs displaying the distribution of select properties of 1000 randomly selected compounds from this scaffold.

2.1.1.11 Ugi- deprotective Cyclization - Dihydrobenzodiazepine-carboxamide

In this BDA scaffold described by Dömling et al.¹¹¹ aminophenylketones are used as an amine component with a protected N-Boc- α -amino-aldehyde, an isocyanide and a carboxylic acid to form the Ugi product. Once deprotected, the free amine immediately cyclizes with the

ketone functionality to form the 1,4,BDA. This method allows for four different point of diversity as many aminophenylketones are commercially available.

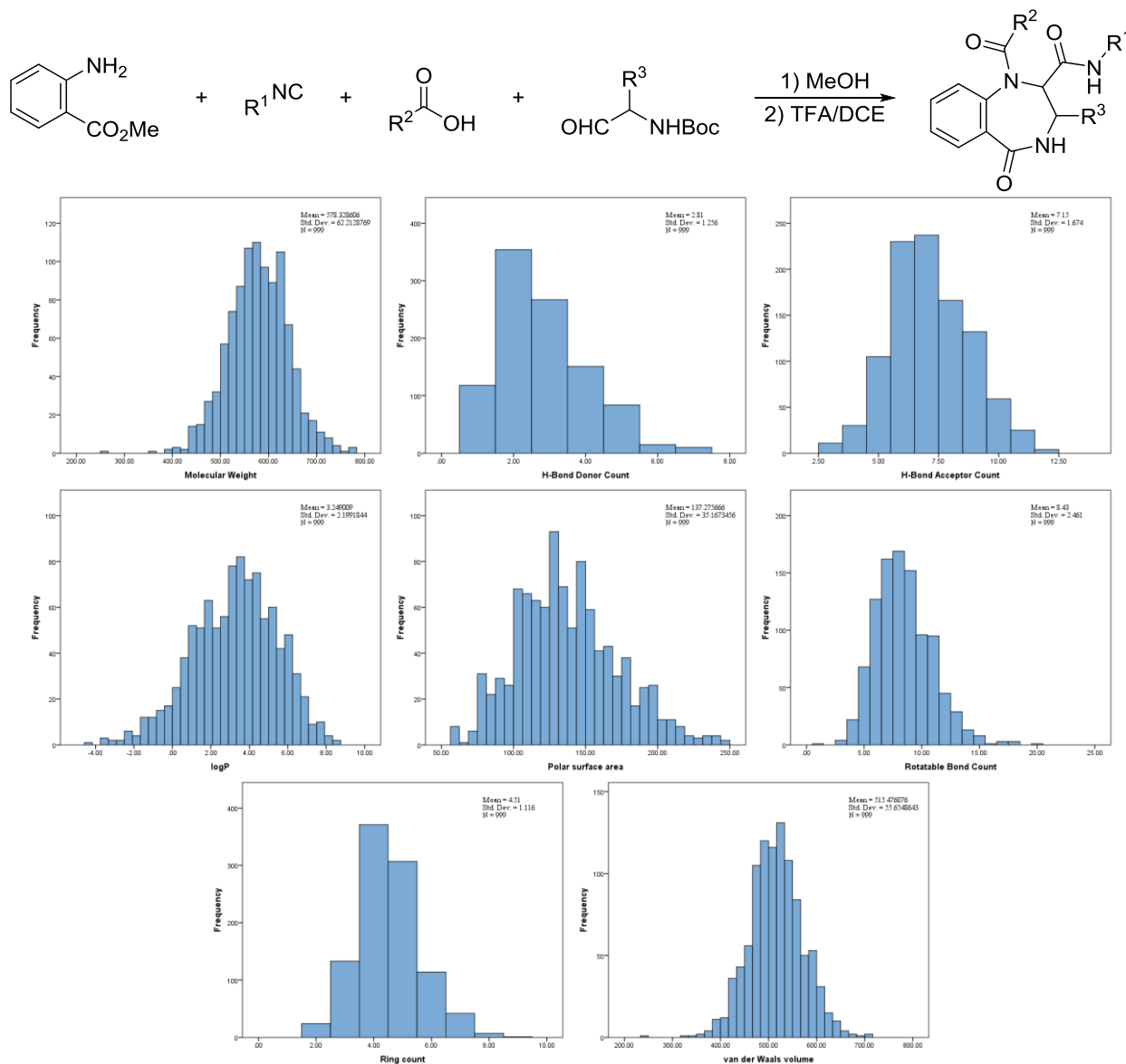


Figure 2.14 Benzodiazepine reaction implemented in the AnchorQuery library as well as graphs displaying the distribution of select properties of 1000 randomly selected compounds from this scaffold.

2.1.1.12 Ugi- deprotective Cyclization - Tetrazolyl-dihydrobenzodiazepine

Building off of the Dihydrobenzodiazepine scaffold, Dömling et al. applied a similar technique to the Ugi-tetrazole reaction.¹¹¹ Using an aminophenylketone as an amine component, an N-Boc- α -amino-aldehyde, an isocyanide, and trimethyl azide as an acid functionality, the Ugi-tetrazole product can be formed. As in the dihydrobenzodiazepine, once the amine is deprotected, spontaneous cyclization to the ketone affords the 1,4-BDA ring with three points of diversity.

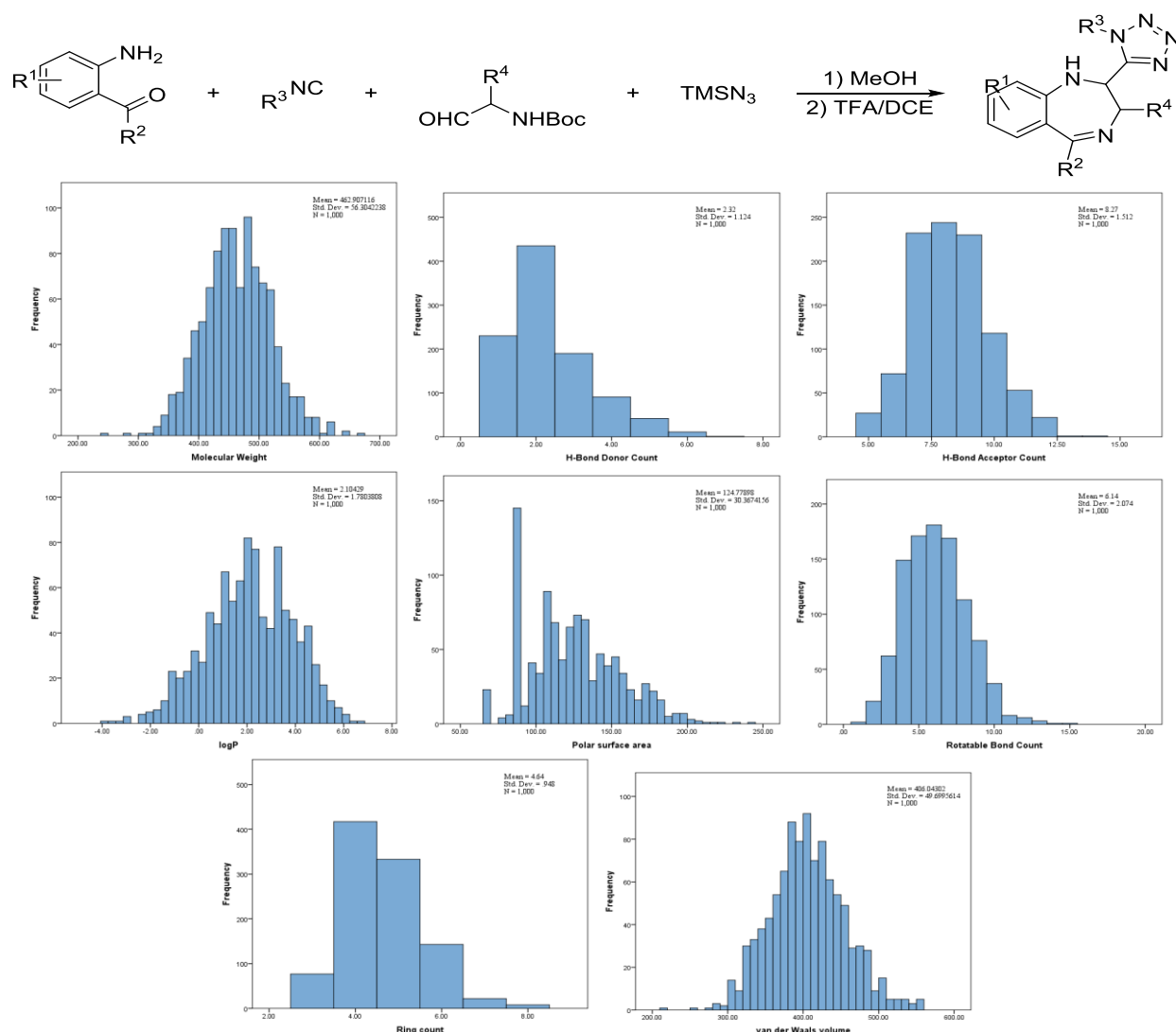


Figure 2.15 Benzodiazepine reaction implemented in the AnchorQuery library as well as graphs displaying the distribution of select properties of 1000 randomly selected compounds from this scaffold.

2.1.1.13 Groebke/Blackburn/Bienayme

In 1998, Groebke,¹¹² Blackburn,¹¹³ and Bienayme¹¹⁴ reported, independently, an efficient method for the synthesis of an imidazo annulated hetero-bicyclic scaffold. This Ugi-type condensation is carried out in the presence of a Brønsted or Lewis Acid with an isocyanide, an aldehyde and a heterocyclic aromatic 5- or 6-membered 2-aminoazine acting as the primary

amine. One major advantage of the Groebke type reactions is their potential to mimic nucleobases adenine, guanine, and cytosine.¹¹⁵

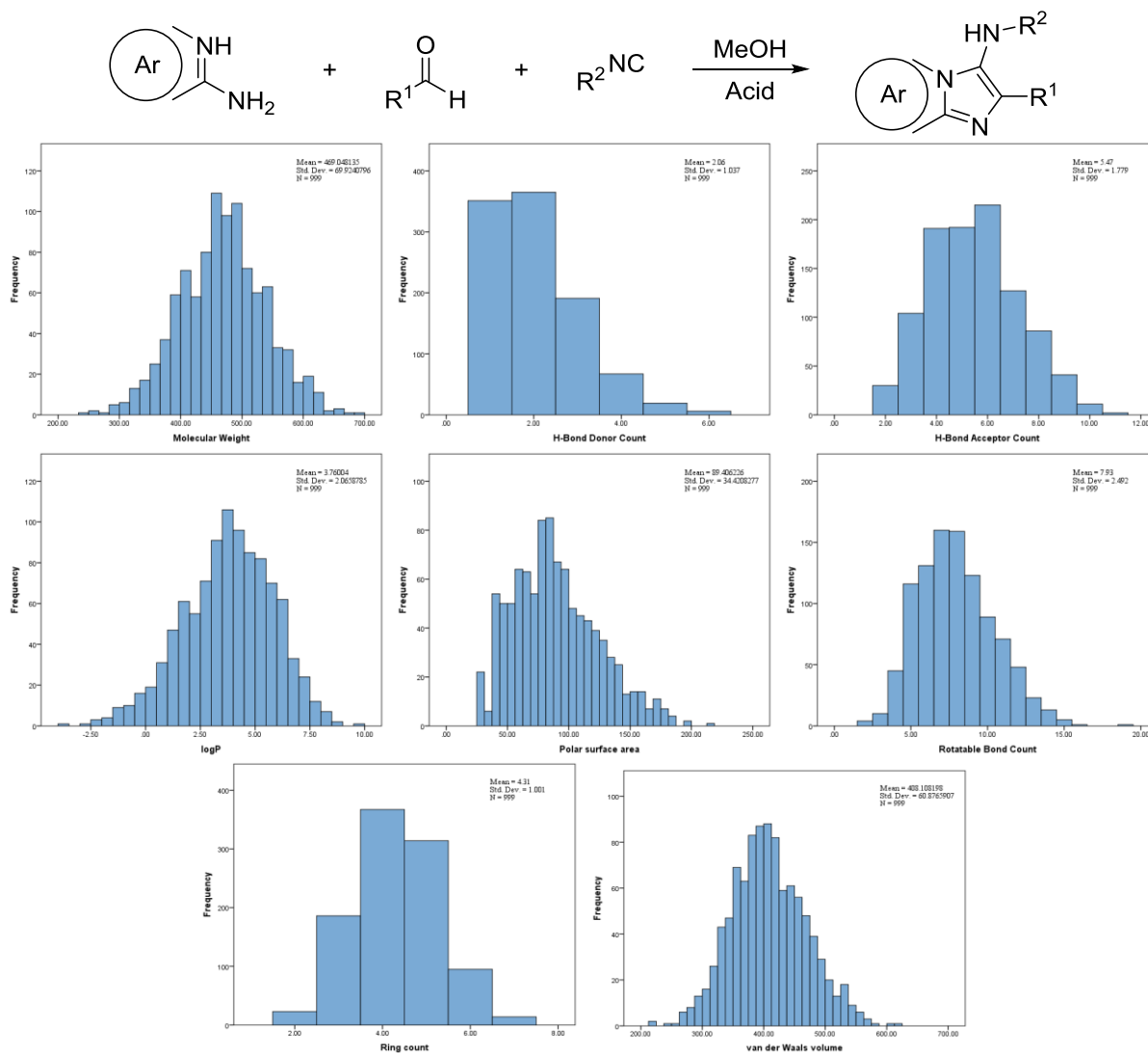


Figure 2.16 Groebke reaction implemented in the AnchorQuery library as well as graphs displaying the distribution of select properties of 1000 randomly selected compounds from this scaffold.

2.1.1.14 Thienodiazepine

Utilizing the Gewald reaction followed by an Ugi-Deprotection-Cyclization, Dömling et al. was able to synthesize 1,4-Thienodiazepine-2,5-diones. In this reaction, the final product from

the Gewald reaction is amine Boc protected and used as an acid component in the Ugi reaction with an isocyanide, a primary amine, and ethyl glyoxalate as an aldehyde component. After the Ugi product is formed, deprotection of the N-Boc is performed and subsequent cyclization to form the 1,4-Thienodiazepine-2,5-diones is observed.

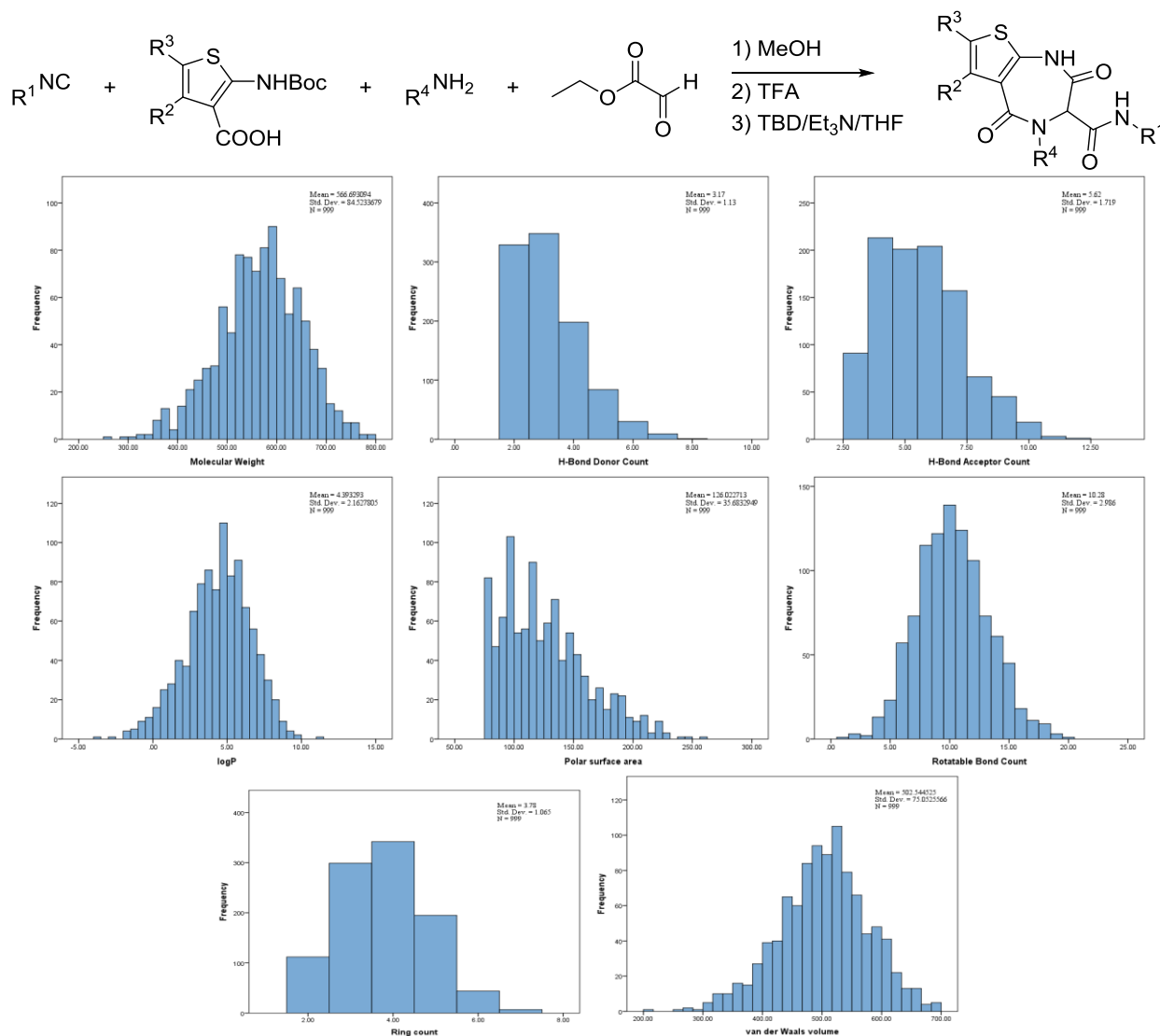


Figure 2.17 Thienodiazepine reaction implemented in the AnchorQuery library as well as graphs displaying the distribution of select properties of 1000 randomly selected compounds from this scaffold.

2.1.1.15 Orru

Orru introduced a novel 2-imidazoline synthesis using an amine, an aldehyde, and an α -acidic isocyanide which can be easily derived from the commercially available amino acids. Both aliphatic and aromatic aldehydes have been seen to be successful in this reaction. However only aliphatic amines gave reasonably good yields, most likely due to steric hindrance around the Schiff base. As the final product of the Orru reaction gives a methyl ester, amidation of the final product allows for a fourth point of diversity to be introduced. This scaffold, in fact, has been shown by Dömling et al. to produce potent p53/MDM2/MDMX inhibitors (unpublished).¹¹⁶

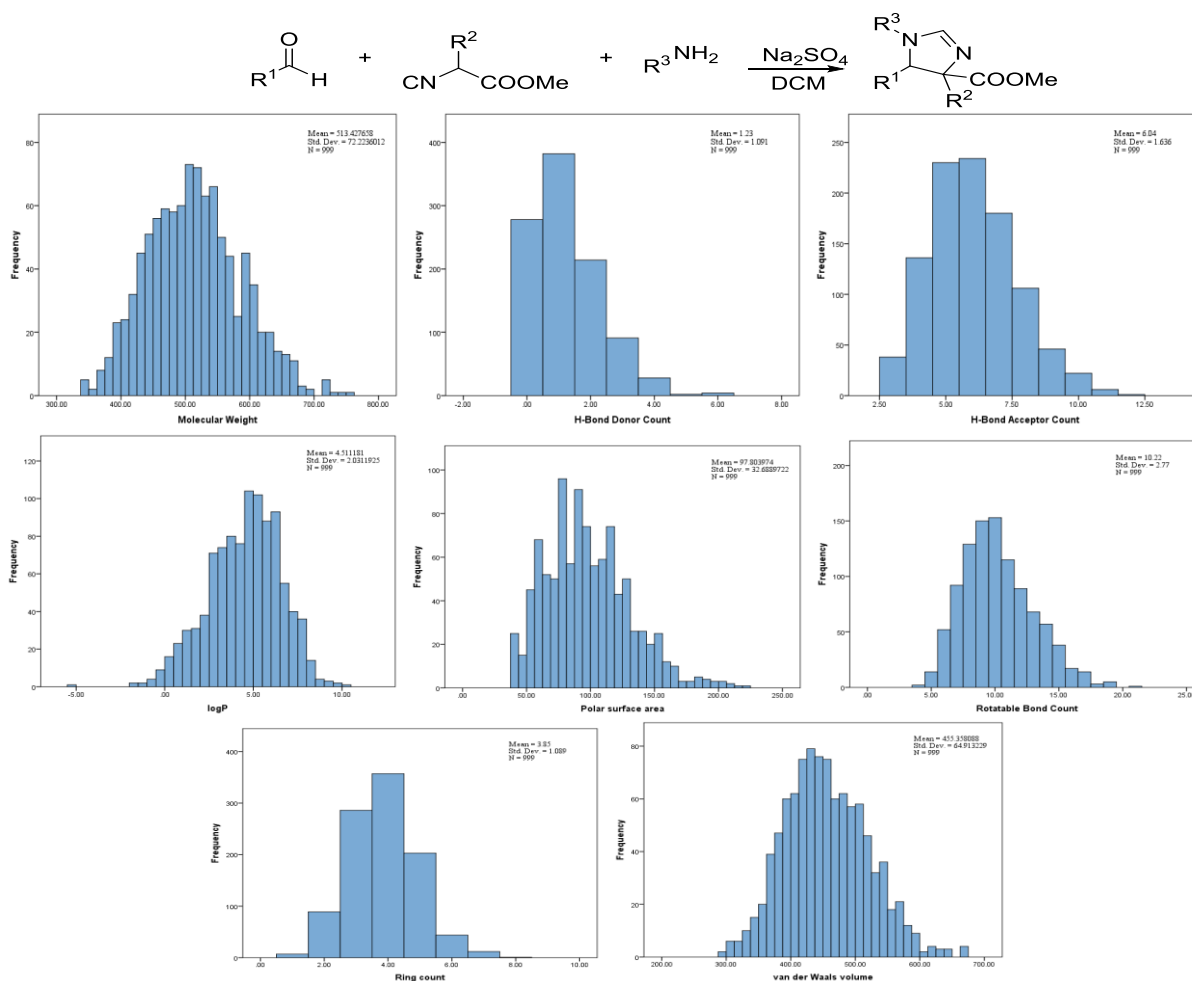


Figure 2.18 Orru reaction implemented in the AnchorQuery library as well as graphs displaying the distribution of select properties of 1000 randomly selected compounds from this scaffold.

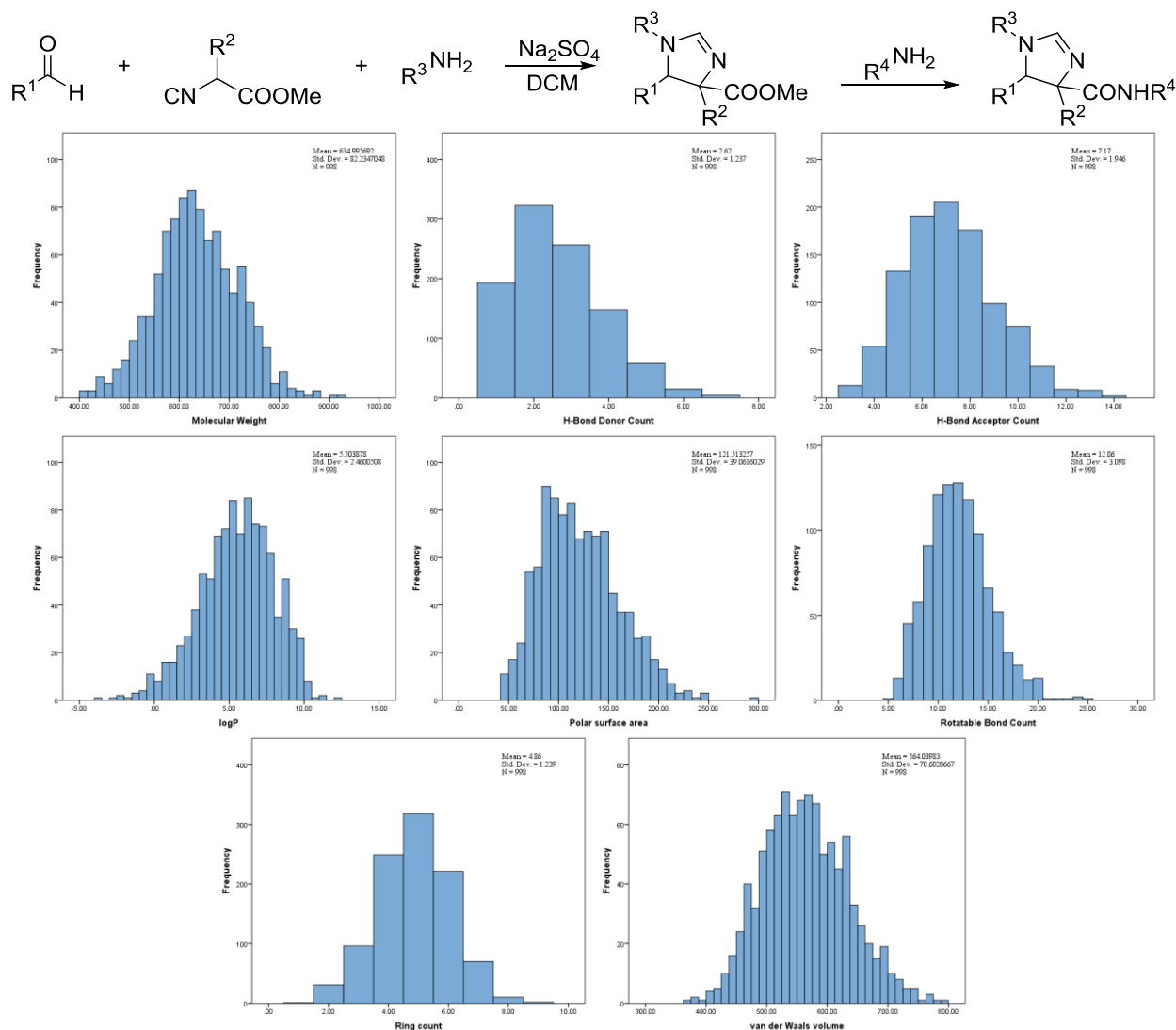


Figure 2.19 Orri amidation reaction implemented in the AnchorQuery library as well as graphs displaying the distribution of select properties of 1000 randomly selected compounds from this scaffold.

2.1.1.16 Schöllkopf reaction

Use of Schöllkopf's isocyanide, which contains a dimethyl amino leaving group in the beta-position has allowed for many novel scaffolds to be produced. One such reaction involves Schöllkopf's isocyanide, an aldehyde, and a primary amine which leads to the formation of 6-oxo-1,4,5,6-tetrahydro-pyrazine-2-carboxylic acid methyl esters. The reaction can be thought of

as an Ugi type reaction, so similar aldehydes and amines which work in the Ugi reaction are seen to work in this specific reaction. As the final compound produces a methyl ester, amidation of the ester can allow for a third point of diversity.

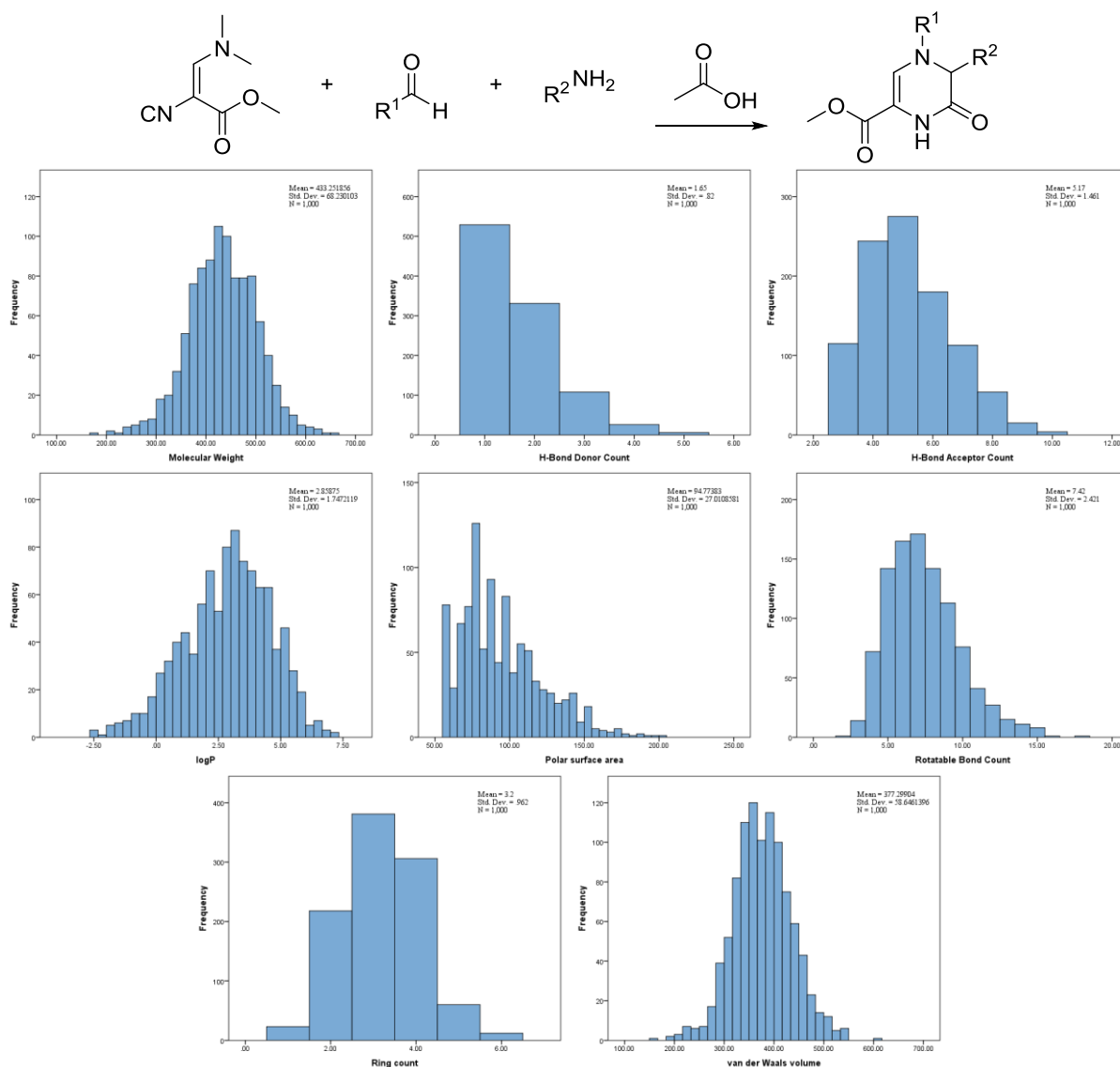


Figure 2.20 Schöllkopf reaction implemented in the AnchorQuery library as well as graphs displaying the distribution of select properties of 1000 randomly selected compounds from this scaffold.

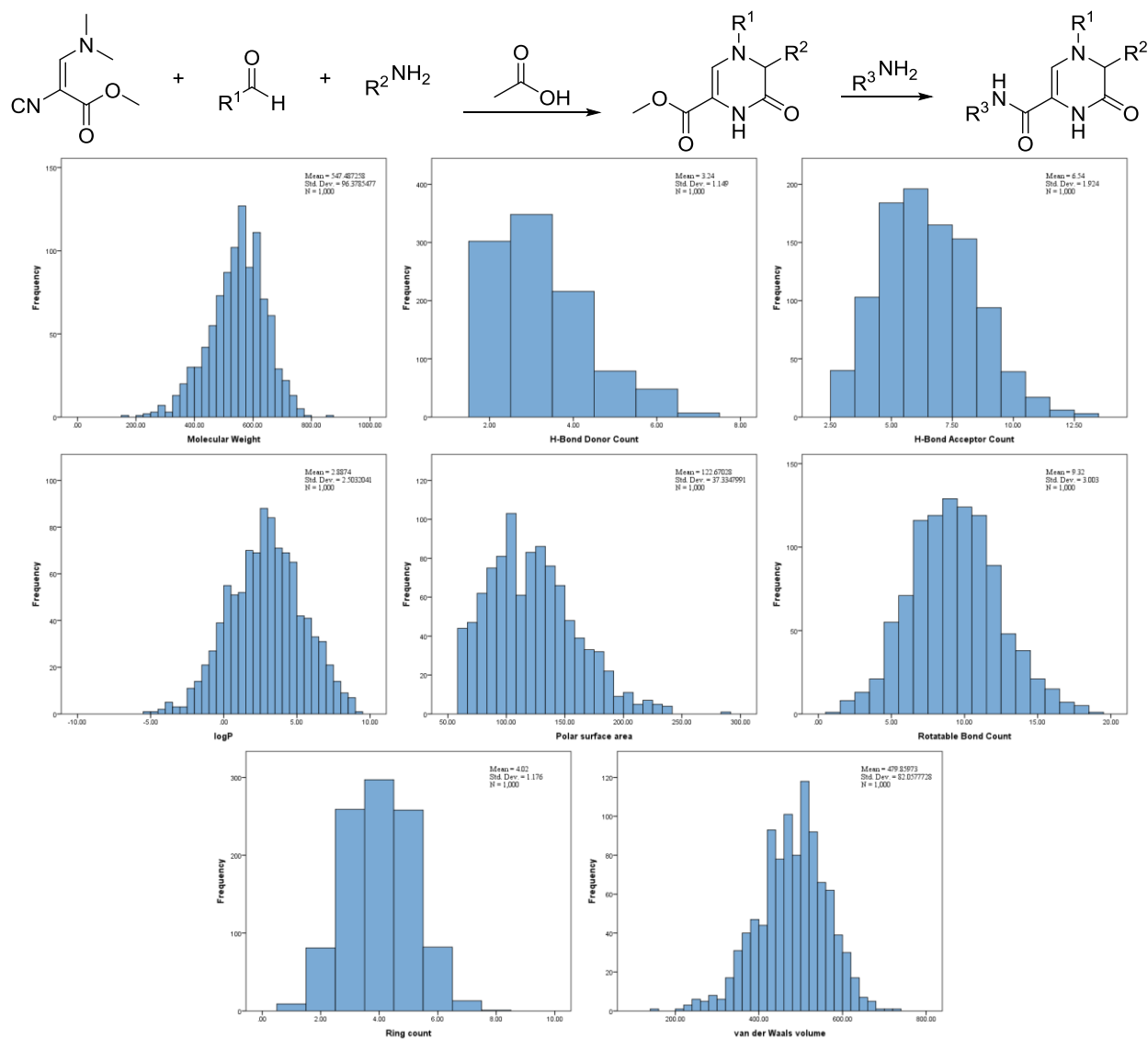


Figure 2.21 Schöllkopf amidation reaction implemented in the AnchorQuery library as well as graphs displaying the distribution of select properties of 1000 randomly selected compounds from this scaffold.

2.1.1.17 Thiazole Amidation

Utilizing Schöllkopf's isocyanide Dömling et al. was able to synthesize 2,4-disubstituted thiazoles in just one step.¹¹⁷ This Ugi type reaction, using a primary amine, an aldehyde or ketone, a thioacid, and Schöllkopf's isocyanide, allows for a highly substituted thiazole ring system: a common heterocyclic motif in natural products. In addition, as the final product

produces a carboxylic acid, amidation can be introduced to provide a fourth point of diversity.

Using this method, Dömling et al. was able to synthesize bacillamide C, a natural product with diverse bioactivity including algicidal and antibacterial.¹¹⁸

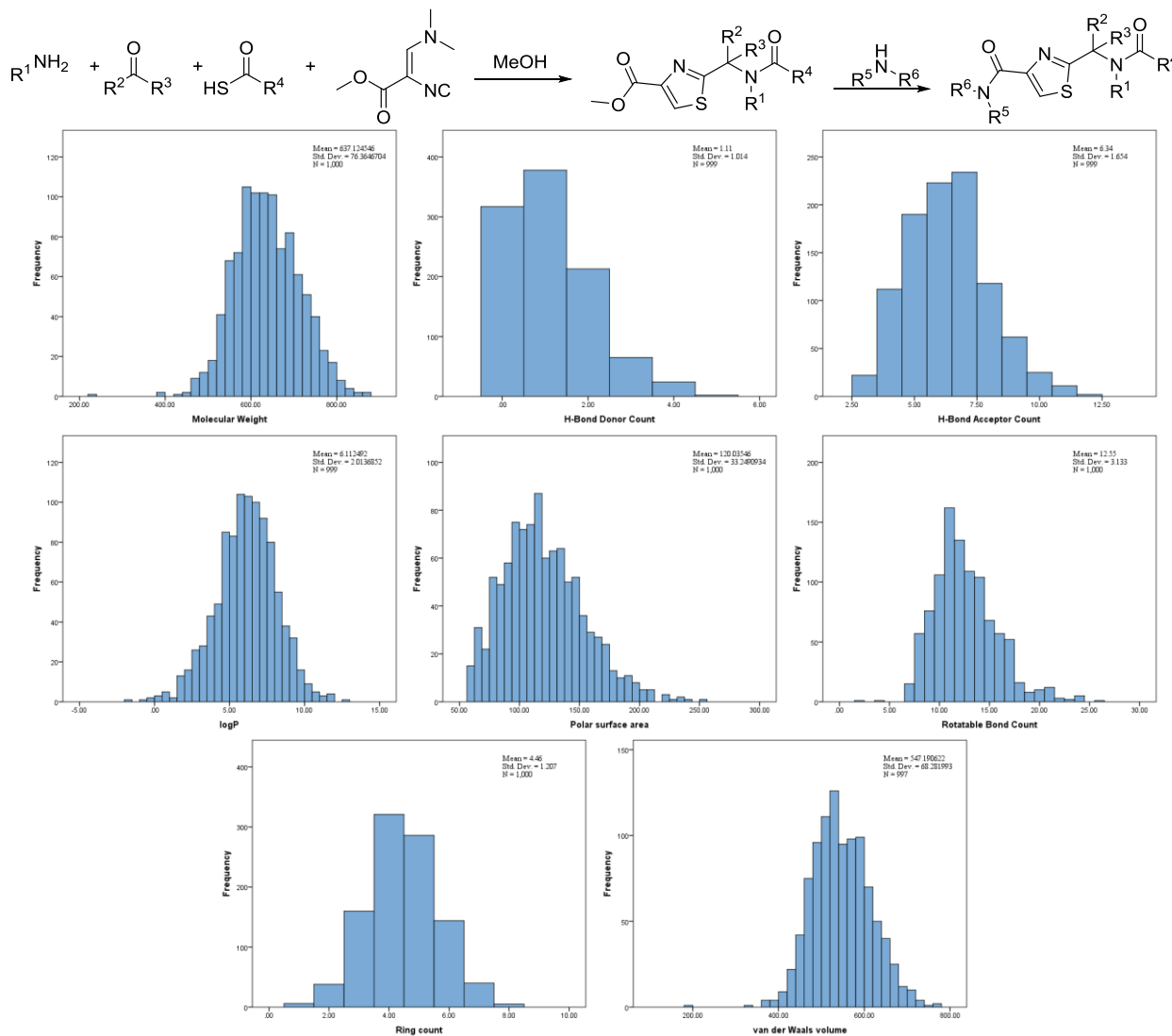


Figure 2.22 Thiazole amidation reaction implemented in the AnchorQuery library as well as graphs displaying the distribution of select properties of 1000 randomly selected compounds from this scaffold.

2.1.2 Non-Isocyanide Based Multicomponent Reactions

2.1.2.1 Döbner

The Döbner reaction, first introduced by Oscar Döbner in 1887,¹¹⁹ utilizes an aromatic amine, an aldehyde and a pyruvic acid (or ester) derivative to produce a cinchoninic acid (or ester) derivative. As this reaction is over 100 years old, the scope and limitation is well documented. Briefly, deactivating substituents in the amine lead to poor or even negligible yields. All types of aldehydes have been described; however aromatic aldehydes tend to produce the best yields. The pyruvic acid component can also be varied as both an acid and an ester, though as an acid it tends to produce better yields.¹²⁰ Such compounds have been seen to have activity in a number of different disease targets such as malaria,¹²¹ quinoline tachykinin receptor antagonists,¹²² and secretory phospholipase A2 inhibitors.¹²³

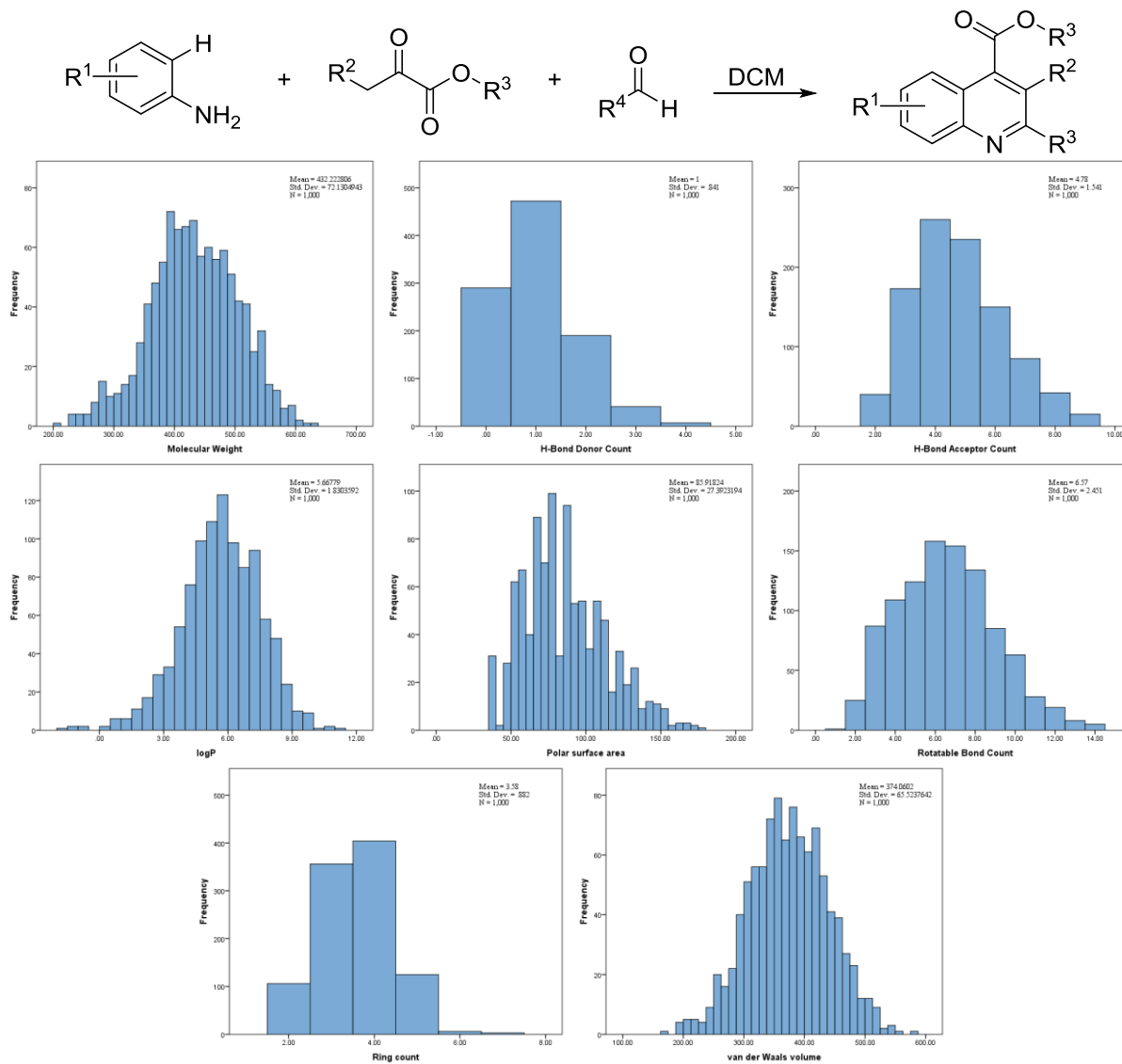


Figure 2.23 Döbner reaction implemented in the AnchorQuery library as well as graphs displaying the distribution of select properties of 1000 randomly selected compounds from this scaffold.

2.1.2.2 Gewald

The Gewald reaction, introduced by Karl Gewald in 1966,¹²⁴ is a versatile reaction and has seen diverse applications in combinatorial and medicinal chemistry. The reaction utilizes sulfur, a nitrile derivative, and an oxo-component, which yields a highly substituted 2-aminothiophene derivative. The nitrile must be an activated nitrile such as cyanoacetic acid (or

ester), or malonodinitrile in order for the reaction to work. Recently Dömling et al. introduced a fast, diverse and efficient method to produce cyanoacetamides suitable for the Gewald reaction on a multi-gram scale involving a very convenient filtration workup.¹²⁵ This method greatly increases the number of available products to be synthesized. The Gewald reaction has been rewarding for the pharmaceutical industry with such drugs as Olanzapine and Tinoridine being derived from the Gewald reaction.¹²⁶

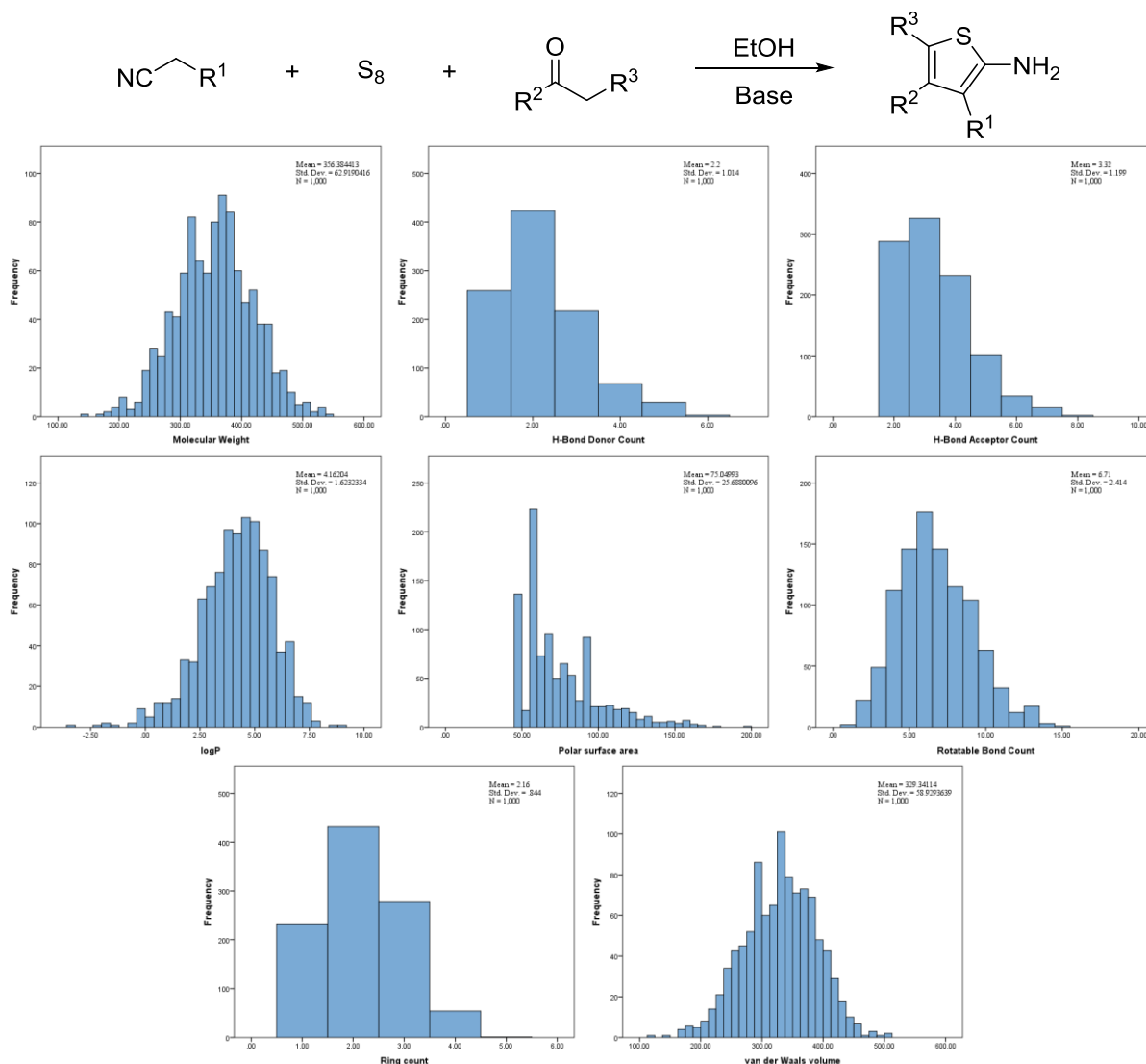


Figure 2.24 Gewald reaction implemented in the AnchorQuery library as well as graphs displaying the distribution of select properties of 1000 randomly selected compounds from this scaffold.

2.1.2.3 Isoquinoline Amidation

Use of homophthalic acid with a Schiff base leads to the synthesis of isoquinolines as described by Ognyanov et al.¹²⁷ Use of both aromatic and aliphatic amines and aldehydes has been seen to work well for this reaction, however it is often necessary to isolate the Schiff base before reacting with the homophthalic acid. While there are not many homophthalic acid derivatives commercially available as this reaction produces a free carboxylic acid in the final product, potential amidation of the acid allows for another point of diversity. Such a technique was used by Holak et al. for discovery of p53/MDM2 inhibitors.¹

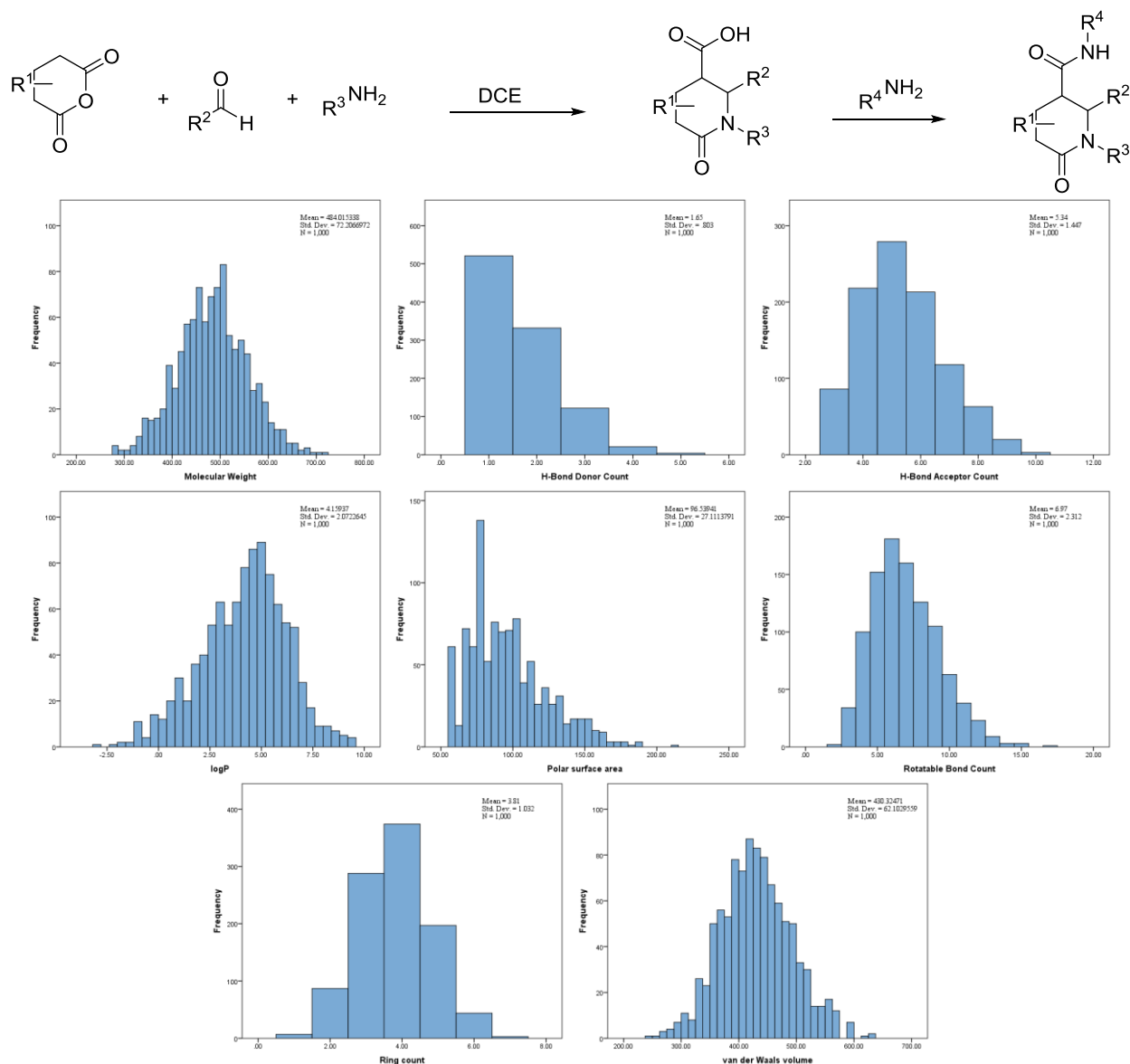


Figure 2.25 Isoquinoline reaction implemented in the AnchorQuery library as well as graphs displaying the distribution of select properties of 1000 randomly selected compounds from this scaffold.

2.1.2.4 Reaction mapping and smarts codes

All reactions were written using SMILES arbitrary target specification (SMARTS) language which is a language that allows you to specify substructures using rules that are straightforward extensions of SMILES. Reactions were written such that the products formed

would have a high probability of success should synthesis be attempted. Starting materials were hand selected using SciFinders database and Reactions were carried out using ChemAxons Reactor software.

SMARTS codes:

Beta Lactam

[H][#8]-[#6](=O)-[#6]-[#6]-[#7]([H])([H].[H][#6:3](-[#1,#6])=O.[#6:6][N+:5]#[C-]>>[#6:6]-
[#7:5]-[#6](=O)-[#6:3](-[#1,#6])-[#7]-1-[#6]-[#6]-[#6]-1=O

DKP

[#7:3]-[#6:2](-[#1,#6:1])-[#6:4](-[#8])=[O:5].[#7:6]-[#6:7](-[#1,#6:8])-[#6:9](-[#8])=O.[#6:10]-
[#6:11](-[#1,#6:15])=O.[#6:14][N+:13]#[C-:12]>>[#6:14]-[#7:13]-
[#6:12](=O)[C:11]([#6:10])([#1,#6:15])[#7:3]-1-[#6:2](-[#1,#6:1])-[#6:4](=[O:5])-[#7:6]-
[#6:7](-[#1,#6:8])-[#6:9]-1=O

Döbner

[H][#7:1]([H])-[#6:2]-1=[#6:7]-[#6:6]=[#6:5]-[#6:4]=[#6:3]-1[H].[#1,#6:15]-[#6:13]-
[#6:12](=O)-[#6:10](=[O:11])-[#8:9]-[#1,#6:8].[H][#6:16](-[#1,#6:14])=O>>[#1,#6:8]-[#8:9]-
[#6:10](=[O:11])-[#6:12]-1=[#6:13](-[#1,#6:15])-[#6:16](-[#1,#6:14])=[#7:1]-[#6:2]-2=[#6:3]-1-
[#6:4]=[#6:5]-[#6:6]=[#6:7]-2

Groebke

[H][#7:6]([H])-[c:7]1[n:8][#6,#7,#8,#16;a][#6,#7,#8,#16;a][#6,#7,#8,#16;a]1.[H][#6:4](-
[#1,#6:5])=O.[#6:2][N+:1]#[C-:3]>>[H][#7:1](-[#6:2])-[#6:3]-1=[#6:4](-[#1,#6:5])-
[#7:6]=[#6:7]-2-[#6,#7,#8,#16;a][#6,#7,#8,#16;a][#6,#7,#8,#16;a]-[#7:8]-1-2

[H][#7:7]([H])-[#6:6]-1=[#7:5]-[*:1]=[*:2]-[*:3]=[*:4]-1.[H][#6:8](-
 [#1,#6:9])=O.[#6:12][N+:11]#[C-:10]>>[#6:12]-[#7:11]-[#6:10]-1=[#6:8](-[#1,#6:9])-
 [#7:7]=[#6:6]-2-[*:4]=[*:3]-[*:2]=[*:1]-[#7:5]-1-2

Gewald

[H][#7;A;X3;!(NC=O):3]([#6:5])[#1,#6:4].[H][#6:1](=O)[C:2]([H])([H])[#1,#6:6]>>[H][#7]([
 H])-[#6]-1=[#6](-[#6:1]=[#6:2](-[#1,#6:6])-[#16]-1)-[#6](=O)-[#7:3](-[#6:5])-[#1,#6:4]

Hydantoine

[#6:1][N+:2]#[C-:3].[#1,#6:5]-[#6:4](-[#1,#6:6])=O.[H][#7:7]([H])-
 [#6;!(C=[!#6])!\$(C#[!#6]):8]>>[#6:1]\[#7:2]=[#6:3]1\[#7]-[#6](=O)-[#7:7](-
 [#6:8])[C:4]1([#1,#6:5])[#1,#6:6]

Imidazole

[H][#6:3](=O)-[#6:2](-[#6:1])=O.[H][#7;A;X3;!(NC=O):7]([H])[#6:8].[H][#8]-[#6:10](-
 [#1,#6:9])=O.[#6:6][N+:5]#[C-:4]>>[#6:6]-[#7:5]-[#6:4](=O)-[#6:3]-1=[#6:2](-[#6:1])-
 [#7]=[#6:10](-[#1,#6:9])-[#7:7]-1-[#6:8]
 [H][#6:3](=O)-[#6:2](-[#6:1])=O.[H][#7;A;X3;!(NC=O):7]([H])[#6:8].[H][#8]-
 [#6:10](=O)~[#6:9]~[#6:11](=[O:12])-[#8:13]-[#6].[#6:6][N+:5]#[C-:4]>>[H][#8:13]-
 [#6:11](=[O:12])~[#6:9]~[#6:10]-1=[#7]-[#6:2](-[#6:1])=[#6:3](-[#7:7]-1-[#6:8])-[#6:4](=O)-
 [#7:5]-[#6:6]

Isoquinoline

[O:2]=[#6:1]-1-[#6:11]-[#6:10]-[#6:7]-[#6:8](=O)-[#8:9]-1.[H][#6:5](-
 [#1,#6:6])=O.[H][#7:3]([H])-[#6:4]>>[H][#8:9]-[#6:8](=O)-[#6:7]-1-[#6:10]-[#6:11]-
 [#6:1](=[O:2])-[#7:3](-[#6:4])-[#6:5]-1-[#1,#6:6]

[H][C:7]1([H])[#6:10]-[#6:11]-[#6:1](=[O:2])-[#8:9]-[#6:8]1=O.[H][#6:5](-
 [#1,#6:6])=O.[H][#7:3]([H])-[#6:4].[H][#7:12]([H])-[#6:13]>>[H][#7:12](-[#6:13])-
 [#6:8](=O)[C:7]1([H])[#6:10]-[#6:11]-[#6:1](=[O:2])-[#7:3](-[#6:4])-[#6:5]1-[#1,#6:6]

Orru

[H][#7:1]([H])-[#6:2].[H][#6:3](-[#1,#6:4])=O.[#6:10]-[#8:9]-[#6:8](=[O:11])-[#6:7](-
 [#1,#6:12])[N+:6]#[C-:5]>>[#6:10]-[#8:9]-[#6:8](=[O:11])[C:7]1([#1,#6:12])[#7:6]=[#6:5]-
 [#7:1](-[#6:2])-[#6:3]1-[#1,#6:4]
 [H][#7:1]([H])-[#6:2].[H][#6:3](-[#1,#6:4])=O.[#8]-[#6:8](=[O:11])-[#6:7](-
 [#1,#6:12])[N+:6]#[C-:5].[H][#7:A;X3;!\$(NC=O):9]([#6:10])[#1,#6:13]>>[#6:10]-[#7:9](-
 [#1,#6:13])-[#6:8](=[O:11])[C:7]1([#1,#6:12])[#7:6]=[#6:5]-[#7:1](-[#6:2])-[#6:3]1-[#1,#6:4]

PZQ

[H][c:13]:[#6,#7;a:1](:[c:5])-[#6:2]-[#6:3][N+:4]#[C-:21].[H][#6:6](-[#6:7])=O.[H][#8]-
 [#6:11](-[#6:12])=O.[H][#7:8]([H])-[#6:9]-[#6:10](-[#8]-[#6])-[#8]-[#6]>>[#6:7]-[#6:6]-1-
 [#7:8](-[#6:9]-[#6:10]-2-[c:13][#6,#7;a:1](:[c:5])-[#6:2]-[#6:3]-[#7:4]-2-[#6:21]-1=O)-[#6:11](-
 [#6:12])=O
 [H][c:13]:[#6,#7;a:1](:[c:5])-[#6:2]-[#6:3][N+:4]#[C-:21].[H][#6:6](-[#6:7])=O.[H][#8]-
 [#6:11](=O)~[#6:12]~[#6:14](=[O:15])-[#8:16]-[#6].[H][#7:8]([H])-[#6:9]-[#6:10](-[#8]-[#6])-
 [#8]-[#6]>>[H][#8:16]-[#6:14](=[O:15])~[#6:12]~[#6:11](=O)-[#7:8]-1-[#6:9]-[#6:10]-2-
 [c:13][#6,#7;a:1](:[c:5])-[#6:2]-[#6:3]-[#7:4]-2-[#6:21](=O)-[#6:6]-1-[#6:7]

Reductive amination

[H][#7:A;X3;!\$(NC=O):1]([H])[#6:2].[H][#6:3](-[#1,#6:4])=O.[#6:8]-
 [#7:7]=[C:5]=[O:6]>>[H][#7:7](-[#6:8])-[#6:5](=[O:6])-[#7:1](-[#6:2])[C:3]([H])([H])[#1,#6:4]

[H][#7;A;X3;!\$(NC=O):1]([H])[#6:2].[H][#6:3](-[#1,#6])=O.[H][#8]-[#6:7](-
 [#6:8])=[O:5]>>[H][C:3]([H])([#1,#6])[#7:1](-[#6:2])-[#6:7](-[#6:8])=[O:5]
 [H][#7;A;X3;!\$(NC=O):1]([H])[#6:2].[H][#6:3](-[#1,#6])=O.[#6:8]-
 [#6:7](Cl)=[O:5]>>[H][C:3]([H])([#1,#6])[#7:1](-[#6:2])-[#6:7](-[#6:8])=[O:5]
 [H][N:1]([H])[CH3:2].[H:7][C:3]([CH3:4])=O.[CH3:6][S:5](Cl)(=[O:8])=[O:9]>>[H:7][C:3]([H
])([CH3:4])[N:1]([CH3:2])[S:5]([CH3:6])(=[O:8])=[O:9]

Schöllkopf

[H][#7:2]([H])-[#6;!\$(C=[!#6])!\$(C#[!#6]):1].[H][#6:4](-
 [#6:3])=O.[H][#7;A;X3;H2,H1;!\$(NC=[!#6])!\$(NC#[!#6]):7]([#6:6])[#1,#6:5]>>[#6:3]-[#6:4]-
 1-[#7:2](-[#6:1])-[#6]=[#6](-[#7]-[#6]-1=O)-[#6](=O)-[#7:7](-[#6:6])-[#1,#6:5]
 [H][#7:2]([H])-[#6;!\$(C=[!#6])!\$(C#[!#6]):1].[H][#6:4](-[#6:3])=O>>[#6]-[#8]-[#6](=O)-[#6]-
 1=[#6]-[#7:2](-[#6:1])-[#6:4](-[#6:3])-[#6](=O)-[#7]-1

Thienodiazepine

[CH3:7][N+:5]#[C-
 :6].[H][CH:2]([H])[C:1]([H])=O.[H][N:3]([H])[CH3:4]>>[H][N:5]([CH3:7])[C:6](=O)C1[N:3](
 [CH3:4])C(=O)C2=C(S[CH:2]=[CH:1]2)N([H])C1=O

Tetrazole

[#6:3][N+:1]#[C-:2].[#6:6]-[#6:5](-[#1,#6:4])=O.[H][#7:7]([#6;A:8])-
 [#1,#6:9]>>[#6;A:8][#7:7](-[#1,#6:9])[C:5]([#6:6])([#1,#6:4])[#6:2]-1=[#7]-[#7]=[#7]-[#7:1]-1-
 [#6:3]

Thiazole

[H][#7](-[#6:1])-[#1,#6:3].[H][#16]-[#6:4](-
 [#1,#6:5])=O.[H][#7:6]([H])[#6;A;!\$(C=[!#6])!\$(C#[!#6]):7].[#6:9]-[#6:8](-

[#1,#6:10])=O>>[#6:1]-[#7:2](-[#1,#6:3])-[#6](=O)-[#6]-1=[#6]-[#16]-[#6](=[#7]-
1)[C:8]([#6:9])([#1,#6:10])[#7:6](-[#6:7])-[#6:4](-[#1,#6:5])=O

Ugi4C5Cr

[#6:8]-[#6:7](-[#7:6])-[#6:9](-[#8])=[O:10].[#6:4]-[#6:5](-[#1,#6:13])=O.[#6:3][N+:1]#[C-
:2].[#8:11]-[#1,#6:12]>>[#6:3]-[#7:1]-[#6:2](=O)[C:5]([#6:4])([#1,#6:13])[#7:6]-[#6:7](-[#6:8])-
[#6:9](=[O:10])-[#8:11]-[#1,#6:12]
[#6:8]-[#6:7](-[#7:6])-[#6:9](-[#8])=[O:10].[#6:4]-[#6:5](-[#1,#6:13])=O.[#6:3][N+:1]#[C-
:2].[H][#7]([#6;A:12])[#1,#6;A:11]>>[#6:3]-[#7:1]-[#6:2](=O)[C:5]([#6:4])([#1,#6:13])[#7:6]-
[#6:7](-[#6:8])-[#6:9](=[O:10])-[#7]([#6;A:12])[#1,#6;A:11]

UDC_Benzimidazole

[H][#7]([H])-[#6]-1=[#6]-[#6]=[#6,#7:1]-[#6:3]=[#6]-1-[#7]([H])[H].[#6:6]-[#6:5](-
[#1,#6:7])=O.[H][#8]-[#6:8](-[#1,#6:9])=O.[#6:11][N+:10]#[C-]>>[#6:11]-[#7:10]-
[#6](=O)[C:5]([#6:6])([#1,#6:7])[#7]-1-[#6:8](-[#1,#6:9])=[#7]-[#6]-2=[#6]-[#6]=[#6,#7:1]-
[#6:3]=[#6]-1-2
[H][#7:15]([H])-[#6:4]-1=[#6]-[#6]=[#6,#7:1]-[#6:3]=[#6:2]-1-[#7:16]([H])[H].[#6:6]-[#6:5](-
[#1,#6:7])=O.[H][#8]-[#6:8](=O)~[#6:9]~[#6:12](=[O:13])-[#8:14]-[#6].[#6:11][N+:10]#[C-
>>[H][#8:14]-[#6:12](=[O:13])~[#6:9]~[#6:8]-1=[#7:15]-[#6:4]-2=[#6]-[#6]=[#6,#7:1]-
[#6:3]=[#6:2]-2-[#7:16]-1[C:5]([#6:6])([#1,#6:7])[#6](=O)-[#7:10]-[#6:11]

Ugi-4-component

[H][#8]-[#6:2](-[#1,#6:1])=O.[H][#7:4]([H])[#6;A:3].[#6:5]-[#6:6](-
[#1,#6:10])=O.[#6:9][N+:8]#[C-:7]>>[#6:9]-[#7:8]-
[#6:7](=O)[C:6]([#6:5])([#1,#6:10])[#7:4]([#6;A:3])-[#6:2](-[#1,#6:1])=O

[H][#7:15]([H])-[#6:4]-1=[#6]-[#6]=[#6,#7:1]-[#6:3]=[#6:2]-1-[#7:16]([H])[H].[#6:6]-[#6:5](-
 [#1,#6:7])=O.[H][#8]-[#6:8](=O)~[#6:9]~[#6:12](=[O:13])-[#8:14]-[#6].[#6:11][N+:10]#[C-
]>>[H][#8:14]-[#6:12](=[O:13])~[#6:9]~[#6:8]-1=[#7:15]-[#6:4]-2=[#6]-[#6]=[#6,#7:1]-
 [#6:3]=[#6:2]-2-[#7:16]-1[C:5]([#6:6])([#1,#6:7])[#6](=O)-[#7:10]-[#6:11]

Van Leusen

[H][N:1]([H])[CH3:2].[H][C:3]([CH3:4])=O.[H][C:5]([CH3:6])=O.[H][N:7]([H])[C:8]([H:9])=
 O>>[H:9][C:8]1=[N:7][C:5]([CH3:6])=[C:3]([CH3:4])[N:1]1[CH3:2]

Zhu

[H][#7:2]([#1,#6;A:1])[#1,#6;A:3].[H][#8]-[#6](=O)-[#6:4](-[#6:5])-
 [#7].[H][#7:6]([#6;A:7])[#1,#6;A:12].[#6:10]-[#6:9](-
 [#1,#6:11])=O>>[#6;A:7][#7:6]([#1,#6;A:12])[C:9]([#6:10])([#1,#6:11])[#6]-1=[#7]-[#6:4](-
 [#6:5])=[#6](-[#8]-1)-[#7:2]([#1,#6;A:1])[#1,#6;A:3]

2.1.3 Principal Moment of Inertia

One particular property we were interested in was the measurement of the 3D nature of our compounds compared to existing popular Zinc library. 1000 randomly selected compounds from the Zinc database, as well as 1000 randomly selected compounds from each of our scaffolds were plotted for their principal moment of inertia. Normalized ratios of principal moment of inertia are plotted into two dimensional triangular graphs and then used to compare the shape space covered by different compound sets. It has been suggested that molecular shape diversity is a prerequisite for broad bioactivity.¹²⁸ As can be seen in Figure 2.26 our reactions cover a wide range of both 2D and 3D characteristics. These plots were done for all scaffolds uploaded to AnchorQuery and can be found in Appendix B.

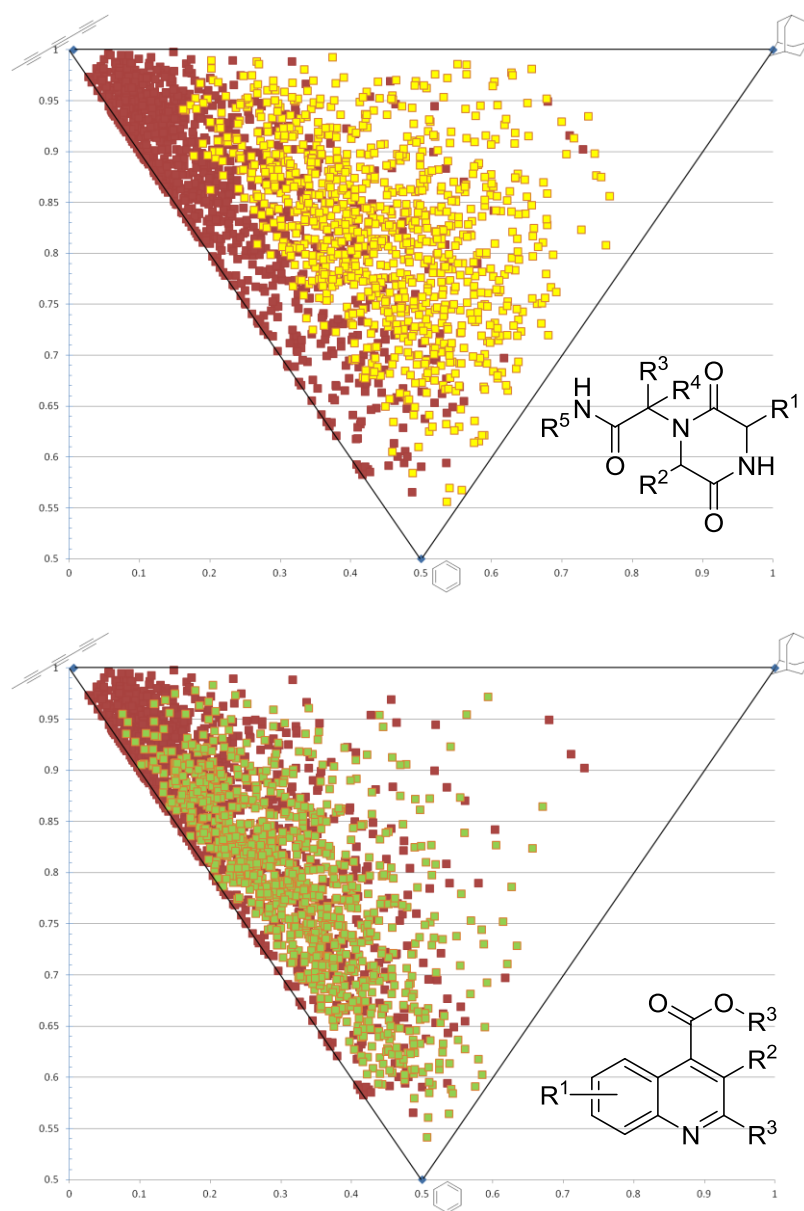


Figure 2.26 Principal moment of inertia for 1000 randomly selected compounds from the Diketopiperazine (Top, yellow squares) and Döbner (bottom green squares) reactions plotted against 1000 randomly selected compounds from the Zinc database (red squares).

2.2 ANCHORQUERY IMPLEMENTATION⁶⁸

AnchorQuery performs an exact pharmacophore search of anchor-oriented virtual libraries of explicit conformations. The computational performance of most pharmacophore search implementations is directly proportional to the size of the database limiting the effective size of virtual libraries. *AnchorQuery* pharmacophore search, like inverted-key fingerprint screening¹²⁹ and Recore,¹³⁰ scales with the breadth and complexity of the query, not the size of the database. However, unlike inverted-key fingerprint screening, *AnchorQuery* does not require a highly reduced and discretized search space nor is it limited to scaffold hopping.

AnchorQuery is provided as an open-access, full-featured web based program available at <http://anchorquery.ccbb.pitt.edu>. The ultimate goal of this technology is to facilitate true collaborations between biologists, experts on specific PPIs, and chemists interested in the rational design of small molecules. Pharmacophore features are automatically identified and can be edited within the graphical interface, shown in **Figure 2.1B**. Additional information, examples, and a user guide are provided at the website. Search performance is a function of the query, not the size of the database, and searches of almost one billion conformations can be performed in a matter of seconds (see online Interactive Examples). Screens can further prune the number of hits by setting a maximum number for hits per compound, pharmacophore matches, or molecular weight. The list of hits satisfying the query is ranked according to several possible criteria: pharmacophore matches, pharmacophore RMSD (pRMSD), MCR chemistry or molecular weight (MW). The user interface includes Jmol (<http://jmol.org>) based visualization of pharmacophore aligned or energy minimized hits. Equally important is that compounds are

linked to their “one-step one-pot” synthesis protocols, a key component in our goal to fast track the development of novel probes for chemical biology.

AnchorQuery has been validated as part of a drug discovery effort targeting the anti-cancer p53/MDM2 PPI. Concurrent to the development of *AnchorQuery*, we identified, synthesized and validated, using fluorescence polarization, 80 inhibitors (< 60μM binding activity) of p53/MDM2 that contain an indole tryptophan anchor analog.¹³¹ Additionally, we derived 13 active compounds from the results of *AnchorQuery* searches.

The pharmacophore of **Figure 2.1** is used to quickly generate an enriched subset of posed compounds. In **Figure 2.27A**, we keep the three lowest pRMSD conformational poses for each compound resulting in 77343 conformations (0.08% of the library conformations) of 34876 compounds (5.9% of the library compounds). The results include 78.5% of the known inhibitors resulting in an enrichment factor of more than 10x. The inset in **Figure 2.27a** shows the lowest pRMSD hit in the screen. This compound has a 20 μM binding affinity and belongs to a family of compounds that include sub-micromolar inhibitors.¹³¹ Note that the visualization tool of *AnchorQuery* provides a straightforward visual validation of the pharmacophore design, and allows the user to rapidly identify scaffolds that are a good starting point for rational modifications.

The accurate scoring of a diverse set of compounds is still an open problem¹³², and *AnchorQuery* does not directly facilitate such a secondary screening. Instead, we allow the user to download the results for in-house refinement. We use a multi-step energy-based secondary screen with pharmacophore filtering to refine and rank the results (see Methods). **Figure 2.27B** shows our hits re-ranked after a fast energy minimization and pharmacophore filtering of the docked structures predicted by *AnchorQuery*. This secondary screening quickly identifies

complexes with bad clashes (i.e., interaction energy > 0) resulting in a substantial enrichment of known actives in the top 5000 compounds (an enrichment factor of more than 50x relative to the full library). Energy minimization with a fixed receptor confirms that 89% of docked structures of validated inhibitors do not change much from their original pharmacophore aligned poses, strongly suggesting that our fast and exact pharmacophore alignments yield satisfactory low-resolution models. However, the best evidence that *AnchorQuery* selects a meaningful set of compounds is shown in **Figure 2.27C**, where a physically meaningful scoring function that includes solvation effects places almost all our previously developed high-affinity inhibitors in the top 150.

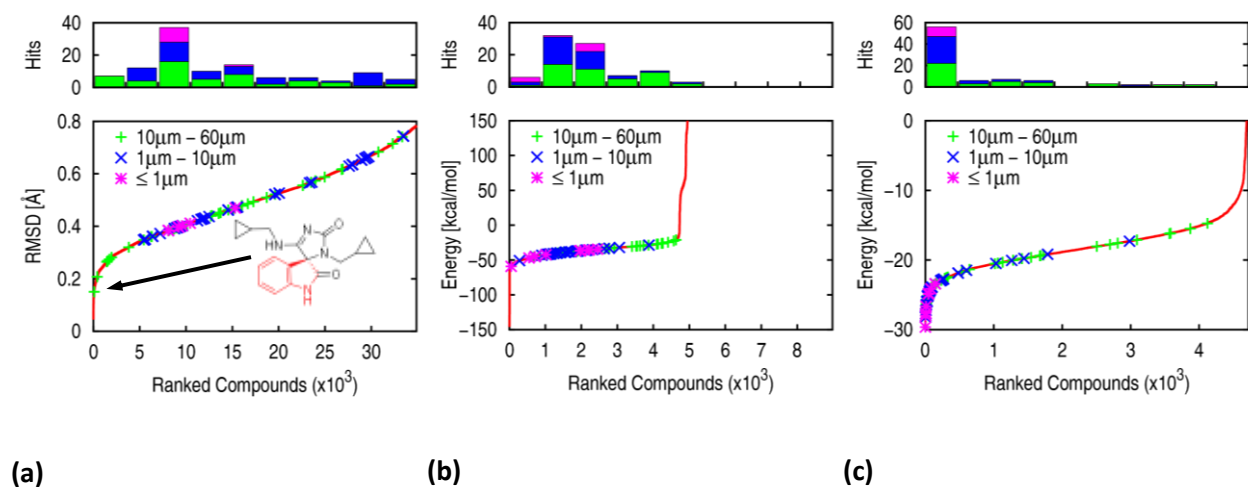


Figure 2.27 An evaluation of an AnchorQuery-based virtual screen. A prototype tryptophan-biased library was seeded with 93 validated inhibitors. Each active compound was annotated with the binding affinity of the racemic mixture. The resulting library was searched using the pharmacophore of **Figure 2.1**. (a) The position of active compounds of three affinity classes (points and histogram) within the RMSD ranked *AnchorQuery* pharmacophore search results (red line). Pharmacophore RMSD successfully extracts all the high affinity (sub-μM) known actives from the library. (b) A similar plot after fast minimization and pharmacophore filtering. This step effectively identifies compounds with unresolvable steric and electrostatic clashes and provides a more efficient starting configuration for the next minimization step. (c) After minimization using a Poisson-Boltzman solvent model, high-affinity compounds are noticeably differentiated from low-affinity compounds.

Our platform builds on the role anchor side chains, i.e., those that bury a large amount of surface area in the acceptor protein, have in PPIs. At the onset of the recognition process anchors target well-defined “druggable” pockets. We use chemical mimicry of these side chains to design small molecule inhibitors using fast and efficient MCR chemistry. Contrary to traditional stepwise multistep sequential synthesis, MCR assembles advanced starting materials into a new product in a “one-pot” procedure thus saving tremendous time and effort when testing the computational hypotheses. This approach has been successful in the development of a large set of novel and diverse active inhibitors of MDM2 and p53 interactions, with crystal structures confirming the benefits of targeting the known chemistry of anchor side chains.

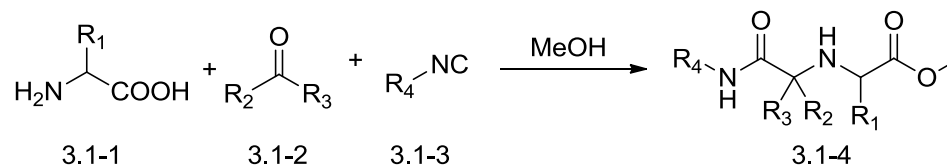
Despite the thousands of validated protein-protein interactions, the pace of discovery of chemical probes that can dissect the role of individual protein interactions in signaling pathways remains slow. Besides technical barriers, a major shortcoming in these efforts is the lack of synergy between mature disciplines like chemistry, which seeks to develop molecules with “drug-like” properties, and biology, which often inquires about protein-protein interactions. *AnchorQuery* is a unique open-access technology that facilitates truly integrative and interdisciplinary research as it allows diverse communities to come together with little or no effort to incorporate their PPI expertise and test their own insights and assays in discovery strategies of chemically accessible small molecular weight probes of protein function.

3.0 DISCOVERY OF NEW MULTICOMPONENT REACTIONS FOR VIRTUAL SCREENING

Multicomponent reaction technology (MCR) is now widely recognized for its impact on drug discovery projects and is strongly endorsed by industry in addition to academia.¹³³ Thus an increasing number of products based on MCRs are marketed or in development. Recent examples include boceprevir,¹³⁴ retosiban¹³⁵ or mandipropamide,¹³⁶ just to name a few. While the number of described MCRs is enormous, only a small number has a wide breath in all classes of educts and allows for the quasi infinite variation of all starting materials.^{49,106,137,138} The size of the chemical space of the different MCR scaffolds, however, has major implications on the usefulness of the particular MCR. For example, the classical Ugi four component reactions allows for the simultaneous variation of four very common starting materials (amine, oxo-component, carboxylic acid and isocyanide, which is derived from a primary amine).⁹² Thus the number of synthesizable products is very large.⁹³ On the other hand, the three component reaction of sulfur, carbon monoxide and epoxides yielding oxathiolan-2-ones, although synthetically very useful can yield only a rather limited number of products.¹³⁹ Different strategies for the design of molecular complexity using MCR chemistry have been devised.¹⁴⁰⁻¹⁴² We would like to report here on a novel stereoselective Ugi-type reaction of the four highly variable starting materials α -amino acid, oxo-component, isocyanide and primary or secondary amine, thus comprising a novel true 4-CR.

3.1 IMINODICARBOXAMIDES BY VARIATION OF THE UGI-4-COMPONENT-5-CENTERED REACTION¹⁴³

Years ago Ugi et al. described the first time the discovery of a novel variant of his now classic isocyanide based reaction. (**Scheme 3-1**).¹⁴⁴ The reaction was termed U-5C-4CR (5-center-4-component) because of the use of bireactive α -amino acids, oxo-components, isocyanides and alcohol as a solvent and reactant. The reaction proved to be versatile and several reports document their usefulness.¹⁴⁵⁻¹⁵² Remarkably, this reaction also led to the first orally available potent, selective and non peptide oxytocin antagonist, currently undergoing clinical trials for preterm birth.^{135,153}

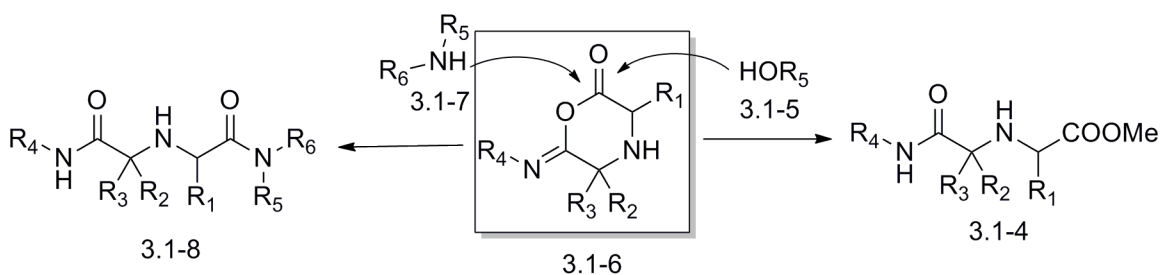


Scheme 3-1 Classic Ugi-4-Component-5-Centered Reaction

This reaction, however only comprises a MCR where three components show a great variability: the α -amino acid (**3.1-1**), the oxo-component (**3.1-2**) and the isocyanide (**3.1-3**). The variability of the alcohol component, which is also the solvent, is rather restricted towards low molecular weight liquids, for example methanol or ethanol. The restriction is a result of the poor solubility of the amino acids in higher alcohols and their reduced nucleophilic reactivity.

The key reaction intermediate is the six-membered α -adduct (**3.1-6**) which is formed by the α -amino acid, the oxo-component and the isocyanide which classically react with an alcohol (**3.1-5**) to form the linear product (**3.1-4**) by the nucleophilic attack of the solvent methanol (**Scheme 3.1-2**). We envisioned that an *N*-nucleophile of a primary or secondary amine (**3.1-7**), could potentially also work as a nucleophile and successfully compete with the alcohol solvent to

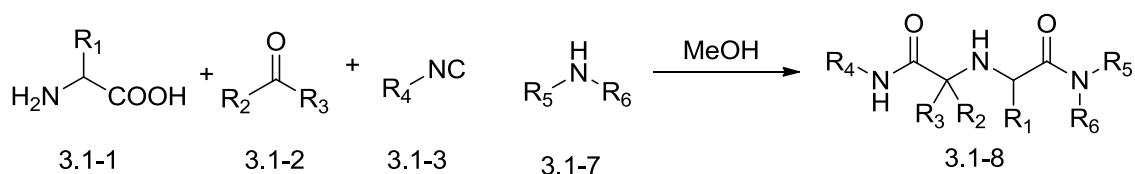
attack the 6-membered α -adduct (**3.1-6**) leading to the iminodicarboxamide derivative (**3.1-8**). The outcome of the projected reaction however was a priori unclear since the amino acid amine (**3.1-1**) and the external primary or secondary amine (**3.1-7**) could compete for the oxo-component and result into different types of Ugi or Passerini products (e.g. via U-5C-4CR, U-4CR, U-3CR or P-3CR) or mixtures thereof. As intramolecular reactions tend to be more favorable, we hypothesized that use of the amino acid as a bifunctional starting material would preferentially form the α -adduct over the intermolecular classic Ugi reaction. Additionally a reaction funneling into the projected reaction pathway would be of high value since this would comprise one of the very few four component reactions which are truly variable in all components.



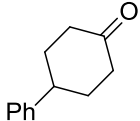
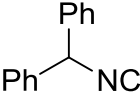
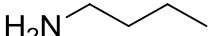
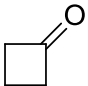
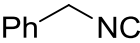
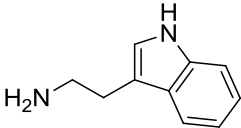
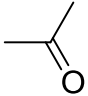
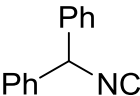
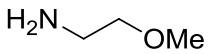
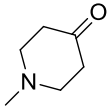
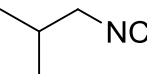
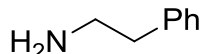
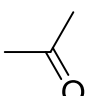
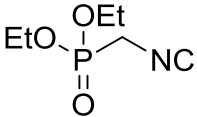
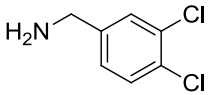
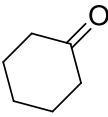
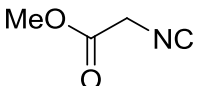
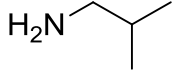
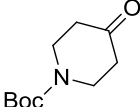
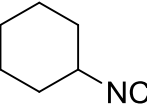
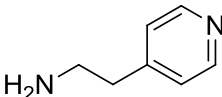
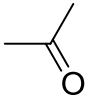
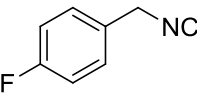
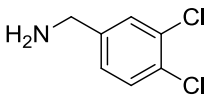
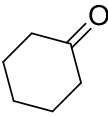
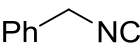
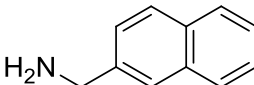
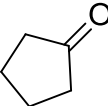
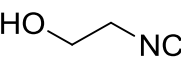
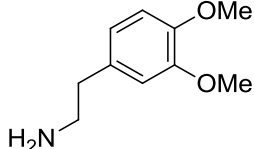
Scheme 3-2 Ugi Proposed Intermediate

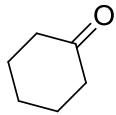
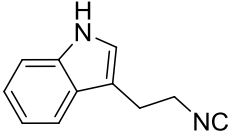
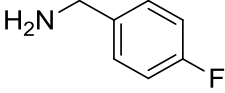
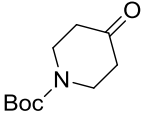
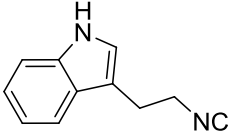
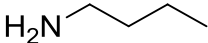
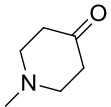
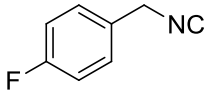
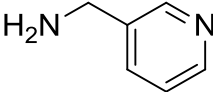
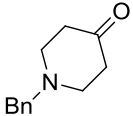
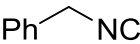
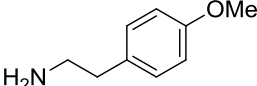
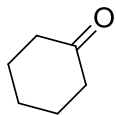
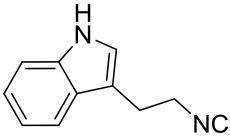
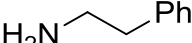
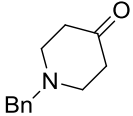
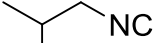
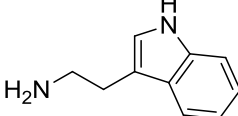
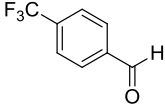
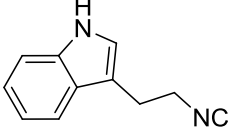
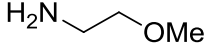
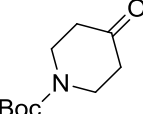
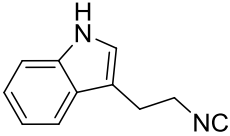
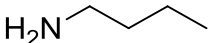
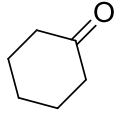
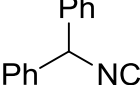
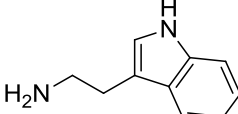
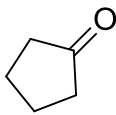
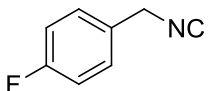
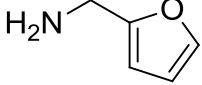
To test our MCR hypothesis we first reacted alanine, 2-fluorobenzaldehyde, 4-fluorobenzyl isocyanide, and morpholine and surprisingly found the expected compound **3.1-8AN** as the major product. Extensive optimization was performed including the parameter solvent, temperature, w/o microwave, reaction time and catalyst and their influence on different combinations of starting materials. In previous Ugi type reactions where intramolecular cyclization of the α -adduct occurs trifluoroethanol (TFE) or similar solvents were advantageously used due to their reduced nucleophilicity.^{154,155} Unexpectedly when TFE was used as a solvent in this reaction it was found to produce a significant amount of

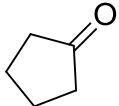
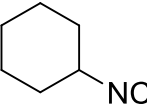
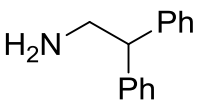
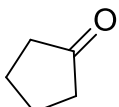
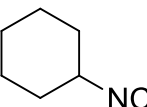
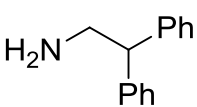
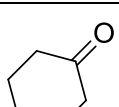
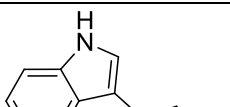
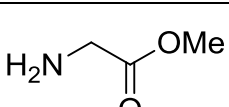
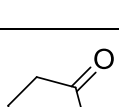
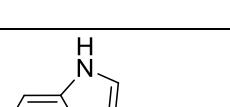
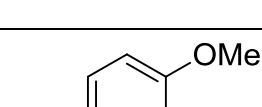
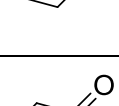
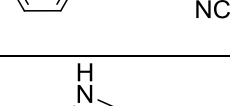
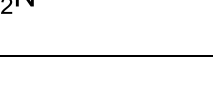
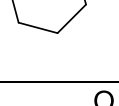
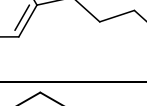
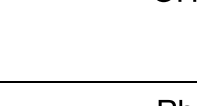

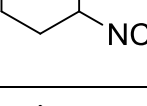
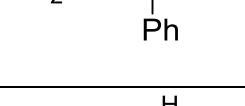
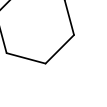
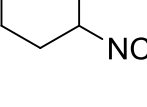
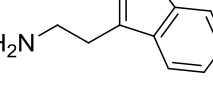
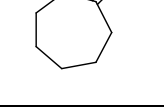
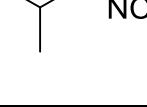
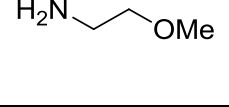
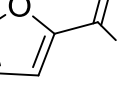
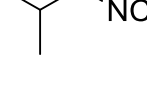
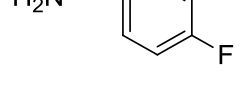
trifluoroethylester **3.1-4'** as side product. An optimal solvent mixture was found to be MeOH/water 4/1, which is a compromise in solubility for the different classes of starting materials. Due to the poor solubility of most amino acids we attempted to speed up the reaction via microwave conditions, from 60-120 °C for anywhere from 30min to 2 hours. While under these conditions the amino acid completely solubilized in the reaction mixture, however no increase in yield was found. Due to the formation of unwanted side products, and therefore an increased difficulty in separation, the benefit from the time gained by using microwave conditions was outweighed by the amount of extra time spent optimizing separation conditions; instead room temperature for 3 days was used.



Entry	Amino Acid (3.1-1)	Oxo-component (3.1-2)	Isocyanide (3.1-3)	Amine (3.1-6)	Yield (%)
3.1-8A	Ala				54
3.1-8B	Leu				44
3.1-8C	Trp				43
3.1-8D	Phe				40 6:1 ^[b]

3.1-8E	Gly				42 1:1 ^[b]
3.1-8F	Ile				54
3.1-8G	Pro				40
3.1-8H	Trp				51
3.1-8I	Trp				52
3.1-8J	O- tBut- Tyr				47
3.1-8K	O- tBut- Ser				41
3.1-8L	Pro				45
3.1-8M	O- tBut- Glu				41
3.1-8N	Ile				33

3.1-8O	Val				54
3.1-8P	O- tBut- Tyr				47
3.1-8Q	Ile				51
3.1-8R	Val				53
3.1-8S	SelenoMet				50
3.1-8T	Met				40
3.1-8U	Leu				34 10:1 ^[a]
3.1-8V	Tyr				25
3.1-8W	O- tBut- Ser				40
3.1-8X	N-Trt- Gln			 6{20}	41

3.1-8Y	Phe				38
3.1-8Z	Trp				37
3.1-8AA	Phe				63
3.1-8AB	N-Boc-Lys				62
3.1-8AC	Phe				30
3.1-8AD	Leu				48
3.1-8AE	Leu				46
3.1-8AF	O-tBut-Tyr				23
3.1-8AG	O-tBut-Tyr				31 8:1 ^[a]
3.1-8AH	Ser				23

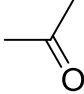
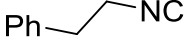
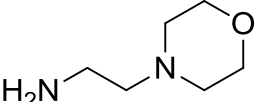
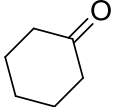
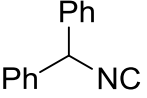
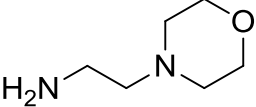
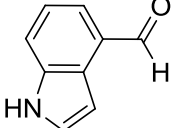
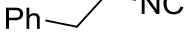
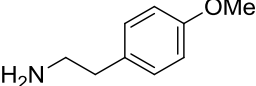
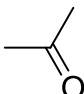
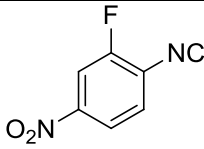
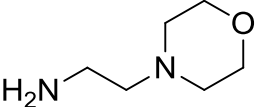
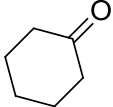
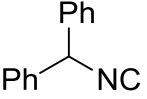
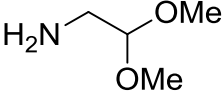
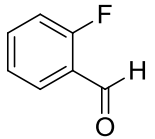
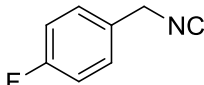
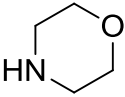
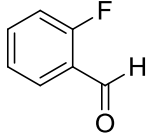
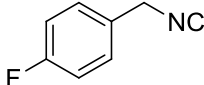
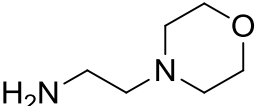
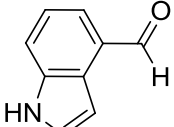
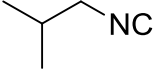
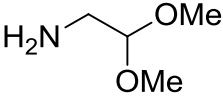
3.1-8AI	Trp				38
3.1-8AJ	5-HTP				34
3.1-8AK	Gly				41
3.1-8AL	Phe				25
3.1-8AM	Trp				47
3.1-8AN	Ala				32 9:1 ^[a]
3.1-8AO	Ala				28 6:1 ^[a]
3.1-8AP	Aib				30

Table 3-1 Ugi-4C-5Cr reaction products and yields [a] d.r. determined by UV [b] d.r. determined by NMR

Next we investigated the scope of the reaction by using representative starting materials of each class and synthesizing a library of iminobisamides (**Table 3-1**). Not surprisingly it was found that the identity of the starting materials and their specific combinations played a role for the overall yields and selectivity of the reaction. We successfully used virtually all natural α -

amino acids and some non natural ones, including hindered aminoisobutyric acid (**3.1-8AP**) or oxidation labile selenomethionine (**3.1-8S**) and 5-hydroxy tryptophan (**3.1-8AJ**). It was found that while use of tyrosine gave the desired product, (**3.1-8V**); using tert-butyl protected tyrosine gave product (**3.1-8P**) in much better yields (25% vs 47% respectively). Similar results were seen between serine and tert-butyl protected serine for products **3.1-8AH** and **3.1-8W** (23% and 40% respectively). Therefore amino acids with reactive side chains (e.g. Ser, Glu, Asp, Lys) were used in their side chain protected form. As oxo-components (**3.1-2**), we often used symmetrical ketones for the sake of formation of only one stereoisomer, however either aldehydes or ketones worked equally well in this reaction. Cyclic ketones, cyclobutanone, cyclopentanone, and cyclohexanone worked well in the reaction, while cycloheptanone and ketones of higher ring size worked with sub-optimal yields, e.g. (**3.1-8AF**, 23%). Different isocyanides (**3.1-3**) were used including aromatic, heteroaromatic, aliphatic and bulky ones and worked generally well. Primary and secondary amines were used as the forth component (**3.1-7**), and generally worked well including functionalized, heterocyclic, aromatic and heteroaromatic ones. As part of the NIH roadmap initiative, a project aiming to address roadblocks to research and to transform the way biomedical research is conducted by providing a large and diverse publicly available compound library for the discovery of molecular probes, we synthesized up to now more than 400 compounds based on this reaction.¹⁵⁶ Yields of representative compounds are summarized in **Table 3-1**.

All reactions were performed on a 0.5 mmol scale and the products were purified to their enantiomers by efficient and fast supercritical fluid carbon dioxide (SFC) technology. The yields in most cases are satisfactory taking into account the complexity of the reaction, between 40 and 60% after chromatographic separation.

Next we asked the question of the stereochemical integrity of the formed products. Thus all reactions performed were investigated by chiral supercritical fluid chromatography (SFC, SI). We investigated the influence of the amine component on the integrity of the amino acid stereocenter. We found that primary amines lead to retention of the stereochemical integrity of the amino acid stereocenter, whereas secondary amines are leading to partial racemization. This can be rationalized by the typical 1-2 units higher pK_B of secondary amines. For example use of 2-fluorobenzaldehyde with L-Alanine, benzyl isocyanide and morpholine, lead to the formation of 4 stereoisomers which have been conveniently separated using chiral SFC; when 2-morpholinoethylamine was used only 2 stereoisomers were found. Racemic D,L-Ala in these reactions was used as a control (Appendix A). As a further proof of the structures, we solved several compounds in molecular detail using single crystal x-ray analysis; **3.1-8Z** is shown in **Figure 3.1**. An example of a noteworthy combination is the use of phenylacetaldehyde, phenylalanine, iso-butyl isocyanide, and iso-butyl amine, which leads to C_2 and C_s symmetrical products in a ratio of 6:1 (**3.1-8D**) (**Figure 3.1**). Such, otherwise difficult to access, C_2 symmetrical compounds could potentially serve as chiral tridentate ligands for catalytic organic transformations.

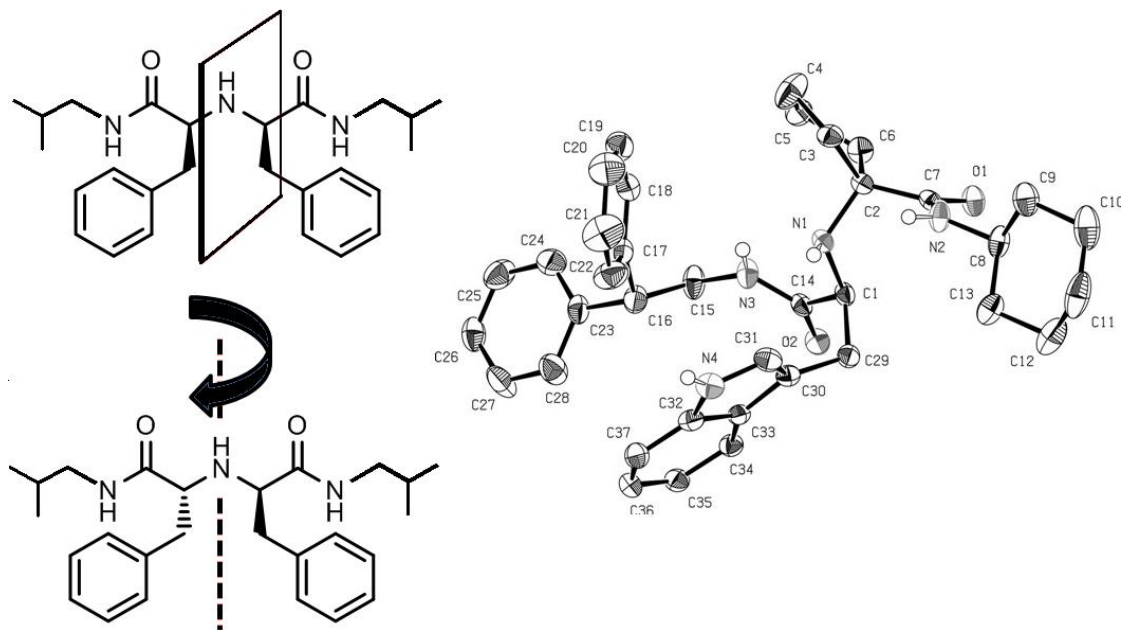


Figure 3.1 Ugi4C5Cr Xray: Left) Example of C_s and C_2 symmetrical products conveniently formed by the new 4CR. Right) ORTEP style plot of compound 3.1-8Z in the solid state.

Iminodicarboxamides are a particular useful class of scaffold and have been reported annotated with divers biological activities, including factor Xa,¹⁵⁷ HIV-1 protease,¹⁵⁸ renin¹⁵⁹, thrombin,¹⁶⁰ and most recently p53/mdm2 inhibition.⁶⁵ Our herein reported one-pot synthesis towards this scaffold comprises a major advancement and is superior to reported stepwise sequential or MCR approaches, in terms of yield, time, effort, stereochemistry and breath of useful starting materials.¹⁶¹⁻¹⁶³ The scope of the extended Ugi 4-CR is good in all investigated starting materials and a very large number of products are theoretically accessible. This is significant since recent trends in drug discovery using MCR chemistry more and more leverage the usage of virtual screening tools.^{65,164,165} Towards this end, we introduced a freely accessible virtual compound library of ~5 million compounds based on this backbone in the recently published ANCHOR.QUERY software for the discovery of protein-protein interaction antagonists.⁶⁵ In conclusion we described a novel and rare case of a 4CR where all four starting material classes can be widely combined which each other.

3.1.1 Materials and Methods

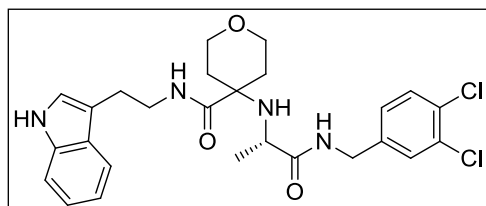
Generalities

Dry solvents were purchased from Aldrich, Fisher Scientific, AcrosOrganics or Alfa Aesar and used as received. ^1H - and ^{13}C NMR spectra were recorded on a Bruker Ultrashield Plus 600. Chemical shift values are in ppm relative to TMS. Abbreviations used are s=singlet, brs=broad singlet d=doublet, dd=double doublet, t=triplet, q=quartet, m=multiplet; data in parenthesis are given in the following order: multiplicity, number of protons, and coupling constants in Hz. MS spectra were recorded on a Waters Super Critical Fluid Chromatograph with a 3100 MS Detector using solvent system of Methanol and CO_2 on either an ethyl pyridine, Regis Cell OD, or Chromegachiral CC4 column.

General Procedure for Compounds 3.1-8

A mixture of amino acid **3.1-1** (0.5 mmol) aldehyde/ketone **3.1-2** (0.5 mmol), aryl/aliphatic isocyanide **3.1-3** (0.5 mmol) and primary/secondary amine **3.1-7** (0.5 mmol), in 0.1 M of MeOH/ H_2O (4:1) were stirred for 24 – 72 hours at room temperature. Solvents were evaporated under reduced pressure and 2mls DCM were added to the residue. Unreacted amino acid was filtered off and filtrate was evaporated to get crude product, which was purified on SFC using MeOH to yield title compound.

(S)-N-(2-(1H-Indol-3-yl)ethyl)-4-((1-((3,4-dichlorobenzyl)amino)-1-oxopropan-2-



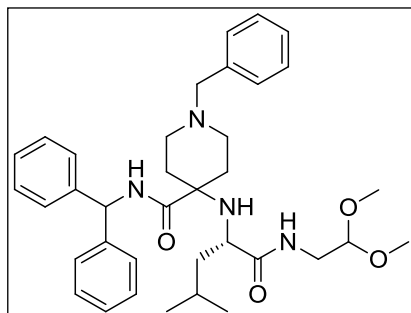
yl)amino)tetrahydro-2H-pyran-4-carboxamide [3.1-

8A]: 54%; yellow solid; HRMS (APCI, m/z): $[\text{M}+\text{H}]^+$: 517.17; found: 517.24; ^1H NMR (600 MHz, CDCl_3)

δ 1.02-1.03 (d, 3H), 1.27-1.29 (t, 1H), 1.47-1.49 (m, 1H), 1.82-1.87 (m, 1H), 1.90-1.94 (m, 1H), 2.07 (m, 1H), 2.77-2.80 (q, 1H), 2.91-2.95 (m, 1H), 3.03-3.07 (m, 1H), 3.52-3.69 (m, 7H), 4.12-

4.15 (m, 1H), 4.21-4.24 (q, 1H), 4.26-4.30 (q, 1H), 6.71-6.73 (m, 1H), 6.91-6.93 (m, 1H), 7.02-7.04 (m, 2H), 7.09-7.12 (m, 1H), 7.17-7.19 (m, 1H), 7.28-7.29 (m, 1H), 7.35-7.37 (m, 2H), 7.59-7.61 (m, 1H), 8.48 (s, 1H); ^{13}C NMR (150 MHz, CDCl_3) δ 14.1, 21.7, 24.9, 31.5, 36.1, 39.8, 42.1, 52.8, 59.4, 60.4, 63.7, 111.4, 112.6, 118.7, 119.4, 122.1, 122.2, 127.0, 129.5, 130.6, 131.5, 132.1, 136.4, 138.6, 175.1, 175.9 ppm.

(S)-N-Benzhydryl-1-benzyl-4-((1-((2,2-dimethoxyethyl)amino)-4-methyl-1-oxopentan-2-



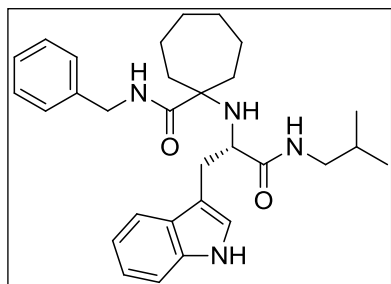
yl)amino)piperidine-4-carboxamide [3.1-8B] 44% as yellow

oil; HRMS (APCI, m/z): $[M]^+$ calc.: 601.37; found: 601.47;

^1H NMR (600 MHz, CDCl_3) δ 0.75-0.76 (d, 3H), 0.77-0.78 (d, 1H), 0.92-0.94 (t, 1H), 1.21-1.23 (m, 1H), 1.42-1.49 (m,

3H), 1.64-1.69 (m, 2H), 1.82-1.87 (m, 1H), 2.04-2.07 (m, 2H), 2.13-2.18 (m, 2H), 3.02-3.06 (t, 1H), 3.25 (s, 1H), 3.30-3.32 (m, 2H), 3.33-3.34 (m, 5H), 3.46 (s, 1H), 3.64 (s, 1H), 4.33-4.35 (m, 1H), 6.16-6.17 (d, 1), 7.22-7.28 (m, 6H), 7.30-7.32 (m, 4H), 7.33-7.36 (5H), 7.54-7.55 (m, 2H); ^{13}C NMR (150 MHz, CDCl_3) δ 22.0, 23.1, 24.5, 40.5, 48.2, 49.4, 49.6, 50.6, 54.2, 56.2, 57.1, 62.2, 98.8, 100.0, 102.2, 127.0, 127.3, 127.4, 127.4, 127.7, 128.5, 128.6, 128.7, 128.8, 129.6, 141.4, 141.5, 174.2, 175.8 ppm.

(S)-1-((3-(1H-Indol-3-yl)-1-(isobutylamino)-1-oxopropan-2-yl)amino)-N-



benzylcycloheptanecarboxamide [3.1-8C]: 28% as yellow oil;

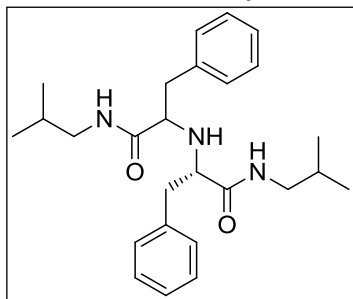
HRMS (APCI, m/z): $[M]^+$ calc.489.32; found: 489.38; ^1H NMR

(600 MHz, CDCl_3) δ 0.76-0.78 (t, 6H), 1.53-1.60 (m, 12H), 2.93-2.95 (t, 2H), 2.97-3.01 (m, 1H), 3.05-3.08 (m, 1H), 3.21-

3.24 (t, 1H), 3.49-3.52 (m, 1H), 4.24-4.27 (m, 1H), 6.08-6.09 (m, 1H), 6.83-6.84 (m, 1H), 6.99 (s, 1H), 7.09-7.10 (m, 2H), 7.11-7.14 (m, 1H), 7.20-7.22 (m, 1H), 7.24-7.26 (m, 1H), 7.28-7.33

(m, 4H), 7.56-7.57 (d, 1H), 8.13 (s, 1H); ^{13}C NMR (150 MHz, CDCl_3) δ 20.0, 22.7, 23.1, 28.2, 30.7, 30.8, 31.5, 34.1, 40.1, 42.7, 46.8, 58.7, 65.6, 99.9, 103.2, 111.4, 111.5, 118.8, 119.8, 122.3, 123.4, 127.1, 127.2, 127.3, 128.5, 136.3, 138.9, 175.5, 176.9 ppm.

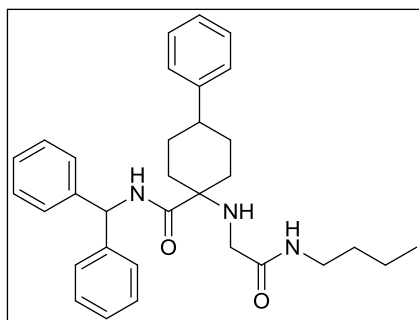
(2'S)-2,2'-Azanediylbis(N-isobutyl-3-phenylpropanamide) [3.1-8D] diastereomeric



mixture]: 40% as white solid; HRMS (APCI, m/z): $[\text{M}]^+$ calc.: 424.29; found: 424.38; ^1H NMR (600 MHz, CDCl_3) δ 0.823-0.847 (m, 12H), 1.67 -1.69 (m, 3H), 2.81-2.84 (m, 2H), 2.92-2.95 (m, 2H), 2.99-3.05 (m, 4H), 3.32-3.34 (m, 2H), 6.92-6.93 (m, 4H),

7.23-7.24 (m, 6H), 7.26-7.28 (m, 2H); ^{13}C NMR (150 MHz, CDCl_3) δ 20.0, 20.0, 28.3, 38.6, 46.6, 63.2, 126.9, 128.5, 128.8, 129.2, 129.3, 136.6, 172.5 ppm.

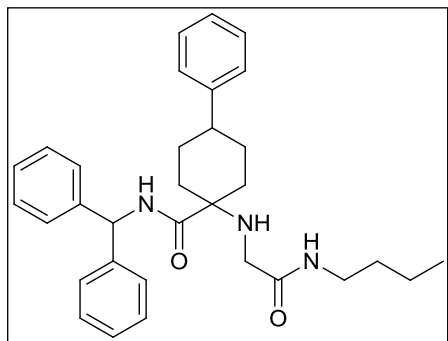
N-Benzhydryl-1-((2-(butylamino)-2-oxoethyl)amino)-4-phenylcyclohexanecarboxamide,



[3.1-8E (Isomer A)]: 19% as white powder (43% yield for both isomers) HRMS (APCI, m/z): $[\text{M}]^+$ calc.: 497.30; found: 498.38; ^1H NMR (600 MHz, CDCl_3) δ 0.825-0.849 (t, 3H), 1.19-1.26 (m, 2H), 1.31-1.36 (quin, 2H), 1.46 -1.54 (m, 2H),

1.78-1.82 (m, 4H), 1.98-2.03 (m, 2H), 2.49-2.53 (m, 1H), 3.02 (s, 2H), 3.11-3.14 (q, 2H), 6.14-1.16 (d, 2H), 7.13-7.15 (m, 6H), 7.18-7.22 (m, 4H), 7.23-7.26 (m, 5H), 7.71-7.73 (d, 1H); ^{13}C NMR (150 MHz, CDCl_3) δ 13.8, 20.1, 30.7, 31.6, 36.0, 38.9, 43.7, 46.5, 56.6, 60.7, 126.1, 126.9, 127.3, 127.5, 128.3, 128.7, 141.6, 146.3, 170.8, 173.6 ppm.

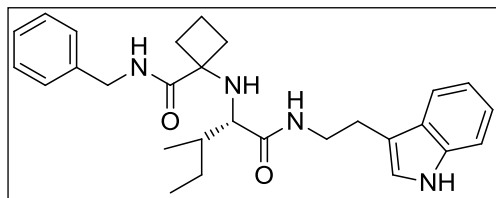
N-Benzhydryl-1-((2-(butylamino)-2-oxoethyl)amino)-4-phenylcyclohexanecarboxamide,



[3.1-8E (Isomer B)]: 23% as white powder (43% yield for both isomers) HRMS (APCI, m/z): $[M]^+$ calc.: 497.30; found: 498.38; ^1H NMR (600 MHz, CDCl_3) δ 0.826-0.851 (t, 3H), 1.21-1.26 (m, 2H), 1.31-1.34 (m, 2H), 1.35-1.41 (m, 2H), 1.75-1.81 (m, 4H), 2.24-2.26 (d, 2H), 2.43-2.47 (m,

1H), 3.04 (s, 2H), 3.06-3.12 (q, 2H), 6.20-6.22 (d, 2H), 7.08-7.10 (m, 3H), 7.15-7.16 (m, 3H), 7.18-7.20 (m, 5H), 7.21-7.26 (m, 4H); ^{13}C NMR (150 MHz, CDCl_3) δ 13.8, 20.1, 28.7, 31.6, 31.9, 39.1, 43.0, 46.6, 56.6, 60.8, 126.3, 126.7, 127.4, 128.4, 128.7, 141.7, 146.1, 170.4, 175.1 ppm.

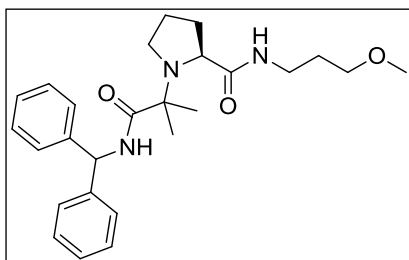
1-((1-((2-(1H-Indol-3-yl)ethyl)amino)-3-methyl-1-oxopentan-2-yl)amino)-N-



benzylcyclobutanecarboxamide, [3.1-8F]: 54% as white powder HRMS (APCI, m/z): $[M]^+$ calc.: 461.28; found: 461.34; ^1H NMR (600 MHz, CDCl_3) δ 0.716-

0.727 (d, 3H), 0.76-0.77 (d, 3H), 1.14-1.16 (quin, 1H), 1.27-1.30 (quin, 1H), 1.381.40 (m, 1H), 1.44-1.45 (m, 2H), 1.86-1.89 (m, 1H), 1.94-1.97 (m, 1H), 2.91-2.93 (t, 1H), 3.51-3.53 (m, 1H), 3.59-3.3.60 (m, 1H), 3.64-3.67 (m, 1H), 3.71-3.76 (m, 1H), 3.92-3.97 (m, 1H), 4.16-4.19 (t, 1H), 4.24-4.27 (m, 1H), 4.40-4.44 (m, 1H), 6.98-7.01 (t, 2H), 7.13-7.15 (m, 1H), 7.21-7.25 (m, 5H), 7.27-7.32 (m, 3H); ^{13}C NMR (150 MHz, CDCl_3) δ 20.1, 20.1, 28.4, 30.6, 35.4, 40.3, 45.9, 46.4, 51.4, 53.5, 57.7, 59.2, 110.8, 111.4, 119.0, 119.6, 122.1, 123.9, 126.4, 127.5, 128.5, 128.6, 136.5, 138.7, 174.9, 175.1 ppm.

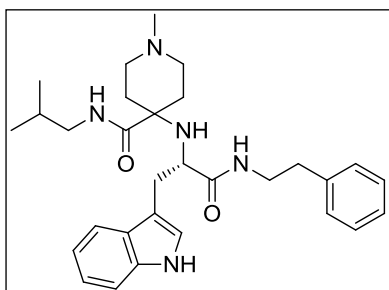
(S)-1-(1-(Benzhydrylamino)-2-methyl-1-oxopropan-2-yl)-N-(3-methoxypropyl)pyrrolidine-



2-carboxamide, [3.1-8G]: 40% as yellow oil; HRMS (APCI, m/z): $[M]^+$ calc.:438.27; found: 438.31; ^1H NMR (600 MHz, CDCl_3) δ 1.30 (s, 3H), 1.32 (s, 3H), 1.60-1.64 (m, 1), 1.67-1.72 (m, 2H), 1.74-1.78 (m, 1H), 1.88-1.92(m, 1H), 2.05-2.10 (m,

1H), 2.75-2.79 (m, 1H), 2.95-2.98 (m, 1H), 3.10 (s, 3H), 3.23-3.36 (m, 4H), 3.40-3.43 (m, 1H), 3.55-3.57 (m, 1H), 6.29-6.30 (d, 1H), 7.24-7.27 (m, 3H), 7.28-7.32 (m, 3H), 7.33-7.36 (m, 4H), 7.52 (s, 1H); ^{13}C NMR (150 MHz, CDCl_3) δ 18.8, 25.1, 25.8, 28.4, 32.1, 38.4, 49.3, 56.8, 58.6, 62.4, 63.3, 72.7, 127.4, 127.6, 128.6, 128.6, 141.52, 141.7 ppm

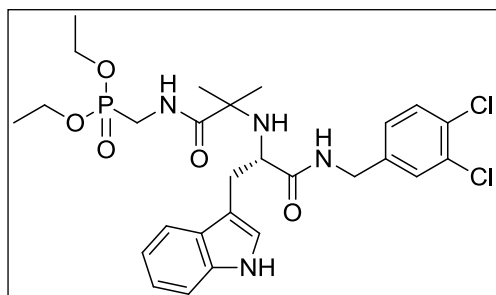
4-((3-(1H-Indol-3-yl)-1-oxo-1-(phenethylamino)propan-2-yl)amino)-N-isobutyl-1-



methypiperidine-4-carboxamide, [3.1-8H]: 51% as white solid; HRMS (APCI, m/z): $[M]^+$ calc.:504.33; found: 504.43 ^1H NMR (600 MHz, CDCl_3) δ 0.781-0.796 (m, 6H), 1.52-1.56 (m, 2H), 1.93-1.96 (m, 1H), 1.99-2.02 (m, 1H), 2.14 (s, 3H), 2.29-

2.33 (m, 1H), 2.36-2.39 (m, 1H), 2.47-2.53 (m, 2H), 2.56-2.59 *m, 1H), 2.88-2.90 (m, 1H), 3.01-3.05 (m, 1H), 3.09-1.13 (m, 1H), 3.25-3.26 (m, 1H), 3.34-3.40 (m, 2H), 6.49 (s, 1H), 6.65 (s, 1H), 6.93-6.94 (d, 2H), 7.08-7.11 (m, 2H), 7.16-7.22 (m, 4H), 7.36-7.37 (d, 1H), 7.62-7.64 (d, 1H), 9.20 (s, 1H); ^{13}C NMR (150 MHz, CDCl_3) δ 20.1, 20.1, 28.4, 30.6, 35.3, 40.3, 45.9, 46.4, 51.4, 51.5, 53.5, 57.7, 59.2, 110.8, 111.4, 119.0, 119.6, 122.1, 123.8, 126.4, 127.5, 128.5, 128.6, 136.5, 138,7, 174.9, 175.1 ppm.

diethyl((2-((1-((3,4-dichlorobenzyl)amino)-3-(1H-indol-3-yl)-1-oxopropan-2-yl)amino)-2-

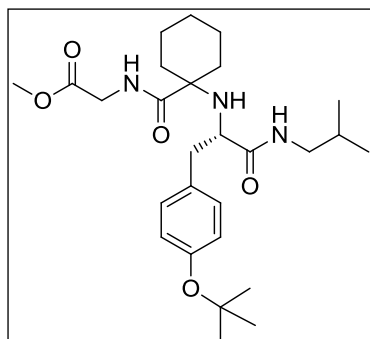


methylpropanamido)methyl)phosphonate, [3.1-8I]:

52% as yellow oil; HRMS (APCI, m/z): $[M]^+$ calc.:597.17; found: 597.30; ^1H NMR (600 MHz, CDCl_3) δ 1.12 (s, 3H), 1.23 (s, 3H), 1.25 - 1.28 (q, 6H),

2.99-3.03 (m, 1H), 3.13-3.16 (m, 1H), 3.32-3.47 (m, 1H), 3.51-3.57 (m, 1H), 3.99-4.04 (m, 4H), 4.25-4.27 (d, 1H), 4.55-4.56 (d, 2H), 6.89-6.91 (m, 1H), 7.01-7.03 (m, 1H), 7.09-7.11 (m, 1H), 7.16-7.20 (m, 1H), 7.29-7.30 (m, 1H), 7.38-7.41 (m, 2H), 7.45 (s, 1H), 7.50-7.51 (d, 1H), 7.60-7.64 (m, 2H), 7.91-7.91 (d, 1H), 8.65 (s, 1H); ^{13}C NMR (150 MHz, CDCl_3) δ 16.4, 23.3, 27.9, 31.1, 42.3, 43.0, 44.8, 58.7, 59.5, 62.6, 62.6, 111.0, 111.6, 118.6, 119.7, 122.3, 123.7, 126.2, 126.8, 127.1, 129.2, 129.4, 129.6, 130.5, 130.7, 131.1, 131.3, 131.7, 132.4, 132.7, 133.1, 133.7, 136.2, 136.4, 138.2, 138.4, 165.4, 175.6, 176.4 ppm.

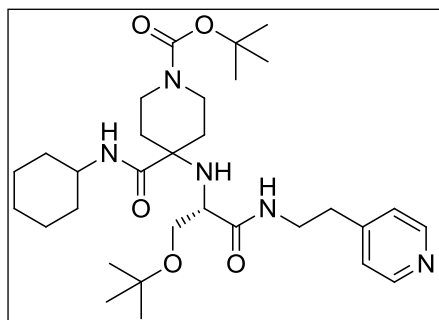
Methyl-2-(1-((3-(4-(tert-butoxy)phenyl)-1-(isobutylamino)-1-oxopropan-2-



yl)amino)cyclohexanecarboxamido)acetate [3.1-8J]: 47% as white solid; HRMS (APCI, m/z): $[M]^+$ calc.:490.32; found: 490.40; ^1H NMR (600 MHz, CDCl_3) δ 0.81-0.82 (m, 6H), 1.34 (s, 9H), 1.48-1.50 (m, 4H), 1.61-1.66 (m, 2H), 1.78-1.80 (m, 2H), 1.94-1.96 (m, 2H), 2.85-2.88 (m, 1H), 2.89-2.90 (m, 1H), 3.00-

3.04 (m, 1H), 3.22-3.24 (m, 1H), 3.74-3.75 (m, 1H), 3.77 (s, 3H), 3.78-3.79 (m, 1H), 3.89-3.92 (m, 1H), 6.91-6.93 (d, 2H), 7.12-7.14 (d, 1H), 7.29 (s, 1H); ^{13}C NMR (150 MHz, CDCl_3) δ 20.1, 21.7, 22.0, 25.2, 28.3, 28.8, 31.8, 35.8, 40.9, 41.0, 46.8, 52.2, 59.5, 61.7, 122.7, 122.9, 124.1, 130.1, 132.4, 154.1, 170.5, 174.7 ppm.

Tert-butyl 4-((3-(tert-butoxy)-1-oxo-1-((2-(pyridin-4-yl)ethyl)amino)propan-2-yl)amino)-



4-(cyclo-hexylcarbamoyl)piperidine-1-carboxylate [3.1-

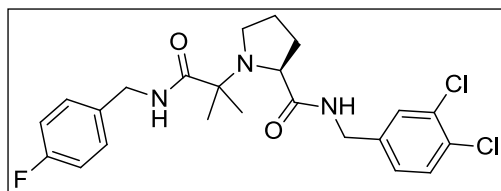
8K]: 41% as white solid; HRMS (APCI, m/z): $[M]^+$

calc.:574.39; found: 574.51; ^1H NMR (600 MHz, CDCl_3) δ

1.05-1.07 (m, 1H), 1.09 (s, 9H), 1.12-1.14 (m, 2H), 1.31-1.34

(m, 2H), 1.44 (s, 9H), 1.46-1.48 (m, 2H), 1.59-1.61 (m, 1H), 1.66-1.70 (m, 2H), 1.77-1.78 (m, 1H), 1.82-1.94 (m, 1H), 1.91-1.96 (m, 1H), 2.03-2.08 (m, 1H), 2.80-2.86 (m, 1H), 3.10-3.11 (m, 1H), 3.25-3.28 (m, 2H), 3.30-3.33 (m, 1H), 1.40-1.43 (m, 1H), 3.51-3.54 (m, 1H), 3.58-3.96 (m, 4H), 6.82-6.83 (m, 1H), 7.14-7.15 (d, 1H), 7.21 (m, 1H), 8.51-8.52 (m, 2H); ^{13}C NMR (150 MHz, CDCl_3) δ 24.9, 25.5, 27.38, 28.4, 32.9, 32.9, 33.3, 33.4, 35.0, 39.5, 48.1, 56.8, 60.3, 63.8, 74.0, 79.5, 124.0, 147.8, 149.9, 154.6, 173.8, 174.3 ppm.

N-(3,4-Dichlorobenzyl)-1-(1-((4-fluorobenzyl)amino)-2-methyl-1-oxopropan-2-



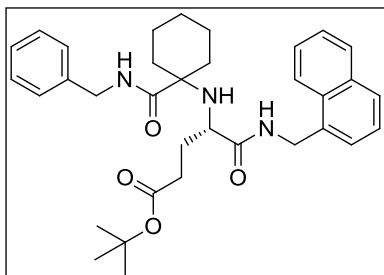
yl)pyrrolidine-2-carboxamide, [3.1-8L]: 45% as white

solid; HRMS (APCI, m/z): $[M]^+$ calc.: 466.14; found:

466.21; ^1H NMR (600 MHz, CDCl_3) δ 1.27 (s, 6H),

1.67-1.71 (m, 1H), 1.76-1.80 (m, 1H), 1.91-1.95 (m, 1H), 2.06-2.11 (m, 1H), 2.74-2.78 (m, 1H), 2.96-2.99(m, 1H), 3.65-3.67 (m, 1H), 4.23-4.40 (m, 4H), 6.80-6.81 (m, 1H), 6.98-7.01 (t, 1H), 7.05-7.06 (m, 1H), 7.17-7.19 (m, 2H), 7.31 (s, 1H), 7.34-7.36 (d, 1H), 7.57-7.59 (m, 1H); ^{13}C NMR (150 MHz, CDCl_3) δ 20.6, 25.0, 25.1, 32.2, 41.9, 42.7, 49.2, 62.0, 62.5, 115.5, 115.6, 126.8, 129.1, 129.4, 130.6, 131.3, 132.6, 134.2, 134.2, 138.9, 161.2, 162.9, 175.5, 176.3 ppm.

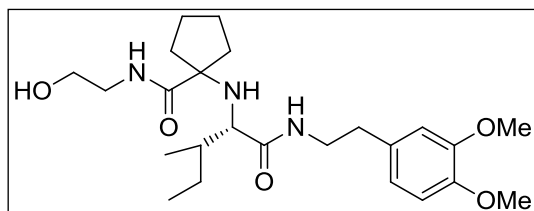
Tert-butyl 4-((1-(benzylcarbamoyl)cyclohexyl)amino)-5-((naphthalen-1-ylmethyl)amino)-



5-oxopentanoate [3.1-8M]: 41% as yellow oil; HRMS (APCI, m/z): $[M]^+$ calc.:558.33; found: 558.44; ^1H NMR (600 MHz, CDCl_3) δ 1.27-1.37 (m, 3H), 1.39 (s, 9H), 1.41-1.44 (m, 4H), 1.69-1.88 (m, 4H), 2.13-2.17 (m, 1H), 2.24-2.29 (m, 1H), 2.24-

2.29 (m, 1H), 3.07-3.09 (m, 1H), 4.27-4.31 (m, 1H), 4.33-4.36 (m, 1H), 4.80-4.87 (m, 2H), 7.06-7.09 (m, 1H), 7.16-7.18 (m, 1H), 7.22-7.26 (m, 2H), 7.28-7.31 (m, 2H), 7.40-7.41 (m, 2H), 7.50-7.53 (m, 2H), 7.80-7.81 (m, 1H), 7.86-7.88 (m, 1H), 7.98-8.00 (m, 1H); ^{13}C NMR (150 MHz, CDCl_3) δ 21.9, 22.1, 25.3, 28.0, 30.5, 31.5, 36.1, 41.4, 43.2, 56.5, 61.9, 80.5, 123.5, 125.3, 125.9, 126.5, 126.7, 127.3, 127.7, 128.5, 128.6, 128.7, 131.3, 133.5, 133.8, 138.6, 172.9, 174.5, 176.1 ppm.

1-(((2S,3R)-1-((3,4-Dimethoxyphenethyl)amino)-3-methyl-1-oxopentan-2-yl)amino)-N-(2-

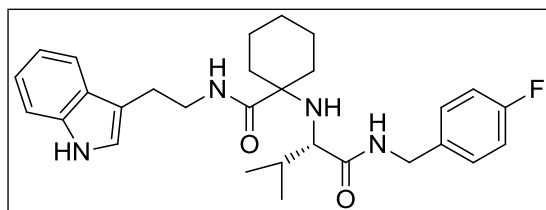


hydroxyethyl)cyclopentanecarboxamide [3.1-8N]:

33% as yellow solid; HRMS (APCI, m/z): $[M]^+$ calc.:450.29; found: 450.36; ^1H NMR (600 MHz,

CD_3OD) δ 0.83 (d, $J = 6.6$ Hz, 3H), 0.92-0.84 (m, 4H), 1.12-1.03 (m, 1H), 1.58-1.49 (m, 3H), 1.72-1.59 (m, 5H), 1.89-1.83 (m, 1H), 1.99 (dt, $J = 13.2, 7.8$ Hz, 1H), 2.81-2.70 (m, 2H), 2.85 (d, $J = 4.8$ Hz, 1H), 3.29 (dt, $J = 2.4, 6.0$ Hz, 1H), 3.44 (t, $J = 7.2$ Hz, 2H), 3.60 (t, $J = 6.0$ Hz, 2H), 3.83 (s, 3H), 3.79 (s, 3H), 6.77 (dd, $J = 8.4, 1.2$ Hz, 1H), 6.90-6.84 (m, 2H); ^{13}C NMR (150 MHz, CD_3OD) δ 12.2, 15.6, 24.7, 25.3, 26.9, 34.8, 35.9, 39.2, 41.2, 41.6, 43.0, 56.4, 56.5, 61.6, 63.7, 71.9, 113.2, 113.7, 122.1, 133.2, 149.1, 150.5, 177.2, 177.2, 179.1 ppm.

(S)-N-(2-(1H-Indol-3-yl)ethyl)-1-((1-((4-fluorobenzyl)amino)-3-methyl-1-oxobutan-2-



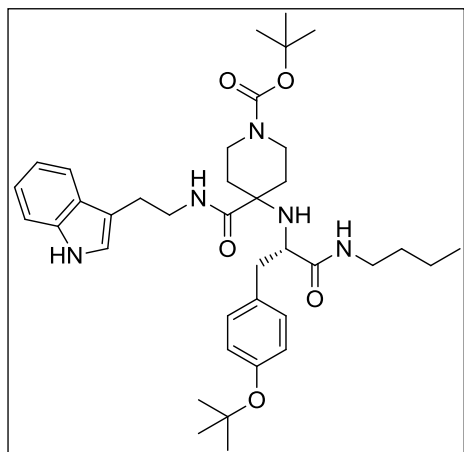
yl)amino)cyclohexanecarboxamide, [3.1-8O]:

54% as yellow solid; HRMS (APCI, m/z): $[M]^+$ calc.:493.29; found: 493.35; ^1H NMR (600 MHz,

CD_3OD) δ 0.79 (d, $J = 7.2$ Hz, 6H), 1.38–1.26 (m, 5H), 1.47–1.39 (m, 2H), 1.54–1.47 (m, 1H), 1.69–1.61 (m, 1H), 1.84 (br q, $J = 10.2$ Hz, 2H), 2.83 (d, $J = 5.4$ Hz, 1H), 3.01–2.89 (m, 2H), 3.46 (t, $J = 7.2$ Hz, 2H), 4.29 (s, 2H), 7.03–6.97 (m, 3H), 7.07 (s, 1H), 7.08 (t, $J = 7.2$ Hz, 1H), 7.29 (dd, $J = 8.4, 5.4$ Hz, 2H), 7.33 (d, $J = 8.4$ Hz, 1H), 7.57 (d, $J = 8.4$ Hz, 1H); ^{13}C NMR (150 MHz, CD_3OD) δ 19.2, 19.4, 23.4, 23.5, 26.2, 26.6, 33.6, 34.1, 36.5, 41.1, 43.3, 62.7, 63.2, 112.3, 113.1, 116.1 (d, $J = 21$ Hz), 119.4, 119.6, 122.4, 123.5, 128.7, 131.0 (d, $J = 9$ Hz), 136.0, 138.2, 163.5 (d, $J_{\text{CF}} = 243$ Hz), 177.2, 177.8 ppm.

(S)-tert-Butyl

4-((2-(1H-indol-3-yl)ethyl)carbamoyl)-4-((3-(4-(tert-butoxy)phenyl)-1-



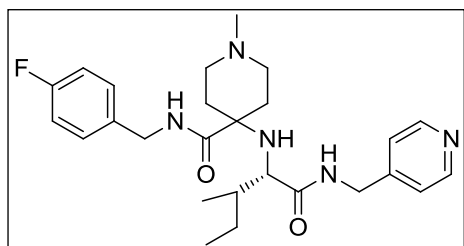
(butylamino)1-oxopropan-2-yl)amino)piperidine-1-

carboxylate, [3.1-8P]: 47% as white solid; HRMS (APCI,

m/z): $[M]^+$ calc.:662.42; found: 662.59; ^1H NMR (600 MHz, CD_3OD) δ 0.87 (t, $J = 7.8$ Hz, 3H), 1.39–1.20 (m, 13H), 1.43 (s, 9H), 1.67–1.58 (m, 1H), 1.92–1.85 (m, 1H), 2.59 (dd, $J = 8.4, 13.2$ Hz, 1H), 2.70 (dd, $J = 6.6, 13.8$ Hz,

1H), 2.86 (t, $J = 7.2$ Hz, 2H), 3.10–2.98 (m, 3H), 3.15 (t, $J = 7.2$ Hz, 1H), 3.30–3.17 (m, 3H), 3.50–3.38 (m, 2H), 6.87 (d, $J = 8.4$ Hz, 2H), 7.05–6.96 (m, 3H), 7.11–7.06 (m, 2H), 7.30 (d, $J = 8.4$ Hz, 1H), 7.57 (d, $J = 7.8$ Hz, 1H); ^{13}C NMR (150 MHz, CD_3OD) δ 14.1, 21.1, 26.1, 28.7, 29.2, 32.3, 32.7, 35.1, 40.1, 41.1, 41.9, 60.2, 60.9, 79.4, 81.0, 112.3, 113.0, 119.4, 119.6, 122.4, 123.5, 125.1, 128.8, 131.2, 134.1, 138.2, 155.4, 156.2, 177.2, 177.3 ppm.

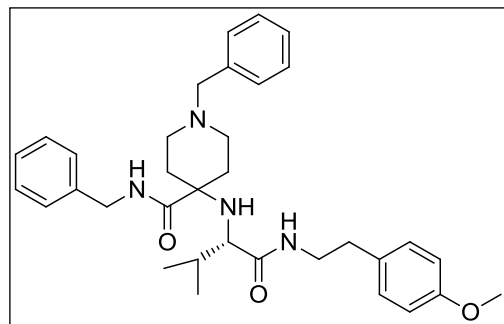
N-(4-Fluorobenzyl)-1-methyl-4-(((2S,3R)-3-methyl-1-oxo-1-((pyridin-4-



ylmethyl)amino)pentan-2-yl)amino)piperidine-4-carboxamide [3.1-8Q]: 51% as yellow oil; HRMS (APCI, m/z): $[M]^+$ calc.: 470.29; found: 470.35; ^1H NMR (600 MHz, CD_3OD) δ 0.83–0.76 (m, 6H), 1.05–0.96 (m, 1H),

1.53–1.43 (m, 2H), 1.59–1.53 (m, 1H), 1.77–1.70 (m, 1H), 2.02 (br s, 2H), 2.20 (s, 3H), 2.25–2.20 (m, 2H), 2.45 (br s, 1H), 2.57 (br s, 1H), 2.94 (d, $J = 4.8$ Hz, 1H), 4.20 (d, $J = 14.4$ Hz, 1H), 4.361 (d, $J = 14.4$ Hz, 1H), 4.364 (s, 2H), 7.03 (t, $J = 8.4$ Hz, 2H), 7.31 (dd, $J = 5.4, 8.4$ Hz, 2H), 7.40 (dd, $J = 4.8, 7.8$ Hz, 1H), 7.81 (d, $J = 7.8$ Hz, 1H), 8.43 (d, $J = 4.2$ Hz, 1H), 8.53 (s, 1H); ^{13}C NMR (150 MHz, CD_3OD) δ 12.2, 15.4, 26.9, 32.9 (br s), 35.3 (br s), 41.2, 41.4, 43.5, 45.9, 52.7 (br s), 60.3, 62.3, 116.1 (d, $J_{\text{CF}} = 21$ Hz), 125.2, 130.8 (d, $J_{\text{CF}} = 7.5$ Hz), 136.3 (d, $J_{\text{CF}} = 3$ Hz), 136.6, 138.2, 148.9, 150.0, 163.4 (d, $J_{\text{CF}} = 243$ Hz), 176.9 ppm.

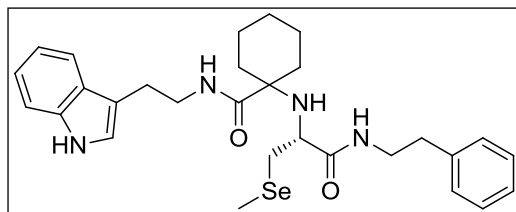
(S)-N,1-Dibenzyl-4-((1-((4-methoxyphenethyl)amino)-3-methyl-1-oxobutan-2-



yl)amino)piperidine-4-carboxamide [3.1-8R]: 53% as yellow powder; HRMS (APCI, m/z): $[M]^+$ calc.: 557.34; found: 557.44; ^1H NMR (600 MHz, CD_3OD) δ 7.35–7.23 (m, 10H), 7.14 (d, $J = 8.4$ Hz, 2H), 6.82 (d, $J = 8.4$

Hz, 2H), 4.39 (d, $J = 14.4$ Hz, 1H), 4.29 (d, $J = 15$ Hz, 1H), 3.74 (s, 3H), 3.51 (d, $J = 12.6$ Hz, 1H), 3.48 (d, $J = 13.2$ Hz, 1H), 3.43–3.34 (m, 2H), 2.82 (d, $J = 5.4$ Hz, 1H), 2.76–2.71 (m, 2H), 2.58 (br s, 2H), 2.43–2.20 (br m, 2H), 2.08–2.00 (br m, 2H), 1.76–1.68 (m, 2H), 1.62–1.55 (m, 1H), 0.84–0.78 (m, 6H). ^{13}C NMR (150 MHz, CD_3OD) δ - 19.2, 33.9, 35.5, 41.7, 44.2, 55.6, 60.8, 63.4, 63.9, 101.4, 102.6, 114.9, 128.2, 128.5, 128.8, 129.4, 129.5, 130.7, 130.8, 132.3, 140.1, 159.8, 177.0, 177.1 ppm.

(R)-N-(2-(1H-Indol-3-yl)ethyl)-1-((3-(methylselanyl)-1-oxo-1-(phenethylamino)propan-2-



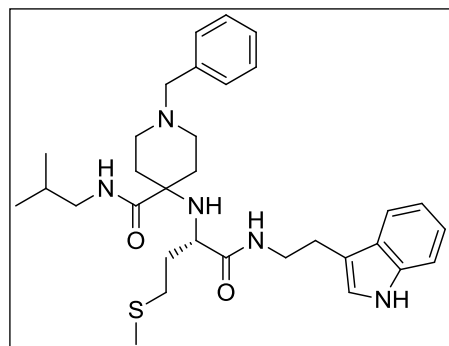
yl)amino)cyclohexanecarboxamide [3.1-8S]: 50% as

yellow oil; (APCI, m/z): $[M]^+$ calc.: 555.22; found:

555.30; ^1H NMR (600 MHz, CD_3OD) δ 1.52–1.26 (m,

8H), 1.90–1.72 (m, 5H), 2.51 (dd, $J = 12.6, 6.0$ Hz, 1H), 2.58 (dd, $J = 13.2, 6.6$ Hz, 1H), 2.84–2.72 (m, 2H), 3.02–2.90 (m, 2H), 3.14 (t, $J = 6.0$ Hz, 1H), 3.40 (t, $J = 7.2$ Hz, 2H), 3.49–3.42 (m, 1H), 3.59–3.52 (m, 1H), 6.99 (t, $J = 7.8$ Hz, 1H), 7.07 (s, 1H), 7.08 (d, $J = 7.8$ Hz, 1H), 7.18 (t, $J = 7.2$ Hz, 1H), 7.20 (d, $J = 7.2$ Hz, 2H), 7.26 (t, $J = 7.8$ Hz, 2H), 7.33 (d, $J = 8.4$ Hz, 1H), 7.57 (d, $J = 7.8$ Hz, 1H); ^{13}C NMR (150 MHz, CD_3OD) δ 4.9, 23.0, 23.1, 26.2, 26.5, 31.2, 32.9, 36.3, 36.5, 41.1, 41.8, 57.4, 62.7, 112.3, 113.1, 119.4, 119.6, 122.4, 123.5, 127.4, 128.7, 129.6, 138.2, 140.3, 176.7, 177.9 ppm.

(S)-4-((1-((2-(1H-Indol-3-yl)ethyl)amino)-4-(methylthio)-1-oxobutan-2-yl)amino)-1-benzyl-



N-isobutylpiperidine-4-carboxamide [3.1-8T]: 40% as

yellow oil; HRMS (APCI, m/z): $[M]^+$ calc.: 564.33; found:

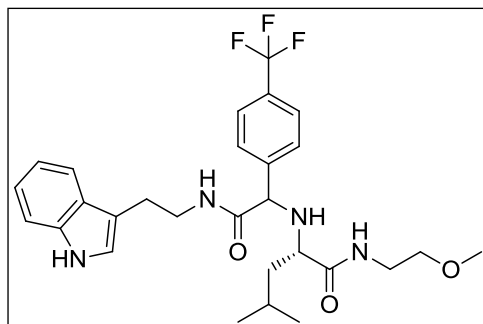
564.44; ^1H NMR (600 MHz, CD_3OD) δ 0.88 (d, $J = 6.6$ Hz,

6H), 1.34 – 1.26 (m, 1H), 1.57 – 1.50 (m, 1H), 1.69 – 1.62

(m, 1H), 1.80 – 1.72 (m, 3H), 2.13 – 1.92 (m, 5H), 2.45 –

2.33 (m, 4H), 2.55 – 2.45 (m, 1H), 3.02 – 2.90 (m, 4H), 3.12 (t, $J = 6.6$ Hz, 1H), 3.51 – 3.39 (m, 3H), 3.59 – 3.52 (m, 1H), 7.00 (t, $J = 7.2$ Hz, 1H), 7.07 (t, $J = 7.2$ Hz, 1H), 7.09 (s, 1H), 7.34 – 7.24 (m, 6H), 7.57 (d, $J = 7.8$ Hz, 1H); ^{13}C NMR (150 MHz, CD_3OD) δ 14.4, 15.2, 20.7, 23.7, 26.1, 29.7, 31.1, 32.2, 32.8, 35.1, 35.7, 40.9, 48.1, 57.5, 60.9, 63.7, 112.4, 113.0, 119.3, 119.7, 122.4, 123.6, 128.6, 128.7, 129.4, 130.9, 137.8, 138.2, 177.3 ppm.

(2S)-2-((2-((2-(1H-Indol-3-yl)ethyl)amino)-2-oxo-1-(4-



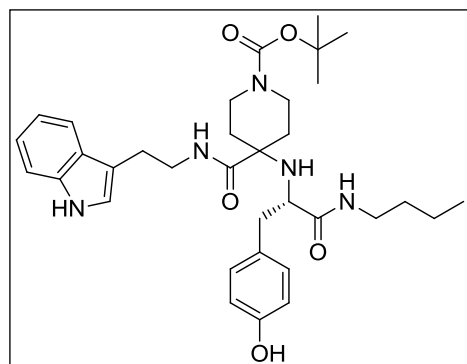
(trifluoromethyl)phenyl)ethyl)amino)-N-(2-

methoxyethyl)-4-methylpentanamide [3.1-8U]: 34% as yellow oil; dr 10/1 by UV, only one diastereomer was isolated. HRMS (APCI, m/z): $[M]^+$ calc.: 533.27; found:

533.38; ^1H NMR (600 MHz, CD_3OD) δ 0.66 (d, $J = 6.6$ Hz, 3H), 0.85 (d, $J = 6.6$ Hz, 3H), 1.37–1.30 (m, 1H), 1.45–1.38 (m, 1H), 1.65–1.57 (m, 1H), 2.88–2.82 (m, 1H), 2.95 (t, $J = 7.2$ Hz, 2H), 3.33 (s, 3H), 3.37–3.33 (m, 2H), 3.44–3.40 (m, 2H), 3.59–3.47 (m, 2H), 4.17 (s, 1H), 7.03–6.96 (m, 2H), 7.10 (t, $J = 7.8$ Hz, 1H), 7.35 (d, $J = 7.8$ Hz, 1H), 7.39 (d, $J = 7.8$ Hz, 2H), 7.59–7.51 (m, 3H); ^{13}C NMR (150 MHz, CD_3OD) δ 22.1, 23.5, 25.7, 25.9, 39.9, 41.3, 44.1, 58.9, 59.4, 65.7, 71.9, 112.3, 113.0, 119.3, 119.7, 122.4, 123.6, 126.5 (q, $J = 5$ Hz), 128.8, 129.8, 131.2 (q, $J = 33$ Hz), 138.2, 144.6, 173.5, 177.1 ppm.

(S)-Tert-butyl

4-((2-(1H-indol-3-yl)ethyl)carbamoyl)-4-((1-(butylamino)-3-(4-



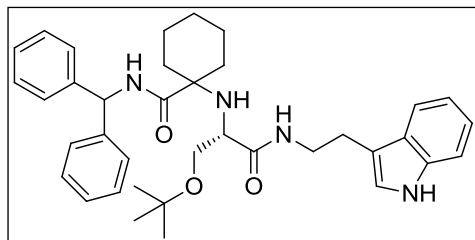
hydroxyphenyl)-1-oxopropan-2-yl)amino)piperidine-1-

carboxylate, [3.1-8V]: 25% as white solid; HRMS (APCI, m/z): $[M]^+$ calc.: 606.36; found: 606.45; ^1H NMR (600 MHz, CD_3OD) δ 0.88 (t, $J = 7.2$ Hz, 3H), 1.27–1.19 (m, 2H), 1.48–1.31 (m, 4H), 1.43 (s, 9H), 1.57–1.50 (m, 1H),

1.95–1.88 (m, 1H), 2.54 (dd, $J = 8.4, 13.8$ Hz, 1H), 2.65 (dd, $J = 6.0, 13.8$ Hz, 1H), 2.89–2.75 (m, 2H), 3.29–3.04 (m, 7H), 3.50–3.39 (m, 2H), 6.73 (d, $J = 8.4$ Hz, 2H), 6.97 (d, $J = 8.4$ Hz, 2H), 7.00 (t, $J = 7.8$ Hz, 1H), 7.05 (s, 1H), 7.07 (t, $J = 7.2$ Hz, 1H), 7.30 (d, $J = 7.8$ Hz, 1H), 7.55 (d, $J = 7.8$ Hz, 1H); ^{13}C NMR (150 MHz, CD_3OD) δ 14.1, 21.1, 26.0, 28.7, 32.3, 35.9, 40.0,

41.1, 41.7, 60.5, 61.0, 81.0, 112.3, 113.0, 116.3, 119.4, 119.6, 122.3, 123.5, 128.8, 129.7, 131.8, 138.1, 156.3, 157.4, 177.1, 177.7 ppm.

(S)-1-((1-((2-(1H-Indol-3-yl)ethyl)amino)-3-(tert-butoxy)-1-oxopropan-2-yl)amino)-N-



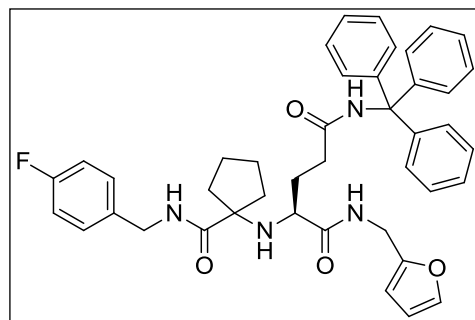
benzhydrylcyclohexanecarboxamide, [3.1-8W]:

40 % as yellow solid; HRMS (APCI, m/z): $[M]^+$ calc.: 595.36; found: 595.45; ^1H NMR (600 MHz, CD_3OD) δ

595.36; found: 595.45; ^1H NMR (600 MHz, CD_3OD) δ

0.99 (s, 9H), 1.56–1.22 (m, 8H), 1.91–1.81 (m, 2H), 2.94–2.82 (m, 2H), 3.12 (t, $J = 4.8$ Hz, 1H), 3.18 (dd, $J = 5.4, 8.4$ Hz, 1H), 3.35–3.27 (m, 1H), 3.39 (dd, $J = 4.8, 9.0$ Hz, 1H), 3.50–3.44 (m, 1H), 7.00 (t, $J = 7.8$ Hz, 1H), 7.05 (s, 1H), 7.09 (t, $J = 7.8$ Hz, 1H), 7.18 (d, $J = 7.8$ Hz, 2H), 7.22 (t, $J = 7.2$ Hz, 1H), 7.25 (d, $J = 7.2$ Hz, 3H), 7.35–7.27 (m, 5H), 7.54 (d, $J = 7.8$ Hz, 1H); ^{13}C NMR (150 MHz, CD_3OD) δ 22.9, 22.9, 26.0, 26.4, 27.7, 33.4, 35.7, 41.0, 58.3, 58.6, 63.0, 64.6, 74.3, 112.3, 112.9, 119.3, 119.6, 122.4, 123.5, 128.3, 128.4, 128.6, 128.6, 128.8, 129.5, 129.6, 138.2, 142.8, 142.9, 176.1, 177.7 ppm.

(S)-2-((1-((4-Fluorobenzyl)carbamoyl)cyclopentyl)amino)-N1-(furan-2-ylmethyl)-N5-



tritylpentanediamide [3.1-8X]: 41% as yellow solid;

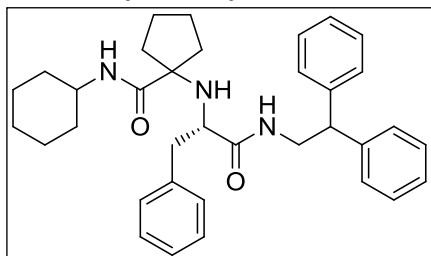
HRMS (APCI, m/z): $[M]^+$ calc.: 687.33; found: 687.45;

^1H NMR (600 MHz, CD_3OD) δ 1.54–1.48 (m, 1H), 1.88–

1.59 (m, 8H), 2.07–1.99 (m, 1H), 2.36–2.26 (m, 2H), 3.01

(t, $J = 6.3$ Hz, 1H), 4.21 (d, $J = 14$ Hz, 1H), 4.34–4.28 (m, 3H), 6.23 (d, $J = 4$ Hz, 1H), 6.32 (t, $J = 2$ Hz, 1H), 6.96 (t, $J = 8.4$ Hz, 2H), 7.30–7.18 (m, 17H), 7.37 (d, $J = 1$ Hz, 1H); ^{13}C NMR (150 MHz, CD_3OD) δ 25.0, 25.3, 31.7, 33.7, 34.6, 36.9, 39.7, 43.4, 59.2, 71.5, 72.0, 108.3, 111.4, 116.1 (d, $J = 21$ Hz), 127.8, 128.7, 130.0, 130.5, 136.4 (d, $J = 3$ Hz), 143.3, 146.0, 152.8, 162.5, 164.2, 174.6, 177.6, 178.8 ppm.

(S)-N-Cyclohexyl-1-((1-((2,2-diphenylethyl)amino)-1-oxo-3-phenylpropan-2-yl)amino)



cyclo-pentanecarboxamide [3.1-8Y]: 38% yield as a white

solid; HRMS (APCI, m/z): $[M]^+$ calc.: 538.73; found 528.46;

^1H NMR (600 MHz, CDCl_3) δ 0.96-1.05 (m, 2H), 1.09-1.16

(m, 1H), 1.23-1.27 (m, 1H), 1.29-1.35 (m, 2H), 1.40-1.48 (m,

3H), 1.52-1.60 (m, 3H), 1.65-1.70 (m, 3H), 1.78-1.86 (m, 4H), 2.08 (bs, 1H), 2.74 (dd, $J = 12.6$,

6.6 Hz, 1H), 2.89-2.95 (m, 2H), 3.61-3.67 (m, 1H), 3.68-3.72 (m 1H), 3.77-3.82 (m, 1H), 3.91 (t,

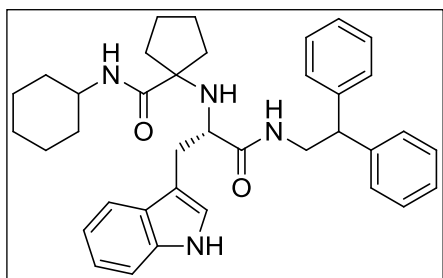
$J = 7.8$ Hz, 1H), 5.88 (t, $J = 6.0$ Hz, 1H), 6.47 (d, $J = 8.4$ Hz, 1H), 7.07-7.11(m, 6H), 7.17-7.20

(m, 2H), 7.24-7.29 (m, 7H); ^{13}C NMR (150 MHz, CDCl_3) δ 23.6, 24.5, 24.8, 24.9, 25.5, 32.9,

33.0, 33.5, 39.1, 41.2, 43.4, 48.0, 50.4, 60.2, 70.6, 126.8, 126.8, 126.9, 127.8, 127.9, 128.6,

128.7, 129.5, 137.2, 141.5, 141.6, 174.4, 174.9 ppm.

(S)-N-Cyclohexyl-1-((1-((2,2-diphenylethyl)amino)-3-(1H-indol-3-yl)-1-oxopropan-2-



yl)amino) cyclopentanecarboxamide [3.1-8Z]: 37% yield

as a white solid; HRMS (APCI, m/z): $[M]^+$ calc.: 577.77;

found 577.45: ^1H NMR (600 MHz, CDCl_3) δ 0.83-0.95 (m,

2H), 1.05-1.12 (m, 1H), 1.29-1.30 (m, 3H), 1.44-1.47 (m,

3H), 1.55-1.66 (m, 5H), 1.73-1.83 (m, 4H), 2.16 (bs, 1H), 2.96 (dd, $J = 14.4$, 6.6 Hz, 1H), 3.07 (J

$= 6.0$ Hz, 1H), 3.12 (dd, $J = 13.8$, 5.4 Hz, 1H), 3.59-3.64 (m, 1H), 3.66-3.72 (m, 3H), 6.10 (bs,

1H), 6.44 (d, $J = 7.8$ Hz, 1H), 6.96 (t, $J = 7.2$ Hz, 3H), 6.99 (d, $J = 7.8$ Hz, 2H), 7.11 (t, $J = 7.8$

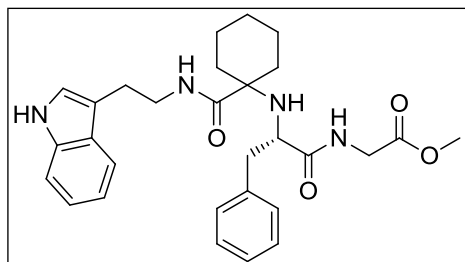
Hz, 1H), 7.14-7.24 (m, 7H), 7.38 (d, $J = 8.4$ Hz, 1H), 7.57 (d, $J = 7.8$ Hz, 1H), 8.42 (s, 1H); ^{13}C

NMR (150 MHz, CDCl_3) δ 23.5, 24.4, 24.8, 24.8, 25.4, 30.7, 32.8, 33.7, 39.0, 43.4, 48.0, 50.2,

59.1, 70.5, 110.9, 111.3, 119.0, 119.6, 122.2, 123.4, 126.6, 127.5, 127.7, 127.8, 128.5, 128.6,

136.3, 141.5, 141.6, 175.0, 175.1 ppm.

(S)-Methyl-2-(2-((1-((2-(1*H*-indol-3-yl)ethyl)carbamoyl)cyclohexyl)amino)-3-



phenylpropan-amido)acetate [3.1-8AA]: 63% yield as a

brownish solid; HRMS (APCI, m/z): $[M]^+$ calc.: 505.62;

found: 505.38; ^1H NMR (600 MHz, CDCl_3) δ 1.29-1.40

(m, 8H), 1.72-1.79 (m, 2H), 2.22 (bs, 1H), 2.73 (dd, $J =$

13.8, 7.8 Hz, 1H), 2.78-2.88 (m, 3H), 3.17-3.23 (m, 2H), 3.43-3.48 (m, 1H), 3.66 (s, 3H), 3.75

(dd, $J = 18.0, 4.8$ Hz, 1H), 3.90 (dd, $J = 18.6, 6.6$ Hz, 1H), 6.48 (bs, 1H), 6.94 (s, 1H), 7.08-7.11

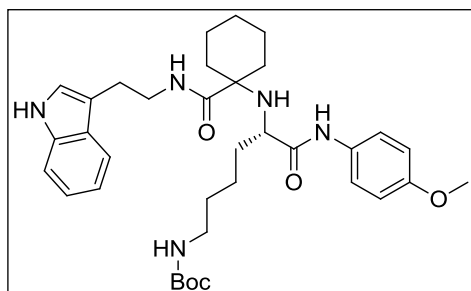
(m, 4H), 7.15-7.22 (m, 4H), 7.33 (d, $J = 8.4$ Hz, 1H), 7.57 (d, $J = 7.8$ Hz, 1H), 8.61 (bs, 1H); ^{13}C

NMR (150 MHz, CDCl_3) δ 21.9, 22.0, 24.9, 25.1, 32.0, 35.0, 39.5, 40.6, 52.2, 58.4, 61.6, 111.2,

112.6, 118.6, 119.1, 121.84, 122.1, 126.8, 127.2, 128.4, 129.5, 136.3, 137.1, 170.2, 175.4, 175.6

ppm.

(S)-Tert-butyl-(5-((1-((2-(1*H*-indol-3-yl)ethyl)carbamoyl)cyclohexyl)amino)-6-((4-



methoxy-phenyl)amino)-6-oxohexyl)carbamate [3.1-

8AB]: 62% yield as a brownish solid; HRMS (APCI, m/z):

$[M]^+$ calc.: 620.79; found: 620.51; ^1H NMR (600 MHz,

CDCl_3) δ 1.13 (bs, 2H), 1.24-1.32 (m, 4H), 1.35-1.50 (m,

17H), 1.72-1.77 (m, 1H), 1.87-1.91 (m, 1H), 2.21 (bs, 1H), 2.87-2.94 (m, 3H), 2.95-3.05 (m,

2H), 3.52-3.60 (m, 2H), 3.76 (s, 3H), 4.73 (bs, 1H), 6.82 (d, $J = 9.0$ Hz, 2H), 6.90 (bs, 1H), 6.99

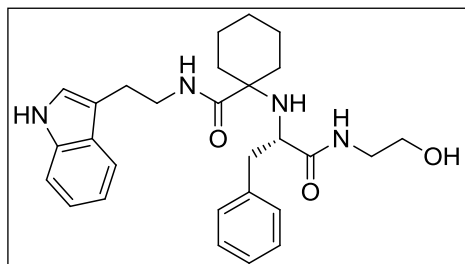
(s, 1H), 7.08 (t, $J = 7.2$ Hz, 1H), 7.17 (t, $J = 7.2$ Hz, 1H), 7.36 (d, $J = 7.8$ Hz, 1H), 7.44 (d, $J =$

9.0 Hz, 2H), 7.57 (d, $J = 7.8$ Hz, 1H), 8.96 (s, 1H), 9.07 (s, 1H); ^{13}C NMR (150 MHz, CDCl_3) δ

21.8, 22.1, 24.9, 25.3, 28.4, 30.0, 34.9, 36.5, 40.1, 55.4, 57.5, 61.9, 79.3, 111.5, 112.5, 114.0,

118.6, 119.0, 121.3, 121.8, 122.1, 127.4, 131.0, 136.5, 156.2, 156.4, 173.6, 176.2 ppm.

(S)-N-(2-(1*H*-Indol-3-yl)ethyl)-1-((1-((2-hydroxyethyl)amino)-1-oxo-3-phenylpropan-2-



yl)amino)cyclohexanecarboxamide [3.1-8AC]: 30%

yield as a yellowish solid; HRMS (APCI, m/z): $[M]^+$ calc.:

477.61; found: 477.37; ^1H NMR (600 MHz, CDCl_3) δ

1.18-1.42 (m, 8H), 1.53-1.59 (m, 1H), 1.74-1.80 (m, 1H),

2.65 (dd, $J = 13.2, 8.4$ Hz, 1H), 2.76-2.86 (m, 3H), 3.08 (t, $J = 7.2$ Hz, 1H), 3.12-3.18 (m, 1H),

3.20-3.28 (m, 2H), 3.43-3.47 (m, 1H), 3.48-3.56 (m, 2H), 6.53 (bs, 1H), 6.96 (s, 1H), 7.04 (d, $J =$

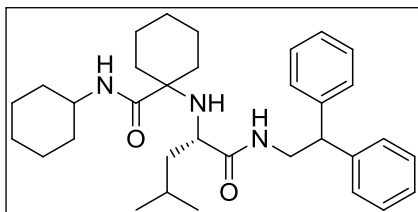
6.6 Hz, 2H), 7.11 (t, $J = 7.8$ Hz, 1H), 7.14-7.20 (m, 5H), 7.34 (d, $J = 8.4$ Hz, 1H), 7.57 (d, $J = 7.8$

Hz, 1H), 8.68 (s, 1H); ^{13}C NMR (150 MHz, CDCl_3) δ 21.6, 21.7, 25.0, 25.1, 32.4, 34.6, 39.5,

41.2, 42.2, 58.8, 61.3, 61.5, 111.3, 112.4, 118.5, 119.2, 121.9, 122.1, 126.8, 127.2, 128.4, 129.5,

136.4, 137.4, 175.7, 176.1 ppm.

(S)-N-Cyclohexyl-1-((1-((2,2-diphenylethyl)amino)-4-methyl-1-oxopentan-2-yl)amino)



cyclo-hexanecarboxamide [3.1-8AD]: 48% yield as a

yellowish solid; HRMS (APCI, m/z): $[M]^+$ calc.: 518.75;

found: 519.48 ^1H NMR (600 MHz, CDCl_3) δ 0.71 (d, $J = 6.6$

Hz, 3H), 0.77 (d, $J = 6.0$ Hz, 3H), 1.07-1.26 (m, 7H), 1.27-1.43 (m, 9H), 1.57-1.61 (m, 1H),

1.66-1.77 (m, 4H), 1.80-1.86 (m, 2H), 1.88 (s, 1H), 2.86 (t, $J = 6.0$ Hz, 1H), 3.63-3.69 (m, 1H),

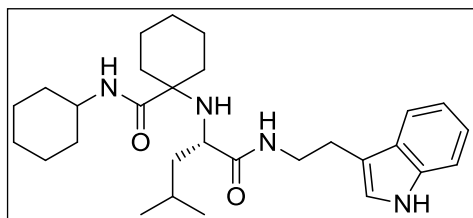
3.70-3.75 (m, 1H), 4.00-4.05 (m, 1H), 4.20 (t, $J = 8.4$ Hz, 1H), 6.24 (d, $J = 7.2$ Hz, 1H), 6.73 (bs,

1H), 7.19-7.22 (m, 2H), 7.23-7.26 (m, 4H), 7.27-7.33 (m, 4H); ^{13}C NMR (150 MHz, CDCl_3) δ

22.2, 22.3, 22.3, 23.1, 24.8, 24.8, 25.3, 25.5, 31.1, 33.0, 33.1, 36.2, 43.5, 45.4, 48.0, 50.6, 56.0,

61.6, 126.8, 126.8, 127.9, 128.0, 128.6, 128.7, 128.8, 141.7, 141.8, 174.3, 175.8 ppm.

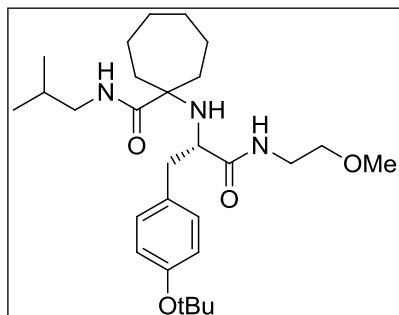
(S)-1-((1-((2-(1*H*-Indol-3-yl)ethyl)amino)-4-methyl-1-oxopentan-2-yl)amino)-*N*-cyclohexyl-



cyclohexanecarboxamid [3.1-8AE]: 46% yield as a yellowish solid; HRMS (APCI, m/z): $[M]^+$ calc.: 481.69; found: 481.40; ^1H NMR (600 MHz, CDCl_3) δ 0.82 (dd, $J =$

10.8, 6.6 Hz, 6H), 1.06-1.18 (m, 3H), 1.22-1.36 (m, 8H), 1.39-1.44 (m, 3H), 1.46-1.54 (m, 2H), 1.57-1.61 (m, 1H), 1.65-1.69 (m, 2H), 1.75-1.78 (m, 1H), 1.81-1.86 (m, 3H), 2.01 (bs, 1H), 2.88-2.91 (m, 1H), 2.93-2.96 (m, 1H), 2.97-3.02 (m, 1H), 3.59 (q, $J = 13.2, 6.6$ Hz, 2H), 3.64-3.71 (m, 1H), 6.41 (d, $J = 7.8$ Hz, 1H), 6.58 (t, $J = 5.4$ Hz, 1H), 7.02 (s, 1H), 7.11 (t, $J = 7.8$ Hz, 1H), 7.19 (t, $J = 15.0$ Hz, 1H), 7.36 (d, $J = 8.4$ Hz, 1H), 7.61 (d, $J = 7.8$ Hz, 1H), 8.39 (s, 1H); ^{13}C NMR (150 MHz, CDCl_3) δ 22.1, 22.2, 22.5, 23.1, 24.6, 24.7, 24.8, 25.2, 25.3, 25.5, 31.5, 33.0, 33.1, 35.9, 39.2, 45.5, 48.1, 56.2, 61.7, 111.2, 112.7, 118.6, 119.3, 122.0, 122.1, 127.2, 136.4, 174.7, 175.9 ppm.

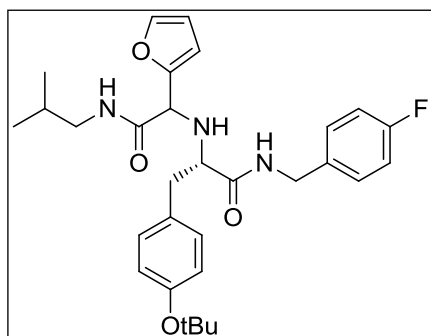
(S)-1-((3-(4-(tert-Butoxy)phenyl)-1-((2-methoxyethyl)amino)-1-oxopropan-2-yl)amino)-*N*-



isobutylcycloheptanecarboxamide [3.1-8AF]: 23% as white solid; ; HRMS (APCI, m/z): $[M]^+$ calc.: 490.36; found: 490.41; ^1H NMR (600 MHz, CD_3OD) δ 0.81 (d, $J = 12$ Hz, 3H), 0.83 (d, $J = 6$ Hz, 3H), 1.33 (s, 9H), 1.62 – 1.41 (m, 12H), 1.91 – 1.41

(m, 1H), 2.06 (m, 1H), 2.49 (dd, $J = 7.2, 13.2$ Hz, 1H), 2.69 (dd, $J = 8.4, 13.2$ Hz, 1H), 2.79 (dd, $J = 5.4, 13.8$ Hz, 1H), 2.88 (dd, $J = 7.2, 13.2$ Hz, 1H), 3.20 (dd, $J = 5.4, 8.4$ Hz, 1H), 3.28 – 3.23 (m, 1H), 3.31 (s, 3H), 3.41 (m, 2H), 6.94 (d, $J = 8.4$ Hz, 2H), 7.16 (d, $J = 8.4$ Hz, 2H). ^{13}C NMR (150 MHz, CD_3OD) δ 20.4, 20.5, 23.8, 24.3, 29.2, 29.8, 31.87, 31.95, 35.5, 40.1, 40.7, 42.0, 47.5, 58.9, 60.5, 66.4, 71.9, 79.4, 125.1, 131.3, 134.1, 155.6, 178.1, 179.2 ppm.

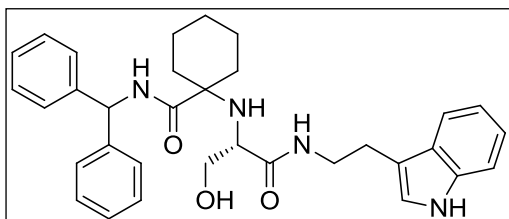
(2S)-3-(4-(tert-butoxy)phenyl)-N-(4-fluorobenzyl)-2-((1-(furan-2-yl)-2-(isobutylamino)-2-



oxoethyl)amino)propanamide [3.1-8AG]: 31% as yellow solid; HRMS (APCI, m/z): $[M]^+$ calc.: 524.28; found: 524.35; ^1H NMR (600 MHz, CD_3OD) δ 0.83 (d, $J = 6.6$ Hz, 6H), 1.32 (s, 9H), 1.76–1.67 (m, 1H), 2.84–2.76 (m, 1H), 3.02–2.91 (m, 3H), 4.28 (s, 1H), 4.32 (s, 2H), 6.13 (d, $J = 3.6$

Hz, 1H), 6.31 (dd, $J = 1.8, 3.0$ Hz, 1H), 6.87 (d, $J = 7.8$ Hz, 2H), 7.08–6.99 (m, 4H), 7.22 (dd, $J = 5.4, 8.4$ Hz, 2H), 7.36 (s, 1H). ^{13}C NMR (150 MHz, CD_3OD) δ 20.4, 29.2, 29.6, 39.6, 43.4, 47.8, 60.0, 63.1, 79.5, 109.8, 111.4, 116.2 (d, $J = 21$ Hz), 125.4, 130.6 (d, $J = 9$ Hz), 130.9, 133.3, 135.9, 143.8, 152.5, 155.5, 163.5 (d, $J = 243$ Hz) ppm (the two carbonyl carbons were not detected),

(S)-1-(((1-((2-(1H-indol-3-yl)ethyl)amino)-3-hydroxy-1-oxopropan-2-yl)amino)-N-

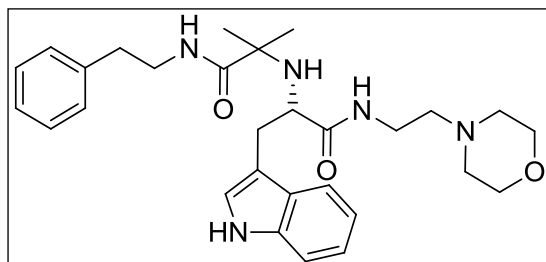


benzhydrylcyclohexanecarboxamide [3.1-8AH]:

23% as yellow oil; ; HRMS (APCI, m/z): $[M]^+$ calc.: 539.29; found: 539.38; ^1H NMR (600 MHz, CD_3OD) δ

1.54–1.20 (m, 8H), 1.92–1.80 (m, 2H), 2.95–2.84 (m, 2H), 3.16 (t, $J = 4.8$ Hz, 1H), 3.39–3.32 (m, 1H), 3.52–3.42 (m, 2H), 3.55 (dd, $J = 6.0, 10.8$ Hz, 1H), 6.12 (s, 1H), 7.00 (t, $J = 7.2$ Hz, 1H), 7.08 (t, $J = 7.8$ Hz, 1H), 7.25–7.17 (m, 4H), 7.37–7.25 (m, 7H), 7.54 (d, $J = 7.8$ Hz, 1H). ^{13}C NMR (150 MHz, CD_3OD) δ 22.8, 22.9, 26.0, 26.4, 32.9, 36.4, 41.0, 58.6, 60.2, 63.2, 64.8, 112.3, 112.9, 119.3, 119.6, 122.4, 123.5, 138.28, 138.31, 128.62, 128.64, 128.8, 129.5, 138.2, 143.0, 176.0, 178.0 ppm.

(S)-2-((3-(1H-indol-3-yl)-1-((2-morpholinoethyl)amino)-1-oxopropan-2-yl)amino)-2-



methyln-N-phenethylpropanamide [3.1-8AI]: 38%

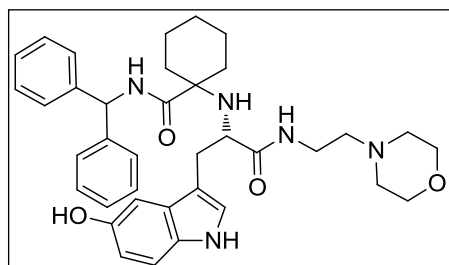
as yellow solid; HRMS (APCI, m/z): $[M]^+$ calc.:

506.31 found: 506.39; ^1H NMR (600 MHz, CD_3OD)

δ 1.15 (s, 3H), 1.22 (s, 3H), 2.25-2.35 (m, 7H), 2.44-

2.51 (m, 2H), 2.59-2.62 (m, 1H), 2.86-2.90 (q, 1H), 3.05-3.08 (dd, 1H), 3.21-3.29 (m, 4H), 3.58-3.61 (m, 3H), 6.63-6.66 (m, 2H), 6.96 (s, 1H), 7.09-7.14 (m, 3H), 7.19-7.26 (m, 2H), 7.28-7.35 (m, 3H), 7.60-7.61 (d, 1H) 8.43 (s, 1H). ^{13}C NMR (150 MHz, CD_3OD) δ 23.1, 28.5, 31.4, 35.5, 40.2, 53.1, 56.8, 59.0, 59.4, 66.8, 100.0, 102.0, 111.4, 118.8, 119.8, 122.4, 123.5, 126.4, 127.2, 128.5, 136.4, 139.3, 175.7, 176.5 ppm.

(S)-N-benzhydryl-1-((3-(5-hydroxy-1H-indol-3-yl)-1-((2-morpholinoethyl)amino)-1-



oxopropan-2-yl)amino)cyclohexanecarboxamide [3.1-

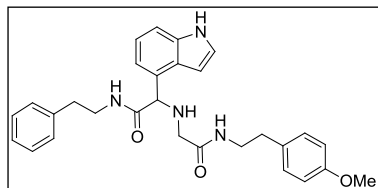
8AJ]: 34% as white solid; HRMS (APCI, m/z): $[M]^+$ calc.:

624.35; found: 624.46; ^1H NMR (600 MHz, CD_3OD) δ 1.27

(brs, 1H), 1.41-1.43 (m, 2H), 1.48-1.49 (m, 2H), 1.56-1.60

(m, 2H), 1.66-1.69 (m, 1H), 1.78-1.81 (m, 1H), 1.92-1.96 (m, 7H), 1.31 (brs, 1H), 2.73-2.77 (dd, 1H), 2.95-2.98 (dd, 1H), 3.10-3.15 (m, 2H), 3.31-3.38 (m, 5H), 6.21-6.22 (d, 1H), 6.67 (s, 1H), 6.76-6.78 (d, 1H), 6.94 (brs, 1H), 7.07-7.09 (m, 2H), 7.22-7.29 (m, 5H), 7.32-7.38 (m, 5H), 8.70 (s, 1H); ^{13}C NMR (150 MHz, CD_3OD) δ 21.9, 22.0, 25.4, 30.5, 35.5, 52.6, 55.7, 57.0, 57.5, 61.8, 66.7, 103.5, 109.5, 111.7, 112.5, 124.4, 127.3, 127.4, 127.6, 127.7, 128.3, 128.8, 128.9, 131.0, 141.4, 141.5, 150.9, 175.8 (missing one carbonyl carbon)

2-(1H-indol-4-yl)-2-((2-((4-methoxyphenethyl)amino)-2-oxoethyl)amino)-N-



phenethylacetamide [3.1-8AK]: 41% as yellow solid; HRMS

(APCI, m/z): $[M]^+$ calc.: 484.25; found: 485.32; ^1H NMR (600

MHz, CD_3OD) δ 2.43-2.50 (m, 2H), 2.55, 2.60 (m, 1H), 2.67-2.71

(m, 1H), 3.08-3.11 (d, 1H), 3.17-3.21 (m, 1H), 3.28-3.32 (m, 2H), 3.39-3.41, (d, 1H), 3.55-3.59

(m, 1H), 3.78 (s, 3H), 4.38 (s, 1H), 5.77 (m, 1H), 6.57 (s, 1H), 6.81-6.83 (m, 3H), 6.95-6.96 (d,

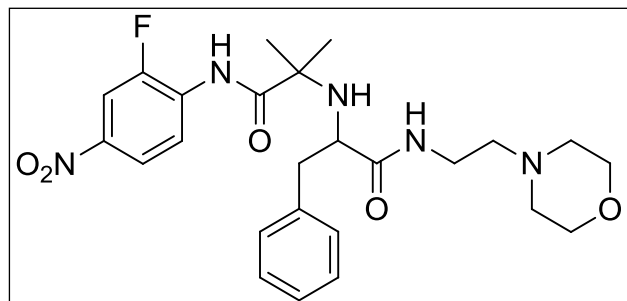
1H), 6.99-7.01 (d, 1H), 7.05-7.09 (m, 1H), 7.12-7.14 (m, 3H), 7.19-7.20 (m, 1H), 7.37-7.39 (d,

1H), 8.87 (s, 1H); ^{13}C NMR (150 MHz, CD_3OD) δ 34.5, 35.5, 40.3, 40.8, 51.5, 55.3, 66.2, 100.6,

111.9, 114.0, 120.0, 122.1, 125.1, 126.1, 126.3, 128.5, 128.6, 129.6, 129.8, 131.0, 136.5, 128.6,

158.1, 171.53, 171.57 ppm

N-(2-fluoro-4-nitrophenyl)-2-methyl-2-((1-((2-morpholinoethyl)amino)-1-oxo-3-



phenylpropan-2-yl)amino)propanamide

[3.1-8AL]: 25% as yellow oil; HRMS (APCI,

m/z): $[M]^+$ calc.: 502.24 ; found: 502.30; ^1H

NMR (600 MHz, CD_3OD) δ 1.32 (s, 3H),

1.43, (s, 3H), 2.20-2.25 (m, 3H), 2.30-2.37 (m, 3H), 2.52 (brs, 1H), 2.90-2.94 (dd, 1H), 2.97-3.00

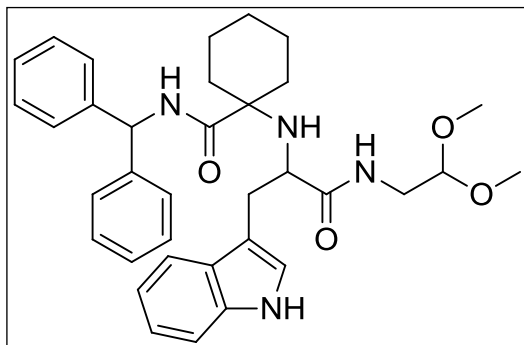
(dd, 1H), 3.13-3.20 (m, 1H), 3.20 (brs, 1H), 3.26-3.31 (m, 1H), 3.58-3.60 (m, 4H), 5.88 (s, 1H),

7.15-7.17 (m, 3H), 7.25-7.29 (m, 3H), 8.00-8.02 (m, 1H), 9.23-9.25 (dd, 2H), 9.70 (s, 1H); ^{13}C

NMR (150 MHz, CD_3OD) δ 22.5, 28.3, 35.3, 42.3, 53.0, 56.4, 60.4, 66.7, 98.0, 100.0, 115.3,

115.5, 117.2, 119.8, 126.9, 128.7, 129.2, 137.2, 174.0, 175.6

(S)-N-benzhydryl-1-((1-((2,2-dimethoxyethyl)amino)-3-(1H-indol-3-yl)-1-oxopropan-2-



yl)amino)cyclohexanecarboxamide [3.1-8AM]:

47% as light yellowish solid; SFCMS (APCI, m/z):

$[M]^+$ calc.: 583.73; found: 583.44; ^1H NMR (600

MHz, CDCl_3) δ 1.37-1.67 (m, 8H), 1.90-1.95 (m, 2H),

2.90-2.95 (m, 1H), 3.00-3.12 (m, 9H), 3.29-3.32 (m,

1H), 3.60 (t, $J = 5.4$ Hz, 1H), 6.23-6.24 (m, 2H), 6.84 (s, 1H), 7.05 (t, $J = 7.8$ Hz, 1H), 7.14 (t, $J = 7.2$ Hz, 1H), 7.22-7.28 (m, 6H), 7.32-7.35 (m, 4H), 7.45-7.46 (m, 2H), 8.68 (s, 1H); ^{13}C NMR (150 MHz, CDCl_3) δ 21.8, 22.0, 30.6, 31.6, 35.6, 40.4, 53.7, 53.8, 57.0, 57.7, 61.7, 102.1, 110.3, 111.1, 119.0, 119.3, 121.9, 123.3, 127.1, 127.3, 127.3, 127.4, 128.5, 128.7, 136.1, 141.4, 141.5, 175.0, 175.4 ppm.

3.2 CYCLIZATION SCAFFOLDS BY VARIATION OF THE UGI-4-COMPONENT- 5-CENTERED REACTION^{166,167}

Chemical diversity and complexity of scaffolds are key for the design- or screening-based discovery of useful materials. Series of compounds based on a particular scaffold are often used to optimize properties. While scaffolds are traditionally built up by sequential multistep syntheses a convergent alternative pathway involves one-pot multicomponent reactions (MCRs).^{168,169} A useful definition of the scaffold in the context of MCR has been introduced recently by us and accordingly it is defined “as the smallest atomic denominator and its connectivity as resulting from a reaction or reaction sequence using starting materials with

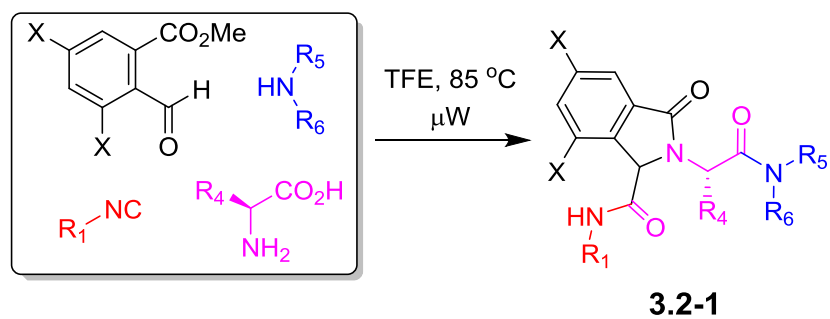
common functional groups."¹⁷⁰ A very large variety of MCR scaffolds have been described in the past based on different strategies.¹⁷¹⁻¹⁷⁶ For example there are more than 40 piperazine scaffolds accessible by MCR.¹⁷⁰ This two step Ugi MCRs/ring forming Pictet-Spengler reaction is of particular interest as it gives access to rather rigid, complex polycyclic products (Scheme 1) which can lead to entropically preferred receptor binding. This reaction sequence has been used for the synthesis of drugs and natural products and chemical biology tools as well.

Ivar Ugi half a century ago pioneered the use of multicomponent reaction technology (MCR) for the discovery of novel agents with preferred properties.¹⁷⁷ MCR is now widely recognized for its impact on drug discovery projects and is strongly endorsed by academia in addition to industry.¹³³ Recent reviews on chemistry and biology of MCRs give comprehensive proof for the increasing number of marketed products based on MCRs including for example boceprevir,¹³⁴ retosiban,¹³⁵ or mandipropamid,¹³⁶ just to name a few. Based on the sheer number of theoretically accessible MCR products, recent trends in drug discovery using MCR chemistry however more and more leverage the usage of virtual screening tools.^{65,164,165} For example the recently introduced ANCHOR.QUERY freeware offers >25 million virtual MCR compounds for structure- and web-based drug design proposes.⁶⁵ While there are hundreds of different MCRs described in the chemical literature only a few are highly variable in all starting materials e.g. Ugi, Passerini and van Leusen.¹⁷⁷⁻¹⁸⁰ The size of the chemical space of the different MCR scaffolds, however, has major implications on the usefulness of the particular MCR serving as a suitable virtual search space. Amongst the different strategies for the design of molecular complexity using MCR chemistry¹⁴⁰⁻¹⁴² the post-Ugi secondary cyclization has been a very fruitful strategy in the past to accomplish novel scaffolds.

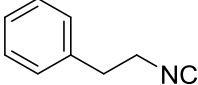
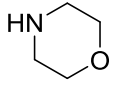
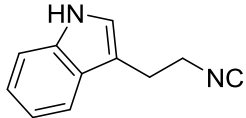
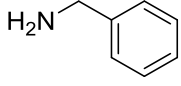
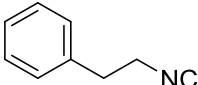
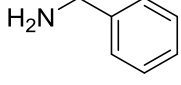
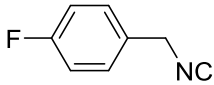
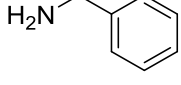
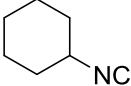
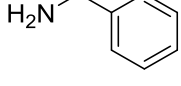
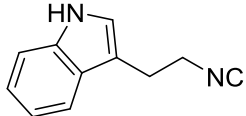
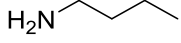
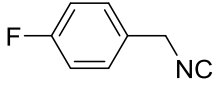
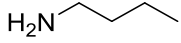
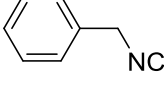
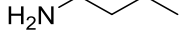
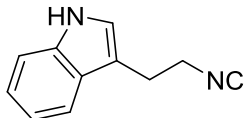
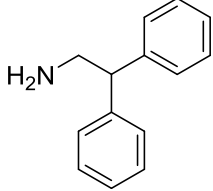
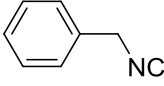
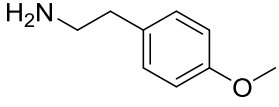
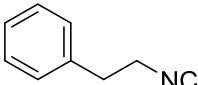
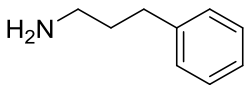
We would like to report here on the design of novel Ugi postcondensations leading to four unprecedented and highly variable heterocyclic scaffolds.

3.2.1 Isoindolinone

One equivalent each of amino acid, isocyanide, primary or secondary amine and o-carboxylmethylester benzaldehyde was added together in a microwave vial in one tenth molar concentration for one hour at 80°C. Crude reaction mixture was checked via SFC-MS and both masses for the Ugi product and the newly cyclized product **3.2-1** could be seen. Work up was done to remove any unreacted amino acid and reaction was heated again in ethanol and SFC-MS then revealed that only cyclized product **3.2-1** remained. Either one diastereomer precipitated out (**3.2-1A** and **3.2-1B**) or crude mixture was purified via SFC (**3.2-1C** and **3.2-1D**). When glycine was used as the amino acid component the cyclized product consistently precipitated out. When primary amines were used (**3.2-1A** and **3.2-1B**) crude SFC traces revealed diastereomeric ratios of 7:3 and only the major diastereomer precipitated (Appendix A). When secondary amines were used (**3.2-1C** and **3.2-1D**) SFC trace using chiral cell OD revealed four stereoisomers in equal ratio suggesting the racemization of the amino acid stereocenter by secondary amines as previously discovered.¹⁴³ (Appendix A)



Entry	Amino Acid	X	Isocyanide	Amine	Yield (%)
3.2-1 A	Iso	H			35 7:3 ^[a]
3.2-1B	Phe	H			42 7:3 ^[a]
3.2-1C	Leu	H			42
3.2-1D	Leu	OMe			40
3.2-1E	Ala	OMe			38
3.2-1F	Trp	H			33 8:1 ^[a]
3.2-1G	Gly	OMe			30

3.2-1H	Gly	OMe			42
3.2-1I	Gly	OMe			20
3.2-1J	Gly	OMe			44
3.2-1K	Gly	OMe			35
3.2-1L	Gly	OMe			30
3.2-1M	Gly	OMe			41
3.2-1N	Gly	OMe			25
3.2-1O	Gly	OMe			43
3.2-1P	Gly	H			37
3.2-1Q	Trp	H			35 8:3 ^[a]
3.2-1R	Gly	OMe			37

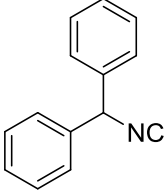
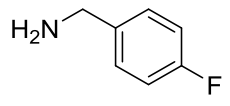
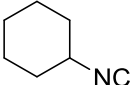
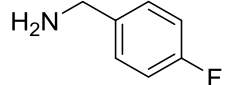
3.2-1S	Ser	H			10 ND
3.2-1T	Gly	OMe			58

Table 3-2 Ugi4C5CR isoindolinone cyclization reaction product isolated yields [a] d.r. determined by

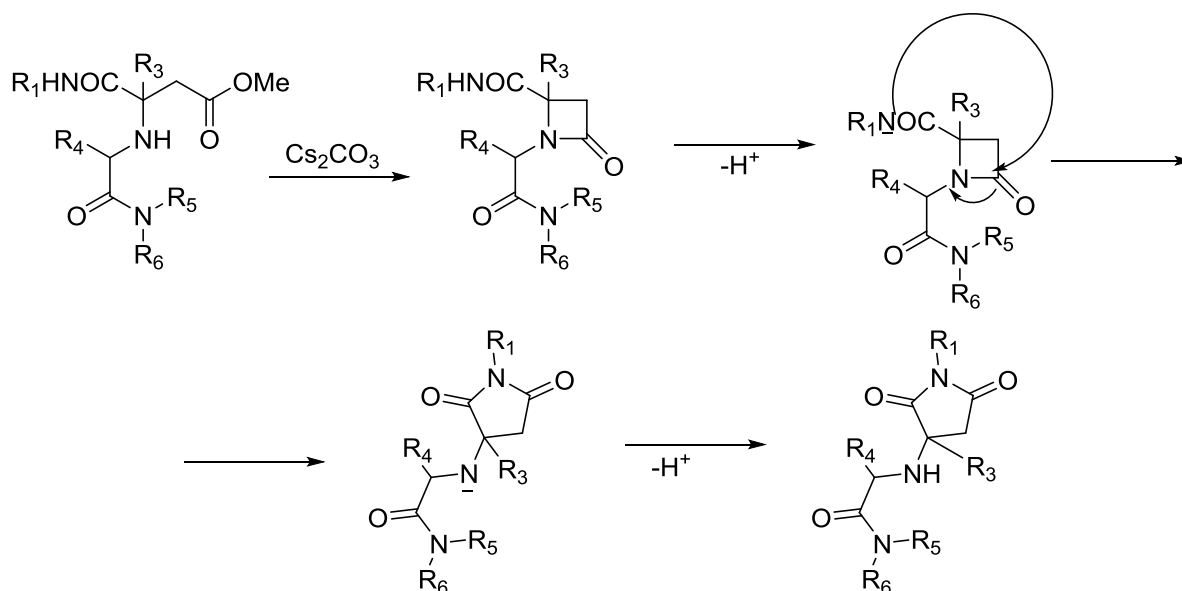
UV

3.2.2 Dioxopyrrolidines

The Ugi reaction generally works well with aromatic and aliphatic aldehydes and ketones. Another available building block of suitable bifunctional orthogonal starting materials is the β -ketoester. In fact when employing 2-oxocyclohexane carboxylic acid ethyl ester under heating conditions at 85 °C, SFC-MS revealed the formation of the Ugi product as well as trace amounts of the corresponding pyrrolidinedione scaffold **3.2-2** (Table 3-3). Upon addition of 3 equivalents of cesium carbonate complete cyclization of the Ugi product to the pyrrolidinedione **3.2-2** was observed. Benzyl 3-oxobutanoate also produced similar pyrrolidinedione **3.2-2**.

What is interesting about this reaction is that it is the amide and not the amine which is reacting with the ester component to form the cyclized product. According to a study done in 1997, it is possible that while initially the amine may react to form the beta-lactam the resulting structure may be formed through ring enlargement.¹⁸¹ It is possible, according to the paper, that the amide NH group is becoming deprotonated followed by the nucleophilic attack on the beta lactam carbonyl group.(Scheme 3-3) This rearrangement appears reasonable as the electron

withdrawing group linked to the amide nitrogen increases the electrophonic character of the CO group.



Scheme 3-3 Proposed reaction mechanism of Ugi cyclization to Dioxopyrrolidines

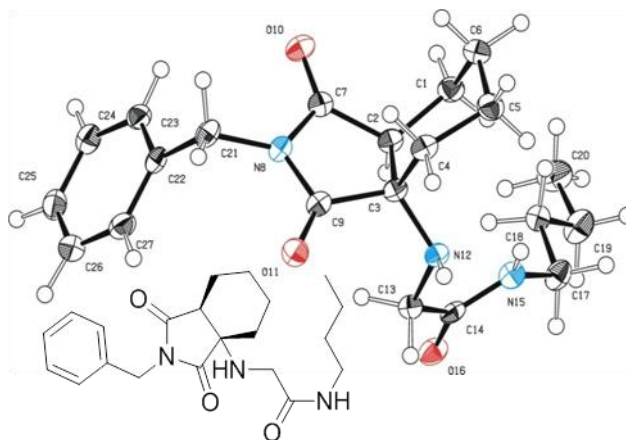
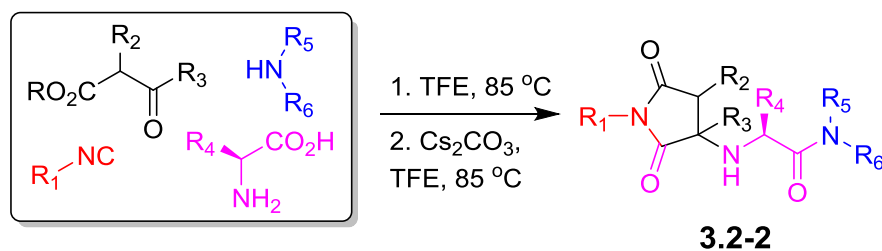


Figure 3.2 Structure of pyrrolidinedione product 3.2-2A in solid state.

Several analogous reactions were performed and all yielded the products in satisfactory yields (**Table 3-3**). The finding of this reaction is remarkable since several other orthogonal methods exist to access the pyrrolidinedione scaffold by isocyanide based MCRs.¹⁸² Stereochemical analysis SFC-mass revealed that compound **3.2-2C** gave a single diastereomer

however **3.2-2B**(9:1) and **3.2-2D** (9.5:0.5) formed mixture of two distereomers (see SI-38,-41). The major distereomers were isolated using preparative TLC plate. Pyrrolidinedione **9a** is exclusively formed as the cis relative stereoisomer. The x-ray structure of **3.2-2A** shows the solid state conformation and also proves the overall structure of the scaffold (**Figure 3.2**).



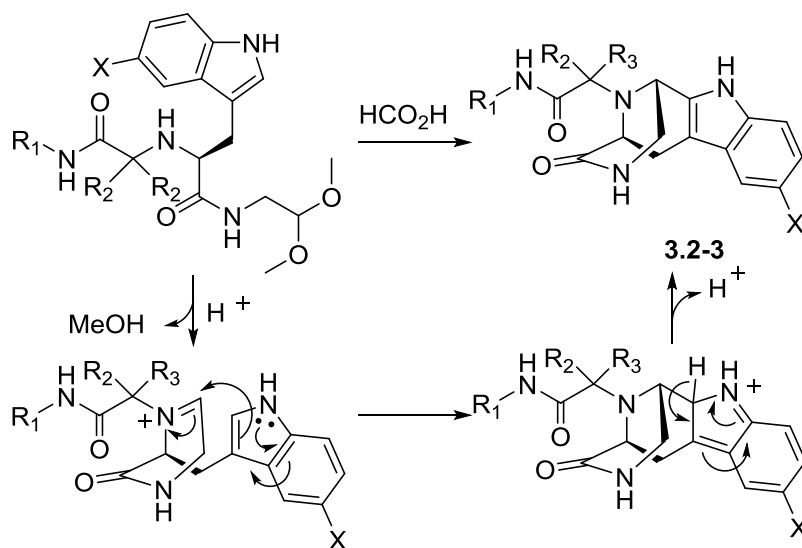
Entry	Amino Acid	Ketone	Isocyanide	Amine	Yield (%)
3.2-2A	Gly				40 1:0^[a]
3.2-2B	Ala				49 9.5:0.5^[a]
3.2-2C	Trp				45 1:0^[a]
3.2-2D	Phe				34 9.5:0.5^[a]

Table 3-3 Ugi4C5CR dioxypyrrolidines cyclization reaction product isolated yields [a] d.r.

determined by UV

3.2.3 Pictet-Spengler

The Pictet-Spengler reaction recently became popular to perform Ugi post condensation reaction to yield complex polycyclic scaffolds.¹⁸³⁻¹⁸⁸ For example the use of suitable starting materials allows for the convergent synthesis of the important schistosomiasis medication praziquantel.^{108,189} The required functional groups of the Pictet-Spengler reaction a electron rich aromatic such as tryptophan and an oxo group can be conveniently introduced via the α -amino acid component and the amine component, respectively (**Table 3-4** and **Table 3-5**). By performing the Pictet-Spengler reaction under formic acid at room temperature condition we indeed could isolate the strained tricyclic 3,9-diazabicyclo[3.3.1]nonane system **3.2-3**. Several analogous reactions show the general character of this transformation (**Table 3-4**).



Scheme 3-4 Proposed reaction mechanism of Pictet-Spengler reaction for indole derivatives.

We first reacted tryptophan amino acid, a ketone, an isocyanide and aminoacetaldehyde dimethyl acetal in MeOH-H₂O (4:1) at room temperature to form the U-5C-4CR product as shown in Scheme 3-4. The Pictet-Spengler reaction product was not obtained by using various conditions such as sulfonic acid, p-toluenesulfonic acid, and camphorsulfonic acid in toluene,

however using concentrated formic acid at room temperature surprisingly gave the Pictet-Spengler cyclization product **3.2-3**. The reaction was also conveniently performed in one-pot without loss of yield of final product by evaporation of the crude U-5C-4CR mixture followed by addition of formic acid. Furthermore we found that the reaction also worked with 5-hydroxy tryptophan according to **Scheme 3-4**. We made variations using different isocyanides and ketones or aldehydes as shown in Table 3-4 and all reactions worked giving satisfactory yields. Use of benzaldehyde (**3.2-3N**) and cyclopentanecarbaldehyde (**3.2-3O**) produced two diastereomers (4:1 by ^1H NMR, table 1). In the case of valeraldehyde **3.2-3V**, two diastereomers in a ratio of 3.6:1 (by HPLC, table 1) were formed. All stereoisomers could be easily separated using preparative SFC-HPLC. All reactions are believed to work by the proposed mechanism shown in Scheme 3-4.^{190,191} The reaction mechanism might occur by initial step deprotection of the acetal groups in acidic condition to form the iminium ion followed by electrophilic substitution. After subsequent deprotonation the desired product (**3.2-3**) is obtained. The x-ray structure of **3.2-3R** shows the solid state conformation and also proves the overall structure of the scaffold (**Figure 3.3**).

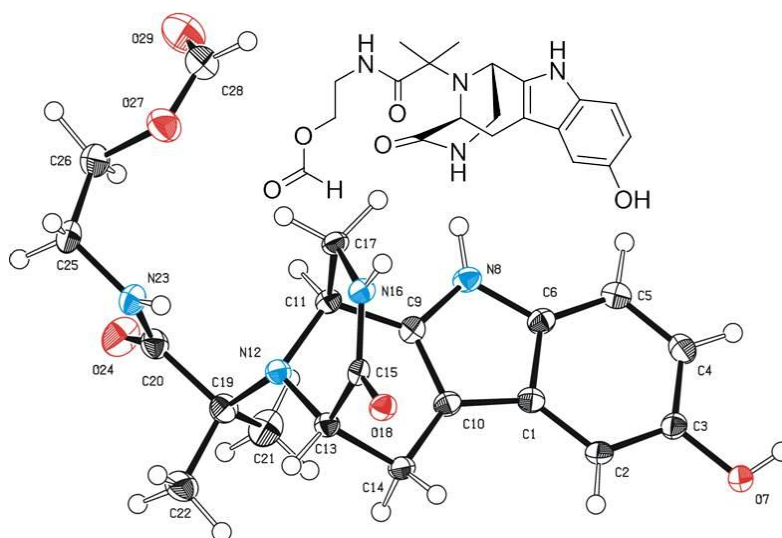
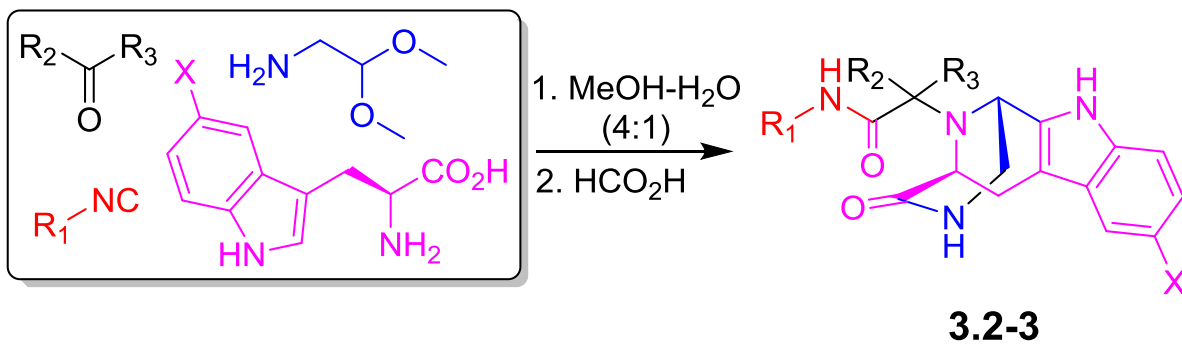


Figure 3.3 Structure of Pictet-Spengler cyclization product **3.2-3R** in solid state.

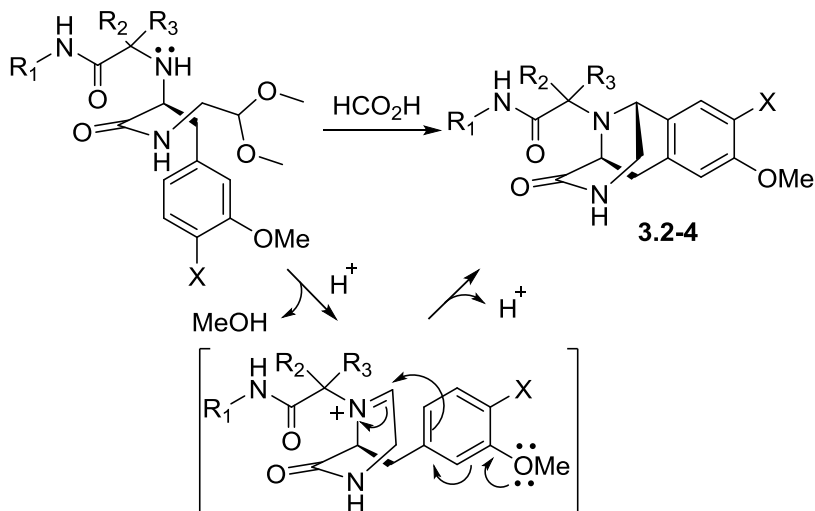


Entry	Aldehyde/Ketone	Isocyanide	X	Yield (%)
3.2-3A			H	44
3.2-3B			H	40
3.2-3C			H	48
3.2-3D			H	30
3.2-3E			H	42
3.2-3F			H	52
3.2-3G			H	48
3.2-3H			OH	35
3.2-3I			H	27
3.2-3J			OH	35

3.2-3K			H	28
3.2-3L			OH	44
3.2-3M			OH	29
3.2-3N			H	61 4:1 ^[a]
3.2-3O			OH	38 4:1 ^[b]
3.2-3P			OH	40
3.2-3Q			OH	27
3.2-3R			OH	51
3.2-3S			H	25
3.2-3T			H	19
3.2-3U			OH	24
3.2-3V			H	52 3.6:1 ^[b]

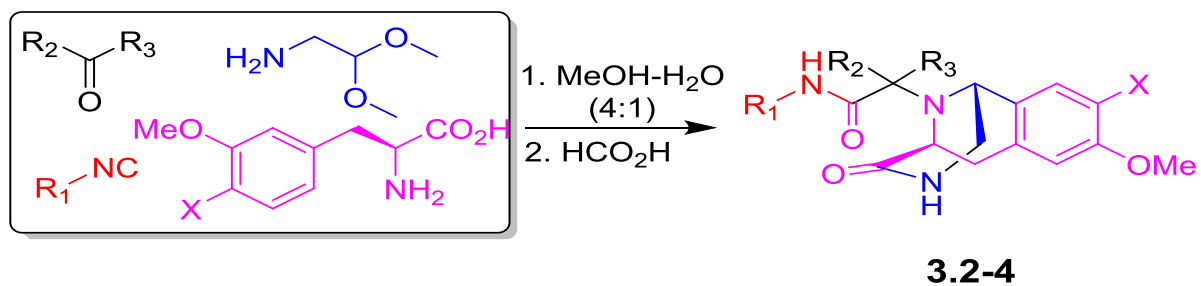
Table 3-4 Ugi4C5CR Pictet-Spengler cyclization reaction product isolated yields over two steps [a]

d.r. determined by UV [b] d.r. determined by NMR



Scheme 3-5 Proposed reaction mechanism of the Pictet-Spengler isoquinoline derivative formation.

We also investigated the use of phenylalanine amino acid derivatives to form the Ugi-Pictet-Spengler isoquinoline (**3.2-4**). While the U-5C-4CR product was formed in all cases only when using 3-methoxy phenylalanine, and 3,4-dimethoxy phenylalanine was the Pictet Spengler isoquinoline product (**3.2-4**) produced. However if no electron donor group is available on the *meta* position of the phenyl ring, such as phenylalanine or 4-methoxy phenylalanine, the Pictet-Spengler isoquinoline was not formed. The reaction might occur as shown in **Scheme 3-5**. The acetal group is removed in acidic condition to form the iminium ion followed by electrophilic substitution and deprotonation to give the desired product.^{190,191} Several analogous reactions were applied and all analogs gave satisfactory yield even with diethyl (cyanomethyl)phosphonate (**3.2-4H**) as shown in **Table 3-5**.



Entry	Aldehyde/Ketone	Isocyanide	X	Yield (%)
3.2-4A			OMe	64
3.2-4B			OMe	59
3.2-4C			OMe	62
3.2-4D			H	35
3.2-4E			OMe	72
3.2-4F			OMe	49
3.2-4G			H	44
3.2-4H			OMe	76
3.2-4I			H	47
3.2-4J			OMe	52

Table 3-5 Ugi4C5CR Pictet-Spengler cyclization reaction product isolated yields over two steps

Next we were interested in the question of how some physicochemical properties of our scaffolds cluster and compare with other commonly used virtual screening libraries. Thus we calculated the descriptors cLogP, Rotatable Bonds, Molecular Weight, and other drug like properties from a randomly generated library of 1000 compounds based on all four scaffolds. The majority of these compounds pass at least 3 out of 4 of Lipinski's rule of 5, most of them however failing the molecular weight rule. Interestingly the two later scaffolds (**3.2-3** and **3.2-4**) possess a low number of rotatable bonds and are highly stiff, increasing their chance of oral bio-availability (**Figure 3.4**). We were especially interested in the recently introduced shape descriptor principal moment-of-inertia (PMI) as a means to differentiate scaffolds based on shape.¹²⁸ These libraries were compared to 1000 randomly selected compounds from the Zinc database^{66,192} and each library was found to possess more 3D characteristics than the Zinc compounds. (**Figure 3.5**) As protein-protein interactions become an increasingly popular yet difficult target for pharmaceutical companies novel chemical space needs to be explored.¹⁹³ With novel scaffolds that possess more 3D features the chances to successfully probe previously unmet medical needs greatly increase. Biological activities of compounds based on the new scaffolds will be reported in due course.

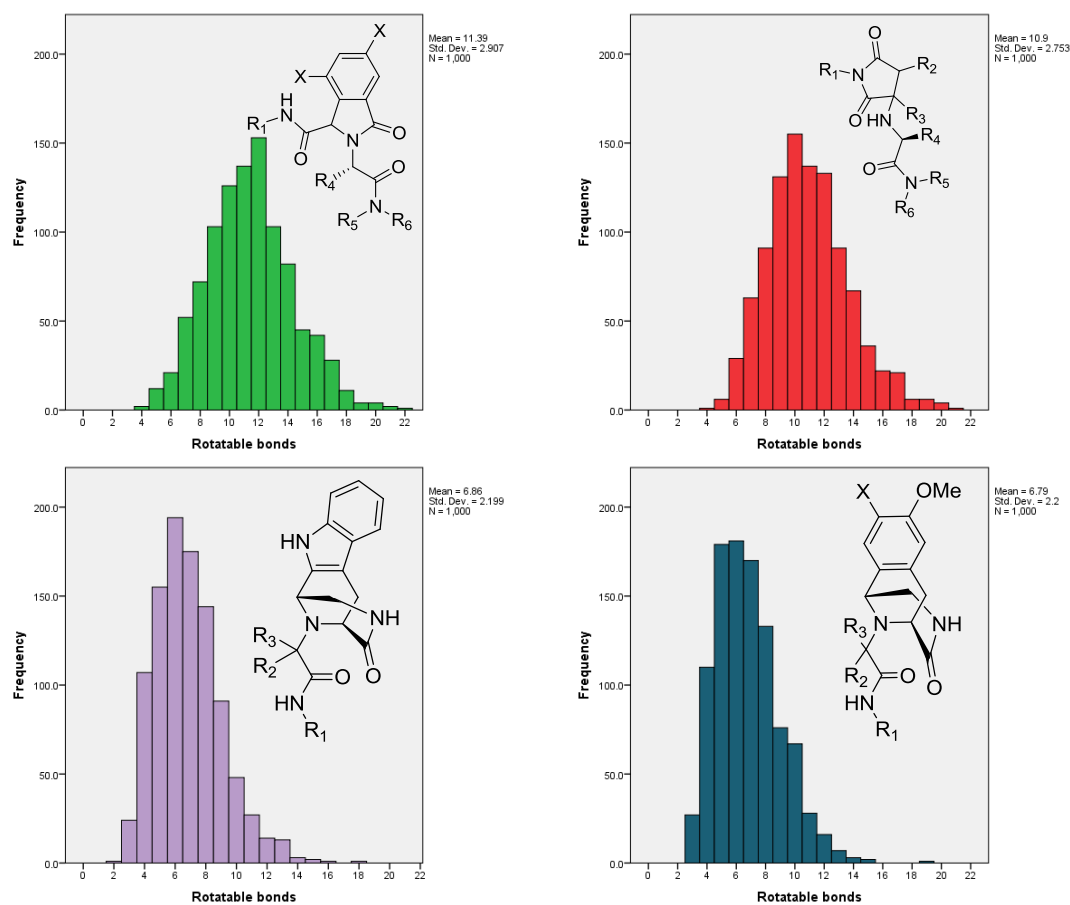


Figure 3.4 Distribution of rotatable bonds of 1000 randomly generated compounds of all four scaffold classes

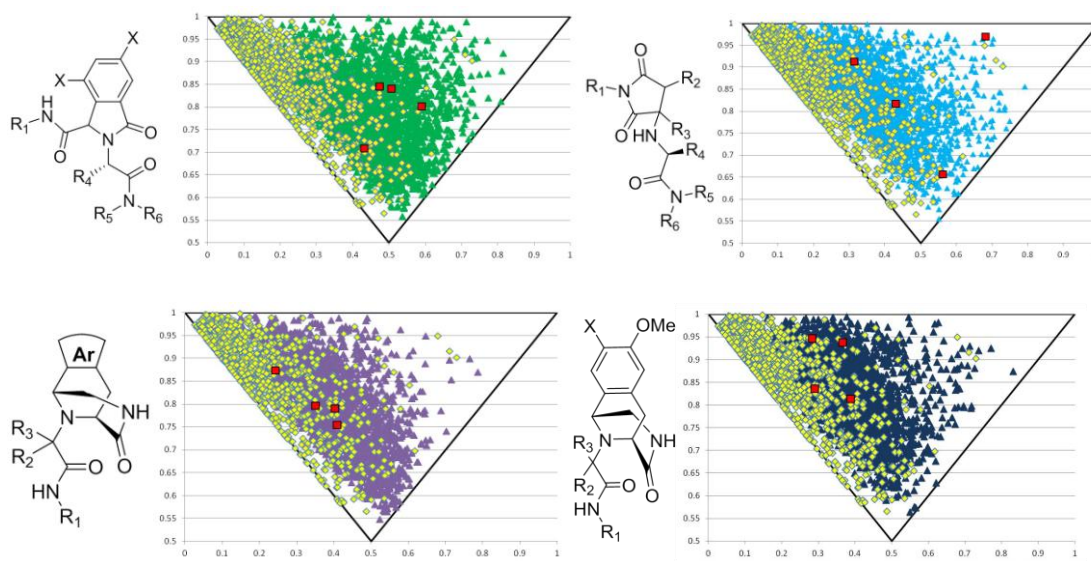


Figure 3.5 Principal Moment of Inertia (PMI) calculated for 1,000 randomly generated compounds for each of the four scaffolds 3.2-1 (green triangles), 3.2-2 (light blue triangles), 3.2-3 (purple triangles) and 3.2-4 (navy blue triangles) compared to 1,000 randomly chosen compounds from the Zinc Library^{194,195} (yellow squares). PMI of specific compounds from this paper can be seen in all four graphs as red squares.

3.2.4 Materials and Methods

Generalities

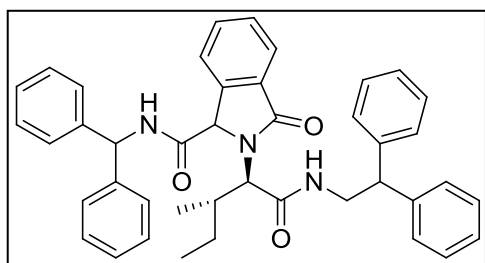
Dry solvents were purchased from Aldrich, Fisher Scientific, Acros Organics or Alfa Aesar and used as received. Starting materials were purchased from Aldrich, Fisher Scientific, Acros Organics or Alfa Aesar. Isocyanides were prepared according to the two step Ugi or one-step Hoffmann methods. ¹H- and ¹³C NMR spectra were recorded on a Bruker Ultrashield Plus 600. Chemical shift values are in ppm relative either to CDCl₃ or DMSO-d₆. Abbreviations used are s = singlet, brs = broad singlet d = doublet, dd = double doublet, t = triplet, td = triple doublet, dt = double triplet q=quartet, m=multiplet; data in parenthesis are given in the following order: multiplicity, number of protons, and coupling constants in Hz. MS spectra were recorded

on a Waters Super Critical Fluid Chromatograph with a 3100 MS Detector using solvent system of Methanol and CO₂ on an ethyl pyridine. Purifications were done on either the Waters Super Critical Fluid Chromatograph Prep 100 system using CO₂ and Methanol or the Teledyne ISCO Combiflash RF System using Hexane/Ethyl Acetate/Dichloromethane/Methanol or silica gel prep TLC plate

General procedure of Ugi-Cyclization reaction yielding oxoisindolines:

A mixture of L-amino acid (0.5 mmol), aldehyde (0.5 mmol), isocyanide (0.5 mmol) and primary or secondary amine (0.5 mmol), in TFE (5 mL) were stirred at 85 °C for 24 – 72 hours. SFC-MS trace showed both the Ugi product as well as the desired cyclized product. TFE was evaporated under reduced pressure and residue was dissolved in DCM. Unreacted amino acid was filtered off and filtrate was evaporated and dissolved in 1 mL EtOH and let sit in an oil bath at 60 °C for 24 hours to allow for the remainder of the Ugi product to cyclize. Precipitate was filtered off and confirmed to be the desired cyclized product by SFC-MS and NMR.

N-benzhydryl-2-(1-((2,2-diphenylethyl)amino)-3-methyl-1-oxopentan-2-yl)-3-



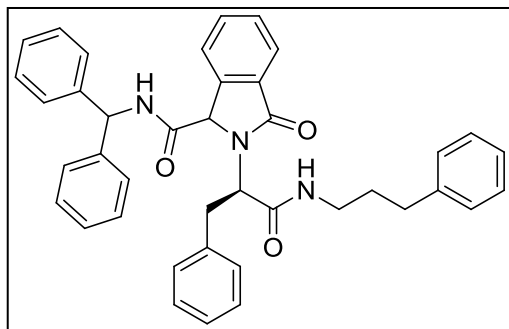
oxoisindoline-1-carboxamide [3.2-1A]: 35% yield as a

white solid ¹H NMR (600 MHz, CDCl₃) δ 0.52 (d, *J* = 6.6 Hz, 3H), 0.66 (t, *J* = 7.2 Hz, 3H), 1.13 – 1.18 (m, 2H), 1.57 (s, 2H), 1.92 – 1.96 (m, 1H), 3.34 – 3.38 (m, 2H),

3.87 – 3.94 (m, 2H), 4.04 (t, *J* = 8.1 Hz, 1H), 5.04 (s, 1H), 6.13 (d, *J* = 8.1 Hz, 1H), 6.95 – 6.97 (m, 2H), 7.04 – 7.13 (m, 10H), 7.16 – 7.21 (m, 9H), 7.43 (t, *J* = 7.4 Hz, 1H), 7.49 (t, *J* = 7.6, 1H), 7.59 (d, *J* = 7.6 Hz, 1H), 7.70 (d, *J* = 7.4 Hz, 1H), 8.46 – 8.47 (m, 1H); ¹³C NMR (150 MHz, CDCl₃) δ 11.0, 15.4, 27.1, 29.7, 34.1, 43.9, 50.5, 57.3, 64.0, 123.3, 123.8, 126.8, 126.9,

126.9, 127.1, 127.5, 128.0, 128.1, 128.3, 128.5, 128.6, 128.7, 129.0, 130.0, 132.6, 140.7, 141.5, 141.7, 142.2, 167.2, 170.8, 170.9 ppm. SFCMS (APCI, m/z): $[M]^+$ calc.: 636.31; found: 636.33.

N-benzhydryl-3-oxo-2-(1-oxo-3-phenyl-1-((3-phenylpropyl)amino)propan-2-yl)isoindoline-



1-carboxamide [3.2-1B]: 50% yield as a yellow oil ^1H

NMR (600 MHz, Chloroform- d) δ 1.52 – 1.61 (m, 2H),

2.41 – 2.48 (m, 2H), 2.90 – 2.94 (m, 1H), 2.99 – 3.04

(m, 1H), 3.14 – 3.20 (m, 2H), 4.58 (dd, J = 10.7, 6.3

Hz, 1H), 5.30 (s, 1H), 5.47 – 5.50 (m, 1H), 6.40 (d, J =

8.8 Hz, 1H), 6.90 (d, J = 7.3 Hz, 1H), 7.11 – 7.13 (m, 1H), 7.19 – 7.33 (m, 12H), 7.47 – 7.48 (m,

1H), 7.52 (t, J = 7.4 Hz, 1H), 7.60 (t, J = 7.5 Hz, 1H), 7.84 (t, J = 8.2 Hz, 1H), 10.29 (d, J = 8.9

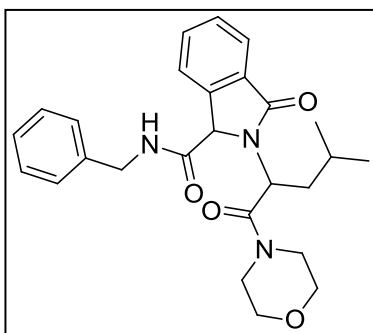
Hz, 1H); ^{13}C NMR (150 MHz, CDCl_3) δ 30.6, 32.9, 35.1, 39.3, 57.1, 60.2, 63.4, 123.5, 123.5,

126.0, 127.0, 127.1, 127.3, 128.4, 128.4, 128.5, 128.5, 128.8, 128.9, 129.0, 129.7, 132.6, 135.7,

140.6, 141.3, 142.2, 142.3, 167.8, 170.7, 171.4 ppm. SFCMS (APCI, m/z): $[M]^+$ calc.: 608.28;

found: 608.36

N-benzyl-2-(4-methyl-1-morpholino-1-oxopentan-2-yl)-3-oxoisindoline-1-carboxamide



[3.2-1C]: 42% yield as a yellow solid ^1H NMR (600 MHz,

CDCl_3) δ 0.79-0.86 (m, 12H), 1.42-1.46 (m, 2H), 1.57-1.61 (m,

1H), 1.64-1.68 (m, 2H), 1.74-1.78 (m, 1H), 3.35-3.47 (m, 4H),

3.51-3.61 (m, 5H), 3.62-3.70 (m, 5H), 3.77-3.88 (m, 2H), 4.16-

4.25 (m, 2H), 4.37 (dd, J =14.6, 6.4Hz, 1H), 4.46 (dd, J =14.6,

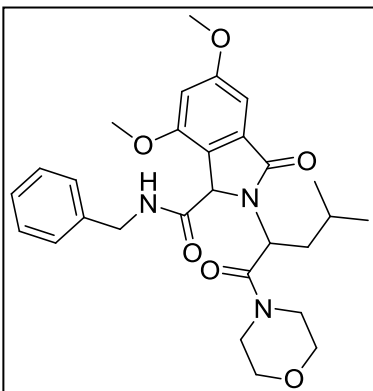
6.3Hz, 1H), 4.94 (t, J =7.4Hz, 1H), 5.12 (s, 1H), 5.29 (t, J =7.5Hz, 1H), 5.41 (s, 1H), 7.01-7.02

(m, 1H), 7.10-7.13 (m, 3H), 7.14-7.18 (m, 4H), 7.19-7.24 (m, 4H), 7.38-7.44 (m, 3H), 7.48 (q,

J =7.7 2H), 7.67 (d, 6.1Hz, 1H), 7.70-7.71 (m, 2H), 9.39-9.40 (m, 1H); ^{13}C NMR (150 MHz,

CDCl₃) δ 22.3, 22.7, 22.8, 23.0, 25.0, 25.4, 38.3, 38.7, 43.0, 43.5, 43.8, 46.7, 49.6, 51.3, 62.8, 63.7, 66.4, 66.6, 122.4, 123.1, 123.5, 124.0, 127.2, 127.7, 127.9, 128.0, 128.4, 128.7, 129.0, 129.0, 129.9, 130.6, 132.5, 132.6, 137.6, 138.1, 142.5, 142.6, 168.4, 168.5, 169.6, 170.1, 170.4, 171.2 ppm. SFCMS (APCI, m/z): [M]⁺ calc.: 450.23; found: 450.21.

N-benzyl-5,7-dimethoxy-2-(4-methyl-1-morpholino-1-oxopentan-2-yl)-3-oxoisindoline-1-

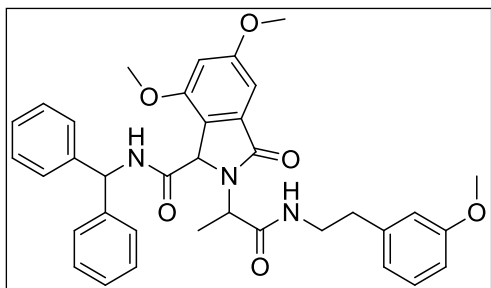


carboxamide [3.2-1D]: 40% yield as a yellow solid

Diastereomer A: ¹H NMR (600 MHz, Chloroform-d) δ 0.93 (d, J = 6.7 Hz, 3H), 0.97 (d, J = 6.6 Hz, 3H), 1.57 – 1.63 (m, 1H), 1.77 – 1.80 (m, 2H), 3.46 – 3.59 (m, 4H), 3.64 – 3.68 (m, 4H), 3.71 (s, 3H), 3.86 (s, 3H), 4.32 (dd, J = 14.8, 4.8 Hz, 1H), 4.72 (dd, J = 14.8, 7.0 Hz, 3H), 5.13 (s, 1H), 5.51 (t, J = 7.6 Hz, 1H),

6.57 (d, J = 2.1 Hz, 1H), 6.87 – 6.89 (m, 1H), 6.93 (d, J = 2.0 Hz, 1H), 7.29 – 7.31 (m, 1H), 7.35 – 7.36 (m, 4H); ¹³C NMR (151 MHz, CDCl₃) δ 22.6, 22.7, 22.8, 24.9, 38.8, 42.5, 43.9, 46.5, 49.0, 55.9, 60.9, 66.8, 67.0, 98.3, 103.1, 122.9, 127.5, 128.0, 128.6, 133.6, 137.9, 154.8, 162.3, 167.7, 169.1, 169.4 ppm **Diastereomer B:** ¹H NMR (600 MHz, Chloroform-d) δ 0.92 (d, J = 6.7 Hz, 3H), 0.94 (d, J = 6.5 Hz, 3H), 1.34 – 1.39 (m, 1H), 1.78 (t, J = 7.2 Hz, 2H), 3.48 – 3.61 (m, 4H), 3.66 (s, 3H), 3.69 – 3.82 (m, 4H), 3.86 (s, 3H), 4.22 (dd, J = 14.8, 4.5 Hz, 1H), 4.63 (dd, J = 14.8, 7.2 Hz, 1H), 4.97 (s, 1H), 5.38 (t, J = 7.5 Hz, 1H), 6.53 – 6.58 (m, 2H), 6.96 (d, J = 2.1 Hz, 1H), 7.25 – 7.37 (m, 5H); ¹³C NMR (150 MHz, CDCl₃) δ 22.52, 23.00, 24.54, 39.23, 42.46, 43.87, 45.96, 48.43, 55.36, 55.91, 59.38, 66.23, 76.84, 77.05, 77.27, 98.64, 103.12, 127.43, 127.93, 128.55, 133.58, 138.06, 154.70, 162.38, 166.37, 167.87, 168.71 ppm. SFCMS (APCI, m/z): [M]⁺ calc.: 510.25; found: 510.28.

N-benzhydryl-5,7-dimethoxy-2-(1-((3-methoxyphenethyl)amino)-1-oxopropan-2-yl)-3-



oxoisindoline-1-carboxamide (3.2-1E) (1:1 mixture

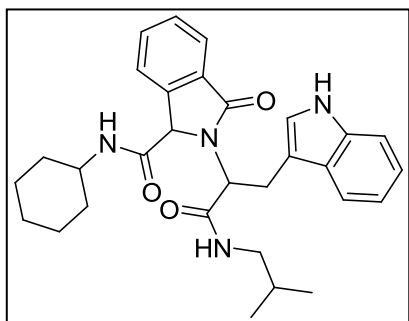
of diastereomers): 38% as white powder; HRMS

(APCI, m/z): $[M]^+$ calc.: 608.27; found: 608.36; ^1H

NMR (600 MHz, CD_3OD) δ 1.46-1.49 (d, 3H), 2.70-

2.75 (m, 2H), 3.40-3.42 (m, 1H), 3.48-3.52 (m, 1H), 3.57 (s, 3H), 3.73 (s, 3H), 3.87 (s, 3H), 4.27-4.29 (q, 1H), 5.21 (s, 1H), 6.25-6.26 (d, 1H), 6.57 (s, 1H), 6.70-6.72 (d, 2H), 6.95-6.96 (d, 1H), 7.06-7.07 (d, 2H), 7.20-7.21 (d, 2H), 7.28-7.35 (m, 6H), 7.38-7.42 (m, 3H); ^{13}C NMR (150 MHz, CD_3OD) δ 14.2, 34.8, 41.2, 53.3, 55.2, 55.3, 56.0, 57.5, 62.2, 98.8, 103.0, 113.8, 120.9, 127.3, 127.6, 128.7, 129.7, 131.2, 134.7, 140.8, 141.3, 154.5, 158.0, 162.5, 167.3, 168.2, 170.1 ppm. SFCMS (APCI, m/z): $[M]^+$ calc.: 607.27 found: 607.33.

2-(3-(1H-indol-3-yl)-1-(isobutylamino)-1-oxopropan-2-yl)-N-cyclohexyl-3-oxoisindoline-1-



carboxamide (3.2-1F) 33% as white powder; ^1H NMR (600

MHz, $\text{DMSO}-d_6$) δ 0.74 – 0.83 (t, J = 6.4 Hz, 6H), 1.13 –

1.20 (m, 1H), 1.22 – 1.30 (m, 4H), 1.53 – 1.58 (m, 1H), 1.62

– 1.68 (m, 1H), 1.67 – 1.75 (m, 2H), 1.75 – 1.83 (m, 2H),

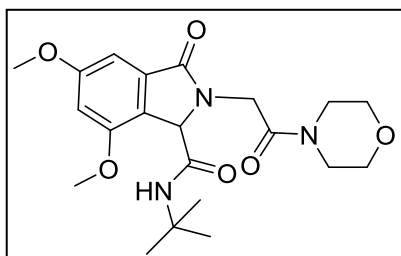
2.79 – 2.86 (dt, J = 12.7, 5.8 Hz, 1H), 2.90 – 2.97 (dt, J =

12.9, 6.4 Hz, 1H), 3.16 – 3.23 (dd, J = 15.2, 9.1 Hz, 1H), 3.35 – 3.39 (m, 2H), 3.52 – 3.61 (m, 1H), 4.87 – 4.93 (dd, J = 9.0, 6.1 Hz, 1H), 5.35 (s, 1H), 6.98 – 7.03 (m, 1H), 7.05 – 7.12 (m, 2H), 7.31 – 7.35 (d, J = 8.1 Hz, 1H), 7.48 – 7.56 (m, 2H), 7.59 – 7.64 (m, 2H), 7.66 – 7.72 (d, J = 7.5 Hz, 1H), 8.43 – 8.47 (t, J = 5.8 Hz, 1H), 9.07 – 9.12 (d, J = 7.8 Hz, 1H), 10.86 (s, 1H); ^{13}C NMR (151 MHz, DMSO) δ 20.4, 24.9, 25.6, 26.5, 28.3, 32.5, 46.7, 48.6, 58.2, 62.4, 98.8, 99.9, 110.4,

111.9, 118.7, 122.9, 123.2, 123.3, 127.3, 129.2, 131.0, 132.6, 136.7, 143.1, 169.6, 170.9 ppm.

SFCMS (APCI, m/z): $[M]^+$ calc.: 501.63 found: 501.35.

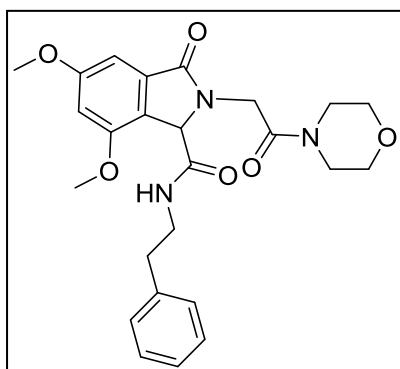
N-(tert-butyl)-5,7-dimethoxy-2-(2-morpholino-2-oxoethyl)-3-oxoisindoline-1-



carboxamide (3.2-1G) 30% as white solid ^1H NMR (600 MHz, DMSO- d_6) δ 1.27 (s, 9H), 3.34 (s, 2H), 3.39-3.41 (m, 2H), 3.48-3.49 (m, 2H), 3.54-3.62 (m, 4H), 3.82 (s, 3H), 3.83 (s, 3H), 5.13 (s, 1H), 6.75 (s, 1H), 6.79 (s, 1H), 8.21 (s,

1H); ^{13}C NMR (151 MHz, DMSO) δ 28.7, 28.8, 51.1, 62.7, 62.8, 67.2, 98.4, 102.94, 123.3, 134.6, 155.56, 162.1, 165.8, 166.8, 168.6 ppm. SFCMS (APCI, m/z): $[M]^+$ calc.: 420.21 found: 420.35.

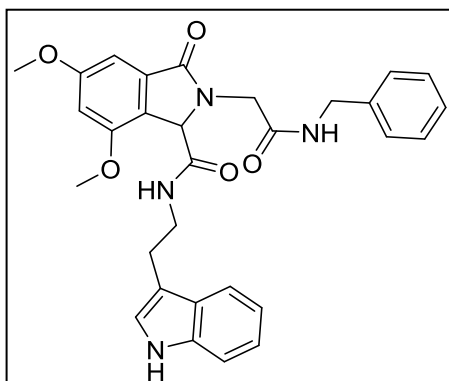
5,7-dimethoxy-2-(2-morpholino-2-oxoethyl)-3-oxo-N-phenethylisindoline-1-carboxamide



(3.2-1H) 42% as white solid. ^1H NMR (600 MHz, DMSO- d_6) δ 2.51 (s, 1H), 2.74-2.75 (m, 1H), 3.36-3.38 (m, 6H), 3.41-3.49 (m, 2H), 3.57-3.59 (m, 4H), 3.78 (s, 3H), 3.84 (s, 3H), 5.06 (s, 1H), 6.76 (s, 1H), 6.82 (s, 1H), 7.22-7.23 (m, 3H), 7.29-7.30 (m, 2H), 8.60 (s, 1H); ^{13}C NMR (151 MHz, DMSO) δ 35.3, 55.7, 55.8, 56.2, 56.3, 56.6, 56.7, 62.4, 62.5, 66.4,

98.5, 98.6, 103.0, 122.8, 128.7, 128.8, 128.9, 129.1, 134.6, 139.7, 155.6, 162.2, 166.3, 166.7, 168.6 ppm. SFCMS (APCI, m/z): $[M]^+$ calc.: 468.21 found: 468.23.

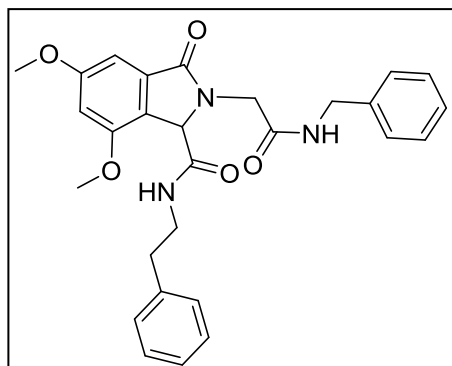
N-(2-(1H-indol-3-yl)ethyl)-2-(2-(benzylamino)-2-oxoethyl)-5,7-dimethoxy-3-



oxoisindoline-1-carboxamide (3.2-1I) 20% at white solid ^1H NMR (600 MHz, DMSO- d_6) δ 2.83-2.86 (m, 2H), 3.32-3.34 (m, 2H), 3.46-3.55 (m, 1H), 3.54 (d, J =17.4Hz, 1H), 3.77 (s, 3H), 3.84 (s, 3H), 4.39-4.31 (m, 2H), 5.18 (s, 1H), 6.77 (s, 1H), 6.84 (s, 1H), 6.98 (t, J =7.2Hz, 1H), 7.07 (t, J =7.8, 1H), 7.16 (s, 1H), 7.24-7.28

(m, 3H), 7.31-7.35 (m, 3H), 7.54 (d, J =7.8Hz, 1H), 8.53-8.55 (m, 1H), 8.73-8.75 (m, 1H), 10.83 (s, 1H). ^{13}C NMR (151 MHz, DMSO) δ 25.5, 55.7, 55.8, 56.2, 56.6, 62.7, 62.9, 98.6, 98.7, 103.0, 111.9, 118.6, 118.7, 121.4, 122.7, 122.9, 123.2, 127.5, 127.6, 127.8, 128.7, 128.8, 135.5, 136.7, 139.5, 155.6, 162.2, 166.7, 168.0, 168.7 ppm. SFCMS (APCI, m/z): $[\text{M}]^+$ calc.:527.22 found: 527.19.

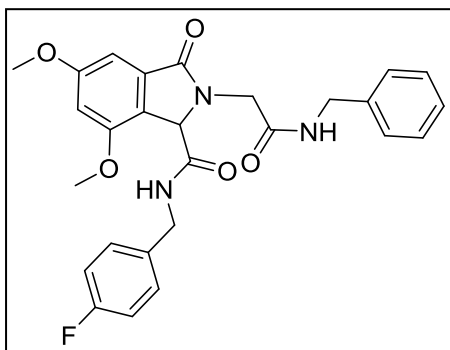
2-(2-(benzylamino)-2-oxoethyl)-5,7-dimethoxy-3-oxo-N-phenethylisindoline-1-



carboxamide (3.2-1J) 44% as white solid ^1H NMR (600 MHz, DMSO- d_6) δ 2.73-2.75 (m, 2H), 3.30-3.39 (m, 4H), 3.79 (s, 3H), 3.85 (s, 3H), 4.26-4.34 (m, 2H), 5.16 (s, 1H), 6.77 (s, 1H), 6.83 (s, 1H), 7.21-7.22 (m, 2H), 7.25-7.30 (m, 5H), 7.32-7.24 (m, 2H), 8.53-8.55 (m, 1H), 8.69-8.71 (m, 1H) ^{13}C NMR (151 MHz, DMSO) δ 55.7, 55.8, 56.2, 56.4,

56.6, 62.7, 62.8, 98.6, 98.7, 103.0, 122.7, 126.5, 127.2, 127.4, 127.7, 127.8, 128.7, 128.8, 128.9, 129.1, 134.6, 139.5, 139.7, 155.6, 162.3, 166.7, 168.0, 168.6 ppm. SFCMS (APCI, m/z): $[\text{M}]^+$ calc.:488.22 found: 488.29.

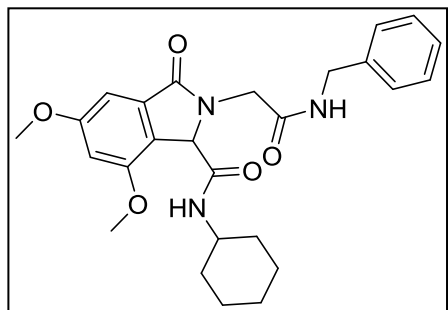
2-(2-(benzylamino)-2-oxoethyl)-N-(4-fluorobenzyl)-5,7-dimethoxy-3-oxoisindoline-1-



carboxamide (3.2-1K) 35% as white solid ^1H NMR (600 MHz, DMSO- d_6) δ 3.52 (d, $J=17.4$, 2H), 3.76 (s, 3H), 3.86 (s, 3H), 4.18-4.21 (m, 1H), 4.30-4.39 (m, 2H), 4.41-4.44 (m, 1H), 5.23 (s, 1H), 6.77 (s, 1H), 6.84 (s, 1H), 7.16 (m, 2H), 7.26-7.32 (m, 7H), 8.57 (s, 1H), 9.16 (s, 1H);

^{13}C NMR (151 MHz, DMSO) δ 55.7, 56.1, 56.4, 56.6, 62.6, 62.7, 98.6, 98.7, 102.9, 115.4, 122.5, 127.6, 127.8, 128.8, 129.4, 129.5, 129.6, 134.6, 135.6, 139.5, 155.5, 160.8, 162.3, 167.0, 167.9, 168.7 ppm. SFCMS (APCI, m/z): $[\text{M}]^+$ calc.:497.19 found: 497.22.

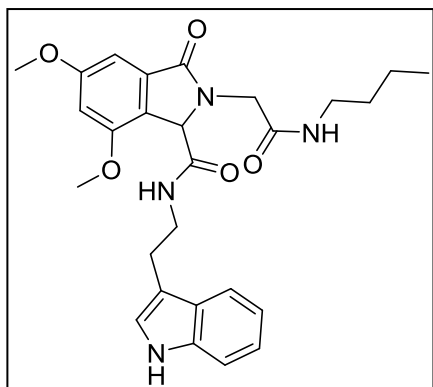
2-(2-(benzylamino)-2-oxoethyl)-N-cyclohexyl-5,7-dimethoxy-3-oxoisindoline-1-



carboxamide (3.2-1L) 30% as white solid ^1H NMR (600 MHz, DMSO- d_6) δ 1.14-1.17 (m, 1H), 1.21-1.26 (m, 4H), 1.55-1.57 (m, 1H), 1.69-1.74 (m, 4H), 3.49-3.52 (m, 2H), 3.55-3.57 (m, 1H), 3.81 (s, 3H), 3.83 (s, 3H), 4.24-4.27 (dd, ***, 1H), 4.33-4.37 (dd, ***, 1H), 5.18 (s, 1H), 6.76 (s,

1H), 6.81 (s, 1H), 7.24-7.28 (m, 2H), 7.31-7.34 (m, 2H), 7.37-7.41 (m, 1H), 8.54-8.56 (m, 2H); ^{13}C NMR (151 MHz, DMSO) δ 24.7, 24.9, 25.6, 32.4, 32.6, 55.6, 56.5, 62.6, 62.7, 98.5, 98.6, 102.9, 122.9, 127.6, 127.7, 128.7, 128.8, 134.6, 139.5, 155.6, 162.2, 165.6, 168.0, 168.7 ppm. SFCMS (APCI, m/z): $[\text{M}]^+$ calc.:466.23 found: 466.25.

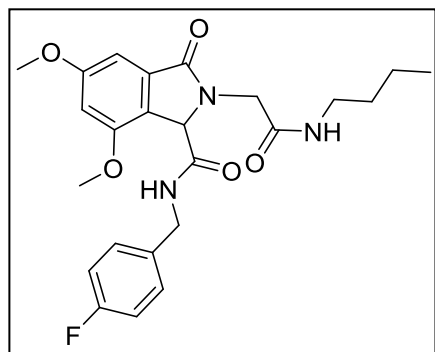
N-(2-(1H-indol-3-yl)ethyl)-2-(2-(butylamino)-2-oxoethyl)-5,7-dimethoxy-3-oxoisindoline-



1-carboxamide (3,2-1M) (Mixture of rotamers) 41% as white solid ^1H NMR (600 MHz, DMSO- d_6) δ 0.86-0.88 (m, 3H), 1.26-1.32 (m, 2H), 1.37-1.51 (m, 2H), 2.82-2.86 (m, 2H), 3.06-3.09 (m, 1H), 3.31-3.36 (m, 1H), 3.45-3.49 (m, 2H), 3.76 (s, 3H), 3.84 (s, 3H), 5.14 (s, 1H), 6.76 (s, 1H), 6.83 (s, 1H), 6.96-6.99 (m, 1H), 7.05-7.08 (m, 1H),

7.15 (s, 1H), 7.33-7.35 (m, 1H), 7.52-7.54 (m, 1H), 7.98-7.99 (m, 1H), 8.73-8.75 (m, 1H), 10.87 (s, 1H); ^{13}C NMR (151 MHz, DMSO) δ 19.6, 20.1, 25.6, 29.8, 31.6, 55.7, 62.7, 62.8, 98.6, 98.7, 102.9, 111.9, 118.7, 122.7, 123.0, 123.2, 134.6, 134.7, 155.6, 162.3, 166.8, 167.7, 168.6, 171.2 ppm. SFCMS (APCI, m/z): $[\text{M}]^+$ calc.:493.24 found: 493.30.'

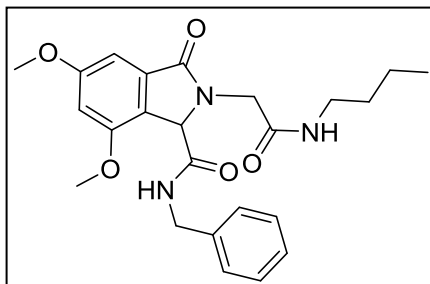
2-(2-(butylamino)-2-oxoethyl)-N-(4-fluorobenzyl)-5,7-dimethoxy-3-oxoisindoline-1-



carboxamide (3,2-1N) 25% as white solid ^1H NMR (600 MHz, DMSO- d_6) δ 0.87 (t, $J=7.2$, 3H), 1.27-1.32 (m, 2H), 1.47-1.50 (m, 2H), 2.72 (t, $J=7.2$, 2H), 3.40-3.46 (m, 2H), 3.77 (s, 3H), 3.84 (s, 3H), 4.12-4.21 (m, 1H), 4.39-4.51 (m, 1H), 5.22 (s, 1H), 6.76 (s, 1H), 6.82 (s, 1H), 7.15-7.18 (m,

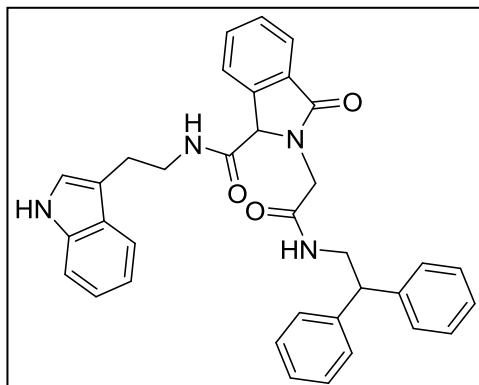
2H), 7.28-7.32 (m, 2H), 7.93-7.94 (m, 1H), 8.01-8.02 (m, 1H); ^{13}C NMR (151 MHz, DMSO) δ 19.6, 19.9, 29.9, 31.6, 55.7, 56.1, 56.5, 98.6, 101.2, 102.9, 122.7, 134.7, 135.7, 155.4, 160.8, 162.3, 166.6, 167.0, 167.2, 168.4, 171.7 ppm. SFCMS (APCI, m/z): $[\text{M}]^+$ calc.:458.20 found: 458.15.

N-benzyl-2-(2-(butylamino)-2-oxoethyl)-5,7-dimethoxy-3-oxoisindoline-1-carboxamide



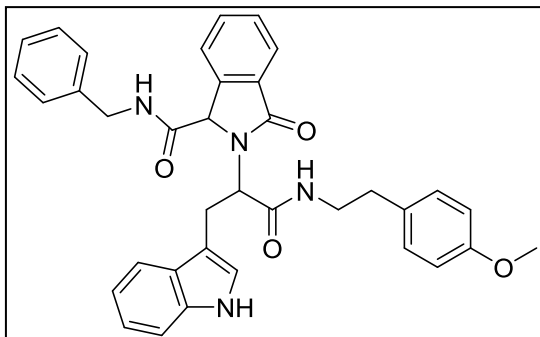
(3.2-1O) 43% as white solid ^1H NMR (600 MHz, DMSO- d_6) δ 0.87 (t, $J=7.2$, 3H), 1.28-1.31 (m, 2H), 1.47-1.49 (m, 2H), 2.71-2.24 (m, 2H), 3.43-3.44 (m, 2H), 3.71 (s, 3H), 3.83 (s, 3H), 4.14-3.17 (m, 1H), 4.50-4.56 (m, 1H), 6.76 (s, 1H), 6.82 (s, 1H), 7.24-7.29 (m, 3H), 7.32-7.35 (m, 2H), 7.91 (s, 1H), 8.03 (s, 1H), 9.58 (s, 1H); ^{13}C NMR (151 MHz, DMSO) δ 19.6, 19.9, 29.9, 44.8, 55.7, 55.8, 56.1, 56.5, 56.7, 98.5, 101.9, 102.8, 122.8, 127.5, 128.7, 139.5, 155.5, 162.2, 166.6, 167.0, 167.2, 167.6, 168.5, 171.5 ppm. SFCMS (APCI, m/z): $[\text{M}]^+$ calc.:440.21 found: 440.28.

N-(2-(1H-indol-3-yl)ethyl)-2-(2-((2,2-diphenylethyl)amino)-2-oxoethyl)-3-oxoisindoline-1-carboxamide (3.2-1P)



carboxamide (3.2-1P) 37% as white solid ^1H NMR (600 MHz, DMSO- d_6) δ 2.77-2.81 (m, 1H), 2.85-2.89 (m, 1H), 3.30-3.33 (m, 1H), 3.49-3.54 (m, 1H), 3.63-3.66 (m, 2H), 3.72-3.74 (m, 1H), 4.02-4.05 (m, 2H)m 4.77 (s, 1H), 6.25-6.26 (m, 1H), 6.75 (m, 1H), 6.92-6.95 (m, 1H), 7.00-7.02 (m, 2H), 7.06-7.10 (m, 6H), 7.14-7.17 (m, 6H), 7.32-7.35 (m, 1H), 7.40-7.45 (m, 1H), 7.51 (d, $J=7.8$, 1H), 7.58 (d, $J=7.2$, 1H), 7.90-7.92 (m, 1H), 8.27 (s, 1H); ^{13}C NMR (151 MHz, DMSO) δ 14.2, 21.1, 24.6, 40.4, 44.1, 50.3, 60.4, 65.6, 111.2, 112.5, 118.6, 119.2, 121.9, 122.2, 123.1, 123.6, 126.9, 127.5, 127.9, 128.0, 128.1, 128.2, 128.3, 128.7, 128.8, 128.9, 129.8, 130.1, 132.6, 136.2, 141.6, 141.7, 141.8, 167.5, 168.4, 170.1, 171.3 ppm. SFCMS (APCI, m/z): $[\text{M}]^+$ calc.:557.26 found: 557.25.

2-(3-(1H-indol-3-yl)-1-((4-methoxyphenethyl)amino)-1-oxopropan-2-yl)-N-benzyl-3-



oxoisindoline-1-carboxamide (3.2-1Q) 35% as

yellow oil ^1H NMR (600 MHz, DMSO- d_6) δ 2.52

– 2.55 (d, J = 7.4 Hz, 2H), 3.10 – 3.18 (ddd, J =

16.2, 13.1, 7.0 Hz, 2H), 3.19 – 3.25 (m, 1H), 3.29

– 3.34 (dd, J = 15.0, 6.9 Hz, 1H), 3.35 – 3.37 (s,

1H), 3.68 – 3.70 (s, 3H), 4.26 – 4.31 (dd, J = 15.0, 5.6 Hz, 1H), 4.37 – 4.42 (dd, J = 15.1, 6.1 Hz,

1H), 4.92 – 4.96 (t, J = 7.6 Hz, 1H), 5.47 – 5.48 (s, 1H), 6.75 – 6.77 (d, J = 8.5 Hz, 2H), 7.00 –

7.02 (d, J = 8.4 Hz, 3H), 7.04 – 7.06 (d, J = 2.3 Hz, 1H), 7.07 – 7.11 (ddd, J = 8.2, 7.0, 1.1 Hz,

1H), 7.25 – 7.28 (q, J = 4.4 Hz, 1H), 7.31 – 7.35 (d, J = 4.5 Hz, 4H), 7.53 – 7.56 (m, 1H), 7.56 –

7.59 (m, 2H), 7.61 – 7.65 (dd, J = 7.5, 1.2 Hz, 1H), 7.71 – 7.74 (d, J = 7.5 Hz, 1H), 8.38 – 8.42

(t, J = 5.7 Hz, 1H), 9.50 – 9.53 (t, J = 5.9 Hz, 1H), 10.84 – 10.85 (d, J = 2.6 Hz, 1H). ^{13}C NMR

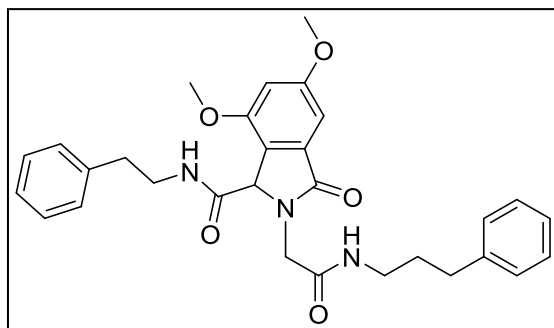
(151 MHz, DMSO) δ 26.54, 34.37, 55.37, 55.39, 57.58, 62.50, 110.28, 111.88, 114.07, 118.80,

118.88, 121.62, 123.00, 123.37, 123.42, 127.44, 127.47, 127.94, 128.77, 129.29, 130.06, 131.21,

131.73, 132.57, 136.62, 139.22, 142.96, 158.02, 168.61, 169.44, 170.36. ppm. SFCMS (APCI,

m/z): $[\text{M}]^+$ calc.: 587.26 found: 587.36

5,7-dimethoxy-3-oxo-2-(2-oxo-2-((3-phenylpropyl)amino)ethyl)-N-phenethylisoindoline-1-



carboxamide (3.2-1R) 37% as white solid ^1H

NMR (600 MHz, DMSO- d_6) δ 1.66 – 1.75 (p, J =

7.2 Hz, 2H), 2.55 – 2.61 (m, 2H), 2.71 – 2.76 (t, J =

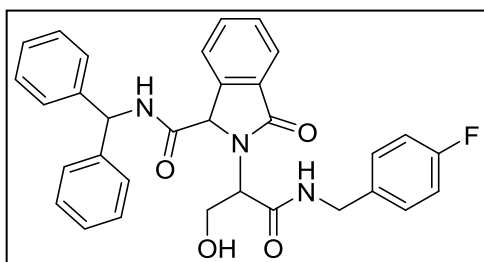
7.4 Hz, 2H), 3.06 – 3.12 (m, 2H), 3.28 – 3.43 (m,

5H), 3.77 – 3.81 (s, 3H), 3.82 – 3.87 (s, 3H), 4.32 –

4.39 (d, J = 16.9 Hz, 1H), 5.10 – 5.15 (s, 1H), 6.75 – 6.79 (d, J = 2.1 Hz, 1H), 6.81 – 6.84 (d, J =

2.0 Hz, 1H), 7.15 – 7.24 (ddt, $J = 13.5, 7.5, 3.7$ Hz, 8H), 7.24 – 7.30 (td, $J = 7.6, 4.1$ Hz, 5H), 8.02 – 8.06 (t, $J = 5.6$ Hz, 1H), 8.67 – 8.72 (t, $J = 5.7$ Hz, 1H); ^{13}C NMR (151 MHz, DMSO) δ 31.33, 32.94, 35.41, 38.71, 41.02, 44.03, 56.29, 62.70, 98.60, 102.97, 122.67, 126.20, 128.73, 128.77, 128.80, 129.02, 134.57, 139.67, 142.14, 155.58, 166.79, 167.74, 168.58 ppm. SFCMS (APCI, m/z): SFCMS (APCI, m/z): $[\text{M}]^+$ calc.: 516.24 found: 516.33.

N-benzhydryl-2-(1-((4-fluorobenzyl)amino)-3-hydroxy-1-oxopropan-2-yl)-3-



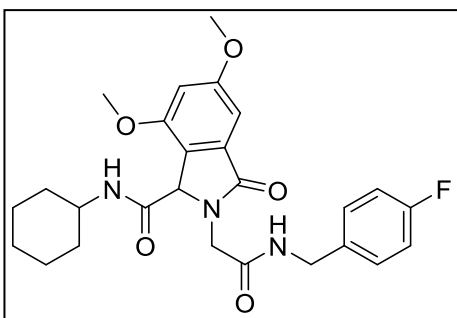
oxoisindoline-1-carboxamide (3.2-1S) 10% as

yellow oil ^1H NMR (600 MHz, DMSO- d_6) δ 3.90-3.93

(m, 2H), 4.26-4.27 (m, 1H), 4.31-4.32 (m, 1H), 4.52 (t, $J=8.4$, 1H), 4.91-4.93 (m, 1H), 5.8 (s, 1H), 6.14 (d,

$J=8.4$), 7.07-7.10 (m, 2H), 7.27-7.30 (m, 4H), 7.31-7.39 (m, 7H), 7.51-7.54 (m, 2H), 7.54-7.59 (m, 1H), 7.71 (d, $J=7.8$, 1H), 8.71-8.73 (m, 1H), 9.94 (d, $J=8.4$, 1H); ^{13}C NMR (151 MHz, DMSO) δ 57.3, 58.7, 59.6, 64.8, 64.9, 115.3, 115.4, 122.9, 123.5, 127.7, 127.8, 128.9, 129.2, 129.3, 131.6, 132.4, 135.7, 142.0, 142.2, 142.6, 160.7, 162.3, 168.5, 168.8, 169.2 ppm. SFCMS (APCI, m/z): $[\text{M}]^+$ calc.: 538.21 found: 538.28.

N-cyclohexyl-2-(2-((4-fluorobenzyl)amino)-2-oxoethyl)-5,7-dimethoxy-3-oxoisindoline-1-



carboxamide (3.2-1T) 58% as white solid ^1H NMR (600

MHz, DMSO- d_6) δ 1.14-1.16 (m, 1H), 1.22-1.25 (m, 4H), 1.55-1.57 (m, 1H), 1.69-1.71 (m, 4H), 3.48-3.51 (m, 1H), 3.54-3.56 (m, 2H), 3.82 (s, 3H), 3.84 (s, 3H), 4.22-4.25 (m, 1H), 4.31-4.35 (m, 1H), 4.42 (d, $J=17.4$, 1H),

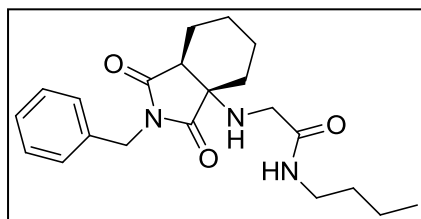
5.16 (s, 1H), 6.76 (s, 1H), 6.82 (s, 1H), 7.13 (m, 2H), 7.30-7.31 (m, 2H), 8.54-8.56 (m, 2H); ^{13}C NMR (151 MHz, DMSO) δ 24.8, 25.6, 32.5, 32.7, 44.1, 48.4, 56.0, 56.1, 56.3, 62.6, 101.9,

102.9, 115.3, 115.5, 122.9, 129.6, 129.7, 134.5, 135.7, 135.8, 155.5, 260.8, 162.2, 165.6, 168.0, 168.7 ppm. SFCMS (APCI, m/z): $[M]^+$ calc.:484.22 found: 484.32.

General procedure of Ugi-Cyclization reaction yielding dioxopyrrolidines:

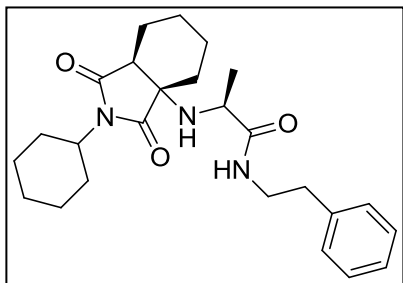
A mixture of L-amino acid (0.5 mmol), ketone (0.5 mmol), isocyanide (0.5 mmol) and primary or secondary amine (0.5 mmol), in TFE (5 mL) were stirred at 85 °C for 24 – 72 hours. Solvents were concentrated under nitrogen to 0.5-1.0 mL and then Cs_2CO_3 was added to mixture. Resultant mixture was heated at 85 °C for overnight. Reaction mixture was diluted with DCM and water, extracted with DCM, dried over MgSO_4 , filtered and solvents were evaporated to get crude product, which was purified by SFC or flash chromatography to yield title compound.

2-((2-benzyl-1,3-dioxooctahydro-1*H*-isoindol-3*a*-yl)amino)-*N*-butylacetamide [3.2-2A]:



40% yield as a white solid; ^1H NMR (600 MHz, CDCl_3) δ 0.93 (t, $J = 7.8$ Hz, 3H), 1.13-1.20 (m, 1H), 1.31-1.41 (m, 3H), 1.45-1.57 (m, 5H), 1.63-1.66 (m, 1H), 1.71-1.74 (m, 1H), 2.21-2.25 (m, 1H), 2.66 (d, $J = 5.4$ Hz, 1H), 3.03 (d, $J = 17.4$ Hz, 1H), 3.26 (q, $J = 13.8, 7.2$ Hz, 2H), 3.45 (d, $J = 17.4$ Hz, 1H), 4.63 (dd, $J = 31.4, 14.4$ Hz, 2H), 7.09 (s, 1H), 7.27-7.33 (m, 5H); ^{13}C NMR (150 MHz, CDCl_3) δ 13.7, 19.7, 20.1, 20.1, 21.5, 31.7, 33.5, 38.8, 42.4, 42.6, 47.4, 62.8, 128.0, 128.5, 128.7, 135.6, 170.6, 175.9, 180.1 ppm. SFCMS (APCI, m/z): $[M]^+$ calc 372.47; found: 372.29.

(2S)-2-((2-cyclohexyl-1,3-dioxooctahydro-1H-isoindol-3a-yl)amino)-N-phenethylpropan-

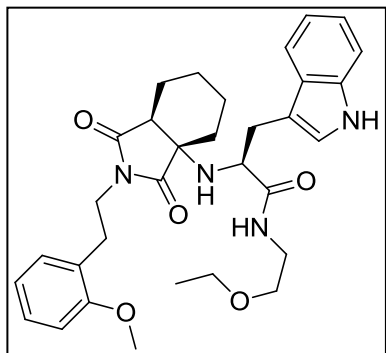


amide [3.2-2B]: 49% yield as a white solid; ^1H NMR (600

MHz, CDCl_3) δ 0.97-1.05 (m, 2H), 1.10-1.30 (m, 5H), 1.38 (d, $J = 6.6$ Hz, 3H), 1.40-1.42 (m, 1H), 1.44-1.47 (m, 1H), 1.51-1.58 (m, 3H), 1.61-1.64 (m, 1H), 1.77-1.81 (m, 2H),

1.99-2.08 (m, 3H), 2.40 (d, $J = 3.6$ Hz, 1H), 2.76-2.81 (m, 1H), 2.84-2.91 (m, 2H), 3.37-3.43 (m, 1H), 3.66-3.71 (m, 1H), 3.85-3.91 (m, 1H), 7.21-7.25 (m, 3H), 7.30-7.34 (m, 3H); ^{13}C NMR (150 MHz, CDCl_3) δ 19.4, 19.7, 21.0, 21.8, 24.9, 25.6, 25.7, 28.4, 29.2, 35.0, 35.3, 39.8, 41.7, 51.5, 55.1, 62.9, 126.7, 128.6, 128.7, 138.5, 174.9, 175.8, 181.4 ppm. SFCMS (APCI, m/z): $[\text{M}]^+$ calc.: 426.56; found: 426.34.

(2S)-N-(2-ethoxyethyl)-3-(1H-indol-3-yl)-2-((2-(2-methoxyphenethyl)-1,3-dioxooctahydro-



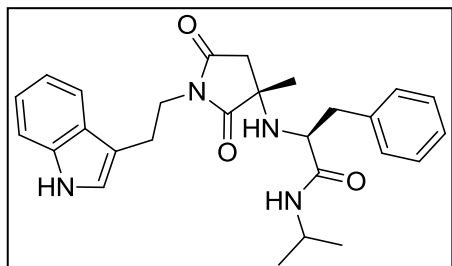
1H-isoindol-3a-yl)amino)propanamide [3.2-2C]: 45% yield as

a light brownish solid; ^1H NMR (600 MHz, CDCl_3) δ 1.00-1.03 (m, 1H), 1.05 (t, $J = 7.2$ Hz, 3H), 1.12-1.17 (m, 1H), 1.21-1.28 (m, 1H), 1.32-1.35 (m, 1H), 1.39-1.45 (m, 2H), 1.52-1.55 (m, 1H), 1.97 (brs, 1H), 2.15 (d, $J = 13.8$ Hz, 1H), 2.47 (d, $J = 6.6$

Hz, 1H), 2.93-2.98 (m, 3H), 3.10 (dd, $J = 14.4, 6.0$ Hz, 1H), 3.12-3.16 (m, 1H), 3.21-3.25 (m, 1H), 3.25-3.29 (m, 1H), 3.30-3.36 (m, 2H), 3.41 (dd, $J = 14.4, 3.6$ Hz, 1H), 3.47-3.54 (m, 1H), 3.82 (t, $J = 6.6$ Hz, 2H), 3.86 (s, 3H), 6.86-6.91 (m, 2H), 7.04-7.06 (m, 2H), 7.09 (t, $J = 7.2$ Hz, 1H), 7.16 (t, $J = 7.2$ Hz, 1H), 7.23 (dt, $J = 8.4, 1.8$ Hz, 1H), 7.34 (d, $J = 7.8$ Hz, 1H), 7.57 (t, $J = 5.4$ Hz, 1H), 7.75 (d, $J = 7.8$ Hz, 1H), 8.43 (s, 1H); ^{13}C NMR (150 MHz, CDCl_3) δ 14.9, 19.4, 20.0, 22.1, 28.3, 28.5, 35.1, 38.0, 38.9, 42.6, 55.4, 57.9, 62.8, 66.2, 68.9, 110.1, 110.6, 111.0,

119.2, 119.6, 120.4, 122.1, 123.5, 126.0, 128.1, 128.3, 130.7, 136.2, 157.9, 174.1, 176.1, 181.2 ppm. SFCMS (APCI, m/z): $[M]^+$ calc.: 561.68; found: 561.42.

(2*S*)-2-((1-(2-(1*H*-indol-3-yl)ethyl)-3-methyl-2,5-dioxopyrrolidin-3-yl)amino)-*N*-isopropyl-



3-phenylpropanamide [3.2-2D]: 34% yield as a light

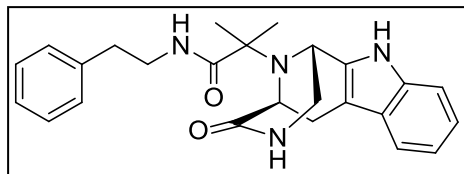
yellowish solid; ^1H NMR (600 MHz, CDCl_3) δ 1.06 (dd, $J = 14.4, 6.6$ Hz, 6H), 1.12 (s, 3H), 1.75 (brs, 1H), 2.36-2.45 (m, 2H), 2.63 (dd, $J = 13.2, 5.4$ Hz, 1H), 2.67 (brs, 1H), 2.94

(dd, $J = 13.2, 4.8$ Hz, 1H), 3.06-3.17 (m, 2H), 3.75-3.80 (m, 1H), 3.89-3.94 (m, 1H), 3.99-4.05 (m, 1H), 6.99 (d, $J = 2.4$ Hz, 1H), 7.03-7.05 (m, 2H), 7.14 (t, $J = 7.2$ Hz, 1H), 7.18 (t, $J = 7.8$ Hz, 1H), 7.22-7.25 (m, 3H), 7.37 (d, $J = 8.4$ Hz, 1H), 7.65 (d, $J = 7.8$ Hz, 1H), 8.36 (s, 1H); ^{13}C NMR (150 MHz, CDCl_3) δ 22.5, 22.6, 22.8, 25.5, 38.7, 39.3, 40.2, 41.0, 58.1, 60.2, 111.4, 111.6, 118.7, 119.5, 122.2, 122.6, 127.1, 127.3, 128.6, 129.7, 135.9, 136.4, 172.3, 174.0, 180.1 ppm. SFCMS (APCI, m/z): $[M]^+$ calc.: 461.57; found: 461.31.

General procedure of Ugi-Pictet-Spengler reaction:

A mixture of amino acid (0.5 mmol), ketone (0.5 mmol), isocyanide (0.5 mmol) and Aminoacetaldehyde dimethyl acetal (0.5 mmol), in 0.1 M of MeOH/ H_2O (4:1) were stirred for 24 – 72 hours at room temperature (In the case of 3,4-Dimethoxy phenylalanine, the reaction mixture was heated at 50 °C for 72 hours). Solvents were evaporated under reduced pressure. The crude Ugi product was dissolved in formic acid (2 mL) and stirred for another 16 h at room temperature. Reaction mixture was diluted with DCM and solid K_2CO_3 was added slowly until the mixture was neutralized. The excess K_2CO_3 was filtered off on celite and solvents were evaporated to obtain crude product, which was purified by SFC, Isco or preparative TLC to yield title compound.

2-methyl-2-((5*S*)-4-oxo-2,3,4,5,6,11-hexahydro-1*H*-1,5-epiminoazocino[4,5-*b*]indol-12-yl)-

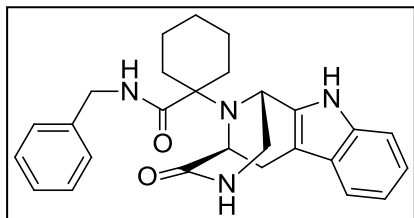


***N*-phenethylpropanamide [4.2-3A]: 44% yield as a light**

yellowish solid; ¹H NMR (600 MHz, CDCl₃) δ 1.07 (s, 3H), 1.35 (s, 3H), 2.81-2.76 (m, 1H), 2.90-2.86 (m, 2H),

3.00-2.95 (m, 2H), 3.11 (dd, *J* = 11.4, 4.2 Hz, 1H), 3.50-3.46 (m, 1H), 3.56-3.52 (m, 1H), 3.76 (d, *J* = 3.6 Hz, 1H), 4.04 (d, *J* = 5.4 Hz, 1H), 6.40 (s, 1H), 7.08 (t, *J* = 7.2 Hz, 1H), 7.13 (t, *J* = 7.8 Hz, 1H), 7.19 (d, *J* = 7.2 Hz, 2H), 7.23 (t, *J* = 7.2 Hz, 1H), 7.31-7.27 (m, 3H), 7.43-7.39 (m, 2H), 8.76 (s, 1H); ¹³C NMR (150 MHz, CDCl₃) δ 20.3, 24.8, 25.2, 35.3, 40.5, 47.1, 47.4, 55.1, 63.6, 108.0, 111.1, 118.2, 119.6, 122.1, 126.5, 126.7, 128.6, 128.7, 131.8, 135.7, 138.6, 173.1, 176.9 ppm. SFCMS (APCI, *m/z*): [*M*]⁺ calc.: 417.52; found: 417.30.

***N*-benzyl-1-((5*S*)-4-oxo-2,3,4,5,6,11-hexahydro-1*H*-1,5-epiminoazocino[4,5-*b*]indol-12-**

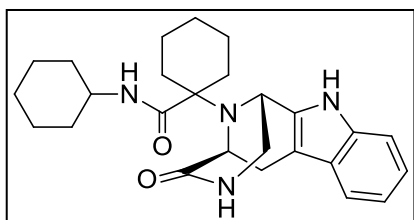


yl)cyclohexanecarboxamide [4.2-3B]: 40% yield as a light

yellowish solid; ¹H NMR (600 MHz, CDCl₃) δ 1.86-1.47 (m, 7H), 1.31-1.12 (m, 3H), 3.04-2.91 (m, 3H), 3.32-3.30 (m,

1H), 4.27-4.15 (m, 4H), 6.24 (s, 1H), 6.97-6.94 (m, 1H), 7.08-7.03 (m, 2H), 7.17-7.14 (m, 2H), 7.26-7.22 (m, 3H), 7.39 (d, *J* = 7.2 Hz, 1H), 8.99 (s, 1H); ¹³C NMR (150 MHz, CDCl₃) δ 22.9, 23.3, 24.9, 25.4, 31.0, 33.6, 43.5, 45.8, 47.9, 54.6, 65.0, 107.7, 111.2, 118.0, 119.3, 121.8, 126.7, 127.5, 127.7, 128.7, 132.9, 135.7, 138.3, 173.4, 175.1 ppm. SFCMS (APCI, *m/z*): [*M*]⁺ calc.: 443.55; found: 443.31.

***N*-cyclohexyl-1-((5*S*)-4-oxo-2,3,4,5,6,11-hexahydro-1*H*-1,5-epiminoazocino[4,5-*b*]indol-12-**

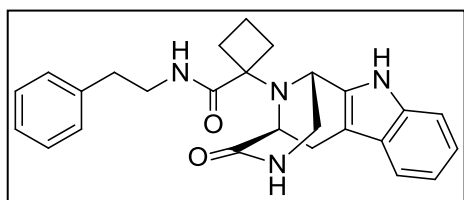


yl)cyclohexanecarboxamide [4.2-3C]: 48% yield as a light

yellowish solid; ¹H NMR (600 MHz, CDCl₃) δ 1.32-0.98 (m, 9H), 1.87-1.51 (m, 11H), 2.99 (d, *J* = 16.2 Hz, 1H), 3.08 (dd,

$J = 16.2, 6.0$ Hz, 1H), 3.21 (dd, $J = 10.8, 3.0$ Hz, 1H), 3.56-3.51 (m, 2H), 4.30-4.27 (m, 2H), 6.35 (d, $J = 7.8$ Hz, 1H), 6.43 (s, 1H), 7.03 (t, $J = 7.2$ Hz, 1H), 7.07 (t, $J = 7.2$ Hz, 1H), 7.16 (d, $J = 7.8$ Hz, 1H), 7.40 (d, $J = 7.8$ Hz, 1H), 9.26 (s, 1H); ^{13}C NMR (150 MHz, CDCl_3) δ 22.8, 23.4, 24.7, 24.8, 24.9, 25.3, 25.4, 30.9, 32.7, 33.0, 34.0, 45.9, 48.2, 48.3, 54.7, 64.8, 107.6, 111.3, 117.9, 119.2, 121.6, 126.8, 132.9, 135.6, 173.4, 174.1 ppm. SFCMS (APCI, m/z): $[\text{M}]^+$ calc.: 435.57; found: 435.37.

1-((5*S*)-4-oxo-2,3,4,5,6,11-hexahydro-1*H*-1,5-epiminoazocino[4,5-*b*]indol-12-yl)-*N*-

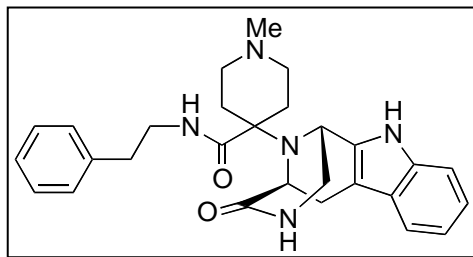


phenethylcyclobutanecarboxamide [4.2-3D]: 30% yield

as a white solid; ^1H NMR (600 MHz, DMSO-d_6) δ 1.46-1.55 (m, 2H), 2.13-2.22 (m, 4H), 2.62-2.72 (m, 2H), 2.74

(d, $J = 15.6$ Hz, 1H), 2.93 (dd, $J = 15.6, 6.0$ Hz, 1H), 3.05 (dd, $J = 11.4, 3.6$ Hz, 1H), 3.23-3.32 (m, 2H), 3.56 (dd, $J = 12.0, 4.8$ Hz, 1H), 3.83 (d, $J = 5.4$ Hz, 1H), 4.20 (d, $J = 4.2$ Hz, 1H), 6.95 (t, $J = 7.2$ Hz, 1H), 7.04 (t, $J = 7.2$ Hz, 1H), 7.14 (d, $J = 7.8$ Hz, 2H), 7.17 (t, $J = 6.6$ Hz, 1H), 7.25 (t, $J = 7.2$ Hz, 2H), 7.31 (d, $J = 7.8$ Hz, 1H), 7.36 (d, $J = 5.4$ Hz, 1H), 10.74 (s, 1H); ^{13}C NMR (150 MHz, DMSO-d_6) δ 13.7, 24.6, 28.4, 28.9, 34.9, 40.5, 46.0, 46.8, 54.9, 66.5, 107.0, 111.2, 117.6, 118.5, 120.8, 126.0, 126.4, 128.3, 128.5, 133.7, 135.6, 139.4, 171.35, 173.9 ppm. SFCMS (APCI, m/z): $[\text{M}]^+$ calc.: 429.53; found: 429.31.

1-methyl-4-((5*S*)-4-oxo-2,3,4,5,6,11-hexahydro-1*H*-1,5-epiminoazocino[4,5-*b*]indol-12-yl)-



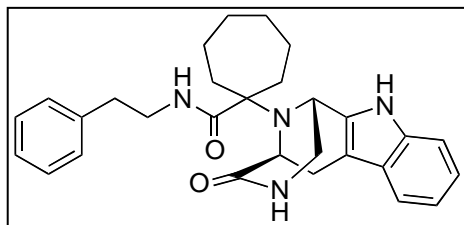
***N*-phenethylpiperidine-4-carboxamide [3.2-3E]:**

Purified by SFC (CO_2/MeOH); Yield 42% (99 mg) as a light yellowish solid; ^1H NMR (600 MHz, DMSO-d_6) δ :

1.56-1.62 (m, 1H), 1.78-1.85 (m, 2H), 1.92-1.99 (m, 2H), 2.04 (s, 3H), 2.04-2.09 (m, 1H), 2.39-2.43 (m, 1H), 2.50-2.59 (m, 3H), 2.69 (d, $J = 15.6$ Hz, 1H),

2.97 (dd, $J = 15.0, 5.4$ Hz, 1H), 3.02 (dd, $J = 10.8, 3.0$ Hz, 1H), 3.10-3.15 (m, 2H), 3.55 (dd, $J = 11.4, 4.2$ Hz, 1H), 3.97 (d, $J = 5.4$ Hz, 1H), 4.35 (s, 1H), 6.93 (t, $J = 7.8$ Hz, 1H), 7.00-7.06 (m, 3H), 7.15 (t, $J = 7.2$ Hz, 1H), 7.23 (t, $J = 7.2$ Hz, 2H), 7.29 (d, $J = 8.4$ Hz, 1H), 7.33 (d, $J = 7.8$ Hz, 1H), 7.40 (d, $J = 3.0$ Hz, 1H), 7.85 (brs, 1H), 10.71 (s, 1H); ^{13}C NMR (150 MHz, DMSO- d_6) δ : 24.6, 30.4, 32.0, 34.6, 40.0, 40.3, 44.9, 45.6, 47.2, 51.9, 52.5, 54.2, 106.9, 111.1, 117.4, 118.4, 120.7, 126.0, 126.6, 128.2, 128.5, 134.3, 135.4, 139.5, 171.6, 172.3 ppm. SFCMS (APCI, m/z): $[\text{M}]^+$ calc.: 472.59; found: 473.24.

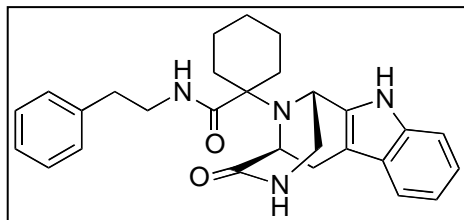
1-((5S)-4-oxo-2,3,4,5,6,11-hexahydro-1H-1,5-epiminoazocino[4,5-*b*]indol-12-yl)-N-



phenethylcycloheptanecarboxamide [3.2-3F]: Purified by SFC (CO_2/MeOH); Yield 52% (122 mg) as a light yellowish solid; ^1H NMR (600 MHz, DMSO- d_6) δ : 1.25-1.55 (m, 9H), 1.73-1.78 (m, 1H), 1.95-2.04 (m, 2H), 2.68-

2.75 (m, 3H), 2.93-2.98 (m, 2H), 3.28 (q, $J = 13.8, 7.2$ Hz, 2H), 3.49 (dd, $J = 11.4, 4.2$ Hz, 1H), 3.85 (d, $J = 5.4$ Hz, 1H), 4.04 (d, $J = 3.6$ Hz, 1H), 6.94 (t, $J = 7.2$ Hz, 1H), 7.03 (t, $J = 7.2$ Hz, 1H), 7.16-7.21 (m, 3H), 7.26-7.31 (m, 3H), 7.35 (d, $J = 7.8$ Hz, 1H), 7.39 (d, $J = 3.6$ Hz, 1H), 7.86 (t, $J = 5.4$ Hz, 1H), 10.73 (s, 1H); ^{13}C NMR (150 MHz, DMSO- d_6) δ : 23.0, 33.8, 24.8, 29.3, 29.5, 32.5, 35.1, 35.3, 40.5, 46.3, 47.2, 54.6, 68.6, 106.9, 111.2, 117.5, 118.5, 120.8, 126.0, 126.5, 128.3, 128.5, 134.3, 135.4, 139.5, 171.5, 175.4 ppm. SFCMS (APCI, m/z): $[\text{M}]^+$ calc.: 471.61; found: 471.25.

1-((5S)-4-oxo-2,3,4,5,6,11-hexahydro-1H-1,5-epiminoazocino[4,5-b]indol-12-yl)-N-



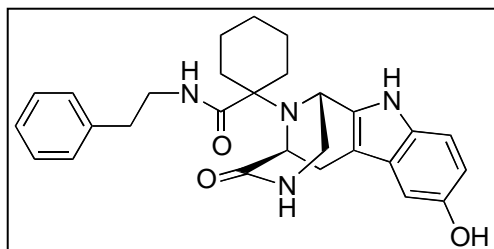
phenethylcyclohexanecarboxamide [3.2-3G]: Purified by

SFC (CO₂/MeOH); Yield 48% (109 mg) as a light yellowish solid; ¹H NMR (600 MHz, DMSO-d₆) δ:

1.07-1.16 (m, 2H), 1.34-1.46 (m, 4H), 1.53-1.57 (m, 1H), 1.62-

1.67 (m, 1H), 1.87-1.94 (m, 2H), 2.53-2.62 (m, 2H), 2.70 (d, *J* = 15.0 Hz, 1H), 2.97 (dd, *J* = 15.6, 5.4 Hz, 1H), 3.02 (dd, *J* = 10.8, 3.0 Hz, 1H), 3.15 (q, *J* = 13.2, 7.2 Hz, 2H), 3.54 (dd, *J* = 11.4, 4.2 Hz, 1H), 3.99 (d, *J* = 5.4 Hz, 1H), 4.33 (d, *J* = 3.6 Hz, 1H), 6.93 (t, *J* = 7.8 Hz, 1H), 7.02 (t, *J* = 7.2 Hz, 1H), 7.07 (d, *J* = 7.2 Hz, 2H), 7.16 (t, *J* = 7.2 Hz, 1H), 7.24 (t, *J* = 7.2 Hz, 2H), 7.29 (d, *J* = 8.4 Hz, 1H), 7.34 (d, *J* = 7.8 Hz, 1H), 7.39 (d, *J* = 3.6 Hz, 1H), 7.81 (t, *J* = 6.0 Hz, 1H), 10.71 (s, 1H); ¹³C NMR (150 MHz, DMSO-d₆) δ: 22.6, 22.8, 24.7, 25.1, 30.9, 32.6, 34.8, 40.4, 45.0, 47.2, 54.1, 63.4, 106.9, 111.1, 117.4, 118.4, 120.6, 126.0, 126.6, 128.2, 128.4, 134.6, 135.4, 139.5, 171.7, 173.1 ppm. SFCMS (APCI, *m/z*): [M]⁺ calc.: 457.58; found 457.25.

1-((5S)-8-hydroxy-4-oxo-2,3,4,5,6,11-hexahydro-1H-1,5-epiminoazocino[4,5-b]indol-12-yl)-



N-phenethylcyclohexane-carboxamide [3.2-3H]:

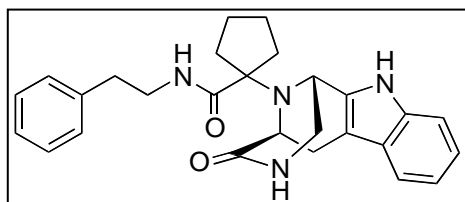
Purified by SFC (CO₂/MeOH); Yield 35% (82 mg) as a light brownish solid; ¹H NMR (600 MHz, DMSO-d₆) δ:

1.05-1.14 (m, 2H), 1.52-1.55 (m, 1H), 1.60-1.64 (m,

1H), 1.85-1.92 (m, 2H), 2.56-2.64 (m, 3H), 2.87 (dd, *J* = 21.0, 6.0 Hz, 1H), 2.98 (dd, *J* = 11.4, 4.2 Hz, 1H), 3.17 (q, *J* = 13.8, 7.2 Hz, 2H), 3.51 (dd, *J* = 11.4, 4.8 Hz, 1H), 3.94 (d, *J* = 5.4 Hz, 1H), 4.25 (d, *J* = 4.2 Hz, 1H), 6.52 (dd, *J* = 8.4, 2.4 Hz, 1H), 6.64 (d, *J* = 1.8 Hz, 1H), 7.06 (d, *J* = 8.4 Hz, 1H), 7.10 (d, *J* = 7.2 Hz, 2H), 7.16 (t, *J* = 7.8 Hz, 1H), 7.25 (t, *J* = 7.8 Hz, 2H), 7.37 (d, *J* = 3.6 Hz, 1H), 7.79 (t, *J* = 5.4 Hz, 1H), 8.55 (s, 1H), 10.35 (s, 1H); ¹³C NMR (150 MHz,

DMSO- d_6) δ : 22.6, 22.8, 25.1, 30.9, 32.5, 34.8, 40.4, 45.1, 47.2, 54.2, 63.5, 101.7, 106.1, 110.5, 111.3, 126.0, 127.3, 128.3, 128.5, 129.9, 135.1, 139.6, 150.4, 171.8, 173.2 ppm. SFCMS (APCI, m/z): $[M]^+$ calc.: 473.58; found: 473.24.

1-((5S)-4-oxo-2,3,4,5,6,11-hexahydro-1H-1,5-epiminoazocino[4,5-b]indol-12-yl)-N-

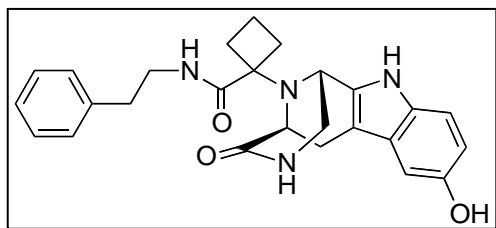


phenethylcyclopentanecarboxamide [3.2-3I]: Purified

by SFC ($CO_2/MeOH$); Yield 27% (60 mg) as a light yellowish solid; 1H NMR (600 MHz, DMSO- d_6) δ : 1.34-

1.40 (m, 1H), 1.44-1.52 (m, 2H), 1.53-1.59 (m, 2H), 1.77-1.83 (m, 1H), 1.88-1.93 (m, 1H), 1.97-2.02 (m, 1H), 2.61 (t, $J = 7.8$ Hz, 2H), 2.72 (d, $J = 15.6$ Hz, 1H), 2.90 (dd, $J = 15.0, 5.4$ Hz, 1H), 3.01 (dd, $J = 11.4, 3.0$ Hz, 1H), 3.21 (q, $J = 13.8, 6.6$ Hz, 2H), 3.57 (dd, $J = 11.4, 4.8$ Hz, 1H), 3.85 (d, $J = 5.4$ Hz, 1H), 4.19 (d, $J = 3.0$ Hz, 1H), 6.94 (t, $J = 7.2$ Hz, 1H), 7.03 (t, $J = 7.2$ Hz, 1H), 7.10 (d, $J = 7.2$ Hz, 2H), 7.16 (t, $J = 7.2$ Hz, 1H), 7.25 (t, $J = 7.8$ Hz, 2H), 7.30 (d, $J = 8.4$ Hz, 1H), 7.35 (d, $J = 7.8$ Hz, 1H), 7.43 (d, $J = 3.0$ Hz, 1H), 7.85 (t, $J = 5.4$ Hz, 1H), 10.74 (s, 1H); ^{13}C NMR (150 MHz, DMSO- d_6) δ : 23.2, 23.3, 24.6, 31.6, 33.6, 34.9, 40.5, 46.9, 47.1, 55.5, 73.4, 107.0, 111.2, 117.5, 118.5, 120.7, 126.0, 126.5, 128.3, 128.5, 134.1, 135.5, 139.5, 171.5, 174.4 ppm. SFCMS (APCI, m/z): $[M]^+$ calc.: 443.55; found: 443.24.

1-((5S)-8-hydroxy-4-oxo-2,3,4,5,6,11-hexahydro-1H-1,5-epiminoazocino[4,5-b]indol-12-yl)-



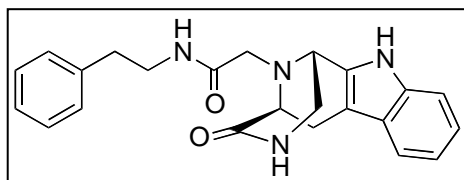
N-phenethylcyclobutane-carboxamide [3.2-3J]:

Purified by SFC ($CO_2/MeOH$); Yield 35% (77 mg) as a light brownish solid; 1H NMR (600 MHz, DMSO- d_6) δ :

1.45-1.54 (m, 2H), 2.08-2.22 (m, 4H), 2.61-2.72 (m, 3H), 2.84 (dd, $J = 15.0, 4.8$ Hz, 1H), 3.01 (d, $J = 8.4$ Hz, 1H), 3.24-3.33 (m, 2H), 3.53 (dd, $J = 11.4, 3.0$ Hz, 1H), 3.79 (d, $J = 4.8$ Hz, 1H), 4.12 (s, 1H), 6.54 (dd, $J = 9.0, 2.4$ Hz, 1H), 6.66 (s,

1H), 7.09 (dd, $J = 9.0, 1.8$ Hz, 1H), 7.14-7.19 (m, 3H), 7.25 (t, $J = 7.2$ Hz, 2H), 7.48 (s, 1H), 7.83 (t, $J = 4.2$ Hz, 1H), 8.62 (brs, 1H), 10.42 (s, 1H); ^{13}C NMR (150 MHz, DMSO- d_6) δ : 13.8, 24.8, 28.4, 29.0, 35.0, 40.5, 46.2, 46.8, 55.0, 66.6, 101.8, 106.2, 110.8, 111.5, 126.1, 127.1, 128.4, 128.6, 130.0, 134.2, 139.5, 150.5, 171.5, 174.0 ppm. SFCMS (APCI, m/z): $[\text{M}]^+$ calc.: 445.53; found: 445.24.

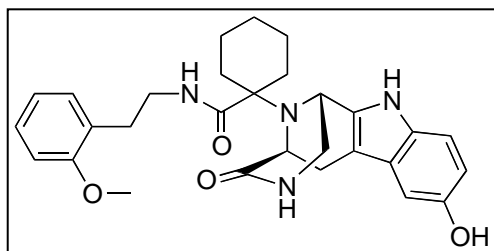
2-((5S)-4-oxo-2,3,4,5,6,11-hexahydro-1H-1,5-epiminoazocino[4,5-*b*]indol-12-yl)-N-



phenethylacetamide [3.2-3K]: Purified by SFC (CO_2/MeOH); Yield 28% (54 mg) as a light yellowish solid; ^1H NMR (600 MHz, DMSO- d_6) δ : 2.66 (d, $J = 16.2$

Hz, 1H), 2.76 (t, $J = 7.2$ Hz, 2H), 2.97 (dd, $J = 15.6, 3.6$ Hz, 2H), 3.07 (dd, $J = 11.4, 4.2$ Hz, 1H), 3.29 (dd, $J = 15.6, 8.4$ Hz, 2H), 3.40-3.46 (m, 1H), 3.56 (d, $J = 5.4$ Hz, 1H), 3.67 (dd, $J = 11.4, 4.2$ Hz, 1H), 3.95 (d, $J = 4.2$ Hz, 1H), 6.97 (t, $J = 7.2$ Hz, 1H), 7.03-7.09 (m, 2H), 7.22 (d, $J = 7.2$ Hz, 2H), 7.29-7.34 (m, 3H), 7.40 (d, $J = 7.8$ Hz, 1H), 7.57 (d, $J = 3.6$ Hz, 1H), 7.91 (t, $J = 6.0$ Hz, 1H), 10.79 (s, 1H); ^{13}C NMR (150 MHz, DMSO- d_6) δ : 21.7, 35.1, 40.0, 46.0, 49.7, 54.8, 58.4, 106.0, 111.2, 117.7, 118.6, 121.1, 126.1, 126.3, 128.4, 128.7, 131.4, 135.8, 139.4, 169.1, 170.7 ppm. SFCMS (APCI, m/z): $[\text{M}]^+$ calc.: 389.46; found: 389.19.

1-((5S)-8-hydroxy-4-oxo-2,3,4,5,6,11-hexahydro-1H-1,5-epiminoazocino[4,5-*b*]indol-12-yl)-



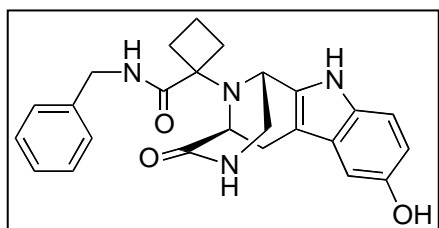
N-phenethylcyclohexane-carboxamide [3.2-3L]:

Purified by SFC (CO_2/MeOH); Yield 44% (110 mg) as a light brownish solid; ^1H NMR (600 MHz, DMSO- d_6) δ : 1.07-1.13 (m, 2H), 1.26-1.30 (m, 1H), 1.36-1.49 (m,

3H), 1.51-1.56 (m, 1H), 1.59-1.64 (m, 1H), 1.84-1.92 (m, 2H), 2.59 (d, $J = 15.0$ Hz, 1H), 2.61-

2.69 (m, 2H), 2.85 (dd, $J = 15.0, 5.4$ Hz, 1H), 2.98 (dd, $J = 11.4, 3.6$ Hz, 1H), 3.12-3.17 (m, 2H), 3.49 (dd, $J = 10.8, 4.2$ Hz, 1H), 3.76 (s, 3H) 3.93 (d, $J = 5.4$ Hz, 1H), 4.21 (d, $J = 3.6$ Hz, 1H), 6.52 (dd, $J = 8.4, 2.4$ Hz, 1H), 6.63 (d, $J = 2.4$ Hz, 1H), 6.84 (t, $J = 7.2$ Hz, 1H), 6.92 (d, $J = 8.4$ Hz, 1H), 7.03 (d, $J = 7.2$ Hz, 1H), 7.06 (d, $J = 8.4$ Hz, 1H), 7.17 (t, $J = 8.4$ Hz, 1H), 7.38 (d, $J = 3.6$ Hz, 1H), 7.77 (t, $J = 5.4$ Hz, 1H), 8.56 (s, 1H), 10.36 (s, 1H); ^{13}C NMR (150 MHz, DMSO- d_6) δ : 22.7, 22.9, 24.9, 25.1, 29.6, 30.9, 32.4, 45.2, 47.2, 54.2, 55.2, 63.7, 101.7, 106.1, 110.6, 111.4, 120.3, 127.5, 129.8, 130.0, 135.2, 150.4, 157.2, 171.8, 173.3 ppm. SFCMS (APCI, m/z): $[\text{M}]^+$ calc.: 503.60; found: 503.28.

***N*-benzyl-1-((5*S*)-8-hydroxy-4-oxo-2,3,4,5,6,11-hexahydro-1*H*-1,5-epiminoazocino[4,5-*b*]-**

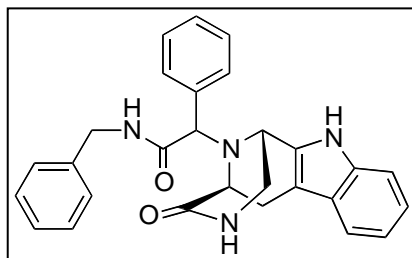


indol-12-yl)cyclobutane-carboxamide [3.2-3M]:

Purified by SFC (CO_2/MeOH); Yield 29% (62 mg) as a light brownish solid; ^1H NMR (600 MHz, DMSO- d_6) δ : 1.47-1.59 (m, 2H), 2.16-2.19 (m, 3H), 2.23-2.29 (m, 1H), 2.64 (d, $J =$

15.0 Hz, 1H), 2.87 (dd, $J = 15.6, 6.0$ Hz, 1H), 3.02 (dd, $J = 10.8, 3.6$ Hz, 1H), 3.57 (dd, $J = 11.4, 4.2$ Hz, 1H), 3.82 (d, $J = 5.4$ Hz, 1H), 4.14 (d, $J = 3.6$ Hz, 1H), 4.24 (dd, $J = 15.0, 6.0$ Hz, 1H), 4.31 (dd, $J = 15.0, 6.6$ Hz, 1H), 6.54 (dd, $J = 8.4, 2.4$ Hz, 1H), 6.66 (d, $J = 1.8$ Hz, 1H), 7.09 (d, $J = 8.4$ Hz, 1H), 7.20-7.24 (m, 3H), 7.29 (t, $J = 7.2$ Hz, 2H), 7.48 (d, $J = 3.6$ Hz, 1H), 8.38 (t, $J = 6.0$ Hz, 1H), 8.61 (s, 1H), 10.43 (s, 1H); ^{13}C NMR (150 MHz, DMSO- d_6) δ : 13.3, 24.6, 28.3, 29.0, 42.5, 46.3, 46.6, 55.2, 66.8, 101.8, 106.2, 110.8, 111.5, 126.7, 127.1, 127.2, 128.3, 130.0, 134.2, 140.1, 150.5, 171.5, 174.2 ppm. SFCMS (APCI, m/z): $[\text{M}]^+$ calc.: 431.50; found: 431.20.

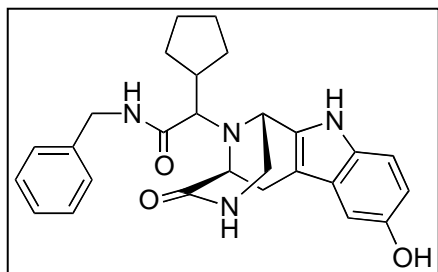
***N*-benzyl-2-((5*S*)-4-oxo-2,3,4,5,6,11-hexahydro-1*H*-1,5-epiminoazocino[4,5-*b*]indol-12-yl)-**



2-phenylacetamide [3.2-3N]: Purified by column flash chromatography (CH₂Cl₂/MeOH); Yield 61% (137 mg) as a light yellowish solid; **Data for 1st diastereomer** (12.2% yield):

¹H NMR (600 MHz, DMSO-*d*₆) δ : 2.56 (d, *J* = 15.6 Hz, 1H), 3.83 (dd, *J* = 16.2, 6.0 Hz, 1H), 3.15-3.17 (m, 1H), 3.28-3.31 (m, 1H), 3.77 (dd, *J* = 11.4, 4.8 Hz, 1H), 4.15 (d, *J* = 4.2 Hz, 1H), 4.21-4.25 (m, 3H), 6.97 (t, *J* = 7.8 Hz, 1H), 7.05-7.08 (m, 3H), 7.18-7.20 (m, 1H), 7.22-7.25 (m, 2H), 7.33-7.41 (m, 5H), 7.58 (d, *J* = 7.2 Hz, 2H), 7.65 (d, *J* = 3.6 Hz, 1H), 8.72 (t, *J* = 6.0 Hz, 1H), 10.85 (s, 1H); ¹³C NMR (150 MHz, DMSO-*d*₆) δ : 21.3, 41.9, 46.2, 48.3, 55.4, 68.9, 106.0, 111.3, 117.9, 118.7, 121.2, 126.4, 126.7, 126.9, 128.1, 128.3, 128.5, 128.6, 131.2, 135.8, 136.8, 139.4, 170.2, 170.6 ppm. SFCMS (APCI, *m/z*): [M]⁺ calc.: 451.53; found: 451.19. **Data for 2nd diastereomer** (48.8% yield): ¹H NMR (600 MHz, DMSO-*d*₆) δ : 2.75 (d, *J* = 16.2 Hz, 1H), 3.07 (dd, *J* = 11.4, 4.2 Hz, 1H), 3.11 (dd, *J* = 15.6, 5.4 Hz, 1H), 3.62 (dd, *J* = 11.4, 4.2 Hz, 1H), 3.81 (d, *J* = 6.0 Hz, 1H), 3.86 (d, *J* = 4.2 Hz, 1H), 4.18 (dd, *J* = 15.6, 6.0 Hz, 1H), 4.30 (dd, *J* = 15.0, 6.0 Hz, 1H), 4.32 (s, 1H), 6.97 (t, *J* = 7.8 Hz, 1H), 7.05 (t, *J* = 7.2 Hz, 1H), 7.09 (*J* = 7.2 Hz, 1H), 7.19-7.22 (m, 1H), 7.24-7.29 (m, 3H), 7.30-7.37 (m, 3H), 7.43 (d, *J* = 7.8 Hz, 1H), 7.48 (d, *J* = 6.6 Hz, 2H), 7.64 (d, *J* = 3.6 Hz, 1H), 8.89 (t, *J* = 6.0 Hz, 1H), 10.65 (s, 1H); ¹³C NMR (150 MHz, DMSO-*d*₆) δ : 21.4, 42.0, 46.5, 46.6, 56.3, 67.5, 106.2, 111.3, 117.8, 118.6, 121.1, 126.3, 126.8, 126.9, 128.1, 128.2, 128.3, 128.6, 131.2, 135.7, 138.2, 139.3, 169.5, 170.8 ppm. SFCMS (APCI, *m/z*): [M]⁺ calc.: 451.53; found: 451.19.

***N*-benzyl-2-cyclopentyl-2-((5*S*)-8-hydroxy-4-oxo-2,3,4,5,6,11-hexahydro-1*H*-1,5-**



epiminoazocino[4,5-*b*]indol-12-yl)acetamide [3.2-30]:

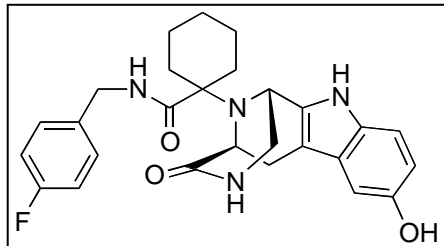
Purified by SFC (CO₂/MeOH); Yield 38% (87 mg) as a brownish solid; **Data for 1st diastereomer** (7.6% yield): ¹H

NMR (600 MHz, DMSO-*d*₆) δ: 0.78-0.87 (m, 1H), 1.31-1.49

(m, 6H), 1.68-1.71 (m, 1H), 2.31-2.39 (m, 1H), 2.57 (d, *J* = 15.6 Hz, 1H), 2.92 (dd, *J* = 15.0, 5.4 Hz, 1H), 3.01-3.06 (m, 2H), 3.64 (dd, *J* = 11.4, 4.2 Hz, 1H), 3.76 (d, *J* = 5.4 Hz, 1H), 4.07-4.14 (m, 2H), 4.21 (d, *J* = 3.0 Hz, 1H), 6.54 (dd, *J* = 8.4, 1.8 Hz, 1H), 6.67 (d, *J* = 1.8 Hz, 1H), 7.07 (d, *J* = 8.4 Hz, 1H), 7.12-7.15 (m, 2H), 7.19-7.26 (m, 3H), 7.44 (d, *J* = 3.0 Hz, 1H), 8.37 (t, *J* = 5.4 Hz, 1H), 8.60 (s, 1H), 10.42 (s, 1H); ¹³C NMR (150 MHz, DMSO-*d*₆) δ: 23.3, 24.7, 25.0, 27.6, 29.6, 42.1, 46.7, 48.0, 57.4, 67.5, 101.8, 105.5, 110.6, 111.4, 126.8, 127.3, 127.7, 128.2, 130.0, 133.7, 139.3, 150.4, 171.3, 171.5 ppm. SFCMS (APCI, *m/z*): [M]⁺ calc.: 459.55; found: 459.24.

Data for 2nd diastereomer (30.4% yield): ¹H NMR (600 MHz, DMSO-*d*₆) δ: 0.83-0.88 (m, 1H), 1.11-1.18 (m, 1H), 1.36-1.47 (m, 3H), 1.52-1.63 (m, 3H), 2.16-2.23 (m, 1H), 2.51 (d, 1H), 3.05-3.10 (m, 2H), 3.15 (d, *J* = 7.2 Hz, 1H), 3.62 (d, *J* = 5.4 Hz, 1H), 3.72 (dd, *J* = 12.0, 4.8 Hz, 1H), 4.20-4.29 (m, 2H), 4.31 (d, *J* = 3.6 Hz, 1H), 6.56 (dd, *J* = 8.4, 1.8 Hz, 1H), 6.68 (d, *J* = 1.8 Hz, 1H), 7.10 (d, *J* = 8.4 Hz, 1H), 7.19-7.23 (m, 3H), 7.25-7.29 (m, 2H), 7.54 (d, *J* = 3.0 Hz, 1H), 8.50 (t, *J* = 5.4 Hz, 1H), 8.62 (s, 1H), 10.40 (s, 1H); ¹³C NMR (150 MHz, DMSO-*d*₆) δ: 21.7, 24.7, 25.0, 27.5, 29.8, 42.1, 46.6, 46.8, 56.7, 66.2, 101.9, 105.6, 110.9, 111.5, 126.8, 127.2, 127.4, 128.3, 130.1, 132.8, 139.5, 150.5, 171.1, 171.2 ppm. SFCMS (APCI, *m/z*): [M]⁺ calc.: 459.55; found: 459.31.

***N*-(4-fluorobenzyl)-1-((5*S*)-8-hydroxy-4-oxo-2,3,4,5,6,11-hexahydro-1*H*-1,5-**



epiminoazocino-[4,5-*b*]indol-12-yl)cyclohexane-

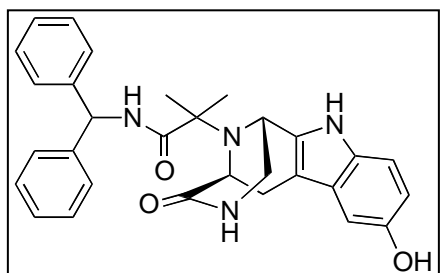
carboxamide [3.2-3P]: Purified by SFC (CO₂/MeOH);

Yield 40% (95 mg) as a brownish solid; ¹H NMR (600 MHz,

DMSO-*d*₆) δ: 1.10-1.14 (m, 2H), 1.24-1.28 (m, 1H), 1.38-

1.51 (m, 3H), 1.57-1.60 (m, 1H), 1.63-1.68 (m, 1H), 1.86-1.89 (m, 1H), 1.98-2.02 (m, 1H), 2.59 (d, *J* = 15.0 Hz, 1H), 2.84 (dd, *J* = 15.0, 5.4 Hz, 1H), 2.94 (dd, *J* = 10.8, 3.6 Hz, 1H), 3.38 (dd, *J* = 11.4, 4.2 Hz, 1H), 3.93 (d, *J* = 5.4 Hz, 1H), 4.10-4.21 (m, 2H), 6.53 (d, *J* = 8.4 Hz, 1H), 6.64 (s, 1H), 7.07 (d, *J* = 8.4 Hz, 1H), 7.08 (t, *J* = 9.0 Hz, 2H), 7.25 (t, *J* = 5.4 Hz, 2H), 7.34 (d, *J* = 3.6 Hz, 1H), 8.30 (t, *J* = 6.0 Hz, 1H), 8.56 (s, 1H), 10.37 (s, 1H); ¹³C NMR (150 MHz, DMSO-*d*₆) δ: 22.8, 23.0, 24.8, 25.0, 30.9, 32.2, 41.7, 45.2, 47.2, 54.2, 64.0, 101.7, 106.1, 110.6, 111.4, 114.7, 114.9, 127.3, 129.3, 129.4, 129.9, 135.1, 136.3, 136.4, 150.4, 171.7, 173.7 ppm. SFCMS (APCI, *m/z*): [*M*]⁺ calc.: 477.54; found: 477.23.

***N*-benzhydryl-2-((5*S*)-8-hydroxy-4-oxo-2,3,4,5,6,11-hexahydro-1*H*-1,5-epiminoazocino[4,5-**



***b*]indol-12-yl)-2-methylpropanamide [3.2-3Q]:** Purified by

SFC (CO₂/MeOH); Yield 27% (66 mg) as a light yellowish

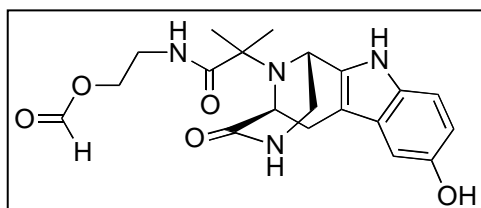
solid; ¹H NMR (600 MHz, DMSO-*d*₆) δ: 0.96 (s, 3H), 1.34

(s, 3H), 2.61 (d, *J* = 15.0 Hz, 1H), 2.73 (dd, *J* = 15.6, 5.4 Hz,

1H), 2.88 (dd, *J* = 10.8, 3.6 Hz, 1H), 3.22 (dd, *J* = 11.4, 4.2 Hz, 1H), 3.84 (t, *J* = 4.8 Hz, 2H), 6.14 (d, *J* = 8.4 Hz, 1H), 6.53 (dd, *J* = 8.4, 2.4 Hz, 1H), 6.62 (d, *J* = 2.4 Hz, 1H), 7.06 (d, *J* = 8.4 Hz, 1H), 7.21-7.25 (m, 1H), 7.28-7.34 (m, 10H), 8.59 (brs, 1H), 8.69 (d, *J* = 9.0 Hz, 1H), 10.36 (s, 1H); ¹³C NMR (150 MHz, DMSO-*d*₆) δ: 20.4, 24.3, 24.6, 46.8, 54.8, 54.9, 56.3, 62.8, 101.8,

106.1, 110.8, 111.5, 126.8, 126.9, 127.2, 127.3, 127.8, 128.3, 128.6, 129.9, 134.4, 142.4, 142.6, 150.4, 171.7, 175.3 ppm. SFCMS (APCI, m/z): $[M]^+$ calc.: 495.58; found: 495.23.

2-(2-((5*S*)-8-hydroxy-4-oxo-2,3,4,5,6,11-hexahydro-1*H*-1,5-epiminoazocino[4,5-*b*]indol-12-

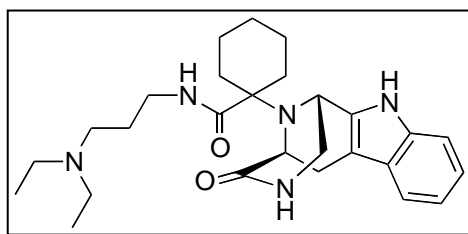


yl)-2-methylpropanamido)ethyl formate [3.2-3R]:

Purified by SFC (CO₂/MeOH); Yield 51% (102 mg) as a light brownish solid; ¹H NMR (600 MHz, DMSO-*d*₆) δ :

0.95 (s, 3H), 1.27 (s, 3H), 2.66 (d, J = 15.6 Hz, 1H), 2.87 (dd, J = 15.6, 6.0 Hz, 1H), 3.03 (dd, J = 11.4, 3.6 Hz, 1H), 3.24-3.30 (m, 1H), 3.45-3.51 (m, 1H), 3.68 (dd, J = 11.4, 4.2 Hz, 1H), 3.78 (d, J = 6.0 Hz, 1H), 3.87 (d, J = 3.6 Hz, 1H), 4.11-4.18 (m, 2H), 6.54 (dd, J = 9.0, 2.4 Hz, 1H), 6.66 (d, J = 1.8 Hz, 1H), 7.08 (d, J = 8.4 Hz, 1H), 7.50 (d, J = 3.6 Hz, 1H), 8.17 (t, J = 6.0 Hz, 1H), 8.22 (s, 1H), 10.40 (s, 1H); ¹³C NMR (150 MHz, DMSO-*d*₆) δ : 20.3, 24.6, 24.7, 37.9, 46.9, 54.9, 59.7, 62.2, 62.7, 101.8, 106.1, 110.8, 111.5, 127.2, 130.0, 134.4, 150.5, 162.1, 171.6, 176.4 ppm. SFCMS (APCI, m/z): $[M]^+$ calc.: 401.43; found 401.17.

***N*-(3-(diethylamino)propyl)-1-((5*S*)-4-oxo-2,3,4,5,6,11-hexahydro-1*H*-1,5-epiminoazocino-**



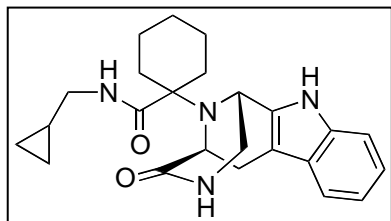
[4,5-*b*]indol-12-yl)cyclohexanecarboxamide [3.2-3S]:

Purified by SFC (CO₂/MeOH); Yield 25% (58 mg) as a light yellowish solid; ¹H NMR (600 MHz, DMSO-*d*₆) δ :

0.90 (t, J = 7.2 Hz, 6H), 1.14-1.19 (m, 2H), 1.35-1.46 (m, 6H), 1.57-1.64 (m, 2H), 1.86-1.94 (m, 2H), 2.28 (t, J = 7.2 Hz, 2H), 2.38 (q, J = 14.4, 7.2 Hz, 4H), 2.70 (d, J = 15.0 Hz, 1H), 2.93-2.97 (m, 3H), 3.04 (dd, J = 10.8, 3.6 Hz, 1H), 3.57 (dd, J = 11.4, 4.8 Hz, 1H), 3.95 (d, J = 5.4 Hz, 1H), 4.31 (d, J = 4.2 Hz, 1H), 6.92 (t, J = 7.2 Hz, 1H), 7.01 (t, J = 7.8 Hz, 1H), 7.38 (d, J = 3.6 Hz, 1H), 7.80 (t, J = 5.4 Hz, 1H), 10.75 (s, 1H); ¹³C NMR (150 MHz, DMSO-*d*₆) δ : 11.5, 22.8, 23.0, 24.8, 25.1, 26.3, 31.0, 32.5, 37.9, 45.0, 46.1,

47.3, 50.5, 54.2, 63.6, 101.5, 106.9, 111.1, 117.4, 118.3, 120.6, 126.6, 134.6, 135.4, 171.7, 172.9 ppm. SFCMS (APCI, m/z): $[M]^+$ calc.: 466.63; found: 466.31.

***N*-(cyclopropylmethyl)-1-((5*S*)-4-oxo-2,3,4,5,6,11-hexahydro-1*H*-1,5-epiminoazocino[4,5-**

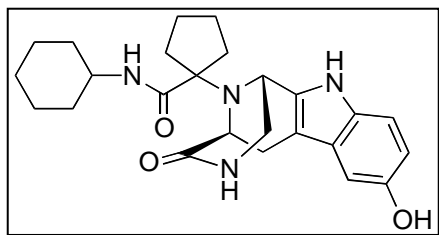


***b*]indol-12-yl)cyclohexanecarboxamide [3.2-3T]:** Purified by SFC (CO₂/MeOH); Yield 19% (38 mg) as a light yellowish solid;

¹H NMR (600 MHz, DMSO-*d*₆) δ : 0.11-0.14 (m, 2H), 0.29-0.35 (m, 2H), 0.83-0.86 (m, 1H), 1.14-1.66 (m, 8H), 1.86-1.95 (m,

2H), 2.72 (d, J = 15.6 Hz, 1H), 2.80-2.88 (m, 2H), 2.96 (dd, J = 15.6, 5.4 Hz, 1H), 3.04 (d, J = 11.4 Hz, 1H), 3.63 (dd, J = 10.8, 4.2 Hz, 1H), 3.99 (d, J = 4.8 Hz, 1H), 4.29 (s, 1H), 6.93 (t, J = 7.2 Hz, 1H), 7.01 (t, J = 7.2 Hz, 1H), 7.28 (d, J = 7.8 Hz, 1H), 7.33 (d, J = 7.8 Hz, 1H), 7.37 (d, J = 3.0 Hz, 1H), 7.82 (t, J = 5.4 Hz, 1H), 10.73 (s, 1H); ¹³C NMR (150 MHz, DMSO-*d*₆) δ : 3.2, 3.2, 10.9, 22.7, 23.0, 24.9, 25.1, 31.0, 32.4, 43.1, 45.1, 47.2, 54.2, 63.8, 107.0, 111.1, 117.4, 118.3, 120.6, 126.6, 134.6, 135.4, 171.7, 173.2 ppm. SFCMS (APCI, m/z): $[M]^+$ calc.: 407.52; found: 407.22.

***N*-cyclohexyl-1-((5*S*)-8-hydroxy-4-oxo-2,3,4,5,6,11-hexahydro-1*H*-1,5-epiminoazocino[4,5-**



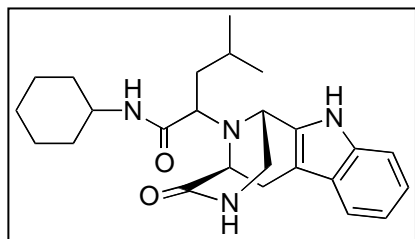
***b*]indol-12-yl)cyclopentane-carboxamide [3.2-3U]:** Purified by SFC (CO₂/MeOH); Yield 24% (52 mg) as a light yellowish solid; ¹H NMR (600 MHz, DMSO-*d*₆) δ : 1.04-1.08

(m, 1H) 1.12-1.22 (m, 4H), 1.36-1.42 (m, 1H), 1.45-1.55 (m,

5H), 1.57-1.65 (m, 4H), 1.76-1.83 (m, 1H), 1.89-1.93 (m, 1H), 1.98-2.02 (m, 1H), 2.63 (d, J = 15.0 Hz, 1H), 2.83 (dd, J = 15.6, 5.4 Hz, 1H), 3.02 (dd, J = 11.4, 4.2 Hz, 1H), 3.83 (d, J = 5.4 Hz, 1H), 4.11 (d, J = 3.6 Hz, 1H), 6.53 (dd, J = 8.4, 2.4 Hz, 1H), 6.64 (d, J = 1.8 Hz, 1H), 7.07 (d, J = 9.0 Hz, 1H), 7.41 (d, J = 4.2 Hz, 1H), 7.47 (d, J = 8.4 Hz, 1H), 8.58 (s, 1H), 10.38 (s,

1H); ¹³C NMR (150 MHz, DMSO-d₆) δ: 23.3, 23.4, 24.8, 24.9, 25.2, 31.4, 32.1, 32.2, 33.5, 47.0, 47.1, 47.8, 55.4, 73.5, 101.8, 106.2, 110.7, 111.4, 127.2, 129.9, 134.6, 150.4, 171.6, 173.5 ppm. SFCMS (APCI, *m/z*): [M]⁺ calc.: 437.55; found: 437.26.

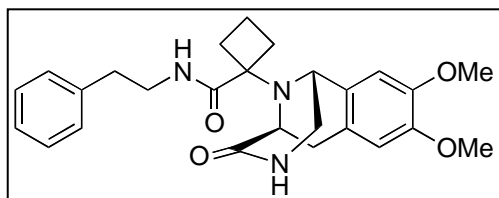
***N*-cyclohexyl-4-methyl-2-((5*S*)-4-oxo-2,3,4,5,6,11-hexahydro-1*H*-1,5-epiminoazocino[4,5-**



***b*]indol-12-yl)pentanamide [3.2-3V]:** Purified by SFC (CO₂/MeOH); Yield 52% (109 mg) as a light yellowish solid; **Data for 1st diastereomer** (11.3% yield): ¹H NMR (600 MHz, DMSO-d₆) δ: 0.83-0.86 (m, 6H), 1.04-1.23 (m, 5H),

1.45-1.68 (m, 8H), 2.68 (d, *J* = 15.6 Hz, 1H), 2.92 (dd, *J* = 15.6, 5.4 Hz, 1H), 3.07-3.13 (m, 2H), 3.46-3.52 (m, 1H), 3.59 (dd, *J* = 15.6, 4.2 Hz, 1H), 3.78 (d, *J* = 4.8 Hz, 1H), 4.05 (d, *J* = 3.6 Hz, 1H), 6.95 (t, *J* = 7.8 Hz, 1H), 7.03 (t, *J* = 7.8 Hz, 1H), 7.30 (d, *J* = 7.8 Hz, 1H), 7.37 (d, *J* = 7.8 Hz, 1H), 7.56 (d, *J* = 3.6 Hz, 1H), 7.76 (d, *J* = 8.4 Hz, 1H), 10.78 (s, 1H); ¹³C NMR (150 MHz, DMSO-d₆) δ: 21.8, 21.9, 24.0, 24.6, 24.7, 24.8, 25.2, 32.2, 32.3, 46.6, 47.2, 48.1, 55.9, 62.3, 106.3, 111.2, 117.7, 118.5, 120.9, 126.5, 132.2, 135.6, 170.9, 171.0 ppm. SFCMS (APCI, *m/z*): [M]⁺ calc.: 423.56; found: 423.32. **Data for 2nd diastereomer** (40.7% yield): ¹H NMR (600 MHz, DMSO-d₆) δ: 0.77 (d, *J* = 6.0 Hz, 3H), 0.81 (d, *J* = 6.6 Hz, 3H), 1.06-1.19 (m, 3H), 1.20-1.29 (m, 2H), 1.33-1.41 (m, 2H), 1.53-1.61 (m, 2H), 1.64-1.72 (m, 4H), 2.63 (d, *J* = 15.0 Hz, 1H), 3.08-3.17 (m, 3H), 3.57-3.61 (m 1H), 3.63 (d, *J* = 6.0 Hz, 1H), 3.67 (dd, *J* = 11.4, 4.8 Hz, 1H), 4.31 (d, *J* = 4.2 Hz, 1H), 6.96 (t, *J* = 7.2 Hz, 1H), 7.04 (t, *J* = 7.2 Hz, 1H), 7.31 (d, *J* = 8.4 Hz, 1H), 7.39 (d, *J* = 7.6 Hz, 1H), 7.55 (d, *J* = 3.6 Hz, 1H), 7.99 (d, *J* = 8.4 Hz, 1H), 10.76 (s, 1H); ¹³C NMR (150 MHz, DMSO-d₆) δ: 22.0, 22.1, 24.0, 24.7, 25.0, 25.2, 32.3, 32.4, 46.1, 46.7, 47.4, 48.7, 56.7, 61.4, 106.5, 111.3, 117.8, 118.5, 121.0, 126.5, 132.2, 135.7, 170.3, 171.1 ppm. SFCMS (APCI, *m/z*): [M]⁺ calc.: 423.56; found 423.32.

1-((5*S*)-8,9-dimethoxy-4-oxo-1,2,3,4,5,6-hexahydro-1,5-epiminobenzo[*d*]azocin-11-yl)-*N*-



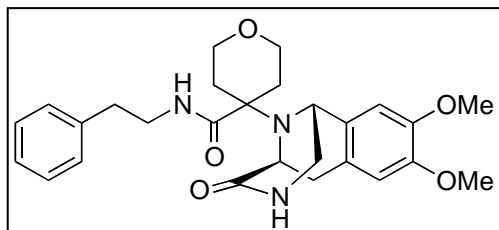
phenethylcyclobutanecarboxamide [3.2-4A]: Purified

by column flash chromatography (Hexanes/EtOAc);

Yield 64% (143 mg) as a light yellowish solid; ¹H NMR

(600 MHz, DMSO-*d*₆) δ: 1.46-1.57 (m, 2H), 2.08-2.14 (m, 2H), 2.16-2.22 (m, 2H), 2.63-2.75 (m, 3H), 2.91-2.97 (m, 2H), 3.25-3.34 (m, 2H), 3.56 (dd, *J* = 11.4, 4.2 Hz, 1H), 3.64 (d, *J* = 6.0 Hz, 1H), 3.69 (s, 3H), 3.71 (s, 3H), 4.08 (d, *J* = 3.6 Hz, 1H), 6.63 (s, 1H), 6.80 (s, 1H), 7.17-7.20 (m, 3H), 7.26 (t, *J* = 7.8 Hz, 2H), 7.50 (d, *J* = 3.0 Hz, 1H), 7.75 (t, *J* = 5.4 Hz, 1H); ¹³C NMR (150 MHz, DMSO-*d*₆) δ: 13.7, 28.3, 29.2, 30.8, 35.0, 40.4, 48.3, 49.6, 54.1, 55.4, 55.5, 66.7, 110.1, 111.4, 125.8, 126.1, 128.3, 128.6, 129.3, 139.5, 147.2, 147.7, 171.1, 173.9 ppm. SFCMS (APCI, *m/z*): [M]⁺ calc.: 450.54; found: 450.21.

4-((5*S*)-8,9-dimethoxy-4-oxo-1,2,3,4,5,6-hexahydro-1,5-epiminobenzo[*d*]azocin-11-yl)-*N*-



phenethyltetrahydro-2*H*-pyran-4-carboxamide [3.2-

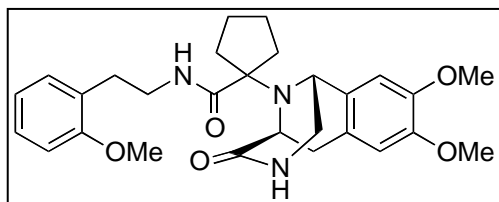
4B]: Purified by column flash chromatography

(Hexanes/EtOAc); Yield 59% (141 mg) as a light

yellowish solid; ¹H NMR (600 MHz, DMSO-*d*₆) δ: 1.54-

1.58 (m, 1H), 1.75-1.78 (m, 1H), 1.91-1.94 (m, 2H), 2.61-2.68 (m, 3H), 2.91-2.99 (m, 2H), 3.10 (t, *J* = 10.8 Hz, 1H), 3.13-3.25 (m, 2H), 3.37 (t, *J* = 10.2 Hz, 1H), 3.61 (dd, *J* = 11.4, 4.8 Hz, 2H), 3.65-3.67 (m, 1H), 3.68 (s, 3H), 3.70 (s, 3H), 3.81 (d, *J* = 6.0 Hz, 1H), 4.21 (d, *J* = 3.6 Hz, 1H), 6.61 (s, 1H), 6.79 (s, 1H), 7.16-7.20 (m, 3H), 7.27 (t, *J* = 7.8 Hz, 2H), 7.43 (d, *J* = 3.6 Hz, 1H), 7.88 (t, *J* = 5.4 Hz, 1H); ¹³C NMR (150 MHz, DMSO-*d*₆) δ: 30.6, 31.9, 32.8, 34.7, 40.5, 48.4, 48.6, 53.2, 55.4, 55.5, 61.4, 63.7, 64.5, 110.1, 111.5, 125.7, 126.1, 128.3, 128.6, 129.8, 139.5, 147.1, 147.6, 171.1, 172.5 ppm. SFCMS (APCI, *m/z*): [M]⁺ calc.: 480.57; found: 480.21.

1-((5S)-8,9-dimethoxy-4-oxo-1,2,3,4,5,6-hexahydro-1,5-epiminobenzo[d]azocin-11-yl)-N-(2-

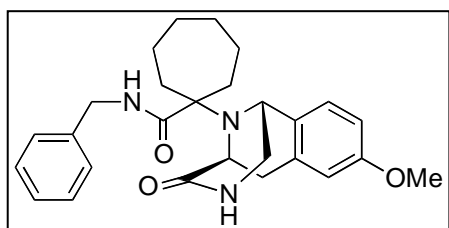


methoxyphenethyl)cyclopentane-carboxamide [3.2-

4C]: Purified by column flash chromatography (Hexanes/EtOAc); Yield 62% (153 mg) as a light

yellowish solid; ^1H NMR (600 MHz, DMSO- d_6) δ : 1.36-1.42 (m, 1H), 1.46-1.53 (m, 3H), 1.54-1.59 (m, 1H), 1.71-1.76 (m, 1H), 1.85-1.90 (m, 1H), 1.99-2.04 (m, 1H), 2.59-2.71 (m, 3H), 2.89-2.93 (m, 2H), 3.20 (q, $J = 14.4, 7.8$ Hz, 2H), 3.57 (dd, $J = 12.0, 4.8$ Hz, 1H), 3.62 (d, $J = 6.0$ Hz, 1H), 3.68 (s, 3H), 3.70 (s, 3H), 3.75 (s, 3H), 4.04 (d, $J = 3.6$ Hz, 1H), 6.60 (s, 1H), 6.79 (s, 1H), 6.84 (t, $J = 7.2$ Hz, 1H), 6.93 (d, $J = 8.4$ Hz, 1H), 7.08 (d, $J = 7.2$ Hz, 1H), 7.18 (t, $J = 9.0$ Hz, 1H), 7.43 (d, $J = 3.6$ Hz, 1H), 7.72 (t, $J = 6.0$ Hz, 1H); ^{13}C NMR (150 MHz, DMSO- d_6) δ : 23.4, 33.6, 29.6, 30.8, 32.1, 33.4, 40.0, 48.5, 50.3, 54.8, 55.2, 55.4, 55.5, 73.3, 110.1, 110.6, 111.4, 120.3, 125.7, 127.3, 127.6, 129.7, 129.9, 147.1, 147.6, 157.2, 171.2, 174.6 ppm. SFCMS (APCI, m/z): $[\text{M}]^+$ calc.: 494.59; found: 494.25.

N-benzyl-1-((1R,5S)-8-methoxy-4-oxo-1,2,3,4,5,6-hexahydro-1,5-epiminobenzo[d]azocin-

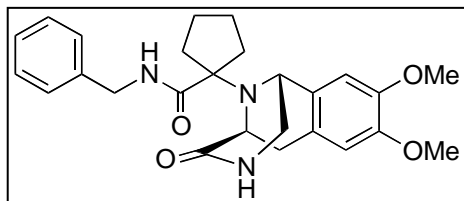


11-yl)cycloheptanecarboxamide [3.2-4D]: Purified by SFC (CO_2/MeOH); Yield 35% (78 mg) as a light yellowish solid; ^1H NMR (600 MHz, CDCl_3) δ : 1.34-1.48 (m, 3H), 1.55-1.75 (m, 6H), 1.90-1.98 (m, 2H), 2.24 (dd, $J = 13.8, 8.4$

Hz, 1H), 2.85 (d, $J = 16.8$ Hz, 1H), 3.01 (dd, $J = 11.4, 3.6$ Hz, 1H), 3.05 (dd, $J = 17.4, 6.6$ Hz, 1H), 3.60 (dd, $J = 11.4, 4.8$ Hz, 1H), 3.75 (s, 3H), 3.84 (d, $J = 6.6$ Hz, 1H), 3.97 (d, $J = 4.2$ Hz, 1H), 4.32 (d, $J = 14.4$ Hz, 1H), 4.46 (d, $J = 14.4$ Hz, 1H), 6.28 (s, 1H), 6.54 (d, $J = 2.4$ Hz, 1H), 6.72 (dd, $J = 8.4, 2.4$ Hz, 1H), 6.90 (d, $J = 8.4$ Hz, 1H), 7.23-7.33 (m, 6H); ^{13}C NMR (150 MHz, CDCl_3) δ : 24.2, 24.8, 30.3, 30.4, 31.8, 33.6, 36.5, 43.3, 49.8, 50.3, 54.4, 55.2, 70.1, 113.2, 127.1,

127.5, 127.8, 128.7, 129.3, 134.5, 138.8, 158.6, 172.7, 176.5 ppm. SFCMS (APCI, m/z): $[M]^+$ calc.: 448.57; found: 448.25.

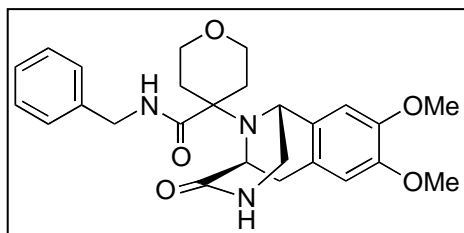
***N*-benzyl-1-((5*S*)-8,9-dimethoxy-4-oxo-1,2,3,4,5,6-hexahydro-1,5-epiminobenzo[*d*]azocin-**



11-yl)cyclopentanecarboxamide [3.2-4E]: Purified by column flash chromatography (Hexanes/EtOAc); Yield 72% (161 mg) as a light yellowish solid; ^1H NMR (600

MHz, DMSO- d_6) δ : 1.39-1.46 (m, 1H), 1.48-1.56 (m, 2H), 1.58-1.63 (m, 2H), 1.74-1.79 (m, 1H), 1.97-2.02 (m, 1H), 2.04-2.09 (m, 1H), 2.63 (d, $J = 16.2$ Hz, 1H), 2.92-2.98 (m, 2H), 3.58-3.64 (m, 2H), 3.69 (s, 3H), 3.70 (s, 3H), 4.08 (d, $J = 4.2$ Hz, 1H), 4.16 (dd, $J = 15.0, 6.0$ Hz, 1H), 4.27 (dd, $J = 14.4, 6.0$ Hz, 1H), 6.61 (s, 1H), 6.77 (s, 1H), 7.20-7.23 (m, 3H), 7.27-7.31 (m, 2H), 7.42 (d, $J = 3.6$ Hz, 1H), 8.26 (t, $J = 6.0$ Hz, 1H); ^{13}C NMR (150 MHz, DMSO- d_6) δ : 23.4, 23.7, 31.1, 32.5, 33.0, 42.5, 48.4, 50.4, 54.8, 55.4, 55.5, 73.8, 110.1, 111.4, 125.8, 126.7, 127.2, 128.2, 129.8, 140.1, 147.1, 147.6, 171.3, 174.9 ppm. SFCMS (APCI, m/z): $[M]^+$ calc.: 450.54; found: 450.21.

***N*-benzyl-4-((5*S*)-8,9-dimethoxy-4-oxo-1,2,3,4,5,6-hexahydro-1,5-epiminobenzo[*d*]azocin-**



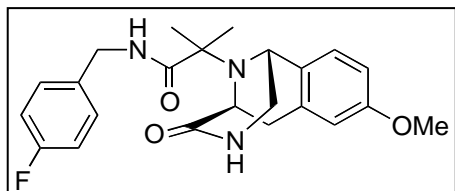
11-yl)tetrahydro-2*H*-pyran-4-carboxamide [3.2-4F]:

Purified by SFC (CO_2/MeOH); Yield 49% (114 mg) as a light yellowish solid; ^1H NMR (600 MHz, DMSO- d_6) δ : 1.55-1.60 (m, 1H), 1.81-1.86 (m, 1H), 1.96-1.99 (m, 1H),

2.01-2.05 (m, 1H), 2.63 (d, $J = 16.2$ Hz, 1H), 2.92-2.97 (m, 2H), 3.21 (t, $J = 10.8$ Hz, 1H), 3.43 (td, $J = 11.4, 1.8$ Hz, 1H), 3.57 (dd, $J = 12.0, 4.8$ Hz, 1H), 3.63-3.67 (m, 1H), 3.69 (s, 3H), 3.71 (s, 3H), 3.73-3.76 (m, 1H), 3.80 (d, $J = 6.6$ Hz, 1H), 4.11 (dd, $J = 14.4, 5.4$ Hz, 1H), 4.20 (d, $J = 3.6$ Hz, 1H), 4.25 (dd, $J = 15.0, 6.0$ Hz, 1H), 6.61 (s, 1H), 6.77 (s, 1H), 7.22-7.24 (m, 3H), 7.29-

7.31 (m, 2H), 7.40 (d, $J = 3.6$ Hz, 1H), 8.35 (t, $J = 6.0$ Hz, 1H); ^{13}C NMR (150 MHz, DMSO- d_6) δ : 30.7, 32.0, 32.6, 40.1, 42.5, 48.5, 53.2, 55.4, 55.5, 61.9, 63.9, 64.7, 110.0, 111.5, 125.6, 126.7, 127.4, 128.2, 129.8, 139.8, 147.1, 147.6, 171.1, 172.7 ppm. SFCMS (APCI, m/z): $[\text{M}]^+$ calc.: 466.54; found: 466.24.

***N*-(4-fluorobenzyl)-2-((1*R*,5*S*)-8-methoxy-4-oxo-1,2,3,4,5,6-hexahydro-1,5-**

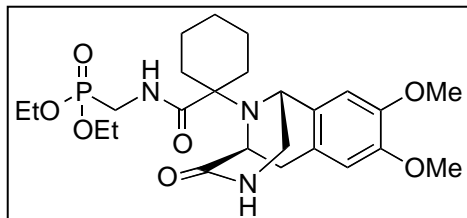


epiminobenzo[d]azocin-11-yl)-2-methylpropanamide

[3.2-4G]: Purified by SFC (CO_2/MeOH); Yield 44% (90 mg) as a light yellowish solid; ^1H NMR (600 MHz, CDCl_3)

δ : 1.25 (s, 3H), 1.39 (s, 3H), 2.87 (d, $J = 16.8$ Hz, 1H), 2.94 (dd, $J = 16.8, 6.0$ Hz, 1H), 3.12 (dd, $J = 11.4, 3.6$ Hz, 1H), 3.63 (dd, $J = 12.0, 4.8$ Hz, 1H), 3.69 (d, $J = 6.6$ Hz, 1H), 3.73 (s, 3H), 4.01 (d, $J = 3.6$ Hz, 1H), 4.24 (dd, $J = 15.0, 5.4$ Hz, 1H), 4.47 (dd, $J = 15.0, 6.6$ Hz, 1H), 6.54 (d, $J = 2.4$ Hz, 1H), 6.73 (dd, $J = 8.4, 2.4$ Hz, 1H), 6.95 (d, $J = 8.4$ Hz, 1H), 6.98-7.02 (m, 3H), 7.21 (dd, $J = 8.4, 5.4$ Hz, 2H), 7.61 (t, $J = 6.0$ Hz, 1H); ^{13}C NMR (150 MHz, CDCl_3) δ : 20.5, 25.1, 31.7, 42.7, 49.3, 50.2, 54.7, 55.1, 63.7, 113.1, 113.2, 115.4, 115.6, 127.2, 128.9, 129.2, 129.3, 134.1, 134.4, 134.5, 158.6, 161.2, 162.9, 172.8, 176.2 ppm. SFCMS (APCI, m/z): $[\text{M}]^+$ calc.: 412.47; found: 412.19.

diethyl-((1-((5*S*)-8,9-dimethoxy-4-oxo-1,2,3,4,5,6-hexahydro-1,5-epiminobenzo[d]azocin-



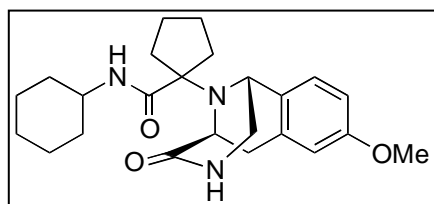
11-yl)cyclohexanecarboxamido)-methyl)phosphonate

[3.2-4H]: Purified by column flash chromatography (Hexanes/EtOAc); Yield 76% (198 mg) as a light yellowish solid; ^1H NMR (600 MHz, DMSO- d_6) δ : 1.11-

1.29 (m, 9H), 1.42-1.47 (m, 2H), 1.53-1.63 (m, 3H), 1.91-1.98 (m, 2H), 2.59 (d, $J = 16.2$ Hz, 1H), 2.93 (dd, $J = 11.4, 3.6$ Hz, 1H), 3.01 (dd, $J = 16.8, 6.6$ Hz, 1H), 3.44 (q, $J = 10.8, 6.0$ Hz,

2H), 3.64 (dd, $J = 12.0, 4.8$ Hz, 1H), 3.69 (s, 3H), 3.70 (s, 3H), 3.73 (d, $J = 6.0$ Hz, 1H), 3.98-4.03 (m, 4H), 4.15 (d, $J = 3.6$ Hz, 1H), 6.60 (s, 1H), 6.73 (s, 1H), 7.38 (d, $J = 3.6$ Hz, 1H), 7.92 (t, $J = 6.0$ Hz, 1H); ^{13}C NMR (150 MHz, DMSO- d_6) δ : 16.2 (q), 22.5, 22.9, 25.0, 30.6, 31.2, 32.3, 33.6, 34.6, 48.7, 48.8, 53.5, 55.4, 55.5, 61.4 (q), 64.3, 109.9, 111.5, 125.8, 130.1, 147.0, 147.5, 171.4, 173.5 ppm. SFCMS (APCI, m/z): $[\text{M}]^+$ calc.: 524.56; found: 524.28.

***N*-cyclohexyl-1-((1*R*,5*S*)-8-methoxy-4-oxo-1,2,3,4,5,6-hexahydro-**

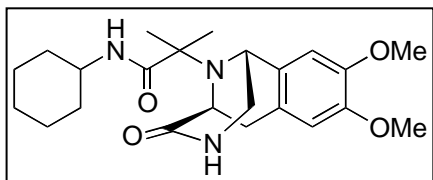


1,5-epiminobenzo[*d*]azocin-11-yl)cyclopentanecarboxamide [3.2-4I]: Purified by SFC

(CO_2/MeOH); Yield 47% (96 mg) as a colorless solid; ^1H

NMR (600 MHz, CDCl_3) δ : 0.97-1.12 (m, 3H), 1.26-1.35 (m, 2H), 1.55-1.73 (m, 8H), 1.78-1.85 (m, 3H), 1.94-1.99 (m, 1H), 2.07-2.10 (m, 1H), 2.92 (d, $J = 16.8$ Hz, 1H), 3.11 (d, $J = 11.4$ Hz, 1H), 3.65-3.70 (m, 1H), 3.74 (s, 3H), 3.76-3.80 (m, 1H), 3.82 (d, $J = 6.6$ Hz, 1H), 4.04 ($J = 4.2$ Hz, 1H), 6.58 (d, $J = 1.8$ Hz, 1H), 6.72 (dd, $J = 8.4, 2.4$ Hz, 1H), 6.94 (d, $J = 8.4$ Hz, 1H); ^{13}C NMR (150 MHz, CDCl_3) δ : 24.8, 24.9, 25.0, 25.4, 32.3, 32.9, 33.0, 33.1, 33.5, 47.8, 49.2, 50.9, 54.5, 55.1, 74.5, 74.6, 113.0, 113.2, 127.2, 129.2, 134.6, 158.5, 172.9, 174.9 ppm. SFCMS (APCI, m/z): $[\text{M}]^+$ calc.: 412.54; found: 412.23.

***N*-cyclohexyl-2-((1*R*,5*S*)-8,9-dimethoxy-4-oxo-1,2,3,4,5,6-hexahydro-1,5-**



epiminobenzo[*d*]azocin-11-yl)-2-methylpropanamide

[3.2-4J]: Purified by SFC (CO_2/MeOH); Yield 52% (108 mg) as a light yellowish solid; ^1H NMR (600 MHz, DMSO-

d_6) δ : 1.01 (s, 3H), 1.09-1.30 (m, 8H), 1.54-1.76 (m, 5H), 2.68 (d, $J = 16.8$ Hz, 1H), 2.95 (dd, $J = 16.8, 6.0$ Hz, 1H), 3.00 (dd, $J = 12.0, 4.2$ Hz, 1H), 3.49-3.54 (m, 2H), 3.62 (dd, $J = 12.0, 4.2$ Hz, 1H), 3.70 (s, 3H), 3.71 (s, 3H), 3.95 (d, $J = 3.6$ Hz, 1H), 6.65 (s, 1H), 6.86 (s, 1H), 7.49 (d, $J =$

3.6 Hz, 1H), 7.62 (d, $J = 9.0$ Hz, 1H); ^{13}C NMR (150 MHz, DMSO- d_6) δ : 20.4, 24.6, 24.7, 24.8, 25.2, 30.4, 32.2, 32.5, 47.6, 48.8, 49.9, 54.4, 55.4, 55.5, 62.5, 110.0, 111.5, 125.3, 129.7, 147.3, 147.6, 171.3, 174.6 ppm. SFCMS (APCI, m/z): $[\text{M}]^+$ calc.: 416.53; found: 416.22.

4.0 UGI-4-COMPONENT-5-CENTERED REACTION FOR USE IN P53/MDM2

Herein, the use of our alternative technique, the web- and structure-based design tool ANCHOR.QUERY is described, which led to the discovery and the subsequent optimization of new, potent p53-MDM2 inhibitors based on our newly described Ugi MCR. The key biophysical insights of ANCHOR.QUERY are that anchor residues define a binding mode and the structural alignment of a chemical mimics the corresponding anchor residue in the PPI structure.¹⁹⁶ An anchor residue is defined as an amino acid side chain that is deeply buried in the protein-protein interaction interface. Another web server, Pocket.Query, is available to calculate the buriedness of the interface amino acid side chains.¹⁹⁶ In the case of the p53-MDM2 interaction, Trp23 is the most deeply buried and central p53 amino acid, and was therefore selected as the anchor. The importance of this amino acid for the p53-MDM2 interaction is also well documented by mutational studies.⁴¹ Other deeply buried amino acid side chains of the p53 hot-spot, Phe19 and Leu26, were selected as hydrophobic pharmacophores.

4.1 ANCHORQUERY SEARCH AGAINST P53/MDM2

In an attempt to discover novel scaffolds to inhibit the protein-protein interaction between p53 and MDM2, a ~1/2 billion conformer library based on ~5 million unique MCR compounds containing the indole anchor were aligned with the Trp23 anchor of p53 and screened for

matches using the anchor/pharmacophore model. The screening results were then sorted and ranked by molecular descriptors. For example, molecular weight ranking is important for the selection of the compounds to potentially achieve good ligand efficiency. The scaffold and individual compounds are chosen for synthesis according to the binding poses and the electrostatic complementarity of the molecules. This method has been validated by several known MCR scaffolds as p53-MDM2 inhibitors, including the van Leusen 3-CR imidazole, the classic Ugi-4-component reaction, the Ugi-4CR hydantoin, and the Orru-3CR imidazolidine.¹⁹⁷⁻²⁰¹ The proposed virtual molecule based on our newly described Ugi-4-component 5-centered reaction (Ugi4C5CR) matching the pharmacophore points is shown in **Figure 4.1**. This serves as a starting point for validation and optimization in the discovery of new p53-MDM2 inhibitors.

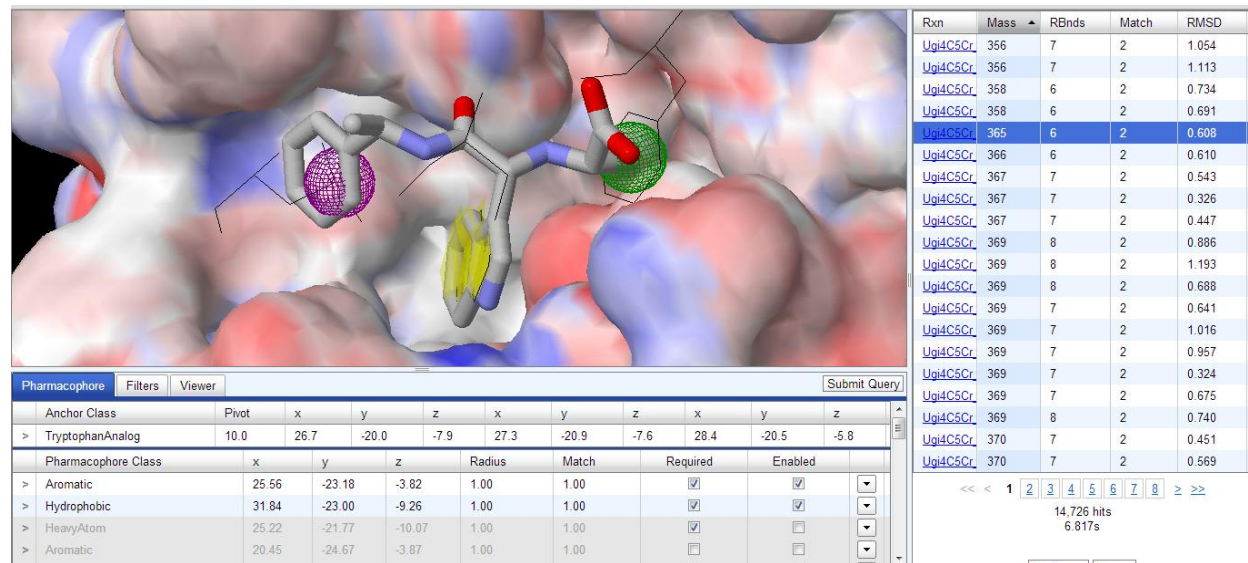


Figure 4.1 Screenshot of pharmacophore-based virtual screening platform ANCHOR.QUERY to discover MCR-derived MDM2 inhibitors. The MDM2 receptor is shown in surface representation (PDB ID: 1YCR). The hot spot p53 derived amino acids Phe19 and Leu26 are shown as lines and green and purple spheres respectively and the Trp23 indole anchor as yellow disk. The virtual U-4C5CR product (grey sticks) with matching pharmacophore model is depicted.

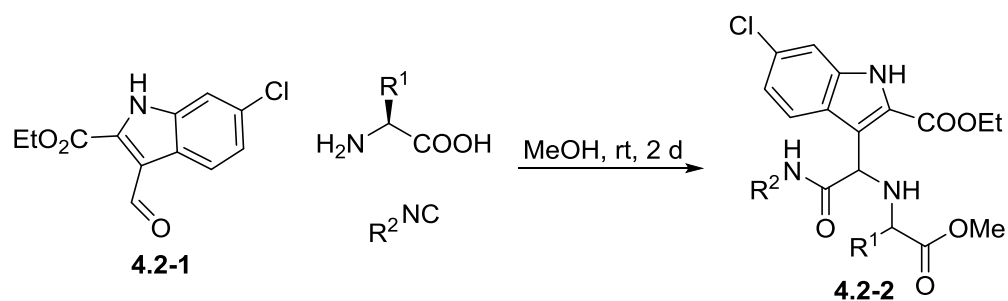
The accurate scoring of a diverse set of compounds is still an open problem ¹³², and *AnchorQuery* does not directly facilitate such a secondary screening. Instead, results were downloaded for in-house refinement. We used a multi-step energy-based secondary screen with pharmacophore filtering to refine and rank the results. Our hits are re-ranked after a fast energy minimization and pharmacophore filtering of the docked structures predicted by *AnchorQuery*. This secondary screening quickly identifies complexes with bad clashes. All energy minimization calculations are performed using the MAB Force Field with Moloc software. The results of *AnchorQuery* pharmacophore search are first quickly minimized within a fixed receptor with no solvent model and Coulomb electrostatics to eliminate ligand poses that are sterically or electrostatically infeasible. Minimized conformations are then filtered against the original pharmacophore. Only conformations that have a pRMSD less than one and an energy score less than zero are retained. The best scoring conformation is then further optimized within a fixed receptor using Poisson-Boltzman electrostatics. Again, minimized results that no longer match the original pharmacophore query (>1.0 Å pRMSD) are filtered out. At the transition between each stage, the number of sampled conformations is reduced to match the available computing resources (the top 3 pharmacophore RMSD conformations are selected from the *AnchorQuery* results and the top conformation of each stereoisomer is selected from the first energy minimization).

Using this technique we were able to identify several promising compounds from the Ugi4C5Cr scaffold which were selected for synthesis.

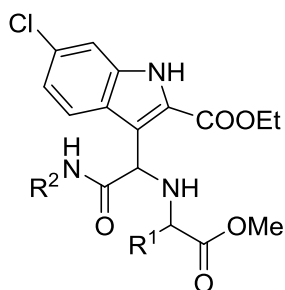
4.2 SYNTHESIS AND IN VITRO ACTIVITY OF SELECTED COMPOUNDS

The Ugi4C5CR is part of the ANCHOR.QUERY scaffolds due to its great scope and the reliability and compatibility of diverse inputs.¹⁴³ A preliminary investigation for the use of the Ugi4C5CR against the p53/MDM2 interaction was done using ethyl-6-chloro-3-formyl-1H-indole-2-carboxylate (**4.2-1**), leucine, and benzyl isocyanide in methanol at room temperature (**Scheme 4-1**) gave the desired product.²⁰²

A fluorescence polarization (FP) assay was employed to measure the binding affinities of small molecules with MDM2 as previously described.²⁰⁰ As a reference compound, Nutlin-3a's K_i was found to be 0.04 μ M, which is in very good agreement with previously reported value.²⁰⁰ Additionally a complementary physically independent assay, AIDA, was used to validate the potency of select p53-MDM2 inhibitor in an NMR competition binding experiment.^{203,204} To our delight, of the first compounds (**4.2-2A-4.2-2D**) tested, two compounds (**4.2-2A** and **4.2-2B**) were identified as hits. Due to fluorescence and water solubility issues, compounds could not be accurately measured via FP. Compound **4.2-2A** was accurately measured by AIDA to show a K_i of 1.7 μ M. Attempts to alter the amino acid (**4.2-2C** and **4.2-2D**) showed no activity leading us to believe that amino acids larger than leucine could not be used. In addition, attempts to alter the isocyanide showed no increase in activity; when using 4-Chlorobenzyl isocyanide (**4.2-2H**) a similar activity was observed.



Scheme 4-1 Classic Ugi4C5CR for use in p53/MDM2 inhibitor discovery



Entry	R1	R2	Ki (μM)
4.2-2A			1.7 ^[a]
4.2-2B			ND
4.2-2C			NI
4.2-2D			NI
4.2-2E			NI

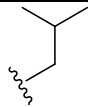
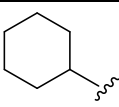
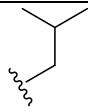
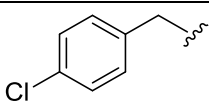
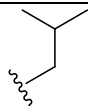
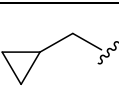
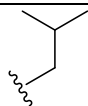
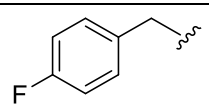
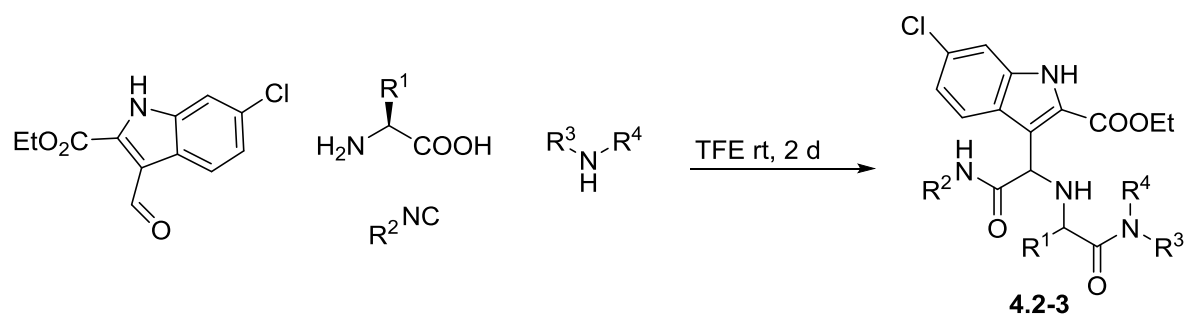
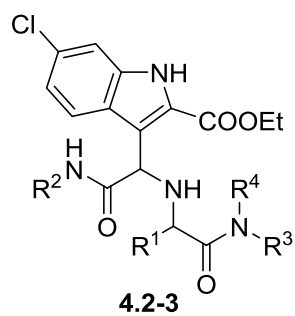
4.2-2F			NI
4.2-2G			3.0
4.2-2H			NI
4.2-2I			ND

Table 4-1 SAR study of compounds 4.2-2 Inhibition constant K_i was measured by FP assay unless otherwise noted. [a] K_i derived by AIDA, Abbreviation NI = No interaction, ND = Not Determinable,

Encouraged by our initial results, we attempted to use our newly modified Ugi4C5CR amidation reaction to increase activity and water solubility. Ethyl-6-chloro-3-formyl-1H-indole-2-carboxylate (**4.2-1**), an amino acid and isocyanide were added at 1/10 molar concentration to Trifluoroethanol. After a half hour primary or secondary amine was added in equal amounts, and allowed to sit for 2 days before work up and purification (**Scheme 4-2**). The addition of the amines was tolerated with respect to activity however did not show a great improvement as compared to our initial results (Table Table 4-2). In attempts to improve the water solubility, morpholine, 2-morpholinoethanamine, and 3-morpholinopropanamine were used, (**4.2-3C -- 4.2-3E**). It was found that as the chain length increased activity decreased causing us to focus on smaller amines.



Scheme 4-2 Modified Ugi4C5CR for use in p53/MDM2 inhibitor discovery



Entry	R ¹	R ²	R ³ /R ⁴	Ki (μM)
4.2-3A				NI
4.2-3B				9.0
4.2-3C				8.0
4.2-3D				10.0
4.2-3E				11.0

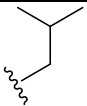
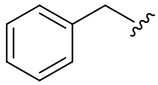
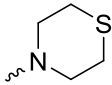
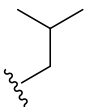
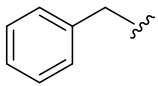
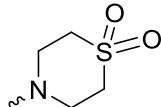
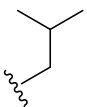
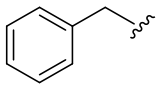
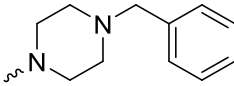
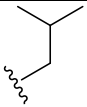
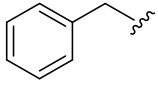
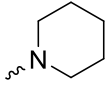
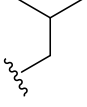
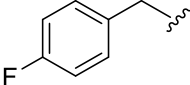
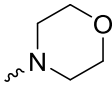
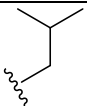
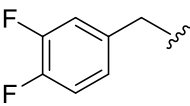
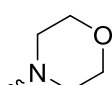
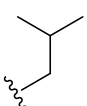
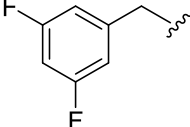
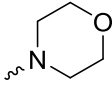
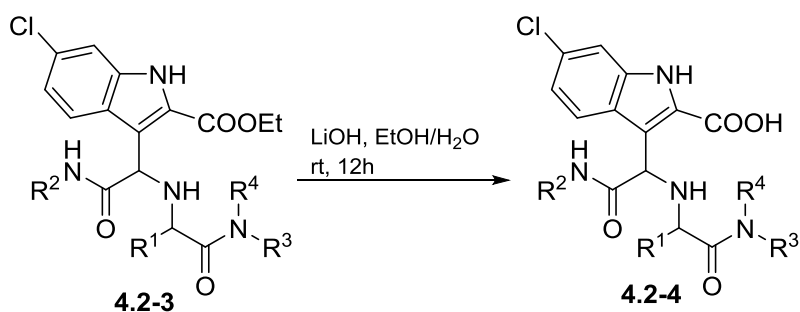
4.2-3F				NI
4.2-3G				3.0
4.2-3H				NI
4.2-3I				NI
4.2-3J				2.7
4.2-3K				1.3
4.2-3L				ND

Table 4-2 SAR study of compounds 4.2-3 Inhibition constant K_i was measured by FP assay unless otherwise noted. Abbreviation NI = No interaction, ND = Not Determinable,

Compounds **4.2-4** were synthesized by hydrolysis of the ethyl ester of the corresponding indole derivatives **4.2-3** (**Scheme 4-3**) and screened with the FP assay (Table 4-3). The binding affinities of **4.2-3** overall greatly improved compared to their corresponding ethyl ester compound. It has previously been shown for the imidazole scaffold that the carboxylic acid group of the indole fragment contributes to the binding with MDM2 (PDB ID: 3LBK).²⁰⁵

It was found that use of fluorine had great potential to increase the binding of our compounds to MDM2 due to an increase in the pi-pi stacking between our compounds and His57

in MDM2.² Three different fluorine substituted benzyl isocyanides were selected based on data available from the Ugi4-component reaction.² Two of these compounds (**4.2-4J** – **4.2-4L**) showed low micro molar activity while the 3,4 substituted benzyl isocyanide-yielded compound **4.4-4K** showed great inhibition of p53 at 85nM Ki. Interestingly, none of the compounds showed comparable binding affinity with MDM4 although MDM4 shows significant overall sequence and very close shape similarity to the p53 binding site.



Scheme 4-3 Synthesis of saponified Ugi4C5CR derivatives

Entry	R ¹	R ²	R ³ /R ⁴	Ki (μM)
4.2-4A				12.0
4.2-4B				9.0
4.2-4C				0.3
4.2-4D				0.4 ^[a]
4.2-4E				7.0

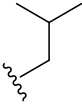
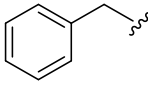
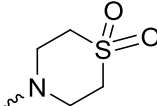
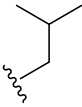
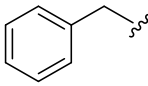
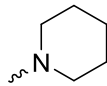
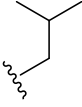
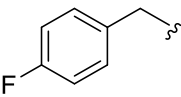
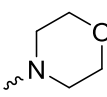
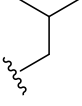
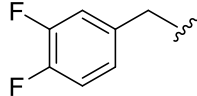
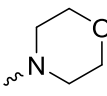
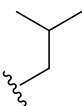
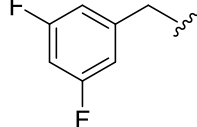
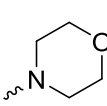
4.2-4G				0.76
4.2-4I				0.42
4.2-4J				0.5
4.2-4K				0.085
4.2-4L				0.26

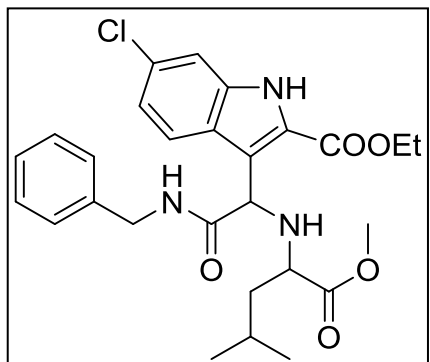
Table 4-3 SAR study of compounds 4.2-4 Inhibition constant K_i was measured by FP assay unless otherwise noted. [a] K_i derived by AIDA Abbreviation NI = No interaction, ND = Not Determinable,

4.2.1 Materials and Methods

General procedure of Compounds 4.2-2

A mixture of ethyl 6-chloro-3-formyl-1*H*-indole-2-carboxylate, amino acid, isocyanide, in 10mL of methanol was stirred under room temperature overnight. The methanol was evaporated under reduced pressure. The residue was dissolved in ethyl acetate, and washed 2 times each with saturated sodium bicarbonate and saturated sodium chloride and dried over sodium sulfate. The ethyl acetate was evaporated under reduced pressure, and the residue was purified via chromatotron in 3:1 hexane/ethyl acetate to afford the final product as a yellow solid.

Ethyl 3-(2-(benzylamino)-1-(((R)-1-methoxy-4-methyl-1-oxopentan-2-yl)amino)-2-

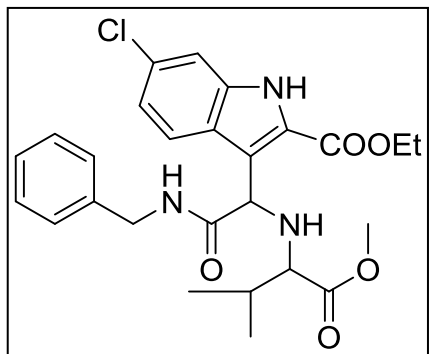


oxoethyl)-6-chloro-1H-indole-2-carboxylate [4.2-2A] 20%

yield as yellow solid. ^1H NMR (600MHz, CDCl_3) δ 0.48-0.49 (d, 3H), 0.75-0.76 (d, 3H), 1.35-1.38 (t, 3H), 1.32-1.67 (m, 3H), 3.19-3.22 (m, 1H), 3.64 (s, 1H), 4.25-4.36 (m, 2H), 4.45-4.58 (m, 2H), 5.28 (s, 1H), 7.00-7.02 (m, 1H), 7.12-7.13 (d,

1H), 7.26-7.27 (m, 2H), 7.30-7.37 (m, 2H), 7.56 (s, 1H), 7.62-7.63 (d, 1H), 9.30 (s, 1H) ^{13}C NMR (600MHz, CDCl_3) δ 14.2, 21.2, 22.9, 24.6, 42.1, 43.4, 51.7, 56.3, 57.6, 61.3, 111.9, 118.7, 120.4, 121.6, 122.5, 125.1, 127.3, 127.6, 127.8, 128.1, 128.6, 128.8, 131.6, 136.1, 138.3, 161.3, 171.7, 175.5ppm. HPLC-MS t_R : 12.48, m/z $[\text{M}+\text{H}]^+$: 513.90, $[\text{M}-\text{H}]^+$:512.03.

Ethyl 3-(2-(benzylamino)-1-(((S)-1-methoxy-3-methyl-1-oxobutan-2-yl)amino)-2-oxoethyl)-

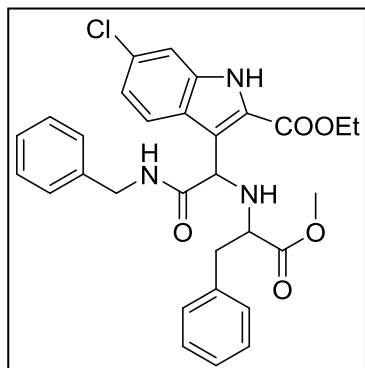


6-chloro-1H-indole-2-carboxylate [4.2-2B] 24% yield as

yellow solid. ^1H NMR (600MHz, CDCl_3) δ 0.73-0.74 (3H, d), 0.82-0.83 (3H, d), 1.24-1.27 (1H, m), 1.33-1.36 (3H, t), 1.87-1.91 (1H, m), 2.89-2.90 (1H, d), 3.65 (1H, s), 4.29-4.32 (2H, q), 4.41-4.52 (2H, m), 5.27 (1H, s), 7.03-7.05 (1H, d), 7.19-

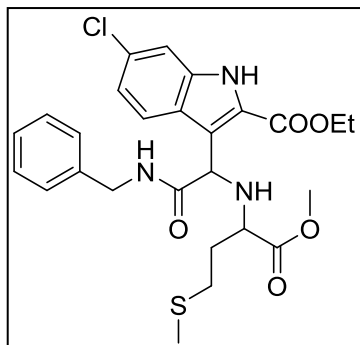
7.20 (3H, d), 7.23-7.29 (3H, m), 7.74-7.75 (1H, m), 9.09 (1H, s); ^{13}C NMR (600MHz, CDCl_3) δ 14.1, 14.2, 18.4, 19.2, 21.0, 31.3, 43.4, 51.5, 56.5, 60.4, 61.3, 62.4, 65.2, 111.9, 112.0, 119.2, 119.9, 121.5, 122.7, 123.9, 124.6, 124.6, 125.0, 125.3, 127.3, 127.5, 127.8, 128.4, 128.6, 127.7, 131.6, 132.2, 132.5, 135.7, 136.1, 138.2, 160.4, 161.3, 167.5, 171.2, 172.0, 174.7ppm. HPLC-MS t_R : 12.35, m/z $[\text{M}+\text{H}]^+$: 500.24, $[\text{M}-\text{H}]^+$:498.11.

Ethyl 3-(2-(benzylamino)-1-(((R)-1-methoxy-1-oxo-3-phenylpropan-2-yl)amino)-2-



oxoethyl)-6-chloro-1H-indole-2-carboxylate [4.2-2C] 48% yield as yellow solid. ^1H NMR (600MHz, CDCl_3) δ 1.07-1.12 (m, 3H), 2.96-2.98 (m, 2H), 3.38 (s, 3H), 3.76-3.77 (m, 1H), 3.86-3.88 (dd, 1H) 4.00-4.01 (m, 2H), 4.13-4.16 (dd, 1H), 5.88 (s, 1H), 6.75-6.77 (m, 2H), 6.80-6.81 (m, 2H), 6.83-6.85 (m, 2H), 6.86-6.88 (m, 3H), 6.99-6.70 (m, 3H), 7.28 (s, 1H); ^{13}C NMR (150MHz, MeOD) δ 13.1, 35.3, 43.1, 52.3, 55.0, 59.2, 61.8, 108.9, 112.3, 121.0, 122.2, 126.9, 127.3, 127.7, 127.9, 128.6, 128.2, 128.8, 131.7, 133.6, 136.7, 137.9, 161.1, 166.1, 168.1 pp. HPLC- MS t_R : 12.35, m/z $[\text{M}+\text{H}]^+$: 547.94, $[\text{M}-\text{H}]^+$: 545.919.

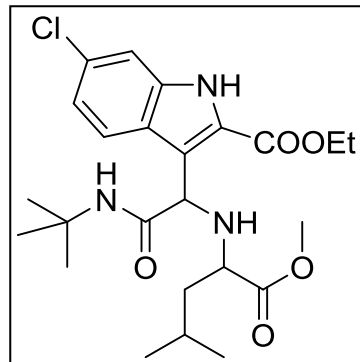
Ethyl 3-(2-(benzylamino)-1-(((R)-1-methoxy-4-(methylthio)-1-oxobutan-2-yl)amino)-2-



oxoethyl)-6-chloro-1H-indole-2-carboxylate [4.2-2D]: 22% as yellow oil ^1H NMR (600MHz, MeOD) δ 1.43-1.47 (m, 3H), 1.99, (s, 3H), 2.20-2.26 (m, 2H), 2.50-2.53 (m, 1H), 2.55-2.62 (m, 1H), 3.32-3.33 (m, 1H), 3.79 (s, 3H), 3.98-4.00 (m 1H), 4.15-4.17 (dd, 1H), 4.26-4.29 (dd, 1H), 4.44-4.47 (m, 2H), 6.21-6.24 (m, 1H),

7.08-7.11 (m, 3H), 7.12-7.18 (m, 3H), 7.55 (s, 1H), 7.68-7.70 (m, 1H); ^{13}C NMR (150MHz, MeOD) δ 13.2, 13.6, 28.2, 29.2, 43.0, 52.4, 54.9, 56.7, 61.5, 109.1, 112.0, 112.2, 121.5, 122.0, 126.8, 127.2, 127.9, 128.4, 131.6, 136.7, 137.8, 161.2, 166.2, 168.6 ppm. HPLC- MS t_R : 12.35, m/z $[\text{M}+\text{H}]^+$: 531.92, $[\text{M}-\text{H}]^+$: 530.01

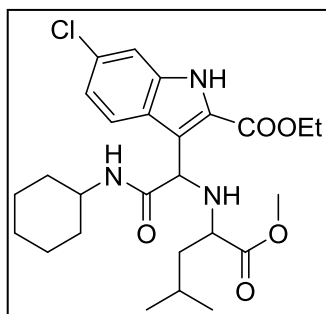
Ethyl 3-(2-(tert-butylamino)-1-(((R)-1-methoxy-4-methyl-1-oxopentan-2-yl)amino)-2-



oxoethyl)-6-chloro-1H-indole-2-carboxylate [4.2-2E]: 14% as yellow oil ^1H NMR (600MHz, MeOD) δ 1.26-1.33 (m, 6H), 1.48-1.51 (m, 9H), 1.59 (m, 2H), 1.90-1.97 (m, 3H), 3.52 (s, 3H), 4.28-4.44 (m, 1H), 4.53-4.57 (q, 2H), 7.32-7.34 (d, 1H), 7.48 (s, 1H), 8.41-8.42 (d, 1H), 9.53 (s, 1H), 10.74 (s, 1H). HPLC- MS t_R : 12.35,

m/z $[\text{M}+\text{H}]^+$: 481.87, $[\text{M}-\text{H}]^+$:478.14

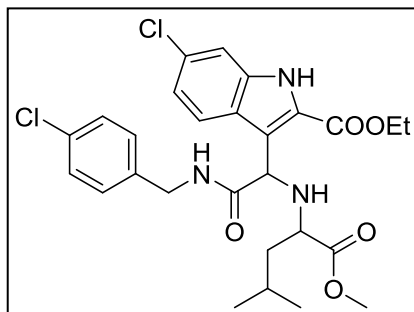
Ethyl 6-chloro-3-(2-(cyclohexylamino)-1-(((R)-1-methoxy-4-methyl-1-oxopentan-2-



yl)amino)-2-oxoethyl)-1H-indole-2-carboxylate [4.2-2F]: 18% as yellow oil ^1H NMR (600MHz, CDCl_3) δ 0.48-0.49 (m, 3H), 0.57-0.58 (m, 3H), 0.76-0.79 (m, 1H), 0.82-0.84 (m, 3H), 0.91-0.92 (m, 3H), 0.99-1.01 (m, 3H), 1.25-1.27 (t, 3H), 3.05 (s, 3H), 3.47-3.50 (m, 1H), 3.77-3.81 (m, 1H), 4.1-4.14 (m, 2H), 6.82-6.84 (m, 1H),

7.00-7.01 (d, 1H), 7.21-7.24 (m, 1H), 7.27-7.28 (m, 1H), 7.31-7.34 (m, 1H); ^{13}C NMR (150MHz, CDCl_3) δ 14.2, 18.9, 20.1, 20.2, 21.1, 35.4, 39.2, 40.6, 48.4, 60.4, 75.8, 91.1, 126.7, 128.5, 128.6, 128.7, 128.9, 130.3, 134.6, 134.7, 138.1, 162.1, 169.0, 171.2 ppm. HPLC- MS t_R : 12.35, m/z $[\text{M}+\text{H}]^+$: 506.10, $[\text{M}-\text{H}]^+$:504.21

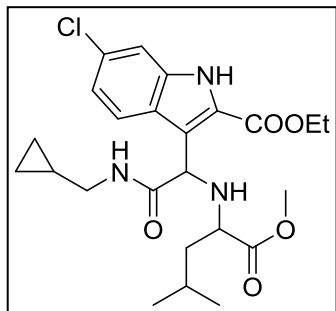
Ethyl 6-chloro-3-(2-((4-chlorobenzyl)amino)-1-(((S)-1-methoxy-4-methyl-1-oxopentan-2-



yl)amino)-2-oxoethyl)-1H-indole-2-carboxylate [4.2-2G] 15% yield as a yellow solid (81mg). ^1H NMR (600MHz, CDCl_3) δ 0.49-0.51 (3H, d), 0.78-0.79 (3H, d), 1.38-1.40 (3H, t), 1.42-1.56 (3H, m), 3.19-3.22 (1H, m), 3.67 (1H, s), 4.35-4.85 (2H, m), 4.39-4.51 (2H, m), 5.27 (1H, s), 7.07-7.09 (1H,

d), 7.17-7.18 (2H, d), 7.26-7.31 (2H, m), 7.41 (1H, s), 7.71-7.72 (1H, d), 8.98 (1H, s). ^{13}C NMR (150MHz, CDCl_3) δ 14.0, 21.4, 23.0, 24.5, 42.4, 42.9, 52.0, 56.2, 56.7, 62.3, 85.7, 115.2, 122.5, 123.3, 124.0, 125.1, 128.6, 128.8, 129.8, 133.1, 136.7, 148.6, 162.5, 170.0, 175.5 ppm. HPLC-MS t_{R} :17.29, m/z $[\text{M}+\text{H}]^+$: 549.87, $[\text{M}-\text{H}]^+$:547.93

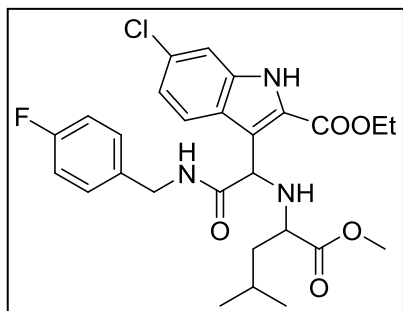
Ethyl 6-chloro-3-(2-((cyclopropylmethyl)amino)-1-(((R)-1-methoxy-4-methyl-1-oxopentan-2-yl)amino)-2-oxoethyl)-1H-indole-2-carboxylate [4.2-2H] 10% as



yellow oil. ^1H NMR (600MHz, MeOD) δ 0.18-0.20 (d, 2H), 0.48-0.50 (d, 2H), 0.66-0.67 (d, 3H), 0.84-0.85 (d, 3H), 0.94-0.98 (m, 2H), 1.32-1.35 (t, 3H), 1.59-1.67 (m, 3H), 3.71 (s, 3H), 3.55-3.57 (m, 1H), 4.21-4.28 (m, 2H), 5.57 (s, 1H), 7.05-7.06 (d, 1H), 7.13 (s, 1H), 7.32

(s, 1H), 7.60-7.61 (d, 1H), 10.18 (s, 1H). ^{13}C NMR (150MHz, MeOD) δ 3.40, 10.5, 14.0, 21.7, 22.4, 24.7, 40.7, 44.6, 52.3, 55.9, 57.8, 61.6, 112.4, 116.3, 121.4, 121.9, 124.6, 125.6, 131.6, 136.2, 161.4, 169.9, 173.3 ppm. HPLC-MS t_{R} : 12.35, m/z $[\text{M}+\text{H}]^+$: 548.00, $[\text{M}-\text{H}]^+$:546.10

Ethyl 6-chloro-3-(2-((4-fluorobenzyl)amino)-1-(((S)-1-methoxy-4-methyl-1-oxopentan-2-yl)amino)-2-oxoethyl)-1H-indole-2-carboxylate [4.2-I] 31 %



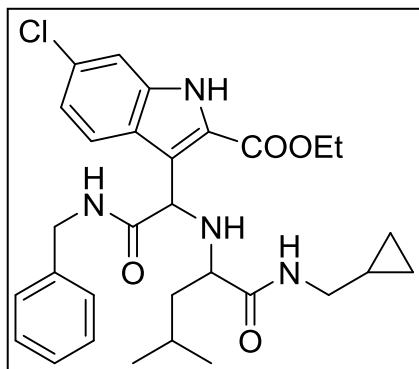
as yellow solid. ^1H NMR (600MHz, CDCl_3) δ 0.42-0.49 (d, 3H), 0.76-0.77 (d, 3H), 0.97-1.01 (1H, m), 1.30-1.33 (m, 3H), 1.42-1.46 (m, 2H), 3.25-3.28 (m, 1H), 3.67 (s, 3H), 4.18-4.27 (m, 2H), 4.47-4.51 (dd, 1H), 4.58-4.61 (dd, 1H), 5.25 (s, 1H),

6.99-7.06 (m, 5H), 7.31-7.33, (m, 2H), 7.51-7.53 (m, 1H), 9.83 (s, 1H); ^{13}C NMR (150MHz, MeOD) δ 14.1, 21.1, 22.6, 24.6, 42.0, 42.7, 51.8, 56.4, 57.8, 61.9, 112.2, 115.3, 119.9, 121.4, 125.0, 129.4, 131.1, 134.2, 136.2, 161.1, 162.2, 172.2, 175.5 ppm. HPLC-MS t_{R} : 12.35, m/z $[\text{M}+\text{H}]^+$: 531.86, $[\text{M}-\text{H}]^+$:529.64

General Procedure for compounds 4.2-3

A mixture of ethyl 6-chloro-3-formyl-1*H*-indole-2-carboxylate, amino acid, isocyanide, in 0.1 M of MeOH/H₂O (4:1) were stirred for 24 – 72 hours at room temperature. Solvents were evaporated under reduced pressure and residue was dissolved in DCM. Unreacted amino acid was filtered off and filtrate was evaporated to get crude product, which was purified on SFC using MeOH to yield title compound.

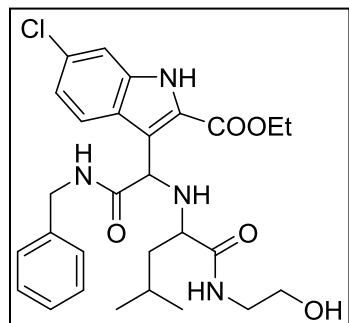
Methyl 3-(2-(benzylamino)-1-(((R)-1-((cyclopropylmethyl)amino)-4-methyl-1-oxopentan-2-yl)amino)-2-oxoethyl)-6-chloro-1*H*-indole-2-carboxylate



[4.2-3A] 20% Yield as a yellow solid. ¹H NMR (600MHz, CDCl₃) δ 0.80-0.81 (d, 3H), 0.94-0.95 (d, 3H), 1.45-1.49 (m, 1H), 1.88-1.93 (m, 1H), 2.74-2.76 (m, 1H), 3.01-3.07 (m, 2H), 3.43-3.49 (m, 3H), 4.21-4.23 (m, 1H), 4.27-4.32 (m, 2H), 4.45-4.48 (m, 1H), 5.93 (s, 1H), 6.88-6.90 (t, 1H), 7.10-7.11 (m,

2H), 7.19-7.21 (m, 1H), 7.24-7.25 (m, 1H), 7.28 (s, 1H), 7.44-7.45 (d, 1H), 7.62 (s, 1H), 11.23 (s, 1H); ¹³C NMR (150MHz, CDCl₃) δ 13.6, 21.3, 22.9, 24.2, 39.3, 42.8, 44.4, 45.3, 54.8, 55.4, 63.3, 65.4, 66.1, 107.8, 113.7, 119.3, 124.0, 124.7, 127.3, 127.8, 127.9, 128.6, 128.8, 133.4, 136.2, 136.5, 160.1, 160.4, 162.4, 165.8, 166.1 ppm. HPLC-MS r_t:16.06, m/z [M+H]⁺: 569.42, [M-H]⁺:567.62

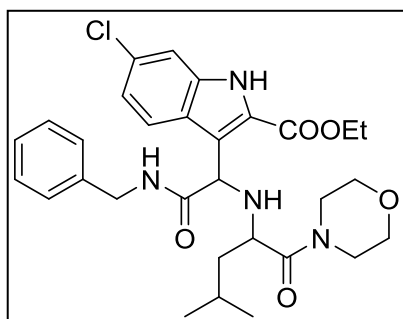
Ethyl 3-(2-(benzylamino)-1-(((S)-1-((2-hydroxyethyl)amino)-4-methyl-1-oxopentan-2-yl)amino)-2-oxoethyl)-6-chloro-1*H*-indole-2-carboxylate. [4.2-



3B] 15% yield as yellow solid. ¹H NMR (600MHz, CDCl₃) δ 0.77-0.78 (d, 3H), 0.87-0.88 (d, 3H), 1.27-1.31 (t, 1H), 1.39-1.42 (t, 3H), 1.56-1.61 (m, 1H), 1.71-1.83 (m, 2H), 3.46-3.50 (m, 1H), 3.66-3.70

(m, 1H), 4.09-4.11 (t, 1H), 4.16-4.20 (q, 1H), 4.27-4.31 (m, 1H), 4.36-4.44 (m, 4H), 4.49-4.52 (m, 1H), 5.68 (s, 1H), 6.20-6.22 (m, 1H), 7.06-7.08 (m, 2H), 7.23-7.27 (m, 3H), 7.48-7.49 (d, 1H), 7.57 (s, 1H), 8.07 (t, 1H), 10.57 (s, 1H); ^{13}C NMR (150MHz, CDCl_3) δ 13.7, 14.0, 21.5, 22.0, 24.5, 38.6, 39.8, 44.6, 55.3, 58.1, 63.7, 65.7, 108.6, 113.6, 115.8, 118.9, 124.4, 125.0, 125.8, 127.6, 128.2, 128.9, 134.2, 135.8, 136.4, 159.9, 160.2, 162.8, 165.9, 168.7 ppm HPLC-MS r_t :15.19, m/z $[\text{M}+\text{H}]^+$:543.10, $[\text{M}-\text{H}]^+$:541.25

Ethyl 3-(2-(benzylamino)-1-(((R)-4-methyl-1-morpholino-1-oxopentan-2-yl)amino)-2-

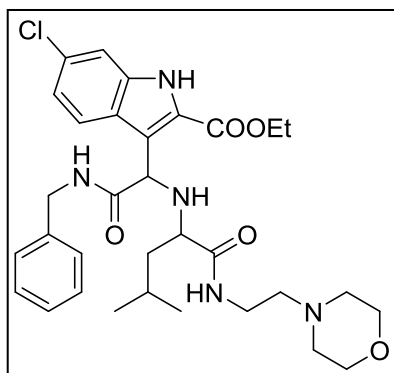


oxoethyl)-6-chloro-1H-indole-2-carboxylate [4.2-3C] 33%

yield as yellow solid. ^1H NMR (600MHz, CDCl_3) δ 0.49-0.50 (d, 3H), 0.89-0.90 (d, 3H), 1.15-1.20 (m, 1H), 1.50-1.53 (m, 5H), 3.06-3.10 (m, 1H), 3.22-3.25 (m, 1H), 3.46-3.51 (m, 2H), 3.54-3.60 (m, 2H), 3.65-3.66 (m, 1H), 3.68-3.71 (m, 2H), 4.46 (s,

2H), 4.47-4.52 (m, 2H), 5.51 (s, 1H), 7.09-7.11 (m, 1H), 7.24-7.25 (m, 2H), 7.28-7.30 (m, 3H), 7.55-7.56 (d, 1H), 7.87-7.88 (d, 1H); ^{13}C NMR (150MHz, CDCl_3) δ 17.0, 17.3, 21.9, 23.8, 26.4, 28.1, 28.6, 46.0, 46.1, 46.6, 49.1, 56.6, 59.2, 64.8, 69.8, 70.2, 115.5, 115.6, 123.1, 124.5, 127.2, 128.8, 130.6, 131.0, 131.9, 134.9, 140.8, 142.6, 165.6, 176.6, 178.1 HPLC-MS r_t :11.49, m/z $[\text{M}+\text{H}]^+$: 569.22, $[\text{M}-\text{H}]^+$:567.15

Ethyl 3-(2-(benzylamino)-1-(((S)-4-methyl-1-((2-morpholinoethyl)amino)-1-oxopentan-2-

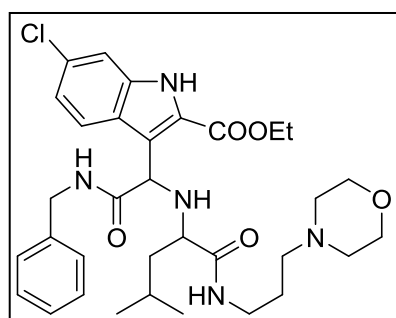


yl)amino)-2-oxoethyl)-6-chloro-1H-indole-2-carboxylate [4.2-

3D] 35% yield as yellow solid. ^1H NMR (600MHz, CDCl_3) δ 0.81-0.82 (d, 3H), 0.90-0.91 (d, 3H), 1.37-1.40 (t, 3H), 1.60-1.62 (m, 1H), 1.74-1.76 (m, 1H), 1.86-1.88 (m, 1H), 2.85-2.86 (m, 2H), 2.95-2.96 (m, 1H), 3.08 (m, 1H), 3.33-3.38 (t, 2H), 3.63 (s,

1H), 3.70-3.78 (m, 3H), 3.85-3.94 (m, 2H), 4.07-4.10 (t, 1H), 4.25-4.29 (m, 1H), 4.32-4.44 (m, 3H), 6.14 (s, 1H), 6.88 (s, 1H), 7.01-7.03 (m, 2H), 7.18-7.19 (d, 1H), 7.21 (s, 1H), 7.28 (s, 1H), 7.52 (s, 1H), 7.71-7.72 (d, 1H), 8.94 (s, 1H), 10.31 (s, 1H); ¹³C NMR (150MHz, CDCl₃) δ 13.8, 21.7, 21.9, 24.6, 33.9, 39.6, 44.2, 52.4, 53.1, 55.7, 57.4, 58.9, 62.9, 63.5, 69.5, 110.3, 113.0, 120.6, 123.5, 126.7, 127.1, 127.8, 128.7, 133.0, 136.2, 136.5, 161.7, 166.6 ppm HPLC-MS r_t:14.01, m/z [M+H]⁺: 612.00, [M-H]⁺:610.00

Ethyl 3-(2-(benzylamino)-1-(((S)-4-methyl-1-((3-morpholinopropyl)amino)-1-oxopentan-2-

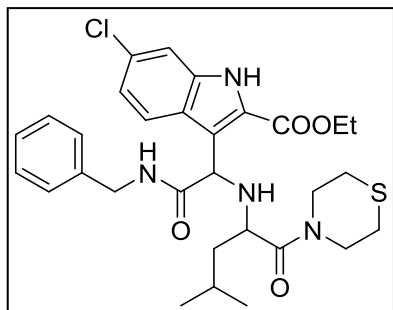


yl)amino)-2-oxoethyl)-6-chloro-1H-indole-2-carboxylate [4.2-

3E] 25% Yield. ¹H NMR (600MHz, CDCl₃) δ 0.73-0.74 (d, 3H), 0.88-0.89 (d, 3H), 1.36-1.51 (m, 3H), 1.58 (s, 2H), 1.67-1.69 (m, 1H), 1.86-1.87 (m, 2H), 1.92-1.94 (t, 2H), 3.13-3.15 (m, 1H), 3.23-3.32 (m, 4H), 3.42-3.46 (d, 1H), 3.50-3.52 (d,

1H), 3.56-3.59 (m, 1H), 3.82-3.89 (m, 4H), 4.00-4.03 (m, 2H), 4.06-4.12 (m, 3H), 4.24-4.27 (m, 1H), 4.45-4.48 (m, 1H), 5.87 (s, 1H) 6.71-6.73 (t, 1H), 7.05 (m, 2H), 7.21 (s, 1H), 7.22 (s, 1H), 7.24 (s, 1H), 7.27-7.28 (m, 1H), 7.54-7.55 (m, 3H), 8.12-8.13 (m, 1H), 9.85 (s, 1H); ¹³C NMR (150MHz, CDCl₃) δ 13.7, 21.0, 22.1, 22.8, 24.5, 27.6, 36.7, 39.9, 44.5, 52.2, 52.5, 54.9, 55.6, 58.5, 63.5, 63.7, 63.8, 63.8 109.1, 112.1, 113.2, 114.0, 115.9, 117.8, 119.6, 124.1, 126.2, 127.0, 127.5, 127.5, 128.7, 128.8, 128.9, 133.7, 136.1, 136.2, 160.1, 160.3, 160.6, 160.9, 162.2, 166.1 ppm. HPLC-MS r_t: 15.03 [M+H]⁺: 626.3.02

Ethyl 3-(2-(benzylamino)-1-(((S)-4-methyl-1-oxo-1-thiomorpholinopentan-2-yl)amino)-2-

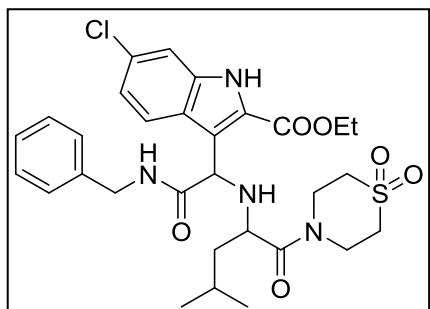


oxoethyl)-6-chloro-1H-indole-2-carboxylate [4.2-3F] 31% as

yellow solid. ^1H NMR (600MHz, CDCl_3) δ 0.52-0.54 (m, 3H), 0.83-0.84 (m, 3H), 1.38-1.51 (m, 6H), 1.65-1.70 (m, 3H), 2.28-2.35 (m, 1H), 2.54-2.58 (m, 1H), 3.28-3.37 (m, 1H), 3.44-3.48 (m, 1H), 3.70-3.74 (m, 2H), 3.81-3.83 (m, 2H), 4.34-4.36 (m,

1H), 4.49-4.53 (m, 2H), 5.46 (s, 1H), 7.02-7.07 (m, 1H), 7.19 (s, 1H), 7.24-7.33 (m, 4H), 7.45 (s, 1H), 7.74-7.77 (m, 1H), 9.37 (s, 1H); ^{13}C NMR (150MHz, CDCl_3) δ 17.2, 17.4, 22.0, 23.8, 26.6, 28.1, 28.8, 45.9, 46.2, 46.6, 49.3, 59.8, 64.8, 69.7, 71.2, 114.9, 123.1, 124.6, 127.2, 128.9, 130.6, 131.1, 131.9, 134.9, 140.6, 142.3, 165.9, 176.3 ppm. SFCMS (APCI, m/z): $[\text{M}]^+$ calc.585.22; found: 585.20

Ethyl 3-(2-(benzylamino)-1-(((S)-1-(1,1-dioxidothiomorpholino)-4-methyl-1-oxopentan-2-yl)amino)-2-oxoethyl)-6-chloro-1H-indole-2-carboxylate

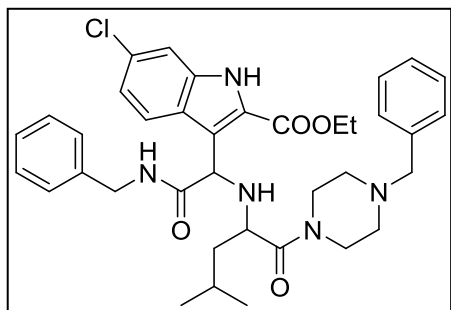


[4.2-3G] 19% as yellow oil. ^1H NMR (600MHz, CDCl_3) δ

0.49-0.51 (m, 3H), 0.82-0.84 (m, 3H), 1.35, (t, 3H), 1.47-1.51 (m, 1H), 1.72-1.77 (m, 2H), 2.63-2.86 (m, 4H), 2.92-3.00 (m, 5H), 3.40-3.41 (m, 1H), 4.29-4.33 (m, 2H), 4.48-4.53 (m, 2H),

5.45 (s, 1H), 7.02-7.04 (m, 1H), 7.11 (s, 1H), 7.22-7.24 (m, 3H), 7.29-7.34 (m, 5H), 7.67-7.70 (m, 1H); ^{13}C NMR (150MHz, CDCl_3) δ 14.2, 23.2, 25.3, 41.3, 43.2, 52.6, 57.8, 60.3, 63.2, 112.3, 120.1, 120.2, 121.3, 124.6, 126.8, 129.9, 129.2, 137.5, 145.6, 161.2, 169.6, 171.2 ppm. SFCMS (APCI, m/z): $[\text{M}]^+$ calc.:617.21; found:617.84

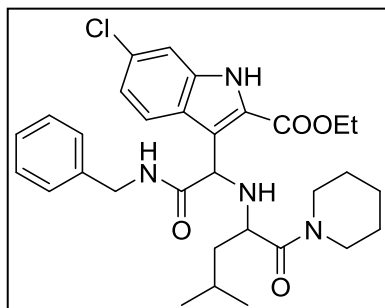
Ethyl 3-(2-(benzylamino)-1-(((S)-1-(4-benzylpiperazin-1-yl)-4-methyl-1-oxopentan-2-yl)amino)-2-oxoethyl)-6-chloro-1H-indole-2-carboxylate



[4.2-3H] 23% as yellow solid ^1H NMR (600MHz, CDCl_3) δ 0.46-0.48 (m, 3H), 0.78-0.81 (m, 3H), 1.34-1.1.36 (t, 3H), 1.41-1.47 (m, 3H), 1.93-2.15 (m, 2H), 2.34-2.38 (m, 2H), 2.89-3.03 (m, 2H), 3.40-3.52 (m, 5H), 4.20-4.24 (m, 2H),

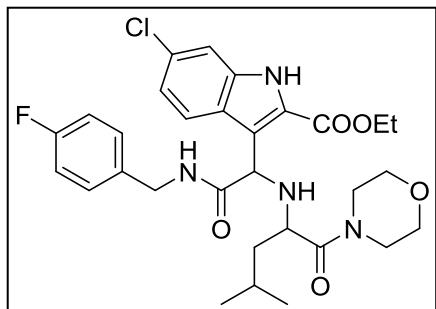
4.51-4.54 (m, 1H), 4.63-4.68 (m, 1H), 5.44 (s, 1H), 6.94 (s, 1H), 7.28-7.32 (m, 7H), 7.36-7.39 (m, 4H), 7.53-7.56 (m, 1H), 8.07 (s, 1H), 10.06 (s, 1H); ^{13}C NMR (150MHz, CDCl_3) δ 15.3, 23.2, 24.7, 41.8, 43.7, 50.2, 54.6, 57.3, 60.8, 64.2, 64.6, 112.6, 120.1, 120.2, 122.3, 125.6, 126.2, 128.4, 128.5, 137.8, 137.9, 143.6, 161.2, 169.9, 171.6 ppm. SFCMS (APCI, m/z): $[\text{M}]^+$ calc.:658.31; found: 658.14

Ethyl 3-(2-(benzylamino)-1-(((S)-4-methyl-1-oxo-1-(piperidin-1-yl)pentan-2-yl)amino)-2-oxoethyl)-6-chloro-1H-indole-2-carboxylate **[4.2-3I]** 13% as



yellow oil. ^1H NMR (600MHz, CDCl_3) δ 0.44-0.45 (d, 3H), 0.76-0.77 (d, 3H), 1.25-1.27 (m, 3H), 1.31-1.34 (m, 3H), 1.40-1.53 (m, 7H), 2.80-2.82 (m, 2H), 2.93-2.97 (m, 1H), 3.38-3.41 (m, 2H), 3.53-3.56 (m, 1H), 4.21-4.24 (m, 2H), 4.46-4.50 (dd, 1H), 4.60-4.64 (dd, 1H), 5.40 (s, 1), 6.93-6.97 (m, 1H), 7.26-7.34 (m, 4H), 7.58-7.60 (d, 1H), 7.95-7.97 (m, 1H), 9.73 (s, 1H); ^{13}C NMR (150MHz, CDCl_3) δ 14.2, 21.2, 23.4, 24.4, 24.5, 25.5, 26.1, 29.6, 42.8, 43.1, 43.9, 45.5, 53.6, 56.2, 61.2, 112.1, 119.6, 121.2, 122.6, 124.9, 125.7, 127.3, 127.8, 128.6, 131.2, 136.2, 138.4, 161.2, 171.3, 172.7 ppm. SFCMS (APCI, m/z): $[\text{M}]^+$ calc.:567.27; found:567.11

Ethyl 6-chloro-3-(2-((4-fluorobenzyl)amino)-1-(((S)-4-methyl-1-morpholino-1-oxopentan-2-

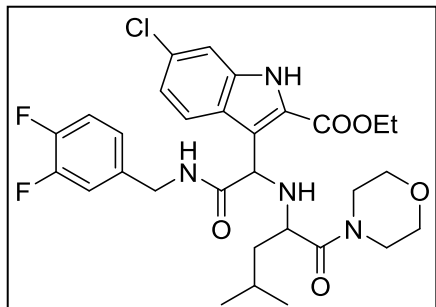


yl)amino)-2-oxoethyl)-1H-indole-2-carboxylate [4.2-3J]

43% as yellow solid] ^1H NMR (600MHz, CDCl_3) δ 0.51-0.52 (m, 3H), 0.89-0.91 (d, 3H), 1.15-1.19 (m, 1H), 1.85-1.89 (m, 2H), 2.50-2.53 (m, 3H), 3.06-3.10 (m, 1H), 3.22-3.25 (m, 1H), 3.46-3.71 (m, 7H), 4.45-4.46 (m, 2H), 4.49-4.52 (m,

2H), 5.51 (s, 1H), 7.09-7.11 (m, 1H), 7.24-7.30 (m, 5H), 7.55 (s, 1H), 7.87-7.88 (m, 1H); ^{13}C NMR (150MHz, CDCl_3) δ 14.3, 20.7, 24.1, 27.3, 43.9, 46.3, 57.8, 61.1, 62.1, 66.0, 112.3, 114.1, 121.2, 121.3, 122.0, 124.2, 127.2, 128.3, 128.4, 133.5, 142.9, 160.8, 169.6, 171.5 ppm. HPLC-MS r_t : 11.49, m/z $[\text{M}+\text{H}]^+$: 586.84, $[\text{M}-\text{H}]^+$: 585.19

Ethyl 6-chloro-3-(2-((3,4-difluorobenzyl)amino)-1-((4-methyl-1-morpholino-1-oxopentan-2-

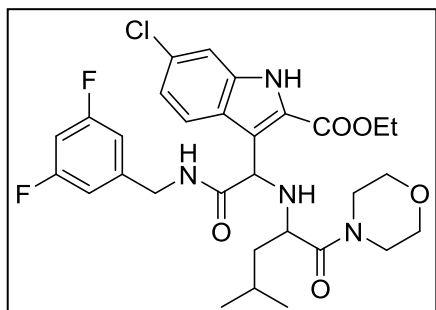


yl)amino)-2-oxoethyl)-1H-indole-2-carboxylate [4.2-3K]

39% as yellow solid] ^1H NMR (600MHz, CDCl_3) δ 0.49-0.50 (m, 3H), 0.85-0.86 (d, 3H), 1.21-1.23 (m, 1H), 1.85-1.89 (m, 2H), 2.48-2.51 (m, 3H), 3.06-3.19 (m, 2H), 3.41-3.56 (m, 2H), 3.60-3.73 (m, 5H), 4.43-4.46 (m, 2H), 4.50-4.54 (m,

2H), 5.49 (s, 1H), 7.02-7.04 (m, 1H), 7.24-7.29 (m, 2H), 7.35-7.39 (m, 2H), 7.46 (s, 1H), 7.95 (s, 1H); ^{13}C NMR (150MHz, CDCl_3) δ 14.2, 18.9, 21.1, 21.3, 23.1, 24.4, 35.3, 42.9, 43.4, 53.2, 56.9, 57.7, 58.9, 60.5, 66.8, 108.7, 111.6, 119.8, 119.9, 126.4, 127.4, 127.5, 128.4, 128.6, 128.7, 128.9, 131.9, 136.4, 138.1, 138.3, 171.1, 172.6 ppm. HPLC-MS r_t : 11.13, m/z $[\text{M}+\text{H}]^+$: 605.33, $[\text{M}-\text{H}]^+$: 603.28

Ethyl 6-chloro-3-(2-((3,5-difluorobenzyl)amino)-1-((4-methyl-1-morpholino-1-oxopentan-2-



yl)amino)-2-oxoethyl)-1H-indole-2-carboxylate [4.2-3L]

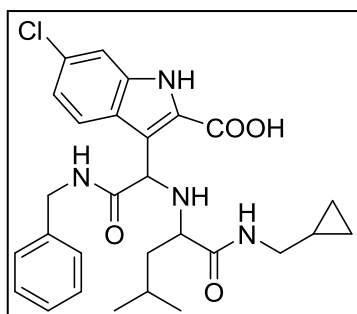
43% as yellow solid. ^1H NMR (600MHz, CDCl_3) δ 0.52-0.53 (m, 3H), 0.98-1.01 (m, 3H), 1.30-1.35 (m, 4H), 1.76-1.79 (m, 2H), 3.59-3.68 (m, 5H), 3.71-3.75 (m, 4H), 4.34-4.36 (q, 2H), 4.46-4.49 (m, 2H), 5.60 (s, 1H), 7.02-7.06 (m, 2H), 7.23-7.25

(m, 1H), 7.36-7.38 (m, 2H), 7.40 (s, 1H), 8.02 (s, 1H); ^{13}C NMR (150MHz, CDCl_3) δ 14.5, 21.2, 23.5, 26.0, 43.2, 47.0, 55.1, 59.6, 61.0, 64.1, 111.0, 115.2, 122.0, 122.1, 123.1, 123.9, 127.4, 128.0, 128.5, 132.3, 141.7, 161.9, 170.1, 171.2 ppm. HPLC-MS r_t : 11.23, m/z $[\text{M}+\text{H}]^+$: 605.41, $[\text{M}-\text{H}]^+$: 603.27

General procedure for Compounds 4.2-4

To one equivalent of the Ugi product (4.2-3) was treated with LiOH in EtOH/water (1:1), and stirred at RT for 2 days. The reaction mixture was then acidified with 1M HCl to a pH of ~ 6 . The mixture was extracted with DCM (10 mL x 3). The combined organic layer was dried over sodium sulfate, and evaporated.

3-(2-(benzylamino)-1-(((R)-1-((cyclopropylmethyl)amino)-4-methyl-1-oxopentan-2-

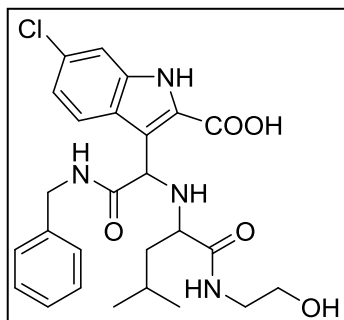


yl)amino)-2-oxoethyl)-6-chloro-1H-indole-2-carboxylic acid

[4.2-4A] 83% as white solid ^1H NMR (600MHz, MeOD) δ 0.12-0.0.15 (m, 2H), 0.39-0.40 (m, 1H), 0.52-0.55 (m, 1H), 0.70-0.78 (m, 3H), 0.86-0.90 (m, 3H), 1.24-1.27 (m, 1H), 1.34-1.67 (m, 3H), 2.50-2.52 (m, 2H), 2.95-3.05 (m, 1H), 4.19-4.27 (m, 2H), 4.50-4.56

(m, 1H), 6.94-6.96 (m, 1H), 7.12-7.26 (m, 3H), 7.28-7.39 (m, 3H), 7.73-7.77 (m, 1H), 8.06-8.15 (m, 1H) ppm. HPLC-MS r_t : 16.16, m/z $[\text{M}+\text{H}]^+$: 525.31, $[\text{M}-\text{H}]^+$: 523.44

3-(2-(benzylamino)-1-(((S)-1-((2-hydroxyethyl)amino)-4-methyl-1-oxopentan-2-yl)amino)-2-



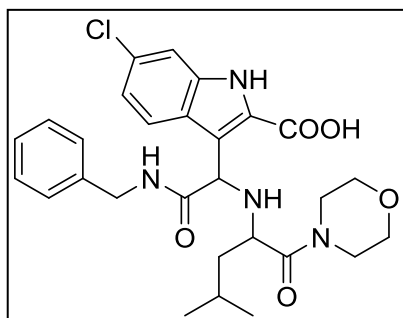
oxoethyl)-6-chloro-1H-indole-2-carboxylic acid [4.2-4B] 76% as

white solid ^1H NMR (600MHz, MeOD) δ 0.32-0.38 (m, 3H), 0.41-0.55 (m, 3H), 0.79-0.89 (m, 1H), 1.12-1.22 (m, 2H), 1.23-1.25 (m, 1H), 1.33-1.39 (m, 2H), 1.44-1.51 (m, 2H), 1.57-1.61 (m, 1H), 4.20-4.22 (m, 2H), 4.98 (s, 1H), 7.02-7.04 (m, 1H), 7.11-7.12 (m, 2H),

7.18-7.19 (m, 1H), 7.29-7.33 (m, 2H), 7.37-7.41 (m, 2H), 7.79-7.81 (d, 1H), 8.10-8.14 (m, 1H)

ppm. HPLC-MS r_t : 15.76, m/z $[\text{M}+\text{H}]^+$: 515.43, $[\text{M}-\text{H}]^+$: 513.69

[KK310] 3-(2-(benzylamino)-1-(((R)-4-methyl-1-morpholino-1-oxopentan-2-yl)amino)-2-



oxoethyl)-6-chloro-1H-indole-2-carboxylic acid [4.2-4C]

93% yield as yellow solid. ^1H NMR (600MHz, MeOD) δ 0.43-0.44 (d, 2H); 0.79-0.80 (d, 2H), 1.26-1.29 (m, 2H), 2.07 (d, 1H), 3.27-3.29 (m, 2H), 3.38-3.41 (m, 2H), 3.47-3.49 (m, 2H), 3.54-3.59 (m, 2H), 4.46-4.49 (m, 1H), 4.61-4.64 (m, 1H), 5.43 (s,

1H), 6.97-6.99 (d, 1H), 7.03 (s, 1H), 7.32-7.34 (m, 2H), 7.35-7.39 (m, 2H), 7.53-7.55 (d, 1H),

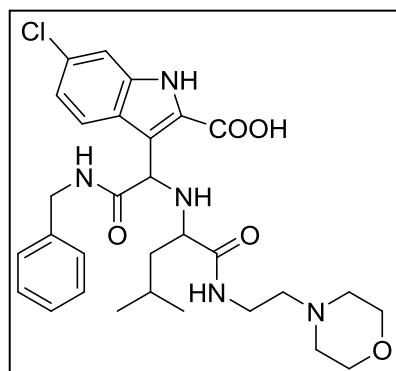
7.89 (s, 1H), 9.93 (s, 1H); ^{13}C NMR (150MHz, MeOD) δ 14.2, 21.4, 23.5, 24.5, 42.2, 42.5, 43.5,

45.0, 52.1, 53.3, 55.8, 60.5, 66.1, 66.8, 112.3, 119.4, 121.5, 122.4, 124.7, 125.6, 127.5, 127.9,

128.7, 131.5, 136.4, 138.3, 161.2, 172.3, 173.2 ppm. HPLC-MS – r_t : 11.36, m/z $[\text{M}+\text{H}]^+$:

569.25, $[\text{M}-\text{H}]^+$: 567.12

3-(2-(benzylamino)-1-((1-((2-hydroxyethyl)amino)-4-methyl-1-oxopentan-2-yl)amino)-2-

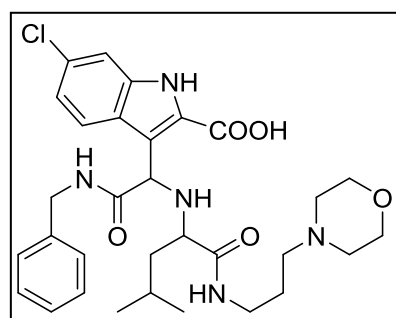


oxoethyl)-6-chloro-1H-indole-2-carboxylic acid [4.2-4D] 91%

Yield as yellow solid. ^1H NMR (600MHz, MeOD) δ 0.34-0.37 (m, 3H), 0.41-0.48 (m, 3H), 0.83-0.90 (m, 1H), 1.12-1.21 (m, 2H), 2.46-2.70 (m, 6H), 2.83-2.88 (m, 2H), 3.01-3.05 (m, 1H), 3.19-3.25 (m, 2H), 3.58-3.96 (m, 1H), 4.20-4.26 (m, 1H), 6.55-6.656 (m, 1H), 6.68-6.76 (m, 3H), 6.79-6.82 (m, 1H), 6.86-6.88

(m, 2H), 6.95-6.97 (m, 1H), 7.03-7.04 (m, 1H), 7.21-7.23 (m, 1H), 7.67-7.689 (m, 1H) ppm. HPLC-MS r_t :15.81, m/z $[\text{M}+\text{H}]^+$: 584.61, $[\text{M}-\text{H}]^+$:582.63

3-(2-(benzylamino)-1-(((S)-4-methyl-1-((3-morpholinopropyl)amino)-1-oxopentan-2-

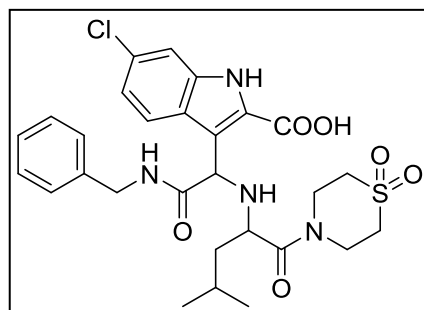


yl)amino)-2-oxoethyl)-6-chloro-1H-indole-2-carboxylic acid

[4.2-4E] 78% as white solid ^1H NMR (600MHz, MeOD) δ 0.74-0.79 (m, 3H), 0.83-0.91 (m, 3H), 1.50-1.65 (m, 5H), 2.34-2.38 (m, 2H), 2.39-2.46 (m, 3H), 2.91-2.2.98 (m, 2H), 3.01-3.09 (m, 3H), 3.17-3.27 (m, 2H), 4.18-4.29 (m, 2H), 5.06-5.08 (m,

1H), 7.09-7.10 (m, 1H), 7.18-7.25 (m, 4H), 7.30-7.40 (m, 5H), 7.82-7.84 (m, 1H), 8.27 (s, 1H) ppm. HPLC-MS r_t :15.41, m/z $[\text{M}+\text{H}]^+$: 598.24, $[\text{M}-\text{H}]^+$:596.61

3-(2-(benzylamino)-1-(((S)-1-(1,1-dioxidothiomorpholino)-4-methyl-1-oxopentan-2-

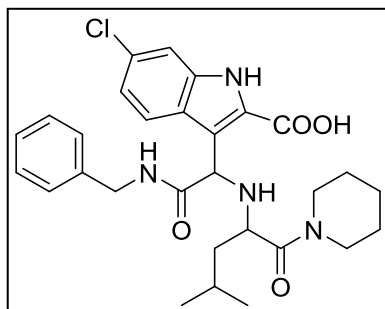


yl)amino)-2-oxoethyl)-6-chloro-1H-indole-2-carboxylic

acid [4.2-4G] ^1H NMR (600MHz, MeOD) δ 0.50-0.49 (d, 3H), 0.77-0.76 (d, 3H), 1.23-1.26 (m, 3H), 3.25-2.23 (m, 1H), 3.63-6.78 (m, 8H), 4.49-4.54 (m 2H), 5.28 (1H, s), 7.01-7.04 (d, 1H, d), 7.29-7.38 (m, 6H), 8.03 (s, 1H), 9.6 (s, 1H) ppm

SFCMS (APCI, m/z): $[M]^+$ calc.:589.18 ; found: 588.43

3-(2-(benzylamino)-1-(((S)-4-methyl-1-oxo-1-(piperidin-1-yl)pentan-2-yl)amino)-2-

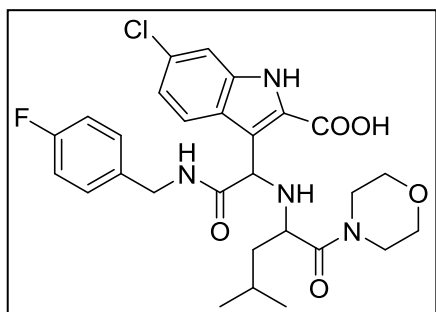


oxoethyl)-6-chloro-1H-indole-2-carboxylic acid [4.2-4I] 93%

as yellow oil ^1H NMR (600MHz, MeOD) δ 0.78-1.80 (m, 3H), 0.88-0.92 (m, 3H), 1.25-1.32 (m, 5H), 1.45-1.50 (m, 2H), 1.56-1.61 (m, 4H), 1.86-1.96 (m, 3H), 2.80-2.94 (m, 2H), 3.47-3.49 (m, 1H), 4.28-4.41 (m, 2H), 4.91 (s, 1H), 5.95 (s, 1H), 7.06-7.09

(m, 2H), 7.15-7.719 (m, 2H), 7.22-7.724 (m, 2H), 7.26-7.29 (m, 1H), 7.36-7.38 (m, 1H), 7.72 (s, 1H) ppm. SFCMS (APCI, m/z): $[M]^+$ calc.:539.23 ; found: 539.32

6-chloro-3-(2-(((4-fluorobenzyl)amino)-1-((4-methyl-1-morpholino-1-oxopentan-2-

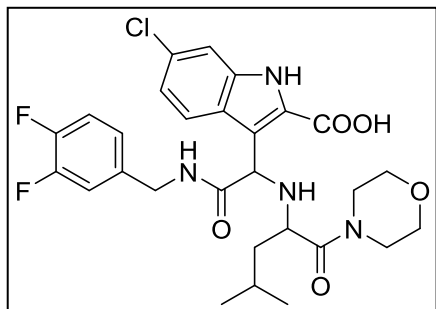


yl)amino)-2-oxoethyl)-1H-indole-2-carboxylic acid [4.2-

4J] 95% as white solid ^1H NMR (600MHz, MeOD) 0.86-0.93 (m, 6H), 1.45-1.49 (m, 3H), 3.27-3.29 (5H), 3.34-3.38 (m, 3H), 4.62-4.79 (m, 2H), 5.33 (s, 1H), 7.07 (s, 1H), 7.23-7.28 (m, 4H), 7.56-7.59 (m, 2H), 8.02 (s, 1H) ppm. HPLC-

MS r_t :15.41, m/z $[M+H]^+$: 558.82, $[M-H]^+$:556.91

6-chloro-3-(2-(((3,4-difluorobenzyl)amino)-1-(((S)-4-methyl-1-morpholino-1-oxopentan-2-

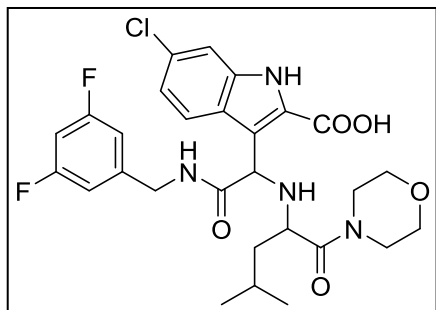


yl)amino)-2-oxoethyl)-1H-indole-2-carboxylic acid [4.2-

4K] 83% as white solid ^1H NMR (600MHz, MeOD) 0.69-0.95 (m, 6H), 1.39-1.47 (m, 1H), 1.85-1.92 (m, 2H), 2.75-2.80 (m, 1H), 3.02-3.09 (m, 1H), 3.42-3.82 (m, 6H), 4.24-4.29 (m, 2H), 5.10 (s, 1H), 6.56-6.59 (m, 1H), 6.80 (s, 1H),

6.87-6.95 (m, 2H), 7.09-7.14 (m, 2H), 7.41-7.56 (m, 2H), 7.86-7.89 (m, 1H) ppm. SFCMS (APCI, m/z): $[M]^+$ calc.:578.20; found: 578.23

6-chloro-3-(2-(((3,5-difluorobenzyl)amino)-1-(((S)-4-methyl-1-morpholino-1-oxopentan-2-



yl)amino)-2-oxoethyl)-1H-indole-2-carboxylic acid [4.2-

2L] 91% as white solid ^1H NMR (600MHz, MeOD) 0.71-0.83 (m, 6H), 1.36-1.41 (m, 1H), 1.84-1.90 (m, 2H), 2.71-2.74 (m, 1H), 2.97-3.08 (m, 2H), 3.53-3.66 (m, 4H), 4.26-4.31 (m, 2H), 5.24 (s, 1H), 6.93 (m, 1H), 7.11-7.19 (m, 2H)

7.43-7.59 (m, 2H), 7.93-7.99 (m, 2H), 8.03 (s, 1H) ppm. SFCMS (APCI, m/z): $[M]^+$ calc.:578.20; found: 578.21

Protein expression, purification (Performed by Holak et al).

Human MDM2 (residues 18-111 or 1-125) was cloned into the pET26 vector and expressed in the *Escherichia coli* BL21(DE3) Rosetta strain (Invitrogen). Cells were grown at 37°C and induced with 1 mM IPTG at an OD_{600nm} of 0.8 and grown for additional 4 h at 37°C. The recombinant protein expressed into inclusion bodies. The inclusion bodies were isolated by centrifugation of the bacterial lysate and washed with PBS containing 0.05% Triton-X100 and subsequently solubilized in 6 M GuHCl in 100 mM Tris-HCl, pH 8.0, including 1 mM EDTA and 10 mM β-mercaptoethanol. The protein was then dialyzed against 4 M GuHCl, pH 3.5, 10 mM β-mercaptoethanol. For renaturation, the protein was diluted (1:100) into 10 mM Tris-HCl, pH 7.0, containing 1 mM EDTA and 10 mM β-mercaptoethanol, by adding the protein in several pulses into the refolding buffer. Refolding was performed overnight at 4°C. Following, ammonium sulphate was added to the final concentration of 1.5 M and after 3 h the sample was mixed with 10 ml of the butyl sepharose 4 Fast Flow (Pharmacia, FRG). The protein was eluted

with 100 mM Tris-HCl, pH 7.2, containing 5 mM β -mercaptoethanol, and further purified on the HiLoad 16/60 Superdex200 gel filtration (Pharmacia) into the buffer containing 5 mM Tris-HCl pH = 8.0, 50 mM NaCl, 10 mM β -mercaptoethanol.

Fluorescence polarization binding assays. (Performed by Holak et al)

All fluorescence experiments were performed as described by Czarna et al.²⁰⁰. Briefly, the fluorescence polarization experiments were read on an Ultra Evolution 384-well plate reader (Tecan) with the 485 nm excitation and 535 nm emission filters. The fluorescence intensities parallel ($Int_{parallel}$) and perpendicular ($Int_{perpendicular}$) to the plane of excitation were measured in black 384-well NBS assay plates (Corning) at room temperature ($\sim 20^{\circ}C$). All fluorescence polarization values were expressed in millipolarization units (mP). The binding affinity of the fluorescent p53-derived peptide of Hu et al.²⁰⁶ towards MDM2 protein was determined in the buffer which contained 50 mM NaCl, 10 mM Tris pH 8.0, 1 mM EDTA, 10% DMSO. Each sample contained 10 nM of the fluorescent P4 peptide and from 0 to 1 μM of MDM2 in a final volume of 50 μl . Next, the competition binding assays were performed using the 10 nM fluorescent P4 peptide, 15 nM MDM2 (75% of the peptide bound), and ligand concentrations ranging from 0 to 100 μM . Plates were read at 30 min after mixing all assay components. Binding constant and inhibition curves were fitted using the SigmaPlot (SPSS Science Software).

AIDA-NMR experiment (Performed by Holak et al)

In this competition experiment, dissociation of MDM2-p53 complex is monitored by 1H NMR spectroscopy and MDM2-antagonist inhibition constant is calculated according to Wang et al. Concentrations used in the assay: 6.3 μM MDM2-p53 complex, 6.8 6.3 μM inhibitor, dissociation constants were assumed to be the same as for the p53 (19-37) peptide used for ITC.

4.3 CO-CRYSTAL AND CELL BASED SCREENING²⁰⁷

Until now, all structurally characterized low-molecular-weight inhibitors of the MDM2-p53 interaction targeted the same “closed” Tyr100 state and were incapable of reaching the N-terminal “lid” segment.^{208-210]} Here we present X-ray structures of two MDM2 complexes that reveal inhibitor molecules bound to the “open” Tyr100 conformation leading to a novel four point pharmacophore model for this pharmacologically important protein-protein interaction. Compound **4.3-1** was found to inhibit the MDM2-p53 interaction with $K_i = 1200$ nM. Crystals of **4.3-1**-MDM2 complex revealed two inhibitor molecules bound to a single protein chain (**Figure 4.2**). The overall fold of MDM2 in complex with **4.3-1** was similar to the native MDM2-p53 structure with the main-chain RMSD of 0.69 Å. The Trp23 pocket of MDM2 is filled with the 6-chloroindole-2-hydroxamic acid, similar to the native Trp23 of p53, forming extensive hydrophobic interactions with Val93, Gly58 and Leu54. The central, peptidic core of the compound was solvent-exposed and did not directly contact the protein, providing the possibility for modifications to improve the drug-likeness. We found that the isobutyl element filled the Phe19 pocket and the benzyl moiety was bound within the Leu26 pocket in spite of structural resemblance between the benzyl and isobutyl substituents of **4.3-1** to the p53 amino acids Phe19 and Leu26, respectively. This represents a mirror image of the native p53 interaction with the indole moiety as a plane of symmetry and is analogous to arrangement already described for a spiro-oxindole inhibitor.²⁰⁵ The isobutyl side chain loosely occupied the Phe19 pocket forming hydrophobic contacts to Ile61, Val93 and Gly58. Binding of the benzyl group to the Leu26 pocket was substantially different from the majority of known inhibitors. Owing to the length and flexibility of the scaffold, this part of the inhibitor binds close to helix IV of MDM2 and was

involved in a parallel aromatic stacking with His96, with 3.7 Å spacing between the rings. Similar π -stacking contacts were observed in a spirocyclic indolone, α -aminoacylamide,²⁰⁵ chromenotriazolopyrimidine,⁵⁷ but not in the structures of an imidazoline nutlin and benzodiazepinedione.^{44,211}

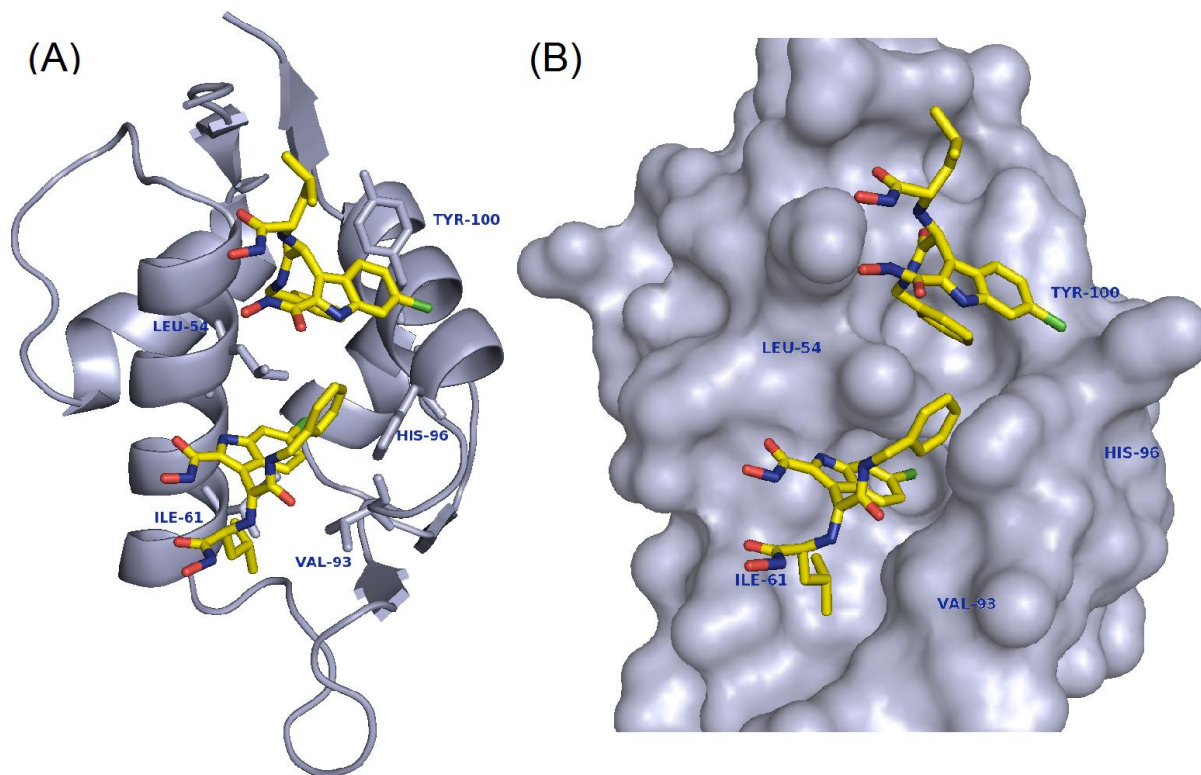


Figure 4.2 Crystallographic structure of 4.3-1 in complex with MDM2. (A) Key residues of MDM2 in proximity of the two inhibitor molecules are highlighted. (B) The extended Leu26 pocket is filled with benzyl rings of two inhibitor molecules.

While the binding mode of the first inhibitor was similar to other known antagonists, the presence of the second inhibitor molecule was a surprise. Strikingly, the benzyl group of the second inhibitor molecule is deeply inserted inside MDM2 occupying a double-sized Leu26 subpocket enlarged by rearrangement of the Tyr100 side chain. The three point pharmacophore model previously used was altered to add a fourth hydrophobic point where the new extended Leu26 subpocket sits. This process yielded a classic Ugi4-component reaction product **4.3-2** with

a K_i of 600nM. The co-crystal structure of **4.3-2** with MDM2 confirmed that the compound exhibited the four point pharmacophore model predicted. (**Figure 4.3**)

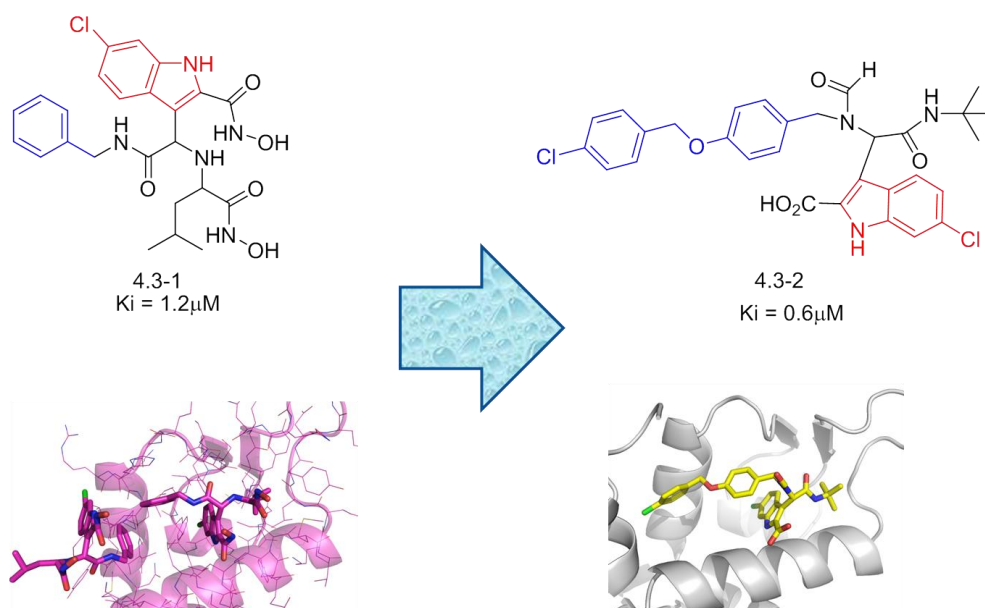


Figure 4.3 Compound 4.3-1 showing two molecules binding to MDM2 opening a never before described pocket led to the discovery of compound 4.3-2; one molecule opening the pocket further

The Phe19 subpocket is occupied by a tert-butyl group and makes van der Waals contacts with Ile61 and Val93 (analogous to those maintained by **4.3-1**). As anticipated, the large 4-chlorobenzyl phenyl ether was found to fill the enlarged Leu26 subpocket. The group forms an extended network of van der Waals contacts with Val93, Leu54, His96 and the Tyr100. The aryl-imidazole π -stacking interaction with His96 is not seen any more in the X-ray lattice due to the shift of the mid phenyl ring by ca. 2.3 Å toward the center of the pocket. The His96 side chain does, however, keep electrostatic contacts with the internal aryl group and the methyleneoxy linker fragment. The position of the terminal, 4-chlorophenyl ring partially overlaps with the phenyl ring of the second **4.3-1** molecule. (**Figure 4.4**)

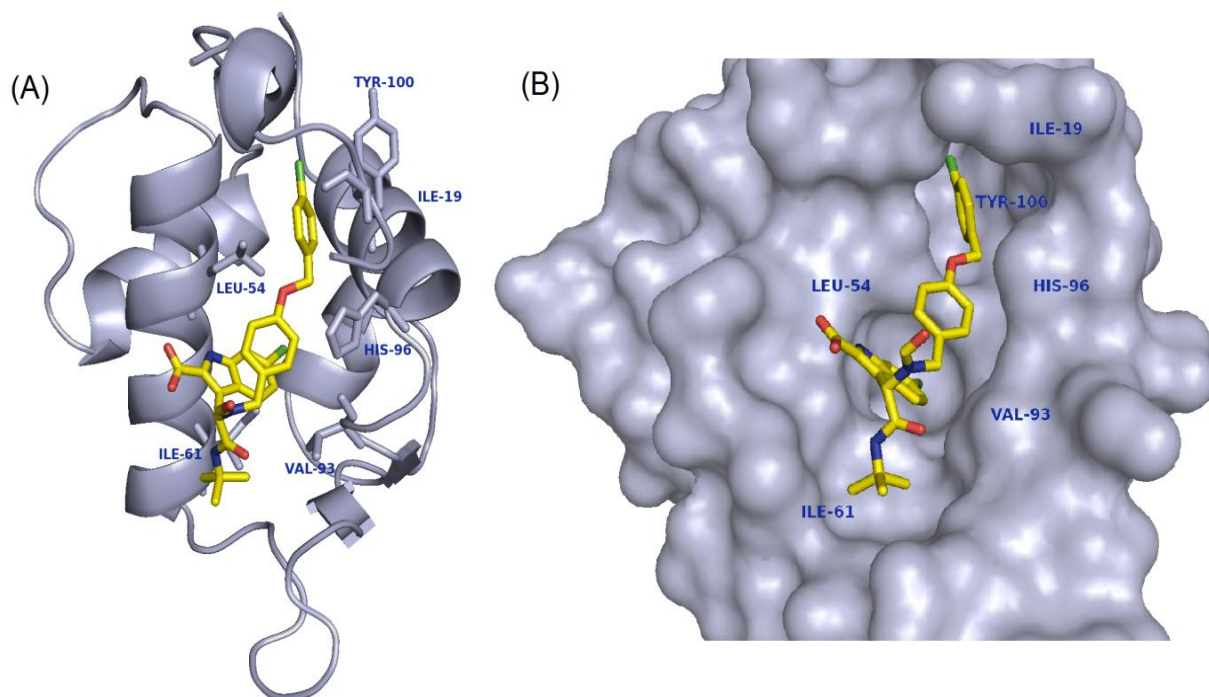
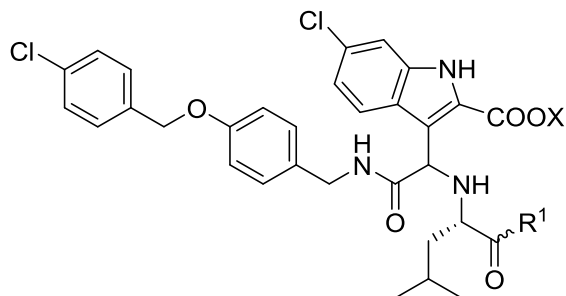


Figure 4.4 Crystallographic structure of 4.3-2 in complex with MDM2. (A) Key residues of MDM2 around the inhibitor are highlighted. (B) The 4-chlorobenzyl phenyl ether fills the hydrophobic cavity formed by an extended L26 pocket and the hydrophobic surface of the N-terminal “lid” helix.

This data encouraged us to attempt to access this pocket with the Ugi4C5CR product. Compounds **4.3-3** were synthesized and fortunately **4.3-3C** and **4.3-3E** showed low micromolar activity. In addition, compound **4.3-3C** showed slight MDMX activity as well ($K_i = 5.41 \mu\text{M}$). As a dual MDM2/MDMX inhibitor would be of great use, both of these scaffolds (Ugi4Component, and the Ugi4C5CR) will be elaborated in the future to try to enhance the MDMX activity while maintaining low micromolar to nanomolar activity against MDM2.



Entry	R ¹	X	MDM2 Ki (μM)	MDMX Ki (μM)
4.3-3A		Et	NI	NI
4.3-3B		H	0.40	5.41

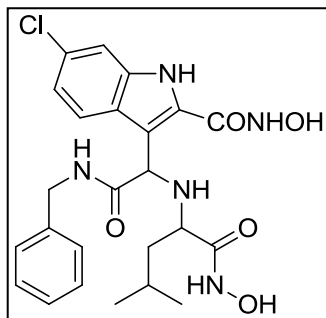
Table 4-4 Use of an extended isocyanide allowed for us to probe the newly discovered MDM2 pocket with the Ugi4C5CR scaffold. In addition to seeing MDM2 activity one compound even showed slight activity against MDMX

4.3.1 Materials and Methods

Procedure for compound 4.3-1

To 1 equivalent of Ugi product 10 equivalents of H₂NOH HCl, 10 equivalents of NaOH, and 3 equivalents of Et₃N, were added and let stir overnight at RT. Product precipitated out as a white solid

3-(2-(benzylamino)-1-((1-(hydroxyamino)-4-methyl-1-oxopentan-2-yl)amino)-2-oxoethyl)-6-



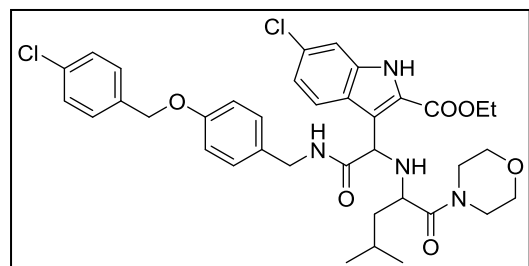
chloro-N-hydroxy-1H-indole-2-carboxamide [4.3-1] 18% Yield as

white solid. ^1H NMR (600MHz, MeOD) δ 0.54-0.53 (d, 3H), 0.57-0.56 (d, 3H), 0.67-0.66 (d, 1H), 0.85-0.84 (d, 3H), 0.93-0.90 (m, 2H), 0.98-0.96 (m, 4H), 2.02 (s, 2H), 3.09-3.07 (t, 1H), 3.69-3.68 (d, 1H), 4.13-4.09 (m, 2H), 4.33-4.28 (m, 2H), 4.37-4.35 (m, 3H), 4.46-4.43

(d, 1H), 5.32 (s, 1H), 7.01-6.98 (m, 2H), 7.34-7.31 (s, 2H), 7.46-7.45 (s, 2H), 7.51 (s, 1H), 7.81-7.73 (m, 2H); ^{13}C NMR (600MHz, MeOD) δ 6.5, 7.0, 7.8, 13.1, 19.5, 20.6, 20.7, 20.9, 21.6, 21.8, 22.0, 22.1, 24.2, 24.3, 24.4, 41.1, 41.9, 42.1, 42.5, 42.5, 42.6, 42.7, 42.9, 43.0, 51.0, 52.0, 54.5, 54.7, 55.7, 55.9, 56.2, 56.7, 57.6, 58.6, 60.1, 111.3, 111.6, 119.6, 119.8, 120.7, 121.0, 121.6, 122.0, 126.0, 126.5, 126.6, 126.7, 126.8, 126.8, 127.1, 127.4, 128.0, 128.0, 128.0, 128.2, 128.6, 128.7, 128.8, 129.0, 129.9, 133.2, 133.3, 135.6, 136.1, 138.4, 138.5, 140.2, 167.4, 167.5 ppm.

HPLC-MS r_t :17.29, m/z $[\text{M}+\text{H}]^+$: 502.31, $[\text{M}-\text{H}]^+$:500.34

Ethyl 6-chloro-3-(2-(((4-((4-chlorobenzyl)oxy)benzyl)amino)-1-(((S)-4-methyl-1-morpholino-



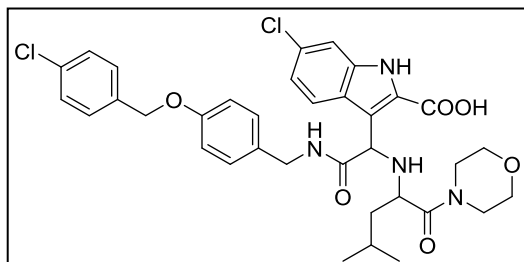
1-oxopentan-2-yl)amino)-2-oxoethyl)-1H-indole-2-carboxylate [4.2-3A] 21% as yellow solid ^1H NMR

(600MHz, CDCl_3) δ 0.43-4.48 (m, 3H), 0.77-0.80 (m, 3H), 1.04-1.10 (m, 1H), 1.28-1.42 (m, 5H), 2.84-2.96

(m, 2H), 3.39-3.41 (m, 2H), 3.51-3.57 (m, 6H), 4.23-4.26 (m, 2H), 4.41-4.46 (dd, 1H), 4.59-4.64 (dd, 1H), 5.07 (s, 2H), 5.46 (s, 1H), 6.87-6.99 (m, 4H), 7.26-7.49 (m, 7H), 8.01 (s, 1H), 9.98 (s, 1H); ^{13}C NMR (150MHz, CDCl_3) δ 14.2, 21.2, 23.4, 24.6, 29.7, 42.2, 42.6, 42.9, 45.0, 53.4, 55.8, 61.1, 66.1, 66.8, 69.3, 112.2, 115.0, 119.3, 121.1, 122.1, 124.6, 125.8, 128.7, 129.3, 131.1,

133.8, 135.5, 136.3, 157.9, 161.1, 172.3, 173.2 ppm. SFCMS (APCI, m/z): $[M]^+$ calc.709.25;;
found: 709.19

6-chloro-3-(2-((4-(4-chlorophenethyl)benzyl)amino)-1-(((S)-4-methyl-1-morpholino-1-



oxopentan-2-yl)amino)-2-oxoethyl)-1H-indole-2-
carboxylic acid [4.3-3B] ^1H NMR (600MHz, CDCl_3)

δ 0.76-0.89 (m, 6H), 1.06-1.12 (m, 1H), 1.24-1.28 (m, 3H), 1.42-4.45 (m, 1H), 1.88-1.89 (m, 1H), 2.97-2.99

(m, 1H), 3.36-3.38 (mm, 1H), 3.55-3.80 (m, 4H), 4.21-4.25 (m, 2H), 4.85 (s, 2H), 5.01 (s, 1H),
6.18 (s, 1H) 6.74-6.76 (m, 1H), 6.97-6.98 (m, 1H), 7.14-7.16 (m, 1H), 7.26-7.41 (m, 4H), 7.70 (s,
1H) ^{13}C NMR (150MHz, CDCl_3) δ 14.2, 21.6, 23.2, 23.4, 24.1, 29.7, 40.8, 42.7, 43.3, 45.5, 52.6,
55.2, 60.4, 65.8, 66.6, 69.1, 69.2, 112.1, 113.7, 115.0, 122.5, 125.9, 128.6, 131.2, 131.8, 133.6,
135.3, 136.1, 157.8, 164.8, 167.4, 168.4, 174.8 ppm. SFCMS (APCI, m/z): $[M]^+$ calc.682.61;;
found: 682.20

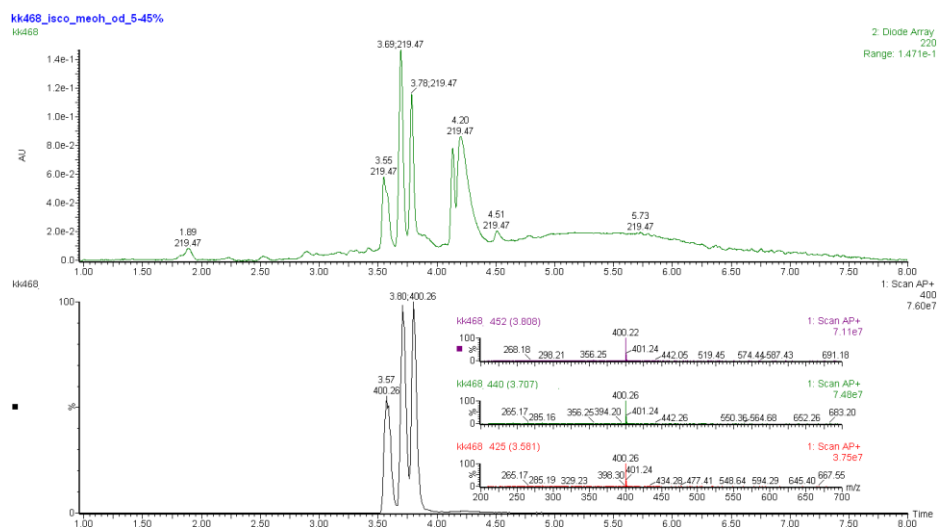
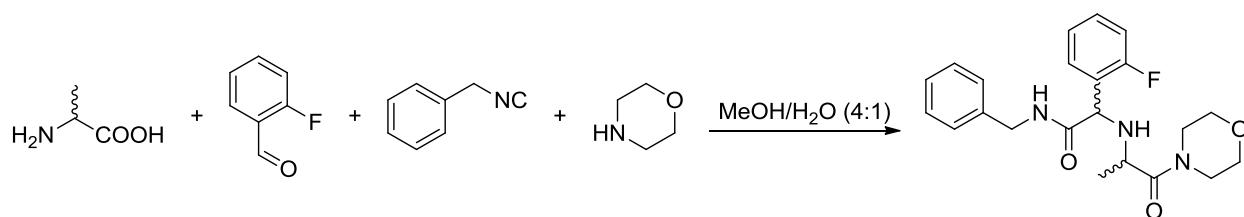
5.0 CONCLUSIONS AND FUTURE WORK

We have introduced ANCHOR.QUERY a novel web-based tool to aid in efforts to find compounds to inhibit protein-protein interactions. The screening library introduced in ANCHOR.QUERY is unique in that it focuses on known multicomponent reactions enriched with various anchor residues. In addition, we have introduced scaffolds explored by our lab into the ANCHOR.QUERY screening library and one such compound showed inhibition of protein-protein interaction p53/MDM2. Exploration of this scaffold led not only to potent inhibitors but also to the co-crystallization of our small molecule with MDM2 to show a newly described binding pocket.

From NMR studies on MDM2 fragments bound to N-terminal p53 peptides, it was suggested that MDM2 is conformationally flexible, and subject to allosteric regulation upon substrate binding.²¹² The structure of the free MDM2 N-terminal domain reveals that the more open conformation of the binding cleft of MDM2 observed in structures of complexes with small molecules and peptides is a more suitable one for ligand discovery and optimization._{ENREF_206} This pocket led us to a new four point pharmacophore screen which allowed us to develop extended inhibitors, one of which showed slight inhibition to MDMX.

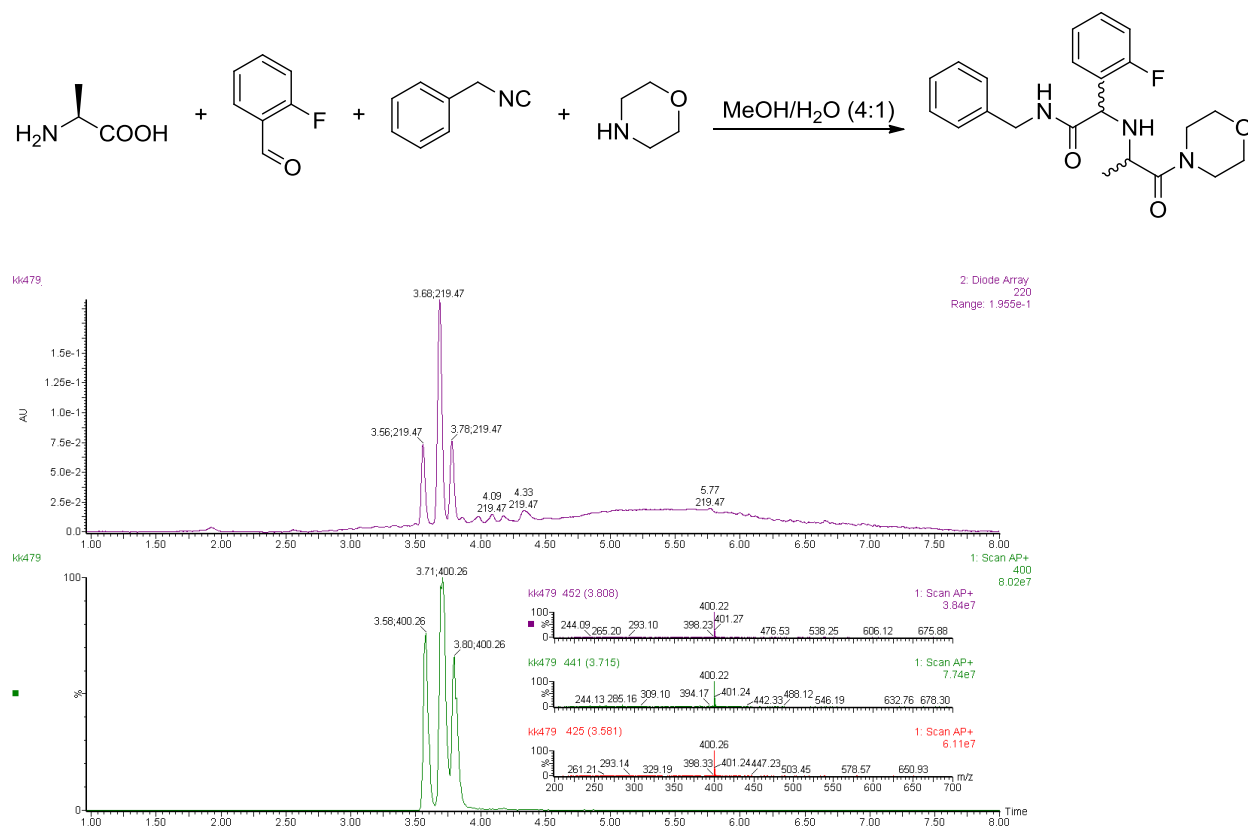
APPENDIX A

CHIRAL SEPARATION OF UGI4C5CR

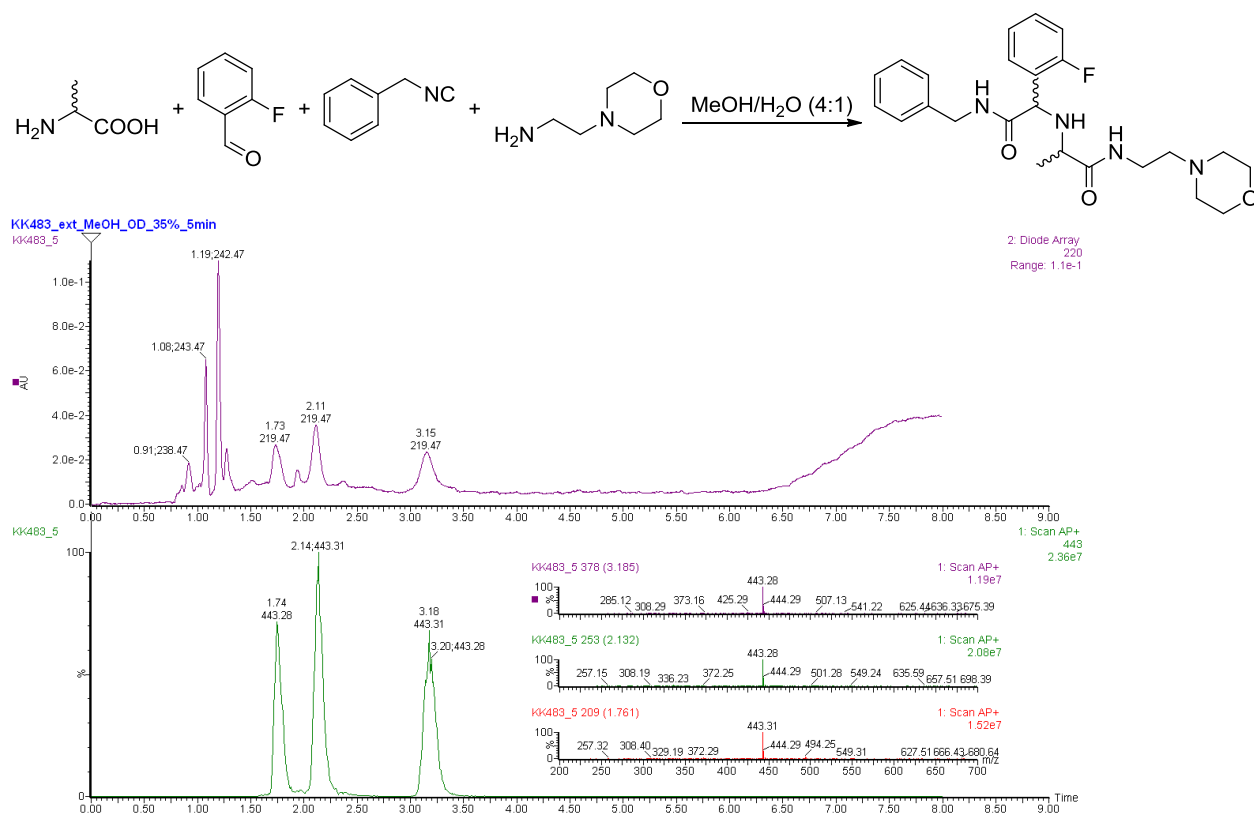


Appendix A Figure 1: As a control D,L-Ala was used with 2-fluorobenzaldehyde, benzyl isocyanide, and morpholine; 3 of the 4 stereoisomers could be separated in the SFC trace, 2 of the enantiomers elute together. Solvent: CO₂ + 5-45 % MeOH over 5.5 min on Regis Cell OD column on Waters Supercritical Fluid Chromatograph. (Top - UV trace at 220λ, Bottom - TIC of

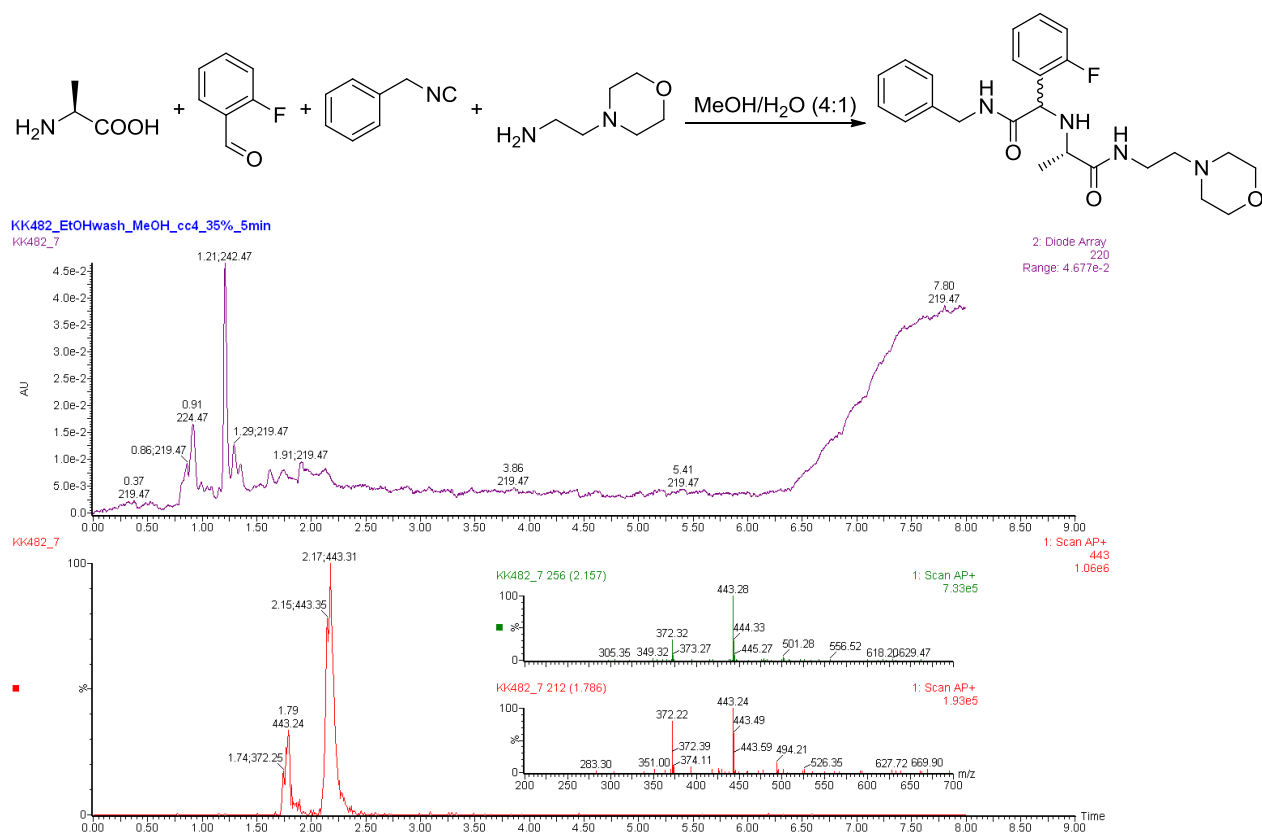
AP+ scan with mass 399.50 - 400.50 extracted, mass spectra of peaks at time 3.808, 3.707, and 3.581 shown to the right of the peaks)



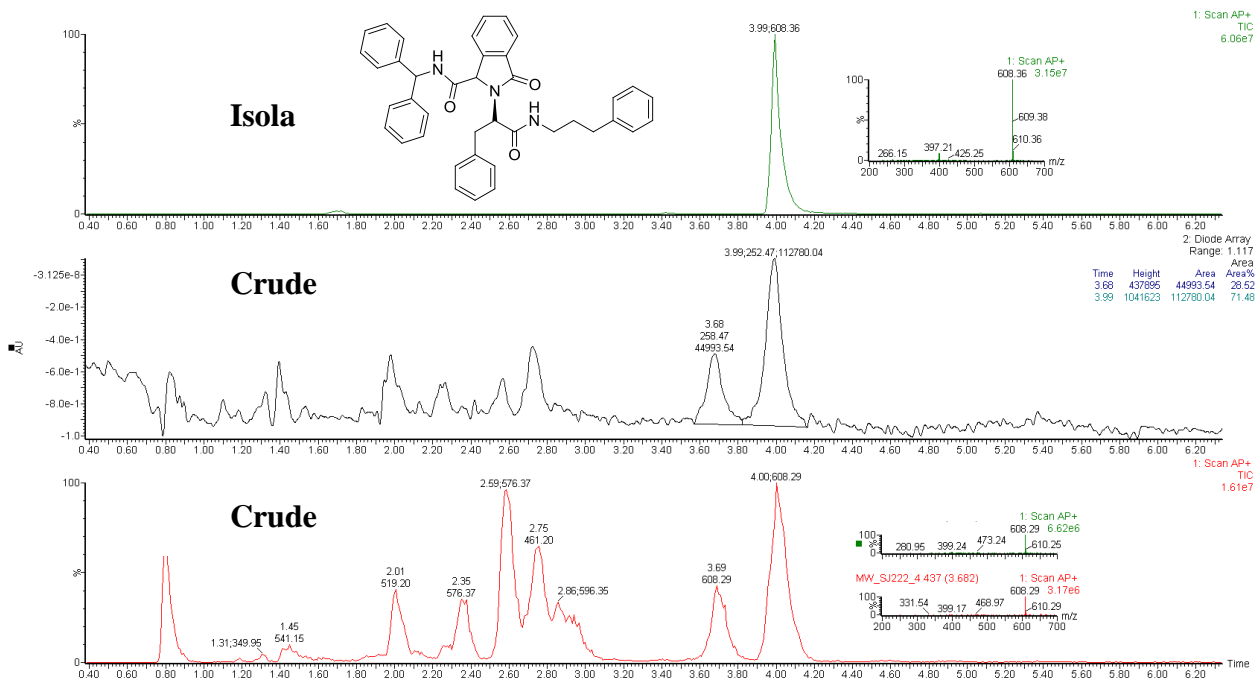
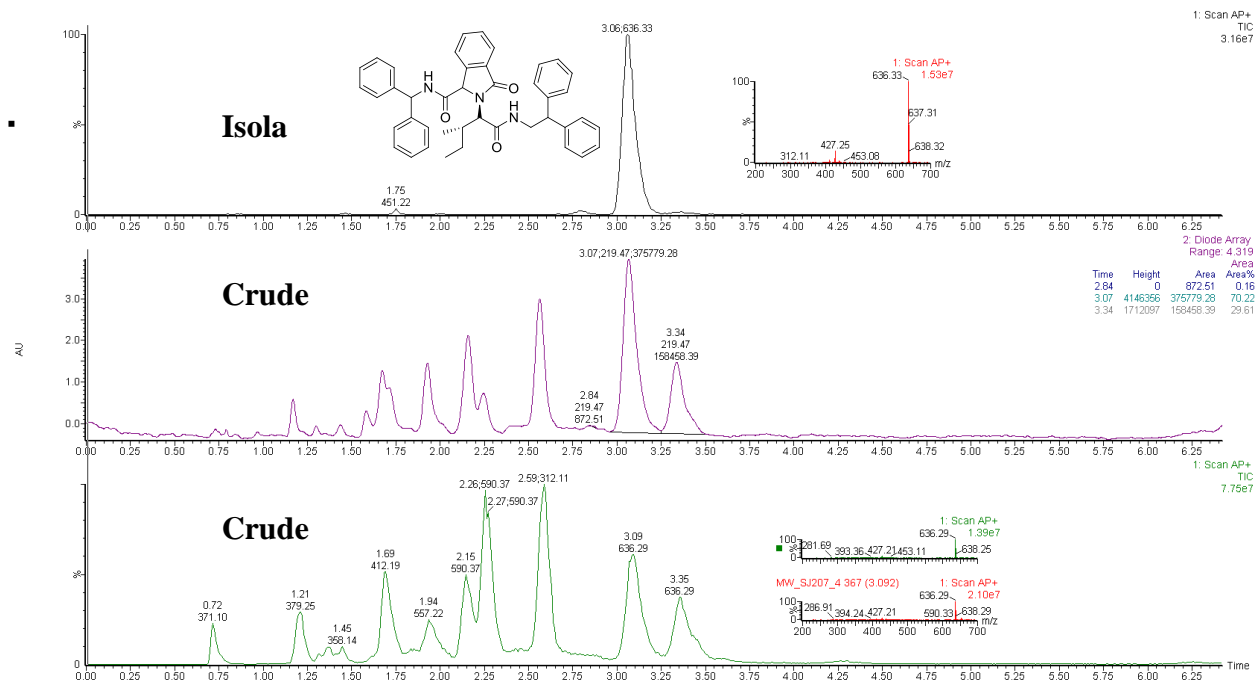
Appendix A Figure 2: When L-Ala was used with 2-fluorobenzaldehyde, benzyl isocyanide, and morpholine, a similar SFC trace could be seen, thereby showing that morpholine caused a racemization of the amino acid stereocenter, most likely due to the higher basicity of the secondary amine. Solvent: CO₂ + 5-45% MeOH over 5.5 min on Regis Cell OD column on Waters Supercritical Fluid Chromatograph. (Top - UV trace at 220λ, Bottom - TIC of AP+ scan with mass 399.50 - 400.50 extracted, mass spectra of peaks at time 3.808, 3.715, and 3.581 shown to the right of the peaks)

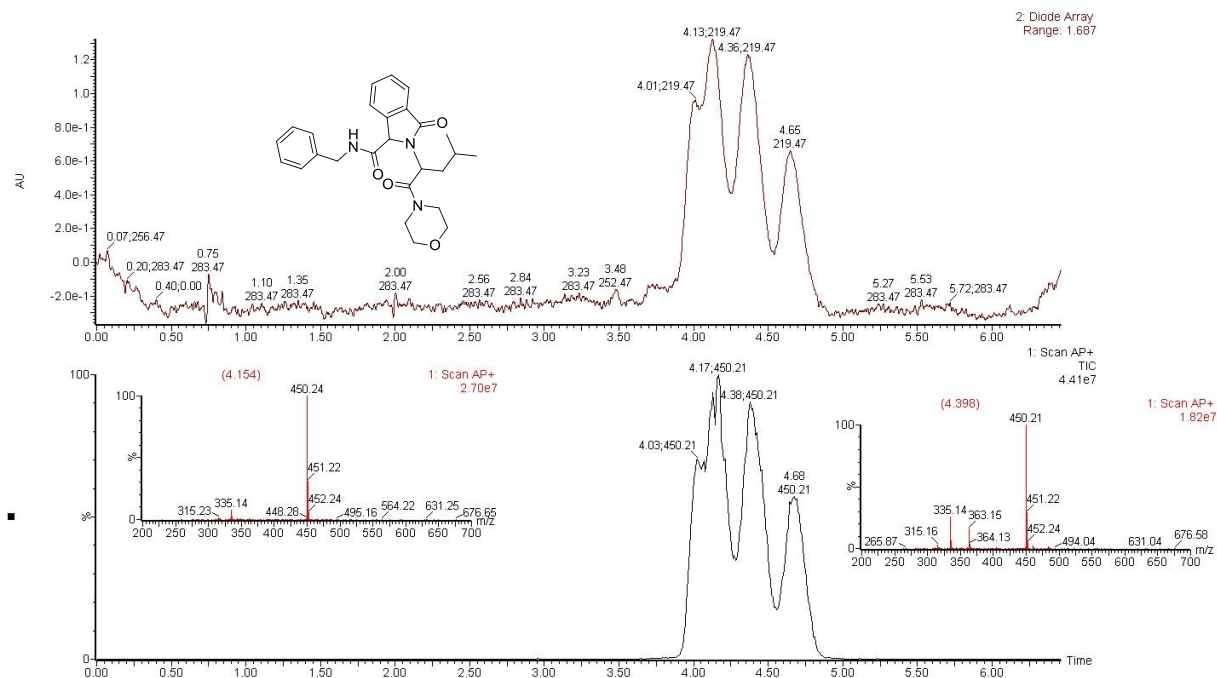


Appendix A Figure 3: As a control D,L-Ala was used with 2-fluorobenzaldehyde, benzyl isocyanide, and 2-morpholinoethanamine; 3 of the 4 stereoisomers could be separated in the SFC trace, most likely 2 of the enantiomers were eluting together. Solvent: CO₂ + 5-45% MeOH over 5.5 min on Regis Cell OD column on Waters Supercritical Fluid Chromatograph. (Top - UV trace at 220 λ , Bottom - TIC of AP+ scan with mass 442.50 - 443.50 extracted, mass spectra of peaks at time 3.185, 2.132, and 1.761 shown to the right of the peaks)



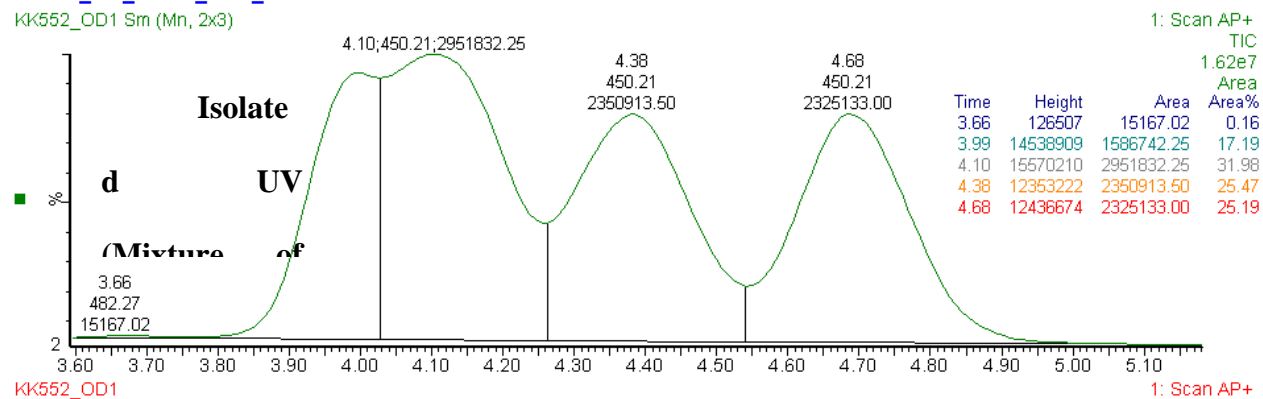
Appendix A Figure 4: When L-Ala was used with 2-fluorobenzaldehyde, benzyl isocyanide, and 2-morpholinoethanamine, only two of the 4 enantiomers were seen. Thereby showing that primary amines do not cause racemization of the amino acid stereocenter. Solvent: CO₂ + 5-45% MeOH over 5.5 min on Regis Cell OD column on Waters Supercritical Fluid Chromatograph. (Top - UV trace at 220λ, Bottom - TIC of AP+ scan with mass 442.50 - 443.50 extracted, mass spectra of peaks at time 2.157, and 1.786 shown to the right of the peaks)



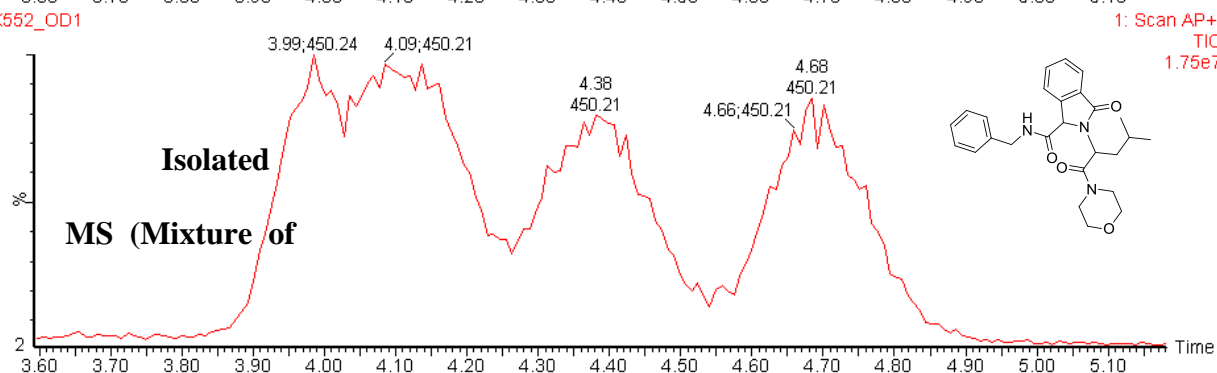


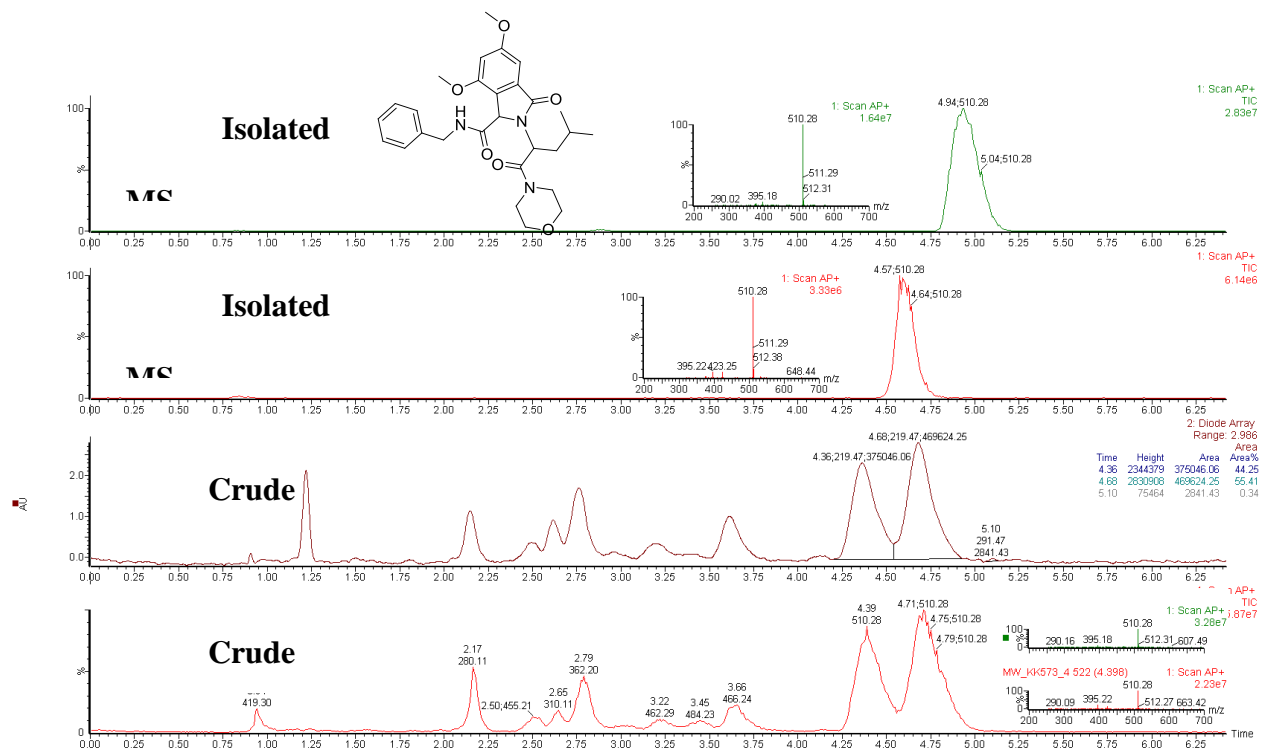
KK552_OD_MeOH_10%_5min

KK552_OD1 Sm (Mn, 2x3)



KK552_OD1

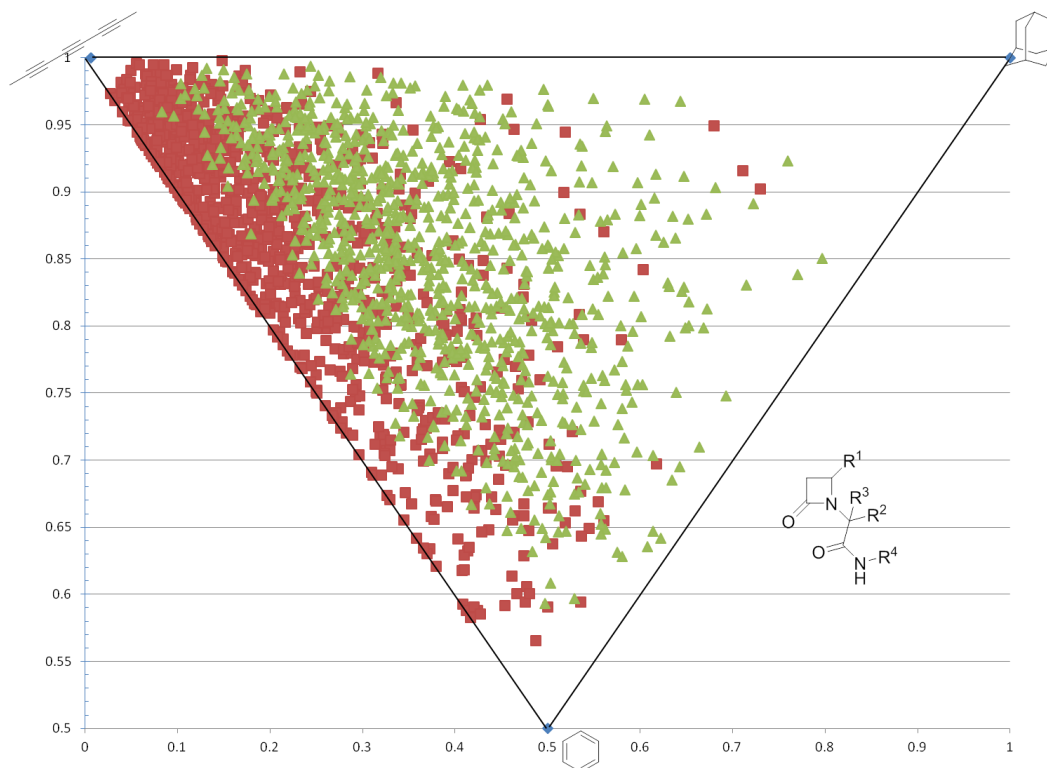


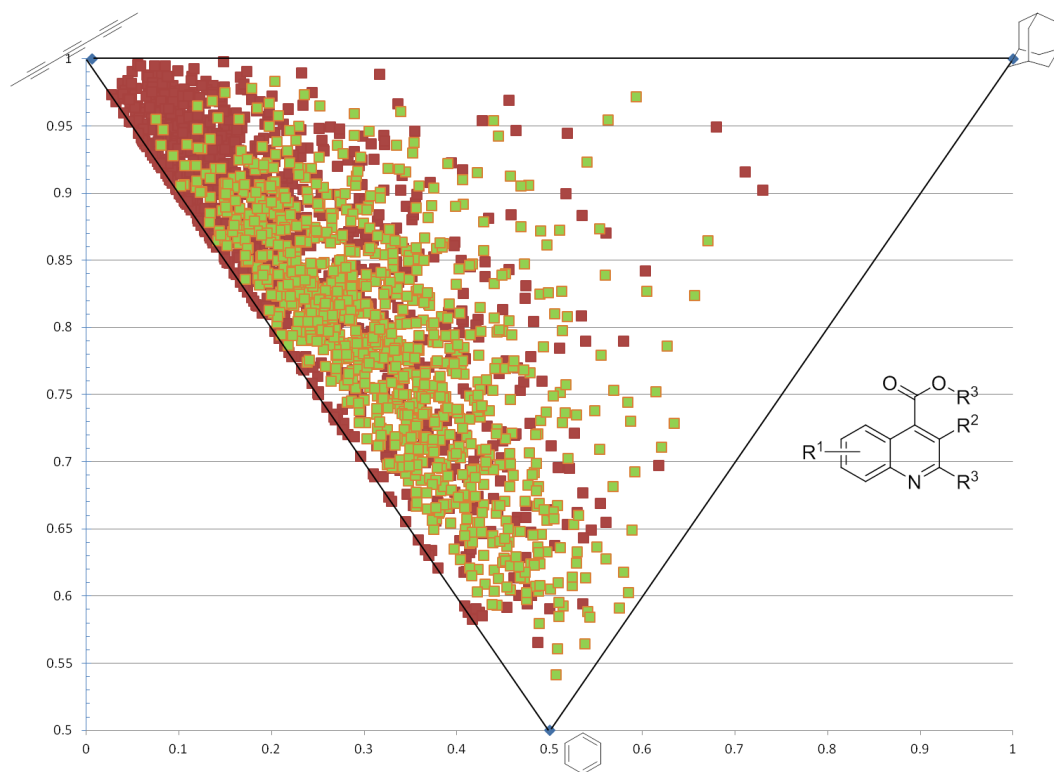
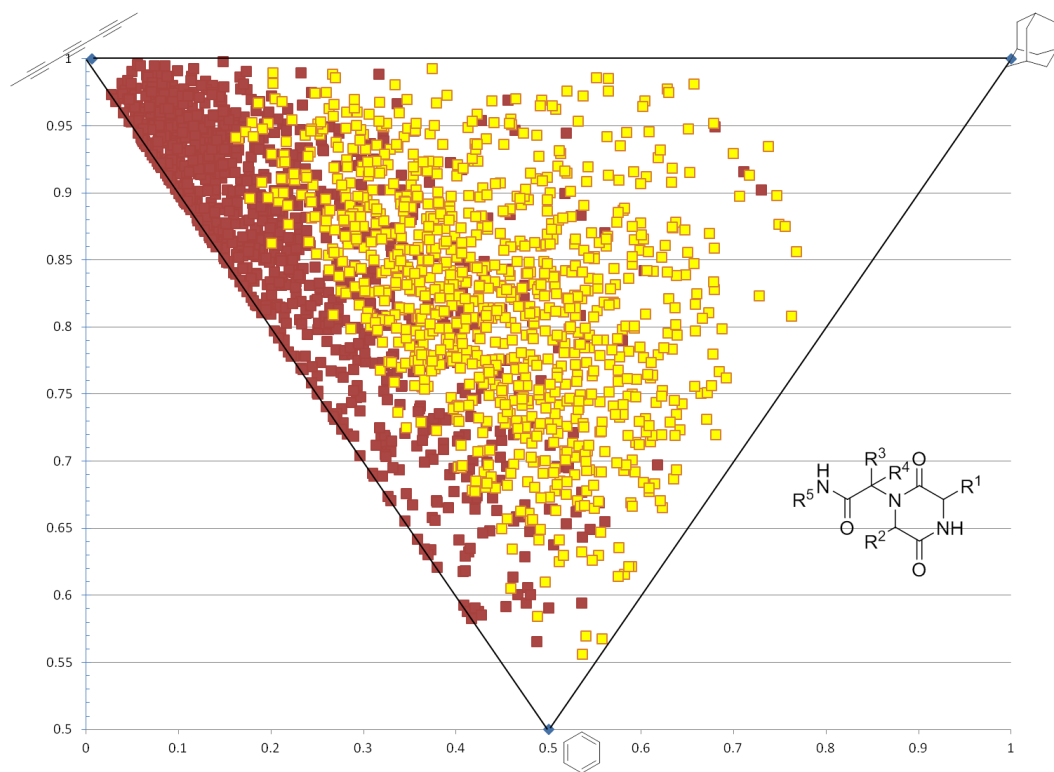


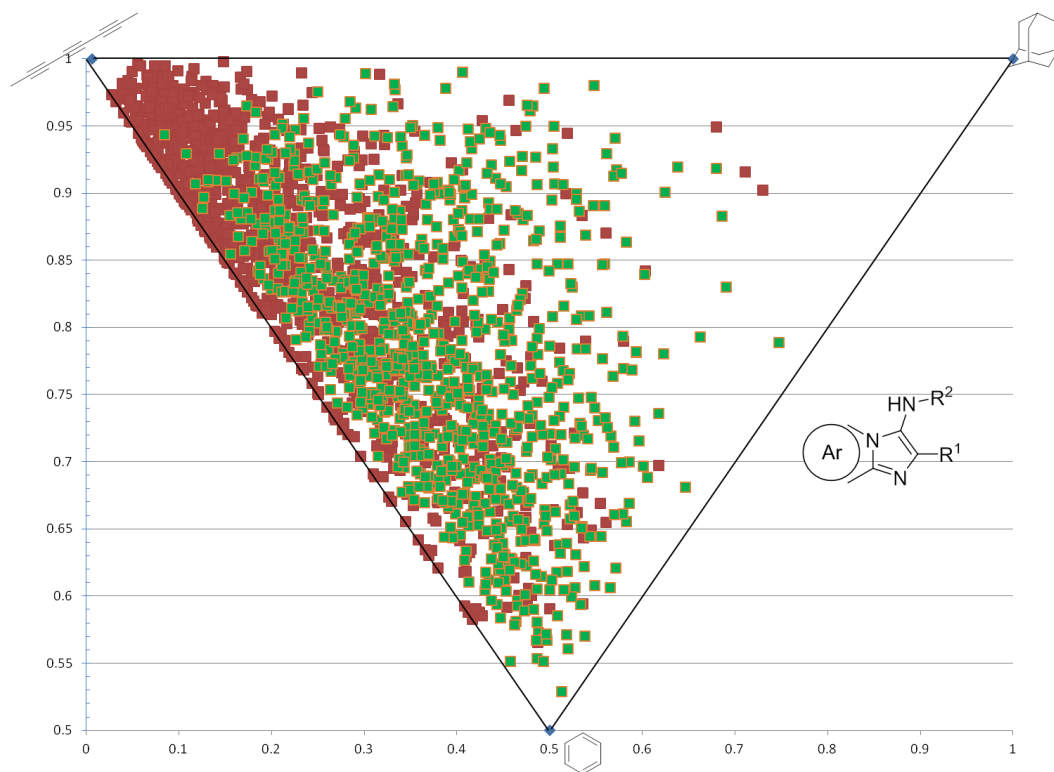
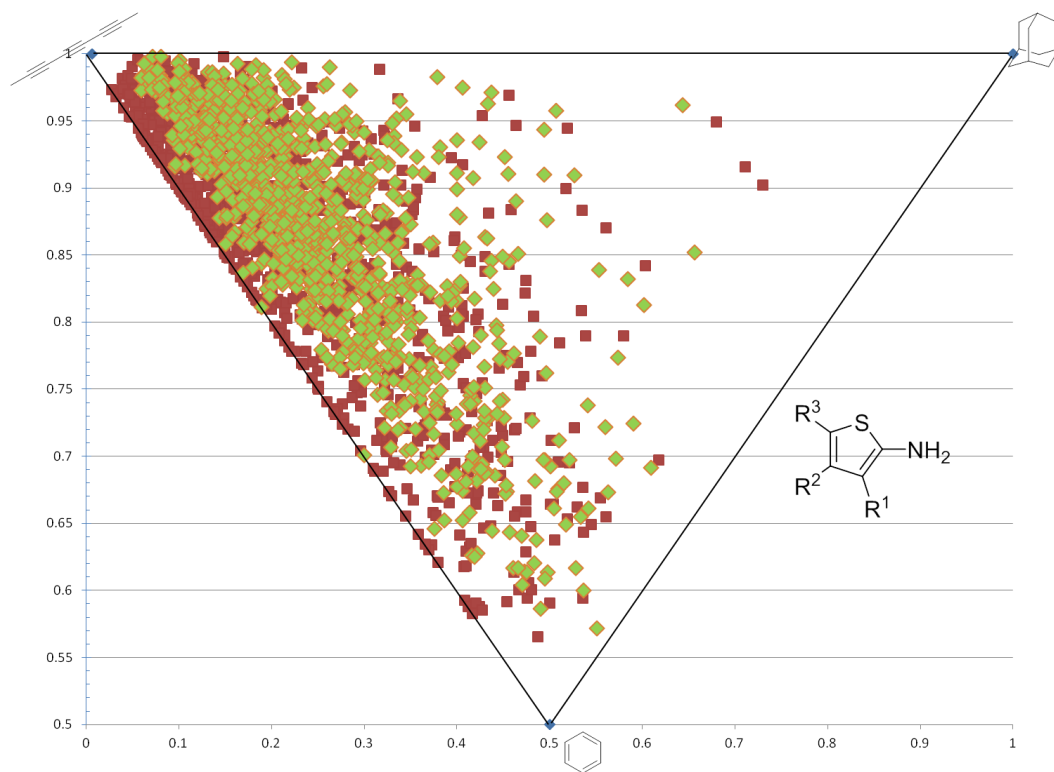
APPENDIX B

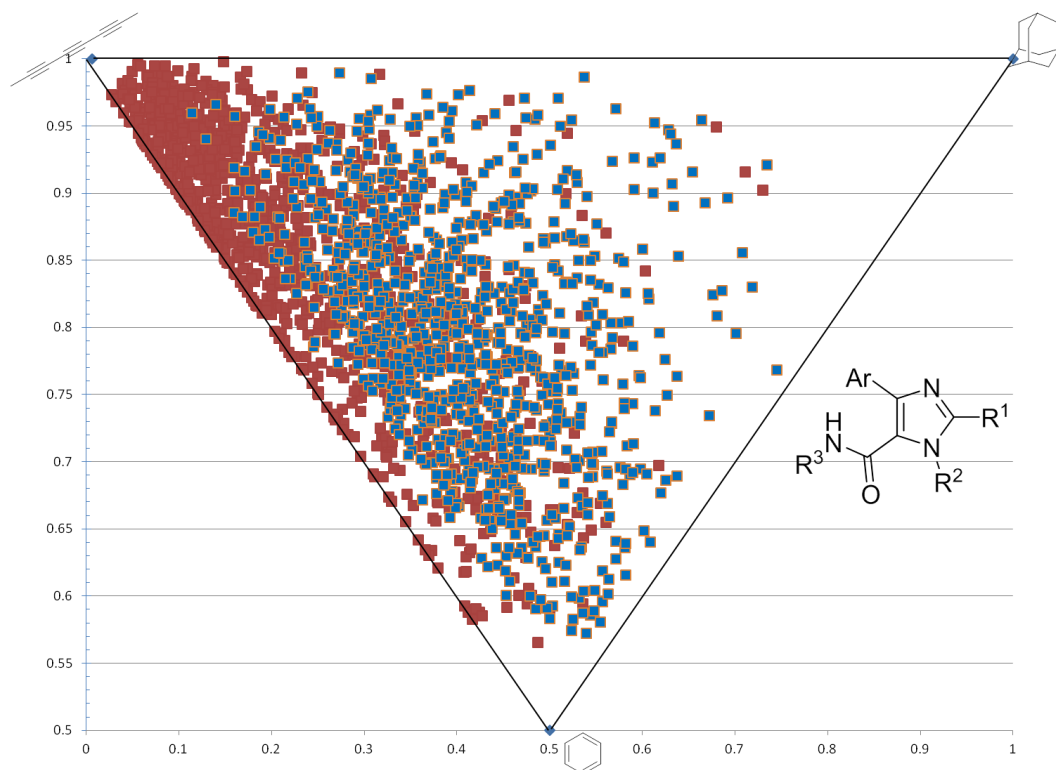
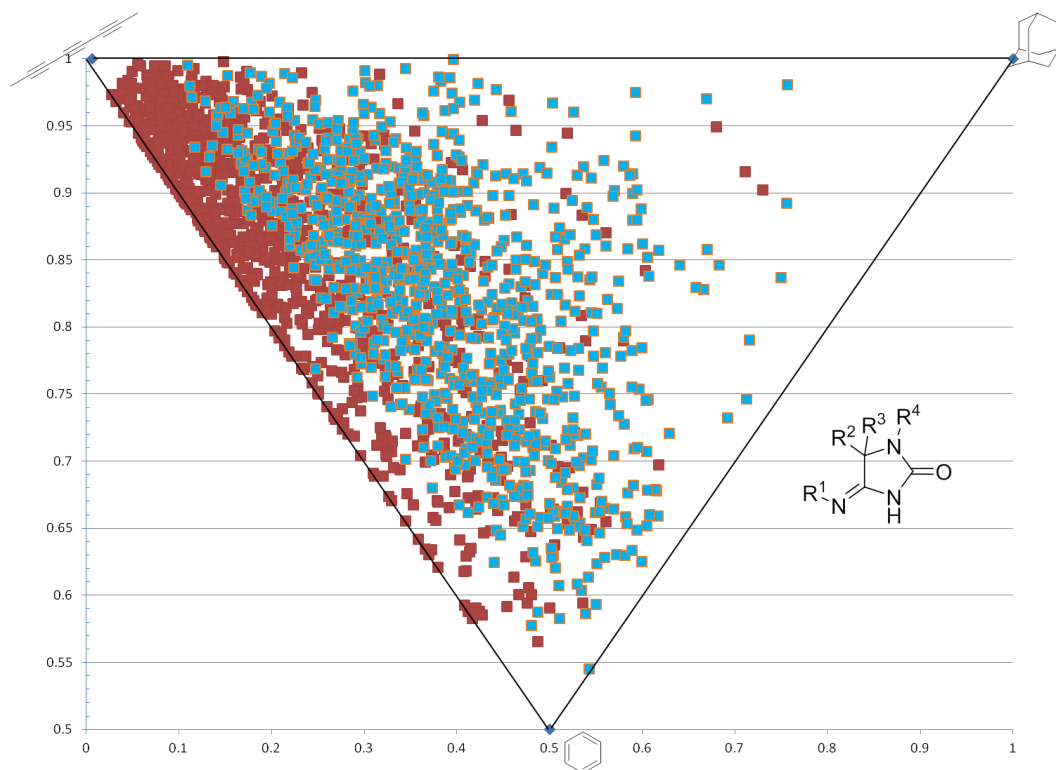
PRINCIPLE MOMENT OF INERTIA

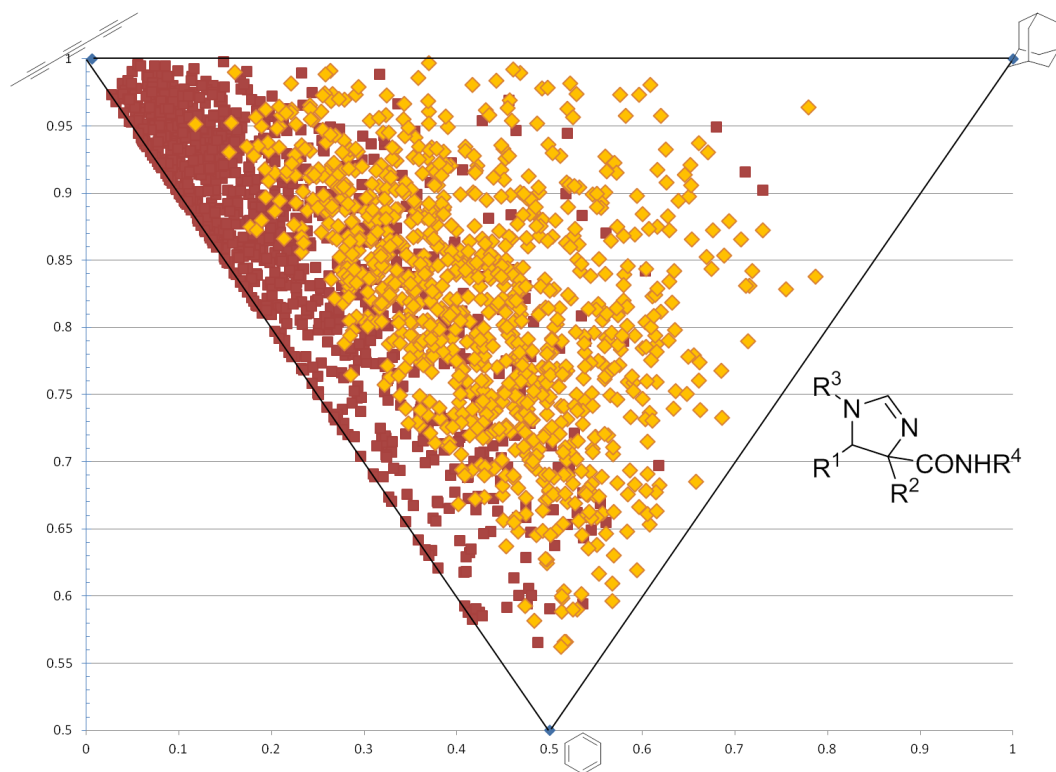
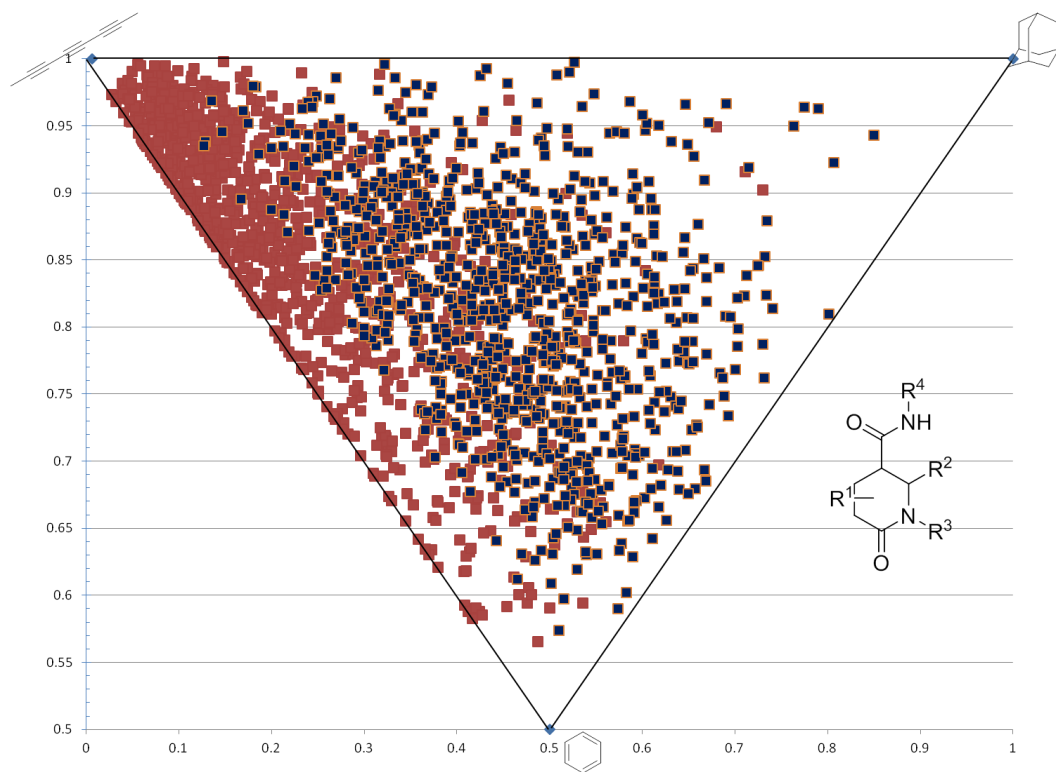
Principal moment of inertia for 1000 randomly selected compounds from the each scaffold reactions plotted against 1000 randomly selected compounds from the Zinc database (red squares).

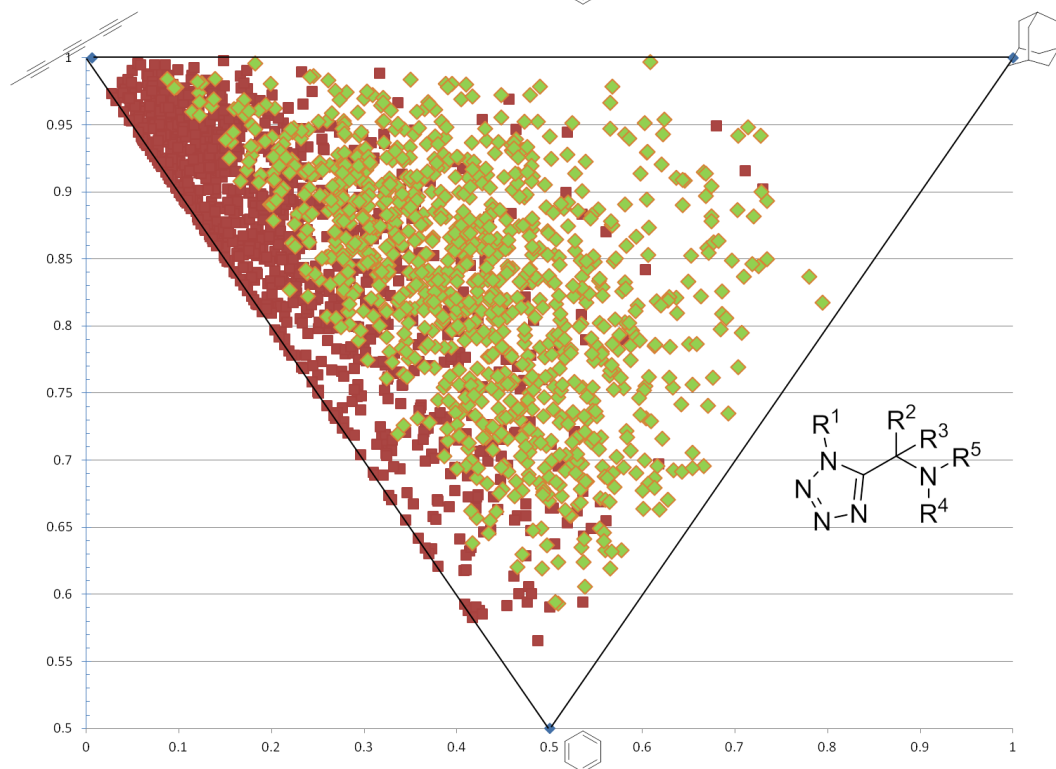
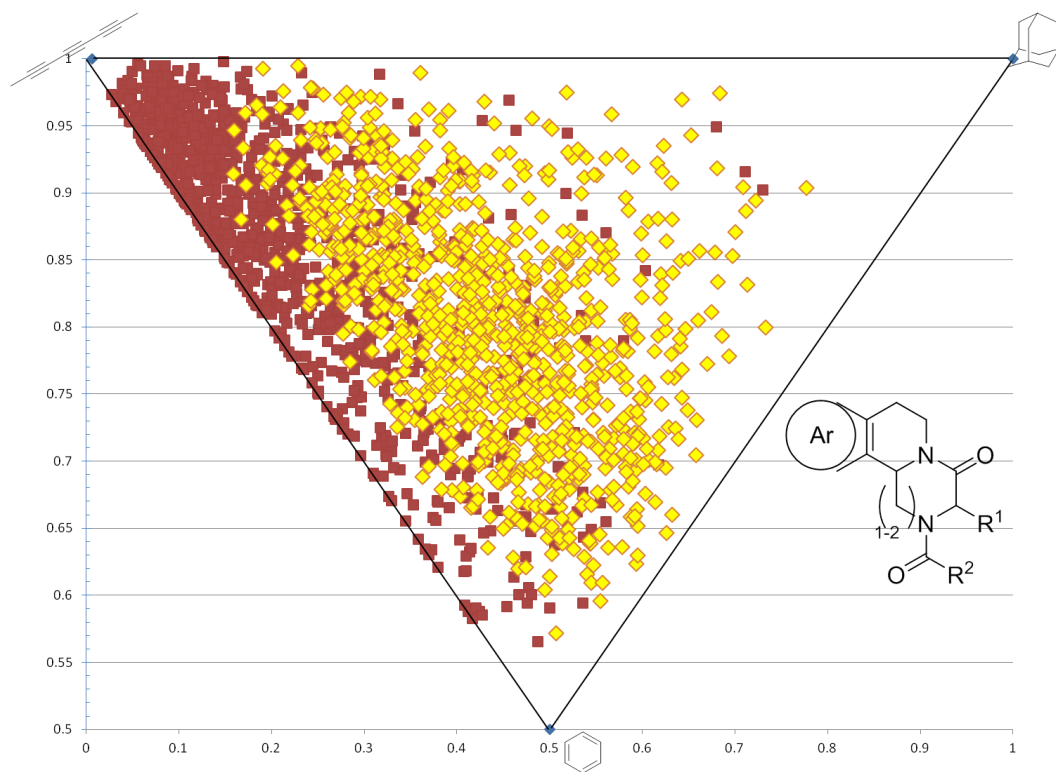


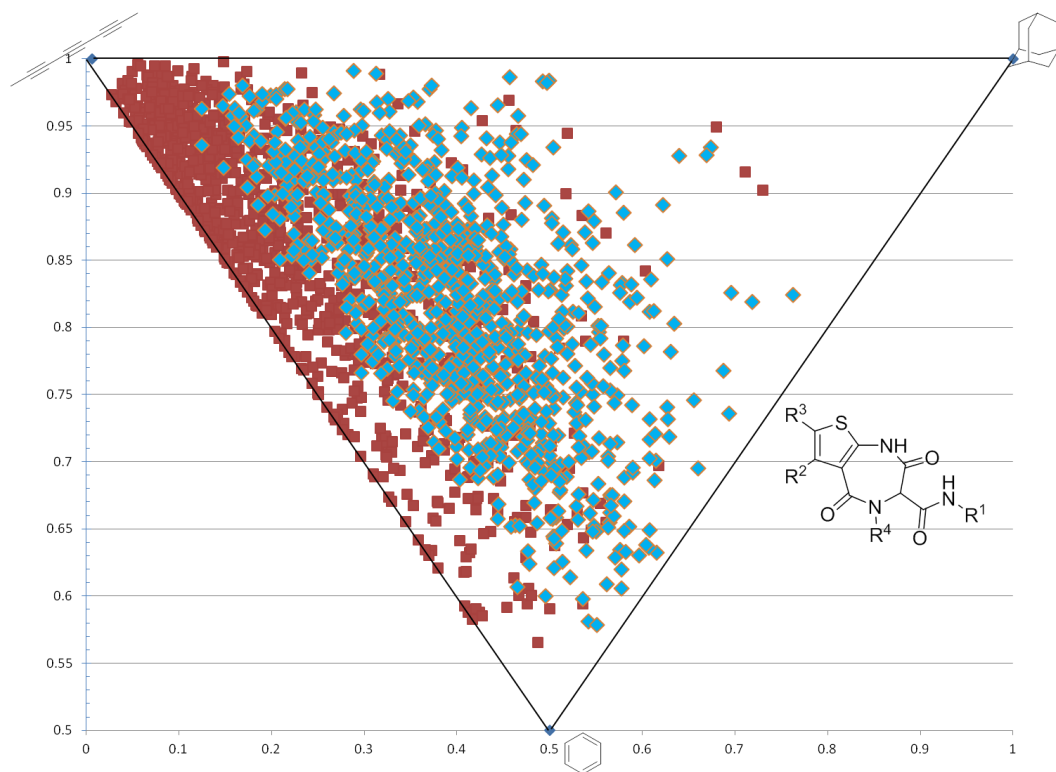
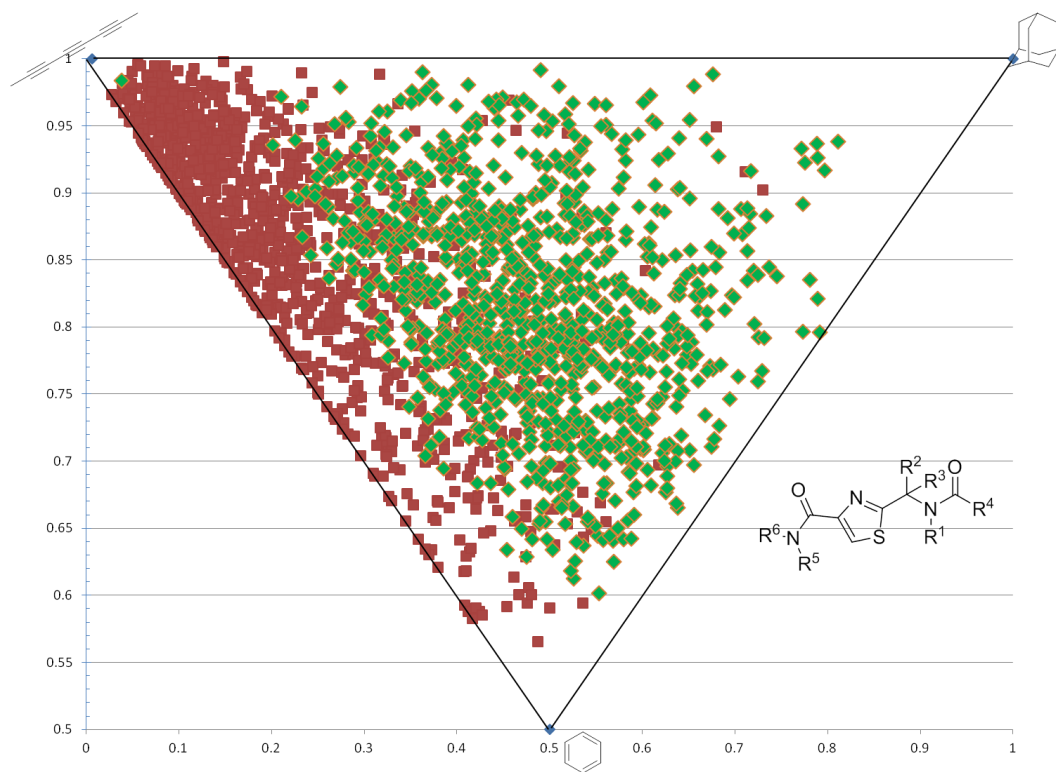


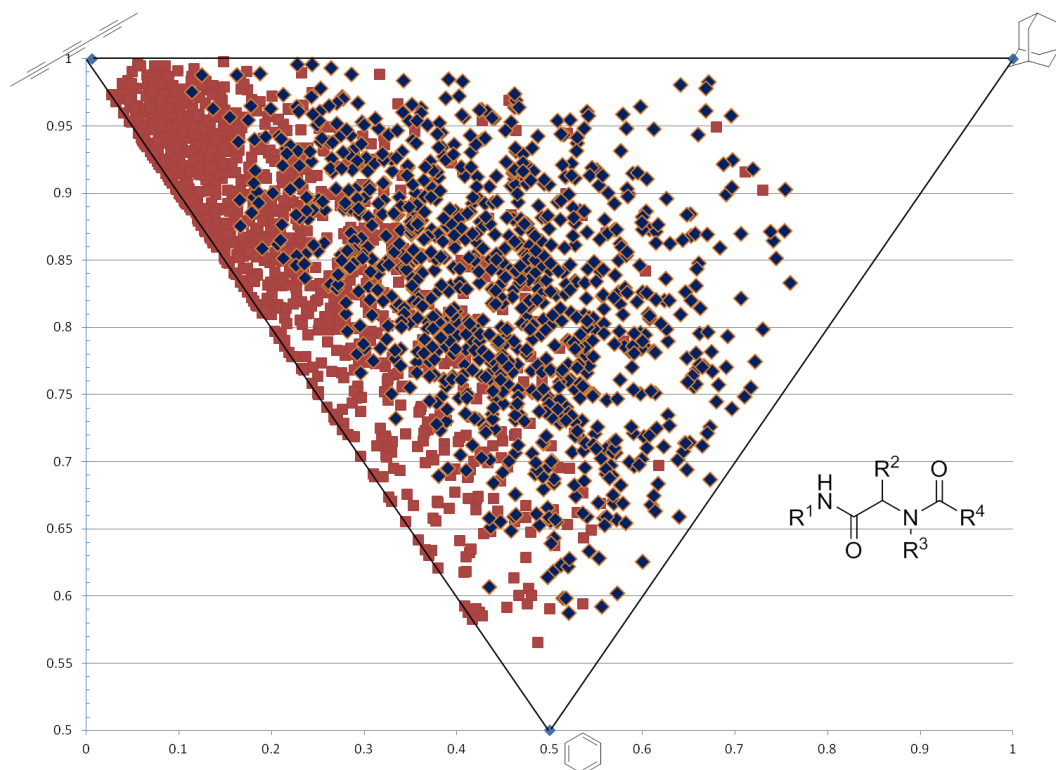
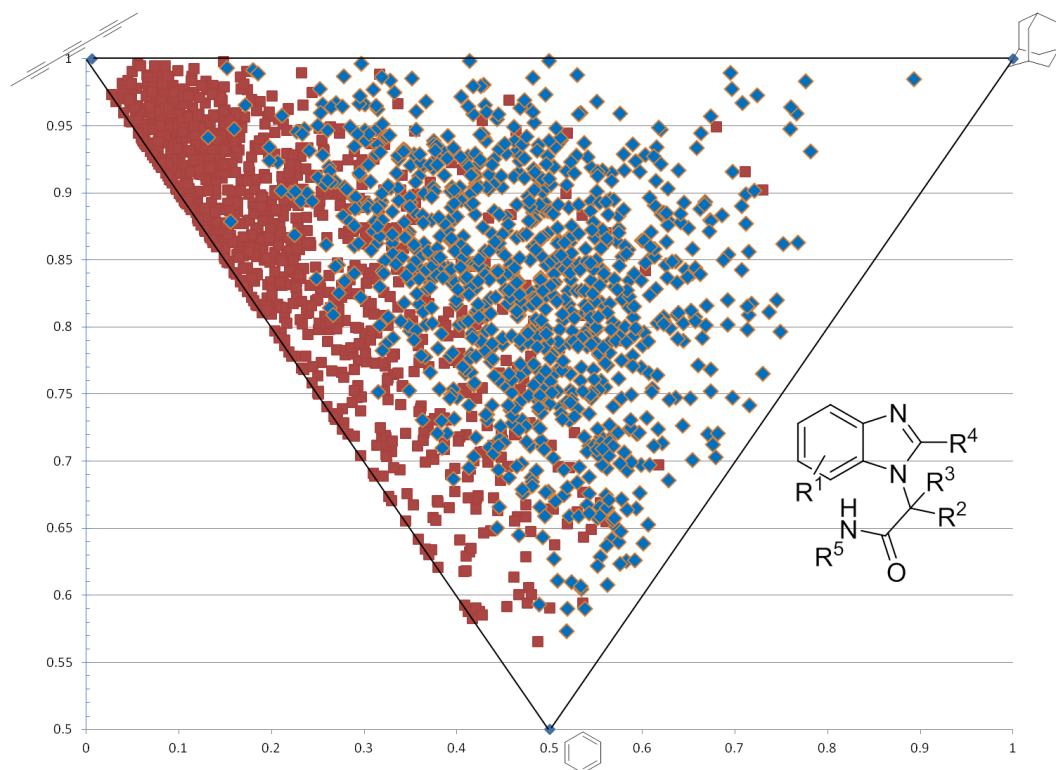












APPENDIX C

All compounds within this dissertation have been previously published, all NMR, HPLC, SFC spectra can be found in the following journals:

Compounds **3.1-8A — 3.1-8AP** can be found in *Angewandte Chemie International Edition*¹⁴³

Compounds **3.2-1A — 3.1-D** can be found in *Organic Letters*¹⁶⁶

Compound **3.2-1E** can be found in *Angewandte Chemie International Edition*¹⁴³

Compounds **3.2-1F — 3.2-1T** have been submitted to *Organic Letters*²¹³

Compounds **3.2-2A — 3.2-2D** can be found in *Organic Letters*¹⁶⁶

Compounds **3.2-3E — 3.2-2V** can be found in *Chemistry - A European Journal*¹⁶⁷

Compounds **3.2-4A — 3.2-4J** can be found in *Chemistry - A European Journal*¹⁶⁷

All compounds in chapter 4 (**4.2-2, 4.2-3, 4.2-4, and 4.3-3**) have been submitted to *Journal of Medicinal Chemistry*²¹⁴

BIBLIOGRAPHY

- (1) Rothweiler, U.; Czarna, A.; Krajewski, M.; Ciombor, J.; Kalinski, C.; Khazak, V.; Ross, G.; Skobeleva, N.; Weber, L.; Holak, T. A. *ChemMedChem* **2008**, *3*, 1118.
- (2) Huang, Y.; Wolf, S.; Koes, D.; Popowicz, G. M.; Camacho, C. J.; Holak, T. A.; Domling, A. *ChemMedChem* **2012**, *7*, 49.
- (3) Antuch, W.; Menon, S.; Chen, Q. Z.; Lu, Y.; Sakamuri, S.; Beck, B.; Schauer-Vukasinovic, V.; Agarwal, S.; Hess, S.; Domling, A. *Bioorg Med Chem Lett* **2006**, *16*, 1740.
- (4) Xu, Y.; Lu, H.; Kennedy, J. P.; Yan, X.; McAllister, L. A.; Yamamoto, N.; Moss, J. A.; Boldt, G. E.; Jiang, S.; Janda, K. D. *J Comb Chem* **2006**, *8*, 531.
- (5) Nishizawa, R.; Nishiyama, T.; Hisaichi, K.; Matsunaga, N.; Minamoto, C.; Habashita, H.; Takaoka, Y.; Toda, M.; Shibayama, S.; Tada, H.; Sagawa, K.; Fukushima, D.; Maeda, K.; Mitsuya, H. *Bioorg Med Chem Lett* **2007**, *17*, 727.
- (6) Liddle, J.; Allen, M. J.; Borthwick, A. D.; Brooks, D. P.; Davies, D. E.; Edwards, R. M.; Exall, A. M.; Hamlett, C.; Irving, W. R.; Mason, A. M.; McCafferty, G. P.; Nerozzi, F.; Peace, S.; Philp, J.; Pollard, D.; Pullen, M. A.; Shabbir, S. S.; Sollis, S. L.; Westfall, T. D.; Woollard, P. M.; Wu, C.; Hickey, D. M. *Bioorg Med Chem Lett* **2008**, *18*, 90.
- (7) Nooren, I. M. A.; Thornton, J. M. *EMBO J* **2003**, *22*, 3486.
- (8) Tuncbag, N.; Gursoy, A.; Guney, E.; Nussinov, R.; Keskin, O. *Journal of Molecular Biology* **2008**, *381*, 785.
- (9) Moreira, I. S.; Fernandes, P. A.; Ramos, M. J. *Proteins: Structure, Function, and Bioinformatics* **2007**, *68*, 803.
- (10) Conte, L. L.; Chothia, C.; Janin, J. *Journal of Molecular Biology* **1999**, *285*, 2177.
- (11) Janin, J.; Chothia, C. *J Biol Chem* **1990**, *265*, 16027.
- (12) Horton, N.; Lewis, M. *Protein Science* **1992**, *1*, 169.
- (13) Fernández, A.; Scheraga, H. A. *Proceedings of the National Academy of Sciences of the United States of America* **2003**, *100*, 113.
- (14) Bogan, A. A.; Thorn, K. S. *Journal of Molecular Biology* **1998**, *280*, 1.
- (15) Rajamani, D.; Thiel, S.; Vajda, S.; Camacho, C. J. *Proceedings of the National Academy of Sciences of the United States of America* **2004**, *101*, 11287.
- (16) von Mering, C.; Jensen, L. J.; Snel, B.; Hooper, S. D.; Krupp, M.; Foglierini, M.; Jouffre, N.; Huynen, M. A.; Bork, P. *Nucl. Acids Res.* **2005**, *33*, D433.
- (17) Berman, H. M.; Westbrook, J.; Feng, Z.; Gilliland, G.; Bhat, T. N.; Weissig, H.; Shindyalov, I. N.; Bourne, P. E. *Nucl. Acids Res.* **2000**, *28*, 235.
- (18) Khoury, K.; Popowicz, G. M.; Holak, T. A.; Domling, A. *Med Chem Comm* **2011**, *2*, 246.
- (19) Lane, D. P.; Crawford, L. V. *Nature* **1979**, *278*, 261.
- (20) Matlashewski, G.; Lamb, P.; Pim, D.; Peacock, J.; Crawford, L.; Benchimol, S. *EMBO J* **1984**, *3*, 3257.

- (21) Oren, M.; Levine, A. J. *Proc Natl Acad Sci U S A* **1983**, *80*, 56.
- (22) Yonish-Rouach, E.; Resnitzky, D.; Lotem, J.; Sachs, L.; Kimchi, A.; Oren, M. *Nature* **1991**, *352*, 345.
- (23) Diller, L.; Kassel, J.; Nelson, C. E.; Gryka, M. A.; Litwak, G.; Gebhardt, M.; Bressac, B.; Ozturk, M.; Baker, S. J.; Vogelstein, B.; et al. *Mol Cell Biol* **1990**, *10*, 5772.
- (24) Momand, J.; Zambetti, G.; Olson, D.; George, D.; Levine, A. *Cell* **1992**, *69*, 1237.
- (25) Brown, C.; Lain, S.; Verma, C.; Fersht, A.; Lane, D. *Nat Rev Cancer* **2009**, *9*, 862.
- (26) Levine, A. J.; Oren, M. *Nat Rev Cancer* **2009**, *9*, 749.
- (27) Brown, C. J.; Lain, S.; Verma, C. S.; Fersht, A. R.; Lane, D. P. *Nat Rev Cancer* **2009**, *9*, 862.
- (28) Liao, L. M.; Weaver, C. H. In *Cancerconnect.com* 2010.
- (29) Halatsch, M. E.; Schmidt, U.; Unterberg, A.; Vougioukas, V. I. *Anticancer Res* **2006**, *26*, 4191.
- (30) Wade, M.; Wahl, G. M. *Mol Cancer Res* **2009**, *7*, 1.
- (31) Vousden, K. H.; Lu, X. *Nat Rev Cancer* **2002**, *2*, 594.
- (32) Donehower, L. A.; Harvey, M.; Slagle, B. L.; McArthur, M. J.; Montgomery, C. A., Jr.; Butel, J. S.; Bradley, A. *Nature* **1992**, *356*, 215.
- (33) Marine, J.-C. W.; Dyer, M. A.; Jochemsen, A. G. *J of Cell Science* **2007**, *120*, 371.
- (34) Toledo, F.; Wahl, G. M. *Nat Rev Cancer* **2006**, *6*, 909.
- (35) Wu, X.; Bayle, J. H.; Olson, D.; Levine, A. J. *Genes Dev* **1993**, *7*, 1126.
- (36) Danovi, D.; Meulmeester, E.; Pasini, D.; Migliorini, D.; Capra, M.; Frenk, R.; de Graaf, P.; Francoz, S.; Gasparini, P.; Gobbi, A.; Helin, K.; Pelicci, P. G.; Jochemsen, A. G.; Marine, J. C. *Mol Cell Biol* **2004**, *24*, 5835.
- (37) Riemenschneider, M. J.; Buschges, R.; Wolter, M.; Reifemberger, J.; Bostrom, J.; Kraus, J. A.; Schlegel, U.; Reifemberger, G. *Cancer Res* **1999**, *59*, 6091.
- (38) Sperandio, O.; Reynes, C. H.; Camproux, A. C.; Villoutreix, B. O. *Drug Discov Today* **2010**, *15*, 220.
- (39) Clackson, T.; Wells, J. A. *Science* **1995**, *267*, 383.
- (40) Kussie, P. H.; Gorina, S.; Marechal, V.; Elenbaas, B.; Moreau, J.; Levine, A. J.; Pavletich, N. P. *Science* **1996**, *274*, 948.
- (41) Picksley, S. M.; Vojtesek, B.; Sparks, A.; Lane, D. P. *Oncogene* **1994**, *9*, 2523.
- (42) Domling, A. *Curr Opin Chem Biol* **2008**, *12*, 281.
- (43) Vassilev, L. T. *Trends Mol Med* **2007**, *13*, 23.
- (44) Vassilev, L. T.; Vu, B. T.; Graves, B.; Carvajal, D.; Podlaski, F.; Filipovic, Z.; Kong, N.; Kammlott, U.; Lukacs, C.; Klein, C.; Fotouhi, N.; Liu, E. A. *Science* **2004**, *303*, 844.
- (45) Wang, Z.; Jonca, M.; Lambros, T.; Ferguson, S.; Goodnow, R. *J Pharm Biomed Anal* **2007**, *45*, 720.
- (46) Fry, D. C.; Emerson, S. D.; Palme, S.; Vu, B. T.; Liu, C. M.; Podlaski, F. *J Biomol NMR* **2004**, *30*, 163.
- (47) Davis, T. A.; Johnston, J. N. *Chemical Science* **2011**, *2*, 1076.
- (48) Parks, D. J.; Lafrance, L. V.; Calvo, R. R.; Milkiewicz, K. L.; Gupta, V.; Lattanze, J.; Ramachandren, K.; Carver, T. E.; Petrella, E. C.; Cummings, M. D.; Maguire, D.; Grasberger, B. L.; Lu, T. *Bioorg Med Chem Lett* **2005**, *15*, 765.
- (49) Grasberger, B. L.; Lu, T.; Schubert, C.; Parks, D. J.; Carver, T. E.; Koblisch, H. K.; Cummings, M. D.; LaFrance, L. V.; Milkiewicz, K. L.; Calvo, R. R.; Maguire, D.; Lattanze, J.; Franks, C. F.; Zhao, S.; Ramachandren, K.; Bylebyl, G. R.; Zhang, M.; Manthey, C. L.; Petrella,

- E. C.; Pantoliano, M. W.; Deckman, I. C.; Spurlino, J. C.; Maroney, A. C.; Tomczuk, B. E.; Molloy, C. J.; Bone, R. F. *J Med Chem* **2005**, *48*, 909.
- (50) Koblisch, H. K.; Zhao, S.; Franks, C. F.; Donatelli, R. R.; Tominovich, R. M.; LaFrance, L. V.; Leonard, K. A.; Gushue, J. M.; Parks, D. J.; Calvo, R. R.; Milkiewicz, K. L.; Marugan, J. J.; Raboisson, P.; Cummings, M. D.; Grasberger, B. L.; Johnson, D. L.; Lu, T.; Molloy, C. J.; Maroney, A. C. *Mol Cancer Ther* **2006**, *5*, 160.
- (51) Marugan, J. J.; Leonard, K.; Raboisson, P.; Gushue, J. M.; Calvo, R.; Koblisch, H. K.; Lattanze, J.; Zhao, S.; Cummings, M. D.; Player, M. R.; Schubert, C.; Maroney, A. C.; Lu, T. *Bioorg Med Chem Lett* **2008**, *16*, 3115.
- (52) Ding, K.; Lu, Y.; Nikolovska-Coleska, Z.; Wang, G.; Qiu, S.; Shangary, S.; Gao, W.; Qin, D.; Stuckey, J.; Krajewski, K.; Roller, P. P.; Wang, S. *J Med Chem* **2006**, *49*, 3432.
- (53) Shangary, S.; Qin, D.; McEachern, D.; Liu, M.; Miller, R. S.; Qiu, S.; Nikolovska-Coleska, Z.; Ding, K.; Wang, G.; Chen, J.; Bernard, D.; Zhang, J.; Lu, Y.; Gu, Q.; Shah, R. B.; Pienta, K. J.; Ling, X.; Kang, S.; Guo, M.; Sun, Y.; Yang, D.; Wang, S. *Proc Natl Acad Sci U S A* **2008**, *105*, 3933.
- (54) Popowicz, G. M.; Czarna, A.; Wolf, S.; Wang, K.; Wang, W.; Domling, A.; Holak, T. A. *Cell Cycle* **2010**, *9*.
- (55) Ding, K.; Wang, G.; Deschamps, J. R.; Parrish, D. a.; Wang, S. *Tetrahedron Letters* **2005**, *2005*, 5949.
- (56) Carry, J. C.; Garcia-Echeverria, C. *Bioorg Med Chem Lett* **2013**, *23*, 2480.
- (57) Allen, J. G.; Bourbeau, M. P.; Wohlhieter, G. E.; Bartberger, M. D.; Michelsen, K.; Hungate, R.; Gadwood, R. C.; Gaston, R. D.; Evans, B.; Mann, L. W.; Matison, M. E.; Schneider, S.; Huang, X.; Yu, D.; Andrews, P. S.; Reichelt, A.; Long, A. M.; Yakowec, P.; Yang, E. Y.; Lee, T. A.; Oliner, J. D. *J Med Chem* **2009**, *52*, 7044.
- (58) Popowicz, G. M.; Czarna, A.; Holak, T. A. *Cell Cycle* **2008**, *7*, 2441.
- (59) Tabernero, J.; Dirix, L.; Schoffski, P.; Cervantes, A.; Capdevila, J.; Baselga, J.; Beijsterveldt, L. v.; Winkler, H.; Kraljevic, S.; Zhuang, S. H. In *Journal of Clinical Oncology, 2009 ASCO Annual Meeting*; J Clin Oncol: 2009; Vol. 27, p 3514.
- (60) ClinicalTrials.gov In *ClinicalTrials.Gov* 2010.
- (61) ClinicalTrials.gov 2010.
- (62) ClinicalTrials.gov **2010**.
- (63) Andreeff, M.; Kojima, K.; Padmanabhan, S.; Strair, R.; Kirschbaum, M.; Maslak, P.; Hillmen, P.; O'Brien, S.; Samaniego, F.; Borthakur, G.; Konopleva, M.; Vassilev, L.; Nichols, G. In *American Society of Hematology Annual Meeting* San Diego, CA, 2010.
- (64) Shen, M.; Schmitt, S.; Buac, D.; Dou, Q. P. *Expert opinion on therapeutic targets* **2013**, *17*, 1091.
- (65) Koes, D.; Khoury, K.; Huang, Y.; Wang, W.; Bista, M.; Popowicz, G. M.; Wolf, S.; Holak, T. A.; Dömling, A.; Camacho, C. J. *PLoS ONE* **2012**, *7*, e32839.
- (66) Irwin, J. J.; Shoichet, B. K. *Journal of chemical information and modeling* **2005**, *45*, 177.
- (67) Maass, P.; Schulz-Gasch, T.; Stahl, M.; Rarey, M. *Journal of chemical information and modeling* **2007**, *47*, 390.
- (68) Koes, D.; Khoury, K.; Huang, Y.; Wang, W.; Bista, M.; Popowicz, G. M.; Wolf, S.; Holak, T. A.; Domling, A.; Camacho, C. J. *PloS one* **2012**, *7*, e32839.
- (69) Nooren, I. M. A.; Thornton, J. M. *EMBO J* **2003**, *22*, 3486.
- (70) Dömling, A. *Current opinion in chemical biology* **2008**, *12*, 281.
- (71) Wells, J. A.; McClendon, C. L. *Nature* **2007**, *450*, 1001.

- (72) Fry, D. C. *Biopolymers* **2006**, 84, 535.
- (73) Fesik, S. W. *Nat Rev Cancer* **2005**, 5, 876.
- (74) Zobel, K.; Wang, L.; Varfolomeev, E.; Franklin, M. C.; Elliott, L. O.; Wallweber, H. J.; Okawa, D. C.; Flygare, J. A.; Vucic, D.; Fairbrother, W. J.; Deshayes, K. *ACS Chem Biol* **2006**, 1, 525.
- (75) Arts, J. *International Conference on Molecular Targets and Cancer Therapeutics* **2007**.
- (76) Rajamani, D.; Thiel, S.; Vajda, S.; Camacho, C. J. *Proc Natl Acad Sci U S A* **2004**, 101, 11287.
- (77) Kimura, S. R.; Brower, R. C.; Vajda, S.; Camacho, C. J. *Biophys J* **2001**, 80, 635.
- (78) Eyrisch, S.; Helms, V. *J. Med. Chem* **2007**, 50, 3457.
- (79) Kick, E. K.; Roe, D. C.; Skillman, A. G.; Liu, G.; Ewing, T. J.; Sun, Y.; Kuntz, I. D.; Ellman, J. A. *Chem Biol* **1997**, 4, 297.
- (80) Wyss, P. C.; Gerber, P.; Hartman, P. G.; Hubschwerlen, C.; Locher, H.; Marty, H. P.; Stahl, M. *J Med Chem* **2003**, 46, 2304.
- (81) Vilar, S.; Cozza, G.; Moro, S. *Current topics in medicinal chemistry* **2008**, 8, 1555.
- (82) Wolber, G.; Langer, T. *Journal of chemical information and modeling* **2005**, 45, 160.
- (83) Macarron, R. *Drug Discovery Today* **2006**, 11, 277.
- (84) Jacoby, E.; Boettcher, A.; Mayr, L. M.; Brown, N.; Jenkins, J. L.; Kallen, J.; Engeloch, C.; Schopfer, U.; Furet, P.; Masuya, K.; Lisztwan, J. In *Chemogenomics: Methods and Applications*; Springer Protocols: 2009; Vol. 575, p 173.
- (85) Berg, T. *Angewandte Chemie International Edition* **2003**, 42, 2462.
- (86) Arkin, M. R.; Wells, J. A. *10.1038/nrd1343* **2004**, 3, 301.
- (87) Sperandio, O.; Reynès, C.; Camproux, A.; Villoutreix, B. *Drug Discovery Today* **2010**, 15, 220.
- (88) Weber, L.; Illgen, K.; Almstetter, M. *Synlett* **1999**, 3, 366.
- (89) Liddle, J.; Allen, M. J.; Borthwick, A. D.; Brooks, D. P.; Davies, D. E.; Edwards, R. M.; Exall, A. M.; Hamlett, C.; Irving, W. R.; Mason, A. M. *Bioorganic & Medicinal Chemistry Letters* **2008**, 18, 90.
- (90) Dömling, A.; Huang, Y. *Synthesis* **2010**, 2010, 2859.
- (91) Irwin, J. J.; Shoichet, B. K. *J. Chem. Inf. Model* **2005**, 45, 177.
- (92) Ugi, I. *Angew. Chem.* **1959**, 71, 386.
- (93) Dömling, A.; Ugi, I. *Angew. Chem., Int. Ed.* **2000**, 39, 3168.
- (94) Ugi, I. *Angew Chem Int Ed Engl* **1962**, 1, 8.
- (95) Tan, C. Y. K.; Weaver, D. F. *Tetrahedron* **2002**, 58, 7449.
- (96) Ugi, I.; Steinbrückner, C. *Chem. Ber.* **1961**, 94, 734.
- (97) Herr, R. J. *Bioorganic & medicinal chemistry* **2002**, 10, 3379.
- (98) Zhao, T.; Boltjes, A.; E, H.; Dömling, A. *Org Lett* **2013**, 15, 639.
- (99) Ugi, I.; Offermann, K. *Chem. Ber.* **1964**, 97, 2276.
- (100) Barrow, J. C.; Stauffer, S. R.; Rittle, K. E.; Ngo, P. L.; Yang, Z.; Selnick, H. G.; Graham, S. L.; Munshi, S.; McGaughey, G. B.; Holloway, M. K.; Simon, A. J.; Price, E. A.; Sankaranarayanan, S.; Colussi, D.; Tugusheva, K.; Lai, M. T.; Espeseth, A. S.; Xu, M.; Huang, Q.; Wolfe, A.; Pietrak, B.; Zuck, P.; Levorse, D. A.; Hazuda, D.; Vacca, J. P. *J Med Chem* **2008**, 51, 6259.
- (101) Zhang, C.; Moran, E.; Woiwode, T.; Short, K.; A., M. *Tetrahedron Lett.* **1996**, 37, 751.
- (102) Sung, K.; Wu, S.; Chen, P. *Tetrahedron* **2002**, 58, 5599.

- (103) Hendlich, M.; Bergner, A.; Gunther, J.; Klebe, G. *Journal of Molecular Biology* **2003**, 326, 607.
- (104) Huang, Y.; Khoury, K.; Domling, A. *Top Heterocycl Chem* **2010**, 23, 85.
- (105) Borthwick, A. D.; Liddle, J. *Medicinal research reviews* **2011**, 31, 576.
- (106) Szardenings, A. K.; Burkoth, T. S.; Lu, H. H.; Tien, D. W.; Campbell, D. A. *Tetrahedron* **1997**, 53, 6573.
- (107) Szardenings, A. K.; Antonenko, V.; Campbell, D. A.; DeFrancisco, N.; Ida, S.; Shi, L. H.; Sharkov, N.; Tien, D.; Wang, Y. W.; Navre, M. *Journal of Medicinal Chemistry* **1999**, 42, 1348.
- (108) Liu, H.; William, S.; Herdtweck, E.; Botros, S.; Dömling, A. *Chemical Biology & Drug Design* **2012**, 79, 470.
- (109) Domling, A.; Khoury, K. *ChemMedChem* **2010**, 5, 1420.
- (110) Tempest, P.; Ma, V.; Thomas, S.; Hua, Z.; Kelly, M. G.; Hulme, C. *Tetrahedron Lett.* **2001**, 42, 4959.
- (111) Huang, Y.; Khoury, K.; Chanas, T.; Domling, A. *Org Lett* **2012**, 14, 5916.
- (112) Groebke, K.; Weber, L.; Mehlin, F. *Synlett* **1998**, 1998, 661.
- (113) Blackburn, C.; Guan, B.; Fleming, P.; Shiosaki, K.; Tsai, S. *Tetrahedron Lett.* **1998**, 39, 3635.
- (114) Bienaymé, H.; Bouzid, K. *Angew Chem Int Ed Engl* **1998**, 37, 2234.
- (115) Guchhait, S.; Madaan, C. *Tetrahedron Lett.* **2011**, 52, 56.
- (116) Bon, R. S.; van Vliet, B.; Sprenkels, N. E.; Schmitz, R. F.; de Kanter, F. J. J.; Stevens, C. V.; Swart, M.; Bickelhaupt, F. M.; Groen, M. B.; Orru, R. V. A. *J. Org. Chem.* **2005**, 70, 3542.
- (117) Heck, S.; Dömling, A. *Synlett* **2000**, 2000, 424.
- (118) Wang, W.; Joyner, S.; Khoury, K. A.; Domling, A. *Organic & biomolecular chemistry* **2010**, 8, 529.
- (119) Döbner, O. *Justus Liebigs Ann. Chem.* **1887**, 242, 265.
- (120) Jones, G. In *The Chemistry of Heterocyclic Compounds*; Jones, G., Ed. 1991; Vol. 32.
- (121) Boa, A. N.; Canavan, S. P.; Hirst, P. R.; Ramsey, C.; Stead, A. M.; McConkey, G. A. *Bioorganic & medicinal chemistry* **2005**, 13, 1945.
- (122) Blaney, F. E.; Raveglia, L. F.; Artico, M.; Cavagnera, S.; Dartois, C.; Farina, C.; Grugni, M.; Gagliardi, S.; Luttmann, M. A.; Martinelli, M.; Nadler, G. M.; Parini, C.; Petrillo, P.; Sarau, H. M.; Scheideler, M. A.; Hay, D. W.; Giardina, G. A. *J Med Chem* **2001**, 44, 1675.
- (123) Wu, Y.; Chen, Z.; Liu, Y.; Yu, L.; Zhou, L.; Yang, S.; Lai, L. *Bioorganic & medicinal chemistry* **2011**, 19, 3361.
- (124) Gewald, K.; Schinke, E.; Böttcher, H. *Chem. Ber.* **1966**, 99.
- (125) Wang, K.; Nguyen, K.; Huang, Y.; Domling, A. *J Comb Chem* **2009**, 11, 920.
- (126) Huang, Y.; Domling, A. *Mol Divers* **2011**, 15, 3.
- (127) Haimova, M.; Mollov, N.; Ivanova, S.; Dimitrova, A.; Ognyanov, V. *Tetrahedron* **1977**, 33, 331.
- (128) Sauer, W. H.; Schwarz, M. K. *Journal of chemical information and computer sciences* **2003**, 43, 987.
- (129) Sheridan, R. P.; Rusinko, A.; Nilakantan, R.; Venkataraghavan, R. *Proceedings of the National Academy of Sciences* **1989**, 86, 8165.
- (130) Maass, P.; Schulz-Gasch, T.; Stahl, M.; Rarey, M. *J. Chem. Inf. Model* **2007**, 47, 390.
- (131) Czarna, A.; Beck, B.; Srivastava, S.; Popowicz, G. M.; Wolf, S.; Huang, Y.; Bista, M.; Holak, T. A.; Dömling, A. *Angew. Chem. Intl. Ed. Engl. In press* **2010**.

- (132) Moitessier, N.; Englebienne, P.; Lee, D.; Lawandi, J.; Corbeil, C. R. *British Journal of Pharmacology* **2008**, *153*, 7.
- (133) Dömling, A.; Wang, W.; Wang, K. *Chem. Rev.* **2012**, *112*, 3083.
- (134) Venkatraman, S.; Bogen, S. L.; Arasappan, A.; Bennett, F.; Chen, K.; Jao, E.; Liu, Y.-T.; Lovey, R.; Hendrata, S.; Huang, Y.; Pan, W.; Parekh, T.; Pinto, P.; Popov, V.; Pike, R.; Ruan, S.; Santhanam, B.; Vibulbhan, B.; Wu, W.; Yang, W.; Kong, J.; Liang, X.; Wong, J.; Liu, R.; Butkiewicz, N.; Chase, R.; Hart, A.; Agrawal, S.; Ingravallo, P.; Pichardo, J.; Kong, R.; Baroudy, B.; Malcolm, B.; Guo, Z.; Prongay, A.; Madison, V.; Broske, L.; Cui, X.; Cheng, K.-C.; Hsieh, Y.; Brisson, J.-M.; Prelusky, D.; Korfmacher, W.; White, R.; Bogdanowich-Knipp, S.; Pavlovsky, A.; Bradley, P.; Saksena, A. K.; Ganguly, A.; Piwinski, J.; Girijavallabhan, V.; Njoroge, F. G. *J. Med. Chem.* **2006**, *49*, 6074.
- (135) Liddle, J.; Allen, M. J.; Borthwick, A. D.; Brooks, D. P.; Davies, D. E.; Edwards, R. M.; Exall, A. M.; Hamlett, C.; Irving, W. R.; Mason, A. M.; McCafferty, G. P.; Nerozzi, F.; Peace, S.; Philp, J.; Pollard, D.; Pullen, M. A.; Shabbir, S. S.; Sollis, S. L.; Westfall, T. D.; Woollard, P. M.; Wu, C.; Hickey, D. M. B. *Bioorg. Med. Chem. Lett.* **2008**, *18*, 90.
- (136) Lamberth, C.; Jeanguenat, A.; Cederbaum, F.; De Mesmaeker, A.; Zeller, M.; Kempf, H.-J.; Zeun, R. *Bioorg. Med. Chem. Lett.* **2008**, *16*, 1531.
- (137) Passerini, M.; Simone, L. *Gazz. Chim. Ital* **1921**, *51*.
- (138) Van Leusen, A. M.; Wildeman, J.; Oldenziel, O. H. *J. Org. Chem.* **1977**, *42*, 1153.
- (139) Nishiyama, Y.; Katahira, C.; Sonoda, N. *Tetrahedron Lett.* **2004**, *45*, 8539.
- (140) Weber, L.; Illgen, K.; Almstetter, M. *Synlett* **1999**, *1999*, 366.
- (141) Dömling, A. *Current opinion in chemical biology* **2000**, *4*, 318.
- (142) Ruijter, E.; Scheffelaar, R.; Orru, R. V. A. *Angew. Chem., Int. Ed.* **2011**, *50*, 6234.
- (143) Khoury, K.; Sinha, M. K.; Nagashima, T.; Herdtweck, E.; Dömling, A. *Angewandte Chemie International Edition* **2012**, *51*, 10280.
- (144) Demharter, A.; Hörl, W.; Herdtweck, E.; Ugi, I. *Angew. Chem., Int. Ed.* **1996**, *35*, 173.
- (145) Ugi, I.; Demharter, A.; Hörl, W.; Schmid, T. *Tetrahedron* **1996**, *52*, 11657.
- (146) Park, S. J.; Keum, G.; Kang, S. B.; Koh, H. Y.; Kim, Y.; Lee, D. H. *Tetrahedron Lett.* **1998**, *39*, 7109.
- (147) Kim, Y. B.; Choi, E. H.; Keum, G.; Kang, S. B.; Lee, D. H.; Koh, H. Y.; Kim, Y. *Org. Lett.* **2001**, *3*, 4149.
- (148) Sung, K.; Chen, F.-L.; Chung, M.-J. *Mol. Diversity* **2003**, *6*, 213.
- (149) Godet, T.; Bonvin, Y.; Vincent, G.; Merle, D.; Thozet, A.; Ciufolini, M. A. *Org. Lett.* **2004**, *6*, 3281.
- (150) Sollis, S. L. *J. Org. Chem.* **2005**, *70*, 4735.
- (151) Ku, I. W.; Cho, S.; Doddareddy, M. R.; Jang, M. S.; Keum, G.; Lee, J.-H.; Chung, B. Y.; Kim, Y.; Rhim, H.; Kang, S. B. *Bioorg. Med. Chem. Lett.* **2006**, *16*, 5244.
- (152) Kadzimirsz, D.; Hildebrandt, D.; Merz, K.; Dyker, G. *Chem. Commun.* **2006**, 661.
- (153) Borthwick, A. D.; Liddle, J.; Davies, D. E.; Exall, A. M.; Hamlett, C.; Hickey, D. M.; Mason, A. M.; Smith, I. E. D.; Nerozzi, F.; Peace, S.; Pollard, D.; Sollis, S. L.; Allen, M. J.; Woollard, P. M.; Pullen, M. A.; Westfall, T. D.; Stanislaus, D. J. *J. Med. Chem.* **2012**, *55*, 783.
- (154) Beck, B.; Srivastava, S.; Khoury, K.; Herdtweck, E.; Dömling, A. *Mol. Diversity* **2010**, *14*, 479.
- (155) Isaacson, J.; Kobayashi, Y. *Angew. Chem., Int. Ed.* **2009**, *48*, 1845.
- (156) NIH In *Probe Reports from the NIH Molecular Libraries Program* [<http://www.ncbi.nlm.nih.gov/books/NBK47352/>]

National Center for Biotechnology Information (US): Bethesda (MD), 2010-.

- (157) Zbinden, K. G.; Anselm, L.; Banner, D. W.; Benz, J.; Blasco, F.; Decoret, G.; Himber, J.; Kuhn, B.; Panday, N.; Ricklin, F.; Risch, P.; Schlatter, D.; Stahl, M.; Thomi, S.; Unger, R.; Haap, W. *European journal of medicinal chemistry* **2009**, *44*, 2787.
- (158) Gehlhaar, D. K.; Verkhivker, G. M.; Rejto, P. A.; Sherman, C. J.; Fogel, D. B.; Fogel, L. J.; Freer, S. T. *Chemistry & biology* **1995**, *2*, 317.
- (159) Jensen, C.; Herold, P.; Brunner, H. R. *Nature reviews. Drug discovery* **2008**, *7*, 399.
- (160) Matthews, J. H.; Krishnan, R.; Costanzo, M. J.; Maryanoff, B. E.; Tulinsky, A. *Biophysical journal* **1996**, *71*, 2830.
- (161) Moderhack, D. *Justus Liebigs Ann. Chem.* **1973**, 1973, 359.
- (162) Smith, H. K.; Beckett, R. P.; Clements, J. M.; Doel, S.; East, S. P.; Launchbury, S. B.; Pratt, L. M.; Spavold, Z. M.; Thomas, W.; Todd, R. S.; Whittaker, M. *Bioorg. Med. Chem. Lett.* **2002**, *12*, 3595.
- (163) Chang, J.-y.; Shin, E.-k.; Kim, H. J.; Kim, Y.; Park, Y. S. *Bull Korean Chem Soc* **2005**, *26*, 989.
- (164) Weber, L.; Wallbaum, S.; Broger, C.; Gubernator, K. *Angew. Chem., Int. Ed.* **1995**, *34*, 2280.
- (165) Shoda, M.; Harada, T.; Kogami, Y.; Tsujita, R.; Akashi, H.; Kouji, H.; Stahura, F. L.; Xue, L.; Bajorath, J. *J. Med. Chem.* **2004**, *47*, 4286.
- (166) Sinha, M. K.; Khoury, K.; Herdtweck, E.; Domling, A. *Organic & biomolecular chemistry* **2013**, *11*, 4792.
- (167) Sinha, M. K.; Khoury, K.; Herdtweck, E.; Domling, A. *Chemistry* **2013**, *19*, 8048.
- (168) Ugi, I.; Domling, A.; Horl, W. *Endeavour* **1994**, *18*, 115.
- (169) Zhu, J.; Bienaymé, H. *Multicomponent reactions*; Wiley-VCH: Weinheim, 2005.
- (170) Dömling, A.; Huang, Y. *Synthesis* **2010**, *42*, 2859.
- (171) Dömling, A. *Curr. Opin. Chem. Bio.* **2000**, *4*, 318.
- (172) Hulme, C.; Gore, V. *Curr. Med. Chem.* **2003**, *10*, 51.
- (173) Ugi, I.; Domling, A.; Gruber, B.; Almstetter, M. *Croat. Chem. Acta* **1997**, *70*, 631.
- (174) Weber, L. *Curr. Opin. Chem. Bio.* **2000**, *4*, 295.
- (175) Weber, L.; Wallbaum, S.; Broger, C.; Gubernator, K. *Angew. Chem. Int. Ed.* **1995**, *34*, 2280.
- (176) Ruijter, E.; Scheffelaar, R.; Orru, R. V. A. *Angew. Chem. Int. Ed.* **2011**, *50*, 6234.
- (177) Ugi, I.; Steinbrückner, C. *Angewandte Chemie* **1960**, *72*, 267.
- (178) Banfi, L.; Riva, R. In *Organic Reactions*; John Wiley & Sons, Inc.: 2004.
- (179) Van Leusen, A. M.; Wildeman, J.; Oldenziel, O. H. *The Journal of Organic Chemistry* **1977**, *42*, 1153.
- (180) Passerini, M.; Simone, L. *Gazz. Chim. Ital* **1921**, *51*, 126.
- (181) Bossio, R.; Marcos, C. F.; Marcaccini, S.; Pepino, R. *Synthesis* **1997**, 1997, 1389.
- (182) Bossio, R.; Marcos, C. F.; Marcaccini, S.; Pepino, R. *Synthesis* **1997**, 1997, 1389.
- (183) Tyagi, V.; Khan, S.; Bajpai, V.; Gauniyal, H. M.; Kumar, B.; Chauhan, P. M. S. *The Journal of Organic Chemistry* **2012**, *77*, 1414.
- (184) Cano-Herrera, M. A.; Miranda, L. D. *Chemical Communications* **2011**, *47*, 10770.
- (185) Wang, W.; Ollio, S.; Herdtweck, E.; Dömling, A. *The Journal of Organic Chemistry* **2010**, *76*, 637.
- (186) Znabet, A.; Zonneveld, J.; Janssen, E.; De Kanter, F. J. J.; Helliwell, M.; Turner, N. J.; Ruijter, E.; Orru, R. V. A. *Chemical Communications* **2010**, *46*, 7706.

- (187) Wang, W.; Herdtweck, E.; Domling, A. *Chemical Communications* **2010**, 46, 770.
- (188) Liu, H.; Dömling, A. *The Journal of Organic Chemistry* **2009**, 74, 6895.
- (189) Cao, H.; Liu, H.; Dömling, A. *Chemistry – A European Journal* **2010**, 16, 12296.
- (190) Pictet, A.; Spengler, T. *Ber.* **1911**, 44.
- (191) Larghi, E. L.; Kaufman, T. S. *Synthesis* **2006**, 37, 187.
- (192) Irwin, J. J.; Sterling, T.; Mysinger, M. M.; Bolstad, E. S.; Coleman, R. G. *Journal of chemical information and modeling* **2012**.
- (193) Dömling, A.; Mannhold, R.; Kubinyi, H.; Folkers, G. *Protein-Protein Interactions in Drug Discovery (Methods and Principles in Medicinal Chemistry)*; Wiley-VCH: Weinheim, Germany, 2013.
- (194) Irwin, J. J.; Shoichet, B. K. *J. Chem. Inf. Model.* **2005**, 45, 177.
- (195) Irwin, J. J.; Sterling, T.; Mysinger, M. M.; Bolstad, E. S.; Coleman, R. G. *J. Chem. Inf. Model.* **2012**, 52, 1757.
- (196) Meireles, L. M. C.; Dömling, A. S.; Camacho, C. J. *Nucleic Acids Research* **2010**, 38, W407.
- (197) Srivastava, S.; Beck, B.; Wang, W.; Czarna, A.; Holak, T. A.; Domling, A. *Journal of Combinatorial Chemistry* **2009**, 11, 631.
- (198) Czarna, A.; Beck, B.; Srivastava, S.; Popowicz, G. M.; Wolf, S.; Huang, Y.; Bista, M.; Holak, T. A.; Doemling, A. *Angewandte Chemie-International Edition* **2010**, 49, 5352.
- (199) Popowicz, G. M.; Dömling, A.; Holak, T. A. *Angewandte Chemie International Edition* **2011**, 50, 2680.
- (200) Czarna, A.; Popowicz, G. M.; Pecak, A.; Wolf, S.; Dubin, G.; Holak, T. A. *Cell Cycle* **2009**, 8, 1176.
- (201) Huang, Y.; Wolf, S.; Bista, M.; Meireles, L.; Camacho, C.; Holak, T. A.; Doemling, A. *Chemical Biology & Drug Design* **2010**, 76, 116.
- (202) Ugi, I.; Demharter, A.; Hörl, W.; Schmid, T. *Tetrahedron* **1996**, 52, 11657.
- (203) Krajewski, M.; Rothweiler, U.; D'Silva, L.; Majumdar, S.; Klein, C.; Holak, T. A. *Journal of Medicinal Chemistry* **2007**, 50, 4382.
- (204) Bista, M.; Kowalska, K.; Janczyk, W.; Domling, A.; Holak, T. A. *Journal of the American Chemical Society* **2009**, 131, 7500.
- (205) Popowicz, G. M.; Czarna, A.; Wolf, S.; Wang, K.; Wang, W.; Domling, A.; Holak, T. A. *Cell Cycle* **2010**, 9, 1104.
- (206) Hu, B.; Gilkes, D. M.; Chen, J. *Cancer Res* **2007**, 67, 8810.
- (207) Bista, M.; Wolf, S.; Khoury, K.; Kowalska, K.; Huang, Y.; Wrona, E.; Arciniega, M.; Popowicz, G. M.; Holak, T. A.; Domling, A. *Structure* **2013**, 21, 2143.
- (208) Popowicz, G. M.; Domling, A.; Holak, T. A. *Angew Chem Int Edit* **2011**, 50, 2680.
- (209) Domling, A. *Curr Opin Chem Biol* **2008**, 12, 281.
- (210) Graves, B.; Thompson, T.; Xia, M.; Janson, C.; Lukacs, C.; Deo, D.; Di Lello, P.; Fry, D.; Garvie, C.; Huang, K. S.; Gao, L.; Tovar, C.; Lovey, A.; Wanner, J.; Vassilev, L. T. *Proc Natl Acad Sci U S A* **2012**, 109, 11788.
- (211) Huang, Y.; Wolf, S.; Koes, D.; Popowicz, G. M.; Camacho, C. J.; Holak, T. A.; Domling, A. *ChemMedChem* **2011**.
- (212) Chi, S. W.; Lee, S. H.; Kim, D. H.; Ahn, M. J.; Kim, J. S.; Woo, J. Y.; Torizawa, T.; Kainosho, M.; Han, K. H. *Journal of Biological Chemistry* **2005**, 280, 38795.
- (213) Khoury, K.; Sinha, M. K.; Jones, S.; E, H.; Dömling, A. *Org Lett* **2014**, Submitted.

(214) Khoury, K.; Huang, Y.; Koes, D.; Bista, M.; Wolf, S.; Beck, B.; Köhler, L.; Popowicz, G.; Holak, T. A.; Camacho, C.; Dömling, A. *Journal of Medicinal Chemistry* **2014**, *Submitted*.